# THE UNIVERSITY
## *of* ADELAIDE

*SUB CRUCE LUMEN*

---

# Small-Scale Batch-Fed Biomass Gasification and Combustion

---

## THOMAS KIRCH

*The University of Adelaide*

*School of Mechanical Engineering*

A THESIS SUBMITTED IN FULFILMENT OF THE REQUIREMENTS FOR THE DEGREE OF DOCTOR OF PHILOSOPHY

July 2019

This page intentionally left mostly blank.

# Abstract

Small-scale solid biomass-fuelled cookstoves are highly important to satisfy the energy demand of nearly half the world's population. With this as a main application, biomass provides the majority of renewable energy worldwide. However, traditional cookstoves, which emit vast amounts of emissions from incomplete combustion, are still the most widely used stoves. Furthermore, recently developed types of cookstoves may not be more efficient than traditional types of stoves, highlighting the necessity for more in-depth research into such combustion systems. Emissions from incomplete biomass combustion have been linked to a number of human health and environmental problems. Particulate matter (PM) emissions contribute substantially to respiratory diseases and black carbon, the second most influential anthropogenic climate forcing emission. These problems can be addressed through widespread use of more efficient and less polluting cookstoves. One type of cookstove, called a gasifier stove, has been identified as providing great potential to achieve the required drastic reduction in emissions from incomplete combustion. Gasifier type cookstoves utilise a staged combustion process. This allows the thermochemical conversion of the solid fuel to form gases, liquids (tars) and solid char, to be separated in time and location from the combustion of the released gases and tars. A much deeper understanding of the ongoing fundamental processes in gasifier stoves is required to enable emissions reductions in future designs, which is the aim of this research.

In gasifier stoves, the separation of the thermochemical conversion process of the fuel and the combustion of the released products is achieved through a staged process. Air staging may be performed by providing a limited amount of primary air from below and secondary air downstream of the solid fuel bed. When lit from the top of the fuel bed this is called a reverse downdraft process. The air supply has a major influence on both the conversion and combustion processes, but the necessary amounts of, and relationships between, the air supply stages are not fully understood.

At a low primary air supply, as is mostly the case in reverse downdraft gasifier cookstoves, the fuel consumption in the thermochemical conversion process scales linearly with the air supply. Increasing air flows lead to higher temperatures in the fuel bed, which in turn alter the product distribution across gases, tars and char. Combustible gases are the preferred product over tars, which may be toxic if released, and soot precursors if combusted. Thus, an intrinsic decomposition of tars may be beneficial. The product distribution can be influenced by specific mechanisms; for example tars can decompose to form gases at high temperatures and this conversion may be supported by the presence of char. In reverse downdraft gasifier stoves, the released tars and gases, together called producer gas, propagate through a layer of hot char where the tar decomposition may be enhanced, but this influence has not been established for small-scale systems. Furthermore, the product composition is dependent on the biomass feedstock and, in application, a wide variety of fuels are

This page intentionally left mostly blank.

being used. The ash content in fuels has been found to be detrimental in many combustion applications and, although the ash and moisture contents can vary substantially between biomass fuels, when comparing the major elements in the composition (i.e. C, H and O) on a dry-ash-free basis, most biomass fuels are similar. The influence of using different fuels with varying ash contents on the conversion and combustion processes in gasifier stoves is largely unknown.

In the present thesis, four studies form the main body and focus on various aspects of the combustion processes in reverse downdraft gasifier stoves. The first study addresses the influence of the draft type (natural or forced) and the relationship between the air supply stages on the overall combustion efficiency. The second and third studies focus on the batch-fed thermochemical biomass conversion process within the solid fuel bed. Specifically, the focus is the influence of an increasing fuel bed depth, thus an increasing char layer thickness to facilitate tar conversion, and the utilisation of various feedstocks, with varying ash contents. The fourth study investigates the secondary combustion process with a particular emphasis on the influence of changing conditions in thermochemical conversion, as provided by the previous two studies. Furthermore, two additional research articles, which were published prior to the official commencement of the degree, on the influence of the air supply, as well as two conference articles, are included in the Appendices.

When investigating the draft type, it was confirmed that utilising forced air achieves a much higher combustion efficiency throughout the different combustion phases in gasifier cookstoves. A relationship of 1:4, of primary to secondary air, provided the best combustion conditions for the utilised wood chips. While focussing on the thermochemical conversion process of wood pellets, a fivefold increase of the primary air led to a rise from approximately 800°C to 1100°C, of the peak temperature, and from 33% to 73%, of the cold gas efficiency. A fourfold extension of the fuel bed depth, at one specific air supply rate, led to an increased production of permanent gases and a rise of the cold gas efficiency by approximately 10%. Similarly, when utilising higher ash content fuels, wheat straw, sheep manure and cow manure, a higher primary air flow was associated with greater process temperatures and a rise in the cold gas efficiency. Conversely, a threefold increase of the air supply led to double the $PM_{2.5}$ combustion emissions from wood pellets and a more than tenfold increase from cow manure. Lower primary air supply rates were associated with lower emissions from incomplete combustion, especially when utilising high ash-content fuels.

Foremost, the combined production of producer gas and char at low air supply rates, when utilising forced air with sufficient secondary air, has been identified to substantially reduce the emissions of incomplete combustion. The conversion of tars and the retention of ash constituents in the produced char contribute to pollutant emissions reduction. By utilising these mechanisms low value agricultural residues and even manures may be burned almost as cleanly as high value wood pellets. Careful reactor design based on the presented results and conclusions may facilitate the development of more efficient and more fuel flexible reverse downdraft gasifier stoves.

This page intentionally left mostly blank.

# Declaration

I certify that this work contains no material which has been accepted for the award of any other degree or diploma in my name, in any university or other tertiary institution and, to the best of my knowledge and belief, contains no material previously published or written by another person, except where due reference has been made in the text. In addition, I certify that no part of this work will, in the future, be used in a submission in my name, for any other degree or diploma in any university or other tertiary institution without the prior approval of the University of Adelaide and, where applicable, any partner institution responsible for the joint-award of this degree.

I acknowledge that copyright of published works contained within this thesis resides with the copyright holder(s) of those works.

I also give permission for the digital version of my thesis to be made available on the web, via the University's digital research repository, the Library Search and also through web search engines, unless permission has been granted by the University to restrict access for a period of time.

07 July 2019

Thomas Kirch                             Date

This page intentionally left mostly blank.

# Acknowledgements

The continuous support, guidance and technical expertise of Paul Medwell has made this thesis possible. I am very thankful that you always made time and had so much good advice to give. The outstanding initiative of Cris Birzer has added rare value to this work, which will always stay with me. The contribution of Phil van Eyk has provided structure and included so many hours of productive discussions of my work. You are such an exceptional, engaged and harmonic group and I am forever grateful that you gave me the opportunity to learn from and work with you.

The financial support of the Studienstiftung des deutschen Volkes, a refreshingly trust, not bureaucracy, based institution, and of the University of Adelaide is gratefully acknowledged. Special gratitude goes out to Marc Simpson, the laboratory facilities manager, for his expertise and problem-solving mentality.

I would also like to thank my friends and colleagues. The elaborate discussions with Mathu Indren and Ben Morton, as well as my office mates Houzhi Wang, Nick Sullivan, Shaun Fitzgerald and Anthony Roccisano, have been invaluable. Learning and using CFD was only possible through patient collaboration with Michael Evans and my writing skills have significantly benefited from workshops and writing sessions with Alison-Jane Hunter.

For giving me the necessary motivation and perseverance, for even moving half way around the world to follow my dreams, for being so lucky as to go through the same challenges together and for so much more I want to thank Sarah Heinrich.

Above all I am grateful to Ursula and Alfred Kirch: you have carried me my whole life, supported all my endeavours and bring me joy with every call. This extends to Brigitte Bornstein and Peter Kirch, I can't begin to explain how lucky I feel to have you.

This page intentionally left mostly blank.

# List of Publications
# Included in this Thesis

**Published**

1. **Kirch, T.,** Birzer, C. H., van Eyk, P. J. & Medwell, P. (2018). "Influence of Primary and Secondary Air Supply on Gaseous Emissions from a Small-Scale Staged Solid Biomass Fuel Combustor." *Energy & Fuels,* vol. 32, pp. 4212–4220.
   DOI: 10.1021/acs.energyfuels.7b03152

2. **Kirch, T.,** Medwell, P., Birzer, C. H. & van Eyk, P. J. (2018). "Influences of Fuel Bed Depth and Air Supply on Small-Scale Batch-Fed Reverse Downdraft Biomass Conversion." *Energy & Fuels,* vol. 32, pp. 8507–8518.
   DOI: 10.1021/acs.energyfuels.8b01699

**Submitted**

3. **Kirch, T.,** Medwell, P., Birzer, C. H. & van Eyk, P. J. (2019) "Small-Scale Autothermal Thermochemical Conversion of Multiple Solid Biomass Feedstock." Submitted to: *Renewable Energy.*

4. **Kirch, T.,** Medwell, P., Birzer, C. H. & van Eyk, P. J. (2019). "Feedstock Dependence of Emissions from Reverse Downdraft Gasifier Cookstove" Submitted to: *Environmental Science & Technology.*

This page intentionally left mostly blank.

# Additional Publications
# Arising from this Project

**Journal Papers**

1. **Kirch, T.,** Medwell, P. & Birzer, C. H. (2016). "Natural Draft and Forced Primary Air Combustion Properties of a Top-Lit Up-Draft Research Furnace." *Biomass & Bioenergy,* vol. 91, pp. 108–115.
   DOI: 10.1016/j.biombioe.2016.05.003

2. **Kirch, T.,** Birzer, C. H., Medwell, P. & Holden, L. (2018). "The Role of Primary and Secondary Air on Wood Combustion in Cookstoves." *International Journal of Sustainable Energy,* vol. 37, pp. 268–277.
   DOI: 10.1080/14786451.2016.1166110

**Conference Articles**

1. **Kirch, T.,** Medwell, P. & Birzer, C. H. (2015) "Assessment of Natural Draft Combustion Properties of a Top-Lit Up-Draft Research Furnace." *Proceedings of the Australian Combustion Symposium.*

2. **Kirch, T.,** Evans, M. J., Medwell, P., Rapp, V. H., Birzer, C. H. & Gadgil, A. J. (2018). "Mixing Uniformity of Emissions for Point-Wise Measurements in Exhaust Ducts" *21st Australasian Fluid Mechanics Conference.*

This page intentionally left mostly blank.

# Contents

This page intentionally left mostly blank.

# List of Figures

This page intentionally left mostly blank.

# List of Tables

This page intentionally left mostly blank.

# Chapter 1

## Introduction

## 1.1 Biomass Fuelled Cookstoves

Solid biomass fuels provide the majority of the renewable energy worldwide [1], supplying $\approx$10% of the total primary energy [2]. A major application is in biomass fuelled cookstoves, which are used by approximately 2.7 billion people [3], making them one of the most widely used combustion systems. Despite this, there has been limited progress in our understanding of the fundamental combustion processes to enable the design of appropriate and technologically advanced cooking systems. Current cookstoves often use traditional or ad hoc improved designs, which may still emit substantial amounts of pollutant emissions [4]. Therefore, a much deeper understanding of the combustion processes in such systems is needed to enable the systematic and reliable development of more efficient designs.

Pollutant emissions, mainly particulates released from incomplete combustion, are the main cause of household air pollution (HAP). HAP contributes considerably to the global burden of disease and it is estimated that approximately 3.8 million people die prematurely from attributed illnesses annually [5]. In particular, air pollution from solid fuels affects women, for whom it is the second highest risk factor worldwide after high blood pressure [6], and children, for whom it is responsible for 50% of premature deaths under five years of age [5]. A recent study has also suggested a link between particulate matter (PM) emissions and Type II diabetes [7]. To achieve any health benefits, a substantial reduction of particulate emissions of nominal diameter $\leq$2.5 $\mu$m ($PM_{2.5}$) is necessary [8]. Discrepancies in cookstove performance determination add difficulty to the analysis of the benefits of particular stove designs [9–12]. Even if current cookstoves designs were optimised and widely used, it is unclear if this alone would achieve the emission reduction goals. Therefore, the investigation of potential systems that could mitigate this significant human environmental health issue is of mortal importance to many.

Particulate matter, together with carbon monoxide (CO), is the main emission

of incomplete combustion and has also been recognised as having a significant environmental impact [13, 14]. Black carbon, a major component of PM, for which residential cooking systems are a main cause [15, 16], has been identified as the second most important anthropogenic emission in terms of its climate forcing potential in the present-day atmosphere [17]. Thus, highly efficient cooking systems, in combination with programs for their dissemination [18, 19], could effect a far-reaching, short-term impact on the environment and the quality of life therein [20].

In order to achieve health and environmental benefits, cleaner-burning cookstoves than are currently in widespread use are needed [8, 21]. One type of cookstove that has been recognised as having great potential to achieve this goal is widely called a "gasifier stove" [22]. A process schematic diagram of a reverse downdraft gasifier stove is presented in Figure 1.1 (a background on gasification technologies is provided in Section 2.2.5). Its main features are a batch-fed solid fuel bed to which primary air is supplied from below and secondary air downstream of the bed. In this type of gasifier stove the thermochemical conversion of the solid fuel and the combustion of released products are separated through the staged provision of air. While nearly all cookstoves rely on natural convection to supply air for combustion, a pathway for the optimisation of gasifier type cookstoves stems from the potential for the simple integration of forced air. Indications have been found that gasifier stoves using a forced air supply achieve better control and more consistent conditions, with the potential to increase the stove's efficiency [23, 24]. The benefit of forced air over natural convection has not been clearly established to date.

In this specific type of gasifier stove, the fuel batch is lit on its top surface. This leads to the formation of a reaction front that moves opposite to the air flow down the fuel bed, which is called a reverse downdraft configuration. In the reaction front, producer gas is released from the solid biomass feedstock, leaving char as a solid product [25]. This combined production of producer gas and solid char in gasifier stoves is enabled by both the staged air supply and the batch-fed configuration,
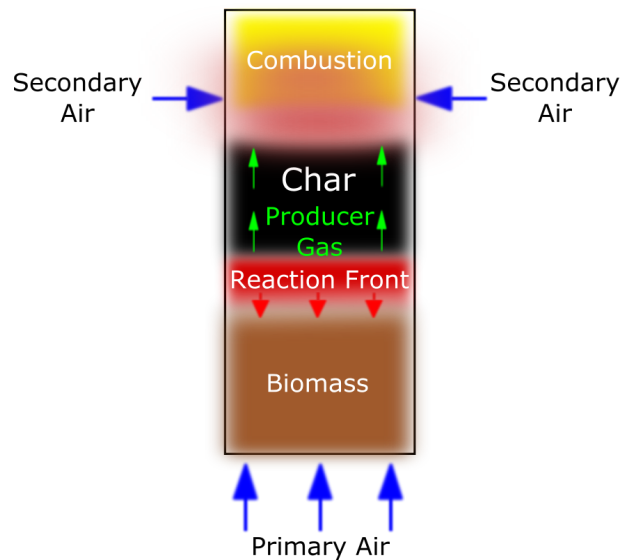
**Figure 1.1:** Process schematic diagram of reverse downdraft gasifier stoves.

which is a distinction from other types of cookstoves. The processes in the reaction front are sustained by heat released from partial oxidation with the limited air supply and is therefore called an autothermal process [26]. The conversion of the solid fuel in the reaction front is dependent on a multitude of parameters which are not fully understood, while the fuel composition and air supply are of central importance. In the reverse downdraft configuration, which is also called top-lit up-draft (TLUD), the producer gas propagates through a layer of the solid char before being combusted with the secondary air. In the char layer, tars (hydrocarbon compounds released from the conversion process) may decompose to combustible gases [27]. The influence of tar decomposition in the char layer on the composition of the released producer gas from the fixed bed is unclear. The combustion of the producer gas with secondary air occurs in a non-premixed jet flame downstream from the solid fuel bed. The produced solid char can be used as a subsequent energy source [28–30], as well as for soil amendment applications, where it is termed biochar [31]. Further understanding of the conversion and combustion processes is necessary to enable environmental and user health benefits.

Many different biomass fuels are used in cookstoves, including wood, agricultural residues and manures. Users may change their fuel source due to availability. Gathering or purchasing of fuel has a substantial impact on low income communities and a reduction in fuel consumption due to the higher efficiency of a stove could provide user benefits [32, 33]. Furthermore, the fuel composition, especially the moisture and ash content [34], can vary widely in between fuels. Optimisation of a particular combustion system for a multitude of solid fuels poses a particular challenge, which may be mitigated by a separation of the conversion and combustion processes, as is the case in gasifier cookstoves.

## 1.2 Aims

The goal of this thesis is to generate a deeper understanding of the fundamental thermochemical conversion processes within a solid fuel bed and the combustion process of the released products in a batch-fed autothermal reverse downdraft reactor. Particular focus is placed on its application in solid biomass-fuelled cookstoves. This thesis specifically aims to:

1. *Examine influences of the supply and distribution of air on the combustion processes.*

   The air supply is of central importance in gasifier cookstoves. The influence of the air supply on the conversion as well as the combustion processes has previously been identified [35–39], but many aspects remain unclear. The influence of the mode of air supply, via natural or forced draft, as well as the relationship between the primary and secondary air, is assessed here. The focus of this assessment is placed on measures that reduce emissions resulting from incomplete combustion.

2. *Investigate the impact of the air supply, the fuel type, and the bed geometry on*

*the autothermal thermochemical conversion process.*

Previous work has provided a basic understanding of the autothermal reverse downdraft solid fuel conversion process utilised in reverse downdraft gasifier cookstoves for a number of fuels [40–44]. The products of this process provide the fuel for the subsequent combustion process and the parameters that control their release require a more in-depth understanding. This is addressed by studying highly influential parameters, the air supply and type of fuel, as well as the heights of the fuel bed and their contribution to the release of products.

3. *Extend the understanding of the producer gas combustion process downstream of the fuel bed, particularly mechanisms that control the emissions.*

   The majority of studies in the literature on gasifier cookstoves focus on the overall combustion process and performance [35–38]. An analysis of the secondary combustion process in isolation, with prior knowledge of the products of the thermochemical conversion of the solid fuel, expands this previous body of work.

## 1.3 Thesis Outline

This research project was initiated by the author before the start of candidature and the preceding work can be found in Appendices A–C. Chapters 2 and 3 provide a background and a literature review tailored to the specific topics addressed in the four research articles in Chapters 4–7 of this thesis by publication. Chapter 4 is an extension of the study presented in Appendix A, with a focus on the air supply mode and the relationship between the primary and secondary air supplies in the system. Subsequent to these studies, the experimental facilities were upgraded. To ensure the validity of measurements taken in these facilities, a computational fluid dynamics (CFD) study was performed, with its main results presented in Appendix D. Furthermore, a new experimental reactor was designed and fabricated for the subse-

quent investigations. The new reactor enabled variation of the fuel bed depth, which is investigated in Chapter 5. Here, the ongoing processes in the fuel bed are scrutinised. In particular, the influence of an increasing char layer thickness, downstream of the reaction front, on subsequent reactions of released products is investigated. In Chapter 6, the thermochemical conversion process in the fuel bed remains a critical focus, concentrating on the influence of a variety of fuels and the influence of the ash content. Chapter 7 investigates the combustion process downstream of the fuel bed, with regard to previous results on the conversion process in the fixed bed, as well as to the composition of the combusted fuel. The results and implications of all the studies are concluded in Chapter 8.

## 1.4 References

[1] WEC, "World Energy Resources: 2013 survey," *World Energy Council*, 2013.

[2] IEA, *World Energy Balances 2018*. World Energy Balances, Paris: OECD Publishing, 2018.

[3] S. Bonjour, H. Adair-Rohani, J. Wolf, N. G. Bruce, S. Mehta, A. Prüss-Ustün, M. Lahiff, E. A. Rehfuess, V. Mishra, and K. R. Smith, "Solid fuel use for household cooking: Country and regional estimates for 1980-2010," *Environmental Health Perspectives*, vol. 121, no. 7, pp. 784–790, 2013.

[4] M. H. Secrest, J. J. Schauer, E. M. Carter, and J. Baumgartner, "Particulate matter chemical component concentrations and sources in settings of household solid fuel use," *Indoor Air*, vol. 27, no. 6, pp. 1052–1066, 2017.

[5] WHO, "Household air pollution and health - Fact sheet N 292," 2014.

[6] S. S. Lim, T. Vos, A. D. Flaxman, G. Danaei, K. Shibuya, and H. Adair-Rohani, "A comparative risk assessment of burden of disease and injury attributable to 67 risk factors and risk factor clusters in 21 regions, 1990-2010: A systematic analysis for the Global Burden of Disease Study 2010," *The Lancet*, vol. 380, pp. 2224–2260, 2012.

[7] S. Rajkumar, M. L. Clark, B. N. Young, M. L. Benka-Coker, A. M. Bachand, R. D. Brook, T. L. Nelson, J. Volckens, S. J. Reynolds, C. L'Orange, N. Good, K. Koehler, S. Africano, A. B. Osorto Pinel, and J. L. Peel, "Exposure to Household Air Pollution from Biomass-Burning Cookstoves and HbA1c and Diabetic Status among Honduran Women," *Indoor Air*, vol. 28, pp. 768–776, 2018.

[8] J. Baumgartner, K. R. Smith, and A. Chockalingam, "Reducing CVD through

improvements in household energy: Implications for policy-relevant research," *Global Heart*, vol. 7, no. 3, pp. 243–247, 2012.

[9] C. L'Orange, *The development of numerical tools for characterizing and quantifying biomass cookstove impact.* PhD thesis, Colorado State University, 2013.

[10] C. L'Orange, D. Leith, J. Volckens, and M. DeFoort, "A quantitative model of cookstove variability and field performance: Implications for sample size," *Biomass and Bioenergy*, vol. 72, pp. 233–241, 2015.

[11] Z. Zhang, Y. Zhang, Y. Zhou, R. Ahmad, C. Pemberton-Pigott, H. Annegarn, and R. Dong, "Systematic and conceptual errors in standards and protocols for thermal performance of biomass stoves," *Renewable and Sustainable Energy Reviews*, vol. 72, no. 17, pp. 1343–1354, 2017.

[12] Y. Zhang, C. Pemberton-Pigott, Z. Zhang, H. Ding, Y. Zhou, and R. Dong, "Key differences of performance test protocols for household biomass cookstove," in *Proceedings of the Twenty-Second Domestic Use of Energy*, (Cape Town), IEEE, 2014.

[13] N. A. MacCarty, D. Ogle, D. Still, T. C. Bond, C. Roden, and B. Willson, "Laboratory comparison of the global-warming potential of six categories of biomass cooking stoves," tech. rep., Aprovecho Research Center, 2007.

[14] N. A. MacCarty, D. Ogle, D. Still, T. Bond, and C. Roden, "A laboratory comparison of the global warming impact of five major types of biomass cooking stoves," *Energy for Sustainable Development*, vol. 12, no. 2, pp. 5–14, 2008.

[15] C. Garland, S. Delapena, R. Prasad, C. L'Orange, D. Alexander, and M. Johnson, "Black carbon cookstove emissions: A field assessment of 19 stove/fuel combinations," *Atmospheric Environment*, vol. 169, pp. 140–149, 2017.

[16] G. Saliba, R. Subramanian, K. Bilsback, C. L'Orange, J. Volckens, M. Johnson, and A. L. Robinson, "Aerosol Optical Properties and Climate Implications of Emissions from Traditional and Improved Cookstoves," *Environmental Science and Technology*, vol. 52, pp. 13647–13656, 2018.

[17] T. C. Bond, S. J. Doherty, D. W. Fahey, P. M. Forster, T. Berntsen, B. J. Deangelo, M. G. Flanner, S. Ghan, B. Kärcher, D. Koch, S. Kinne, Y. Kondo, P. K. Quinn, M. C. Sarofim, M. G. Schultz, M. Schulz, C. Venkataraman, H. Zhang, S. Zhang, N. Bellouin, S. K. Guttikunda, P. K. Hopke, M. Z. Jacobson, J. W. Kaiser, Z. Klimont, U. Lohmann, J. P. Schwarz, D. Shindell, T. Storelvmo, S. G. Warren, and C. S. Zender, "Bounding the role of black carbon in the climate system: A scientific assessment," *Journal of Geophysical Research: Atmospheres*, vol. 118, no. 11, pp. 5380–5552, 2013.

[18] B. Alberts, B. E. Robinson, and J. Baumgartner, "Cultivating a Demand for Clean Cookstoves," *Science - Letters*, vol. 334, pp. 1636–1637, 2011.

[19] E. T. Gall, E. M. Carter, C. M. Earnest, and B. Stephens, "Indoor Air Pollution in Developing Countries : Research and Implementation Needs for Improvements in Global Public Health," *American Journal of Public Health*, vol. 103, no. 4, pp. e1–e6, 2013.

[20] J. Agenbroad, M. DeFoort, A. Kirkpatrick, and C. Kreutzer, "A simplified model for understanding natural convection driven biomass cooking stoves—Part 1: Setup and baseline validation," *Energy for Sustainable Development*, vol. 15, no. 2, pp. 160–168, 2011.

[21] K. R. Smith, J. P. McCracken, M. W. Weber, A. Hubbard, A. Jenny, L. M. Thompson, J. Balmes, A. Diaz, B. Arana, and N. Bruce, "Effect of reduction in household air pollution on childhood pneumonia in Guatemala (RESPIRE): A randomised controlled trial," *The Lancet*, vol. 378, pp. 1717–1726, 2011.

[22] G. L. Simon, R. Bailis, J. Baumgartner, J. Hyman, and A. Laurent, "Current debates and future research needs in the clean cookstove sector," *Energy for Sustainable Development*, vol. 20, pp. 49–57, 2014.

[23] N. A. MacCarty, D. Still, and D. Ogle, "Fuel use and emissions performance of fifty cooking stoves in the laboratory and related benchmarks of performance," *Energy for Sustainable Development*, vol. 14, no. 3, pp. 161–171, 2010.

[24] Y. Zhang, Z. Zhang, Y. Zhou, and R. Dong, "The influences of various testing conditions on the Evaluation of household biomass pellet fuel combustion," *Energies*, vol. 11, no. 5, pp. 1131–1142, 2018.

[25] C. Roth, "Micro-gasification : cooking with gas from dry biomass," tech. rep., GIZ - Deutsche Gesellschaft fuer Internationale Zusammenarbeit, Eschborn, 2014.

[26] S. Karellas, "Production of Hydrogen from Renewable Resources," in *Biofuels and Biorefineries* (Z. Fang, ed.), vol. 5, ch. 4, pp. 97–117, Dordrecht: Springer, 2015.

[27] I. Haberle, Ø. Skreiberg, J. Łazar, and N. E. L. Haugen, "Numerical models for thermochemical degradation of thermally thick woody biomass, and their application in domestic wood heating appliances and grate furnaces," *Progress in Energy and Combustion Science*, vol. 63, pp. 204–252, 2017.

[28] M. Deng, J. Li, S. Zhang, M. Shan, J. Baumgartner, E. Carter, and X. Yang, "Real-time combustion rate of wood charcoal in the heating fire basin: Direct measurement and its correlation to CO emissions," *Environmental Pollution*, vol. 245, pp. 38–45, 2019.

[29] H. Abdullah and H. Wu, "Biochar as a Fuel: 1.1. Properties and Grindability

of Biochars Produced from the Pyrolysis of Mallee Wood under Slow-Heating Conditions," *Energy and Fuels*, vol. 23, no. 8, pp. 4174–4181, 2009.

[30] H. Abdullah, K. A. Mediaswanti, and H. Wu, "Biochar as a fuel: 2. Significant differences in fuel quality and ash properties of biochars from various biomass components of mallee trees," *Energy and Fuels*, vol. 24, no. 3, pp. 1972–1979, 2010.

[31] D. Woolf, J. Lehmann, E. M. Fisher, and L. T. Angenent, "Biofuels from pyrolysis in perspective: Trade-offs between energy yields and soil-carbon additions," *Environmental Science and Technology*, vol. 48, no. 11, pp. 6492–6499, 2014.

[32] N. G. Johnson and K. M. Bryden, "The impact of cookstove adoption and replacement on fuelwood savings," *Proceedings - 2012 IEEE Global Humanitarian Technology Conference*, pp. 387–391, 2012.

[33] N. G. Johnson and K. M. Bryden, "Energy supply and use in a rural West African village," *Energy*, vol. 43, no. 1, pp. 283–292, 2012.

[34] S. V. Vassilev, D. Baxter, L. K. Andersen, and C. G. Vassileva, "An overview of the chemical composition of biomass," *Fuel*, vol. 89, no. 5, pp. 913–933, 2010.

[35] T. B. Reed and R. Larson, "A wood-gas stove for developing countries," *Energy for Sustainable Development*, vol. 3, no. 2, pp. 34–37, 1996.

[36] T. Reed, R. Walt, S. Ellis, A. Das, and S. Deutch, "Superficial Velocity - The Key To Downdraft Gasification," in *4th Biomass Conference of the Americas*, (Oakland), 1999.

[37] S. Varunkumar, *Packed bed gasification-combustion in biomass based domestic stoves and combustion systems*. PhD thesis, Indian Institute of Science, 2012.

[38] J. Tryner, *Combustion Phenomena in Biomass Gasifier Cookstoves*. PhD thesis, Colorado State University, 2016.

[39] A. M. James R, *Simultaneous Biochar and Syngas Production in a Top-Lit Updraft Biomass Gasifier*. PhD thesis, North Carolina State University, 2015.

[40] J. Porteiro, D. Patiño, J. Collazo, E. Granada, J. Moran, and J. L. Miguez, "Experimental analysis of the ignition front propagation of several biomass fuels in a fixed-bed combustor," *Fuel*, vol. 89, no. 1, pp. 26–35, 2010.

[41] J. Porteiro, D. Patiño, J. Moran, and E. Granada, "Study of a fixed-bed biomass combustor: Influential parameters on ignition front propagation using parametric analysis," *Energy and Fuels*, vol. 24, no. 7, pp. 3890–3897, 2010.

[42] M. Fatehi and M. Kaviany, "Adiabatic reverse combustion in a packed bed," *Combustion and Flame*, vol. 99, pp. 1–17, 1994.

[43] M. Horttanainen, J. Saastamoinen, and P. Sarkomaa, "Operational limits of ignition front propagation against airflow in packed beds of different wood fuels," *Energy and Fuels*, vol. 16, no. 3, pp. 676–686, 2002.

[44] M. Rönnbäck, M. Axell, L. Gustavsson, H. Thunman, and B. Lecher, "Combustion processes in a biomass fuel bed - Experimental results," in *Progress in Thermochemical Biomass Conversion* (A. Bridgwater, ed.), ch. 59, pp. 743–757, Bodmin: Blackwell Science Ltd, 2001.

This page intentionally left mostly blank.

# Chapter 2

## Background

## 2.1 Solid Biomass Fuel

### 2.1.1 Definition and Composition

Solid biomass is a widely available fuel for combustion providing up to 90% of energy in certain regions [1] and can be utilised without further preparation. Biomass has been used for millennia [2] and with nearly half the world's population still relying on biomass-fuelled cookstoves [3] it remains likely to be the most widely used fuel. To understand the combustion behaviour of biomass, knowledge of its constituents and composition is essential.

Biomass, used as fuel for combustion processes, can be subdivided into six source groups: 1. Wood and woody biomass; 2. Herbaceous and agricultural biomass; 3. Aquatic biomass; 4. Animal and human biomass waste; 5. Contaminated biomass and industrial biomass waste (semi-biomass); and 6. Biomass mixtures [4]. In the present research, those fuels categorised as groups 1, 2 and 4 are of interest. Specifically, woody biomass, agricultural biomass and animal waste, are widely available for utilisation and are the focus of this research.

Both groups 1 and 2 can be further defined as lignocellulosic materials with the three main constituents being cellulose, hemicellulose and lignin. Cellulose is the carbohydrate that forms the structural framework of the plant [5]. Cellulose is a glucose polymer of recurring $C_6H_{10}O_5$ units, bonded by $\beta$-glycosidic linkages [5]. The $\beta$-glycosidic linkages form linear chains which are supported by hydrogen bonding, leading to high stability and resistance to breakage. Hemicellulose is a highly branched polymer consisting of five sugars ($C_5$: D-xylose and L-arabinose; $C_6$: D-galactose, D-glucose, and D-mannose) and uronic acid. Lignin has a polyphenolic, highly aromatic structure that stabilises cell walls and holds cells together [5]. Group 4, specifically animal manures, is much more heterogenous than those in groups 1 and 2, and can contain faeces, urine, bedding materials and waste feed, as well as

16

fermentation products [6]. Hydrocarbon compounds are the main constituents of all biomass, while it also contains minerals such as Na, P, Ca, and Fe, which are considered as the ash fraction [7].

The composition of the six biomass groups can be highly variable due to differences in the lignocellulose (excluding group 3), moisture, or ash content. Therefore, to classify the biomass composition further, proximate analyses (the determination of the moisture, volatile matter (VM), fixed carbon (FC), and ash content) and ultimate analyses (the determination of the elemental composition of C, H, N and often S) are widely performed. The volatile matter content is the fraction of the original fuel mass that evolves as gases and liquids, in the form of an aerosol, when the fuel is heated to high temperatures. The fixed carbon is the mass of carbon that remains after the volatiles have escaped and ash is the solid product after the carbon is oxidised. All three fractions and their yields are substantially influenced by the heating rate and process temperature, which determine not only the amount but also the physical characteristics of the resulting char [8]. Biomass fuels can also be classified by their heating value (energy content). Extensive databases of biomass compositions are available [9].

The atomic ratios of elements of different fuels can be displayed in a van Krevelen diagram, as shown in Figure 2.1. The atomic ratios of a fuel decrease as its geological age increases, which generally means that the older the fuel, the higher its energy content [7]. When looking at Figure 2.1, this includes a reduction of the O/C ratio. The heating value of a fuel rises also with the increasing H/C ratio, while this ratio decreases with geological age. It can be seen that biomass covers a very wide range of H/C and O/C ratios, and a case-by-case approach is necessary [10].

## 2.1.2 Fuels in Small-Scale Application

In small-scale applications, the utilised fuel is often determined by its local availability. Woody biomass is likely to be most widely used and the focus of a large
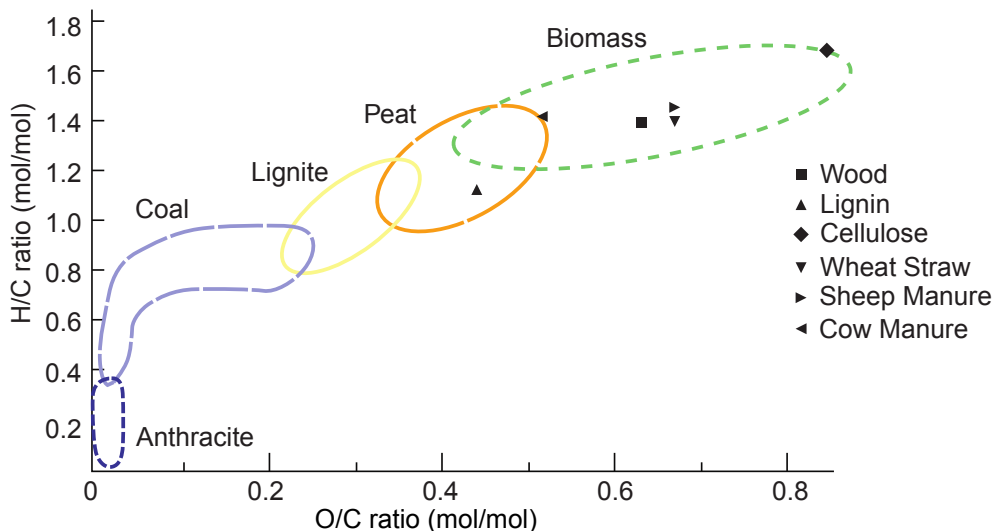
***Figure 2.1:*** The molar H/C ratio as a function of the molar O/C ratios of various solid hydrocarbon fuels in a van Krevelen diagram, adapted after [7].

proportion of combustion research [11]. However, the combustion properties of other biomass fuels have yet to be explored [12, 13]. In certain locations, for example India, agricultural residues and animal manures are used in large quantities as an energy source for domestic application [14, 15], but a relatively small number of investigations have focused on such fuels. Additional fuels utilised in small-scale applications include biomass such as straw [16, 17], husks [18], kernels [19] or manure [20–22].

Table 2.1 presents the structural composition of biomass fuels, with their three constituents: cellulose, hemicellulose and lignin. Most biomass can be classified as containing cellulose>hemicellulose>lignin, including woody biomass, as well as herbaceous and agricultural biomass (grasses, straws, stalks, fibres, shells/husks, residues) [4]. The composition of manures is largely influenced by diet, as well as methods of collection [23]. The decomposition of each structural lignocellulose component behaves differently when exposed to heat.

Table 2.2 presents the proximate and ultimate analyses of commonly used fuels. Although there are many significant differences between biomass fuels, the elemental

**Table 2.1:** Contents of structural components—cellulose, hemicellulose and lignin—of selected biomass on a dry basis (% g/g).

| Biomass | Cellulose | Hemicellulose | Lignin | Reference |
|---|---|---|---|---|
| Softwood | 30–50 | 10–40 | 15–30 | [24–26] |
| Hardwood | 40–75 | 10–40 | 15–25 | [24–26] |
| Wheat Straw | 30–31 | 28–50 | 15–16 | [26, 27] |
| Cattle Manure | 3.2 | 2.3 | 4.2 | [28] |

composition on a dry-ash-free basis of a multitude of biomass materials appears quite similar [4]. Wide variations in fuel composition, which can be noticed from the proximate analyses, mostly stem from variations in the ash and moisture contents.

**Table 2.2:** Proximate (db) and ultimate analyses (dab), and the higher heating value (MJ·kg$^{-1}$) of selected biomass fuels.

| Fuel | M | VM | FC | Ash | C | H | O | N | HHV | Reference |
|---|---|---|---|---|---|---|---|---|---|---|
| Wood | 20.0 | 82.0 | 17.0 | 1.0 | 51.6 | 6.3 | 41.5 | 0.1 | 20.2 | [25] |
| Wheat Straw | 7.8 | 74.6 | 18.5 | 6.8 | 49.2 | 5.8 | 44.0 | 0.6 | 16.3 | [27] |
| Cow Manure | 13.9 | 70.3 | 13.8 | 15.9 | 54.0 | 6.4 | 36.7 | 0.8 | 17.4 | [29] |
| Sheep Manure | 5.2 | 53.5 | 12.5 | 33.9 | 48.1 | 5.4 | 43.0 | 3.5 | 12.0 | [22] |

Apart from the composition, the biomass particle size is a very important parameter in combustion applications [30] and is mostly fuel specific. For example, wood is a solid, dense material ($\rho_{Bulk} = 200$–$500$ kg·m$^{-3}$) and can be formed into various sizes and shapes. Conversely, straws are hollow ($\rho_{Bulk} = 80$–$150$ kg·m$^{-3}$) and often only cut, but usually available in much smaller particle sizes than wood. Husks, pits or kernels are mostly combusted in their original form. Manures may be formed into hand-ball-size pellets. Pellets or briquettes can be fabricated to achieve a more homogeneous particle size, but the biomass feedstock also influences the ability with which and size into which pellets can be formed [31, 32]. When small particle sizes are coupled with low bulk density, for example in the case of rice husks or straw, larger combustion chamber sizes may be required. The use of varying biomass feedstock in any cookstove is still challenging and further understanding of the influencing

parameters is necessary to ensure efficient utilisation.

## 2.2 Thermochemical Conversion and Combustion of Biomass

### 2.2.1 Overview

Thermochemical decomposition of biomass involves a multitude of chemical species and reactions, which are interconnected. Its complexity stems not only from the heterogeneity of the fuel, but is also highly dependent on the process parameters, such as peak temperature, heating rate, or oxidiser availability, leading to wide ranges of product yields. Furthermore, the reactor-specific fluid dynamics and thermodynamics can play a determining role, adding difficulty to reactor designs and up-scaling; therefore, only the basics of the fundamental processes involved and their interplay in the thermochemical biomass conversion are identified. The fundamental processes are drying, pyrolysis, devolatilisation and gasification. In Figure 2.2 the basic subsequent processes in staged combustion are presented. As these fundamental processes may be defined differently in the literature, a short discussion of the use in this thesis is included.

### 2.2.2 Drying

All biomass include a fraction, and in many cases a substantial amount, of water. Untreated biomass can have a moisture content of up to 98% on a wet basis, in the case of sewage sludge [7], and more commonly values up to 60% for freshly harvested green woody biomass [33]. Drying is considered to occur at temperatures ≤100°C. In many applications, the feedstock is air-dried before introduction into the conversion reactor, as the drying process consumes large amounts of energy. A low moisture content is desired for most combustion processes.

20
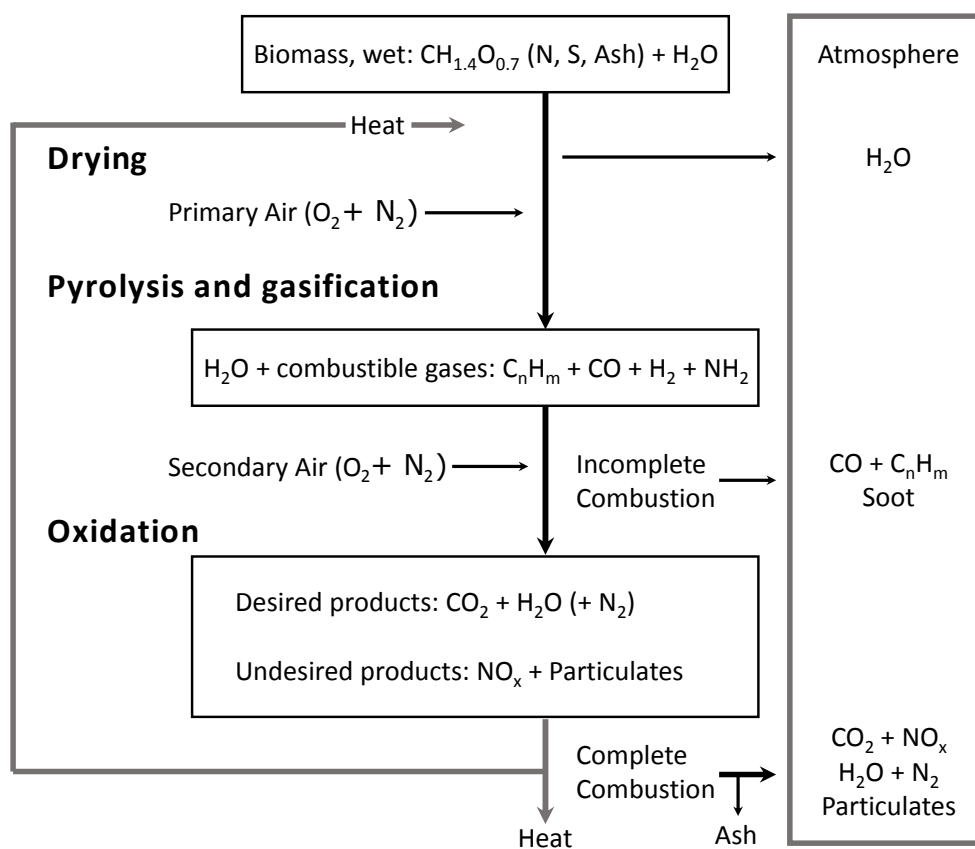
*Figure 2.2:* Overview of the thermochemical conversion and combustion of biomass in an air staged process, adapted after [12].

In gasifier stoves, irrespective of pre-drying of the fuel, additional drying occurs upstream of the reaction front. A higher moisture content of the fuel is linked to lower burning rates and reaction front velocities, due to the consumption of large amounts of energy by vaporisation [34]. In the present study, the influence of the moisture content is not the focus of attention and thus a similar moisture content is ensured for the investigated fuels.

## 2.2.3 Pyrolysis

Pyrolysis can be referred to as the thermochemical conversion of biomass, either in an inert environment [35, 36] or under sub-stoichiometric conditions [7, 37]. In

numerical models, pyrolysis is more clearly defined by reaction R1, which does not involve oxygen [38], as presented in Table 2.3, and this definition is adopted in this thesis. The three product fractions: gaseous, liquid, and solid are formed [39]. The yields of the different products depend on a multitude of factors, while peak temperatures and heating rates are of central importance [40].

**Table 2.3:** Simplified chemical reactions of the processes: pyrolysis, gasification, combustion and tar cracking/reforming [7, 41].

| | Reaction | |
|---|---|---|
| Pyrolysis | Biomass $\rightarrow C_n + C_xH_yO_z + CO_2 + CO + H_2 + CH_4 + H_2O$ | R1 |
| Heterogeneous gasification | $C + 0.5 \cdot O_2 \rightarrow CO$ | R2 |
| | $C + CO_2 \leftrightharpoons 2 \cdot CO$ | R3 |
| | $C + H_2O \leftrightharpoons CO + H_2$ | R4 |
| | $C + 2 \cdot H_2 \leftrightharpoons CH_4$ | R5 |
| | $2 \cdot C + H_2 \leftrightharpoons C_2H_2$ | R6 |
| Homogeneous gasification | $CO + 0.5 \cdot O_2 \rightarrow CO_2$ | R7 |
| | $CH_4 + 0.5 \cdot O_2 \rightarrow CO + 2 \cdot H_2$ | R8 |
| | $CO + H_2O \leftrightharpoons CO_2 + H_2$ | R9 |
| | $CO_2 + 3 \cdot H_2 \rightarrow CH_4 + H_2O$ | R10 |
| | $CH_4 + H_2O \leftrightharpoons CO + 3 \cdot H_2$ | R11 |
| | $2 \cdot CO + 2 \cdot H_2 \rightarrow CH_4 + CO_2$ | R12 |
| Combustion | $C_xH_y + (x + 0.5 \cdot y) \cdot O_2 \rightarrow CO_2 + H_2O$ | R13 |
| | $C + O_2 \rightarrow CO_2$ | R14 |
| | $H_2 + 0.5 \cdot O_2 \rightarrow H_2O$ | R15 |
| Tar Cracking | $C_xH_y \rightarrow C + C_nH_m + gases$ | R16 |
| Tar Reforming | $C_xH_y + x \cdot H_2O \rightarrow x \cdot CO + (n + 0.5 \cdot m) \cdot H_2$ | R17 |
| | $C_xH_y + x \cdot CO_2 \rightarrow 2 \cdot x \cdot CO + (0.5 \cdot y) \cdot H_2$ | R18 |
| | $C_xH_y + 2 \cdot x \cdot H_2O \rightarrow x \cdot CO_2 + (0.5 \cdot y + 2 \cdot x) \cdot H_2$ | R19 |

The pyrolysis process is most commonly divided into slow, intermediate and fast pyrolysis, based on the thermal environment, leading to different distributions of the product fractions [7]. Under fast pyrolysis conditions, the fine biomass—particle size in the millimetre range—is heated at high rates, of approximately 1000°C/s, to reaction temperatures of >400°C, with vapour residence times of 0.5–2 s. High cooling rates are employed to reduce thermal post-decomposition to achieve liquid production of up to 75%. Intermediate pyrolysis occurs at heating rates of 100–

500°C/min of coarser materials of several 10 millimetres in size, with a particle residence time <10 min at a temperature of ≈350–550°C. The vapour residence time is ≈2–4 s and high cooling rates are employed to achieve a ≈55% liquid fraction. Slow pyrolysis can use whole, log-size fuel, with residence times of hours or even weeks, at heating rates of several °C/min, leading to a nearly even distribution between the char, liquid and gaseous products [35]. Boundaries and definitions of the above-mentioned divisions of pyrolysis vary in the literature and further divisions such as flash, intermediate or vacuum pyrolysis [5] are often included, but these are of less importance here.

In the fuel bed of gasifier stoves, pyrolysis occurs once the drying process is concluded and the temperature increases further. The heating rate is in the range of intermediate pyrolysis and peak reaction temperatures are generally >600°C. As the reaction front is only a thin region, the vapour residence time is very short and thus conditions in between fast and intermediate pyrolysis are present. These conditions will lead to thermochemical conversion with a presumably high prevalence of liquid products.

## 2.2.4 Devolatilisation

Devolatilisation is the release of volatile matter from a solid fuel. This term is often not clearly defined, as it appears to be expected to be self-explanatory and is widely used interchangeably with the term pyrolysis [42, 43]. The distinction made in terms of pyrolysis in this thesis is based on the availability of oxygen, a definition that is widely accepted [44]. When a limited amount of the oxidiser is present, partial gasification (R2–R12; refer to Table 2.3), and partial combustion (R13–R15) of the products can occur simultaneously to the pyrolysis (R1) of the feedstock. Devolatilisation then describes the concurrent occurrence of multiple processes with the dominant one being the thermochemical conversion of the feedstock via pyrolysis (R1). Therefore, in this thesis, pyrolysis is considered a subset of devolatilisation.

The products released from devolatilisation are a complex composition of volatile products: a mixture of gases and tars, termed producer gas.

### 2.2.5 Gasification

Gasification is the thermochemical conversion of a solid carbonaceous feedstock into primarily gaseous products. The most basic chemical reactions involved are the heterogeneous reactions of the oxidiser with the solid carbon (R2–R5), as well as homogeneous gas phase reactions (R6–R11) [45]. Extensive research on gasification technology has previously been published [7, 42, 46]. The literature on gasification technologies is mainly focused on coal as the fuel, due to its wider application, while here the focus is on the conversion of biomass.

The term gasification is widely used for any process where an oxidiser is added to a solid fuel to produce gases and liquids. Traditionally it was established for the conversion of coal by limited addition of air, steam or a mixture of air and steam, to generate a producer gas mainly containing CO as a combustible species. When fuels with a higher volatile matter content are being used, pyrolysis and the production of liquid products increases, making it more difficult to create a clean product gas, but simultaneously enabling alternative applications. As the product composition is not only feedstock, but also reactor design dependent, the term gasification is often used in conjunction with the reactor type and the air supply. Reactor types can be distinguished between batch-fed systems, mainly fixed-bed gasification, and continuously-fed systems, including fixed-bed, moving-bed, fluidised bed and entrained flow gasification [47]. The air supply is then further refined: for example, for fixed-bed gasification, it can be up-draft, downdraft or cross-draft. The processes within the solid fuel bed in gasifier stoves can be compared most closely with those in fixed-bed downdraft gasification, because devolatilisation products move through a layer of produced char. Therefore, although the primary air supply moves upwards (updraft), the processes in gasifier stoves are widely called reverse downdraft.

The advantages of downdraft gasification are a comparatively low tar content in the producer gas, the relative simplicity of the process and low cost operation [45].

In the literature, cookstoves using the described process (refer to Section 1.1) are widely called gasifier [48, 49], semi-gasifier [50–53] or micro-gasifier [54] cookstoves. One main difference is that in reverse downdraft gasifier cookstoves the oxidiser is supplied directly to the reaction front where devolatilisation of the fuel occurs, while in downdraft gasifiers, air is supplied to the produced solid char and pyrolysis occurs upstream of the air supply. In gasifier cookstoves this leads to two subsequent processes, separated in time and location. First, the devolatilisation of the supplied fuel to form gases, liquids and char, and second, the gasification of the produced char. It could be argued that only the second process, where the conversion of the char occurs, would be classified as gasification. Therefore, especially when char is seen as a solid product, gasification of the produced char may only play a secondary role in the conversion process—hence the name "gasifier stoves" may be a misnomer.

### 2.2.6 Combustion

Combustion refers to the complete oxidation of chemical species, involving a multitude of chemical reactions. The most basic chemical reactions of the combustion of hydrocarbon compounds are R13–R15, in Table 2.3, with more detailed descriptions provided elsewhere [8, 55, 56].

Combustion can occur in many forms, from explosion [8], with high localised heat release, to flameless combustion [57–59], with more homogeneously distributed reactions and heat release. In gasifier stoves, two main forms of combustion are present at different locations: (1) Within the fuel bed, the thermochemical conversion process is sustained by partial oxidation of the released products, which can be referred to as smouldering combustion; (2) Downstream of the fuel bed, the released aerosol is burned in a non-premixed laminar jet flame.

Smouldering combustion involves the same chemical reactions as gasification and

the main difference is that gasification occurs in a specifically designed reactor, while smouldering combustion is generally uncontrolled in oxygen vitiated locations in the open environment, mainly seen in forest or building fires [60–62]. As these reactions occur in a controlled environment in gasifier stoves, they will be referred to as gasification or partial oxidation.

In non-premixed laminar flames, mixing of fuel with the oxidiser, here air, occurs in the combustion region. Such flames exhibit the entire range of mixture fractions from pure air to pure fuel, including fuel lean to fuel rich combustion, respectively, whilst the highest temperatures are achieved where stoichiometric combustion occurs [63]. The complexity of this kind of flame is exacerbated by the wide range of compounds included in the fuel, which will be discussed subsequently in more detail.

### 2.2.7 Discussion

The complexity of the interplay of the process pyrolysis, devolatilisation, gasification and combustion in application is reflected by the difficulty in forming clear differentiation of these processes. The phenomenon of the moving reaction front, in the gasifier stoves, has been described as stratification and stratified gasification [38, 64–66]. If char is a product of the process, as stated in Section 2.2.5, technically gasification reactions do not contribute substantially to the process and the term gasification could be misleading. Additionally, the term oxidative pyrolysis is widely used for conditions as found in this reaction front, where pyrolysis occurs while oxygen is available [24, 67–70]. The term oxidative pyrolysis appears to refer to the simultaneous occurrence of pyrolysis and further oxidising reactions of released products within the reaction front. In cookstove-specific literature, the term migrating pyrolytic front [71] can also be found as a synonym for the reaction front. In this thesis, the term devolatilisation will be used in preference for the conversion process in the reaction front. When referring to pyrolysis, gasification or combustion, the definitions based on the chemical reactions in Table 2.3 are used. A clearer definition and a deeper

understanding of the interconnection between these processes in gasifier stoves is of importance to the development of more efficient cookstoves and is a goal of this thesis.

## 2.3 References

[1] R. B. Gupta and A. Demirbas, *Gasoline, Diesel, and Ethanol Biofuels from Grasses and Plants.* Cambridge University Press, 2010.

[2] R. L. Youngs and M. F. Hamza, *Encyclopedia of Materials: Science and Technology.* Elsevier Ltd, second ed., 2001.

[3] S. Bonjour, H. Adair-Rohani, J. Wolf, N. G. Bruce, S. Mehta, A. Prüss-Ustün, M. Lahiff, E. A. Rehfuess, V. Mishra, and K. R. Smith, "Solid fuel use for household cooking: Country and regional estimates for 1980-2010," *Environmental Health Perspectives*, vol. 121, no. 7, pp. 784–790, 2013.

[4] S. V. Vassilev, D. Baxter, L. K. Andersen, C. G. Vassileva, and T. J. Morgan, "An overview of the organic and inorganic phase composition of biomass," *Fuel*, vol. 94, pp. 1–33, 2012.

[5] K. K. Pant and P. Mohanty, "Biomass , Conversion Routes and Products - An Overview," in *Transformation of Biomass: Theory to Practice* (A. Hornung, ed.), ch. 1, New York: Wiley & Sons Inc., 2014.

[6] Z. He and H. Zhang, eds., *Applied Manure and Nutrient Chemistry for Sustainable Agriculture and Environment.* Dordrecht: Springer, 2014.

[7] P. Basu, *Biomass Gasification and Pyrolysis and Torrefaction.* Elsevier, second ed., 2013.

[8] I. Glassman, R. A. Yetter, and N. G. Glumac, "Environmental combustion considerations," in *Combustion*, ch. 8, pp. 393–475, Elsevier, fifth ed., 2015.

[9] ECN, "Database for biomass and waste," in *https://phyllis.nl/*, Accessed: Feb., 2019.

[10] M. L. de Souza-Santos, "Solid Fuels," in *Solid Fuels Combustion and Gasification - Modeling, Simulation, and Equipment Operations*, vol. 42, ch. 2, pp. 86–92, Boca Raton: CRC Press, second ed., 2010.

[11] S. D. Fernandes, N. M. Trautmann, D. G. Streets, C. A. Roden, and T. C. Bond, "Global biofuel use , 1850 - 2000," *Global Biogeochemical Cycles*, vol. 21, pp. 1–15, 2007.

[12] M. Kaltschmitt and H. Hartmann, *Energie aus Biomasse.* Springer, second ed., 2009.

[13] L. Han, X. Wang, H. Spiertz, L. Yang, Y. Zhou, J. Liu, and G. Xie, "Spatio-Temporal Availability of Field Crop Residues for Biofuel Production in Northwest and Southwest China," *Bioenergy Research*, vol. 8, no. 1, pp. 402–414, 2015.

[14] H. S. Mukunda, S. Dasappa, P. J. Paul, N. K. S. Rajan, M. Yagnaraman, D. Ravi Kumar, and M. Deogaonkar, "Gasifier stoves – science, technology and field outreach," *Current Science*, vol. 98, no. 5, pp. 627–638, 2010.

[15] A. Pandey, S. Patel, S. Pervez, S. Tiwari, G. Yadama, J. Chow, J. Watson, P. Biswas, and R. Chakrabarty, "Aerosol emissions factors from traditional biomass cookstoves in India: Insights from field measurements," *Atmospheric Chemistry and Physics*, vol. 17, no. 22, pp. 13721–13729, 2017.

[16] G. Chen, K. Gao, B. Yan, Z. Dan, W. Zhou, and Z. Cheng, "Estimation and emissions from crop straw and animal dung in Tibet," *Science of the Total Environment*, vol. 631-632, pp. 1035–1045, 2018.

[17] S. Wei, G. Shen, Y. Zhang, M. Xue, H. Xie, P. Lin, Y. Chen, X. Wang, and S. Tao, "Field measurement on the emissions of PM, OC, EC and PAHs from

indoor crop straw burning in rural China," *Environmental Pollution*, vol. 184, pp. 18–24, 2014.

[18] A. T. Belonio, "Rice husk gas stove handbook," tech. rep., Appropriate Technology Center, Central Philippine University, 2005.

[19] A. A. Ahmad, N. A. Zawawi, F. H. Kasim, A. Inayat, and A. Khasri, "Assessing the gasification performance of biomass: A review on biomass gasification process conditions, optimization and economic evaluation," *Renewable and Sustainable Energy Reviews*, vol. 53, pp. 1333–1347, 2016.

[20] S. Anderson and E.-Y. Fusun, "Fuel Fodder and Faeces : An Ethnographic and Botanical Study of Dung Fuel Use in Central Anatolia," *Environmental Archaeology*, vol. 1, pp. 99–109, 1998.

[21] C. Birzer, P. Medwell, G. MacFarlane, M. Read, J. Wilkey, M. Higgins, and T. West, "A biochar-producing, dung-burning cookstove for humanitarian purposes," *Procedia Engineering*, vol. 78, pp. 243–249, 2014.

[22] A. Vakát, V. Krepl, and J. Kára, "Animal dung as a Source of Energy in Remote Areas of Indian Himalayas," *Agricultura Tropica et Subtropica*, vol. 43, no. 2, pp. 140–142, 2010.

[23] L. P. White and L. G. Plaskett, *Biomass as Fuel*. London: Acedemic Press, 1981.

[24] J. M. Jones, A. R. Lea-Langton, L. Ma, M. Pourkashanian, and A. Williams, *Pollutants Generated by the Combustion of Solid Biomass Fuels*. London: Springer, 2014.

[25] P. McKendry, "Energy production from biomass (part 1): overview of biomass," *Bioresource Technology*, vol. 83, no. 1, pp. 37–46, 2002.

[26] J. Heinonen and T. Sainio, "Chromatographic Fractionation of Lignocellulosic Hydrolysates," in *Advances in Chemical Engineering*, vol. 42, pp. 261–349, Elsevier Inc., 1 ed., 2013.

[27] K. Raveendran, A. Ganesh, and K. C. Khilar, "Influence of mineral matter on biomass pyrolysis characteristics," *Fuel*, vol. 74, no. 12, pp. 1812–1822, 1995.

[28] S. Prasad, A. Singh, and H. C. Joshi, "Ethanol as an alternative fuel from agricultural, industrial and urban residues," *Resources, Conservation and Recycling*, vol. 50, no. 1, pp. 1–39, 2007.

[29] A. Williams, J. Jones, L. Ma, and M. Pourkashanian, "Pollutants from the combustion of solid biomass fuels," *Progress in Energy and Combustion Science*, vol. 38, no. 2, pp. 113–137, 2012.

[30] H. Lu, E. Ip, J. Scott, P. Foster, M. Vickers, and L. L. Baxter, "Effects of particle shape and size on devolatilization of biomass particle," *Fuel*, vol. 89, no. 5, pp. 1156–1168, 2010.

[31] S. Döring, *Power from Pellets*. Berlin: Springer, 2013.

[32] Y. Zhou, Z. Zhang, Y. Zhang, Y. Wang, Y. Yu, F. Ji, R. Ahmad, and R. Dong, "A comprehensive review on densified solid biofuel industry in China," *Renewable and Sustainable Energy Reviews*, vol. 54, no. 17, pp. 1412–1428, 2016.

[33] E. Alakangas, *Biomass and agricultural residues for energy generation*. Elsevier Ltd, 2015.

[34] H. Yibo, H. Li, X. Chen, C. Xue, C. Chen, and G. Liu, "Effects of moisture content in fuel on thermal performance and emission of biomass semi-gasified cookstove," *Energy for Sustainable Development*, vol. 21, no. 1, pp. 60–65, 2014.

[35] A. Hornung, "Pyrolysis," in *Transformation of Biomass: Theory to Practice*, ch. 4, Wiley & Sons, Ltd, first ed., 2014.

[36] S. C. Moldoveanu, "The Chemistry of the Pyrolytic Process," in *Techniques and Instrumentation in Analytical Chemistry*, ch. 2, pp. 7–48, Elsevier B.V., 2010.

[37] D. Mohan, C. U. Pittman, and P. H. Steele, "Pyrolysis of Wood / Biomass for Bio-oil : A Critical Review," *Energy and Fuels*, vol. 20, no. 4, pp. 848–889, 2006.

[38] C. Di Blasi and C. Branca, "Modeling a stratified downdraft wood gasifier with primary and secondary air entry," *Fuel*, vol. 104, pp. 847–860, 2013.

[39] US Department of Energy, "Bioenergy," in *Bioenergy* (A. Dahiya, ed.), pp. 41–52, Elsevier Inc., 2015.

[40] L. Fagbemi, L. Khezami, and R. Capart, "Pyrolysis products from different biomasses," *Applied Energy*, vol. 69, no. 4, pp. 293–306, 2001.

[41] Y. Shen, "Chars as carbonaceous adsorbents/catalysts for tar elimination during biomass pyrolysis or gasification," *Renewable and Sustainable Energy Reviews*, vol. 43, pp. 281–295, 2015.

[42] C. Higman and M. Van der Burgt, *Gasification*. Elsevier Inc., 2008.

[43] Z. Tan, *Air Pollution and Greenhouse Gases - From Basic Concepts to Engineering Applications for Air Emission Control*. Singapore: Springer, 2014.

[44] F. Battin-Leclerc, J. M. Simmie, and E. Blurock, *Cleaner Combustion - Developing Detailed Chemical Kinetic Models*. London: Springer, 2013.

[45] J. G. Speight, *Gasification of Unconventional Feedstock*. Laramie: Elsevier Inc., 2014.

[46] T. Reed and A. Das, "Handbook of Biomass Downdraft Gasifier Engine Systems," tech. rep., Solar Energy Research Institute, Golden, 1988.

32

[47] M. Grabner, "Gasification of Solids: Past, Present, and Future," in *Gasification Processes: Modeling and Simulation* (P. A. Nikrityuk and B. Meyer, eds.), pp. 29–42, Weinheim: Wiley-VCH Verlag GmbH & Co. KG, 2014.

[48] S. K. Babar and P. Karve, "Natural draft gasifier water heater for rural households," *Boiling Point*, no. 57, pp. 37–39, 2009.

[49] E. M. Carter, M. Shan, X. Yang, J. Li, and J. Baumgartner, "Pollutant emissions and energy efficiency of chinese gasifier cooking stoves and implications for future intervention studies," *Environmental Science and Technology*, vol. 48, no. 11, pp. 6461–6467, 2014.

[50] Y. Chen, G. Shen, S. Su, W. Du, Y. Huangfu, G. Liu, X. Wang, B. Xing, K. R. Smith, and S. Tao, "Efficiencies and pollutant emissions from forced-draft biomass-pellet semi-gasifier stoves: Comparison of International and Chinese water boiling test protocols," *Energy for Sustainable Development*, vol. 32, pp. 22–30, 2016.

[51] J. Tryner, J. W. Tillotson, M. E. Baumgardner, J. T. Mohr, M. W. Defoort, and A. J. Marchese, "The Effects of Air Flow Rates, Secondary Air Inlet Geometry, Fuel Type, and Operating Mode on the Performance of Gasifier Cookstoves," *Environmental Science and Technology*, vol. 50, no. 17, pp. 9754–9763, 2016.

[52] J. Tryner, J. Volckens, and A. J. Marchese, "Effects of operational mode on particle size and number emissions from a biomass gasifier cookstove," *Aerosol Science and Technology*, vol. 52, no. 1, pp. 87–97, 2018.

[53] J. Tryner, B. D. Willson, and A. J. Marchese, "The effects of fuel type and stove design on emissions and efficiency of natural-draft semi-gasifier biomass cookstoves," *Energy for Sustainable Development*, vol. 23, pp. 99–109, 2014.

[54] D. Sakthivadivel and S. Iniyan, "Combustion characteristics of biomass fuels in a fixed bed micro-gasifier cook stove," *Journal of Mechanical Science and Technology*, vol. 31, no. 2, pp. 995–1002, 2017.

[55] T. C. Lieuwen, V. Yang, and R. A. Yetter, eds., *Synthesis Gas.* Boca Raton: Taylor & Francis, 2009.

[56] E. Ranzi, A. Frassoldati, R. Grana, A. Cuoci, T. Faravelli, A. P. Kelley, and C. K. Law, "Hierarchical and comparative kinetic modeling of laminar flame speeds of hydrocarbon and oxygenated fuels," *Progress in Energy and Combustion Science*, vol. 38, no. 4, pp. 468–501, 2012.

[57] M. J. Evans, P. R. Medwell, H. Wu, A. Stagni, M. Ihme, I. Chimica, and P. Milano, "Classification and lift-off height prediction of non-premixed MILD and autoignitive flames," *Proceedings of the Combustion Institute*, vol. 36, pp. 4297–4304, 2017.

[58] J. Ye, P. R. Medwell, B. B. Dally, and M. J. Evans, "The transition of ethanol flames from conventional to MILD combustion," *Combustion and Flame*, vol. 171, pp. 173–184, 2016.

[59] J. Ye, P. R. Medwell, E. Varea, S. Kruse, B. B. Dally, and H. G. Pitsch, "An experimental study on MILD combustion of prevaporised liquid fuels," *Applied Energy*, vol. 151, pp. 93–101, 2015.

[60] H. Ohtani, T. Maejima, and Y. Uehara, "In-Situ Heat Release Measurement Of Smoldering Combustion Of Wood Sawdust," *Fire Safety Science*, vol. 3, pp. 557–564, 1991.

[61] H. Wang, P. J. Van Eyk, P. R. Medwell, C. H. Birzer, Z. F. Tian, and M. Possell, "Identification and Quantitative Analysis of Smoldering and Flaming Combustion of Radiata Pine," *Energy and Fuels*, vol. 30, no. 9, pp. 7666–7677, 2016.

[62] H. Wang, P. J. van Eyk, P. R. Medwell, C. H. Birzer, Z. F. Tian, and M. Possell, "Effects of Oxygen Concentration on Radiation-Aided and Self-sustained Smoldering Combustion of Radiata Pine," *Energy and Fuels*, vol. 31, no. 8, pp. 8619–8630, 2017.

[63] J. Warnatz, U. Maas, and R. W. Dibble, *Combustion: Physical and chemical fundamentals, modeling and simulation, experiments, pollutant formation*. Berlin: Springer, fourth ed., 2006.

[64] M. Barrio, M. Fossum, and J. E. Hustad, "A Small-Scale Stratified Downdraft Gasifier Coupled to a Gas Engine for Combined Heat and Power Production," in *Progress in Thermochemical Biomass Conversion* (A. Bridgwater, ed.), pp. 426–440, Bodmin: Blackwell Science Ltd, 2001.

[65] G. Gautam, S. Adhikari, S. Thangalazhy-Gopakumar, C. Brodbeck, S. Bhavnani, and S. Taylor, "Tar analysis in syngas derived from pelletized biomass in a commercial stratified downdraft gasifier," *BioResources*, vol. 6, no. 4, pp. 4652–4661, 2011.

[66] T. B. Reed, B. Levie, and M. S. Graboski, "Fundamentals, Development and Scaleup of the Air-Oxygen Stratified Downdraft Gasifier," tech. rep., Solar Energy Research Institute, Golden, 1988.

[67] E. M. Fitzpatrick, J. M. Jones, M. Pourkashanian, A. B. Ross, A. Williams, and K. D. Bartle, "Mechanistic Aspects of Soot Formation from the Combustion of Pine Wood," *Energy and Fuels*, vol. 22, pp. 3771–3778, 2008.

[68] D. J. Hautman, F. L. Dryer, K. P. Schug, and I. Glassman, "A Multiple-step Overall Kinetic Mechanism for the Oxidation of Hydrocarbons," *Combustion Science and Technology*, vol. 25, no. 5-6, pp. 219–235, 1981.

[69] C. S. McEnally, L. D. Pfefferle, B. Atakan, and K. Kohse-Höinghaus, "Studies of aromatic hydrocarbon formation mechanisms in flames: Progress towards closing the fuel gap," *Progress in Energy and Combustion Science*, vol. 32, no. 3, pp. 247–294, 2006.

[70] S. Varunkumar, N. K. S. Rajan, and H. S. Mukunda, "Single Particle and Packed Bed Combustion in Modern Gasifier Stoves - Density Effects," *Combustion Science and Technology*, vol. 183, no. 11, pp. 1147–1163, 2011.

[71] C. Roth, "Micro-gasification : cooking with gas from dry biomass," tech. rep., GIZ - Deutsche Gesellschaft fuer Internationale Zusammenarbeit, Eschborn, 2014.

# Chapter 3

## Literature Review

# 3.1 Thermochemical Conversion

## 3.1.1 Process Description

In an autothermal reverse downdraft process, air is supplied to a fuel bed from below. To start the thermochemical conversion, a kindling material is supplied to the top surface of the fuel, leading to the incineration of the top layer and the formation of a reaction front that propagates opposite the air flow down the bed [1], as presented in Figure 1.1. With increasing air mass flux ($\varphi_A$), three subsequent regimes have been identified, as presented in Figure 3.1: (1) the oxygen-limited regime, where the fuel conversion increases nearly linearly up to $\varphi_{F1}$ with the air supply $< \varphi_{A1}$; (2) the reaction-limited regime, between $\varphi_{A1}$ and $\varphi_{A2}$, where a further increase of the air supply leads to a stagnation of the fuel conversion increase, between $\varphi_{F1}$ and $\varphi_{F2}$ and; (3) the regime where the fuel conversion is reduced due to cooling by convection, at $> \varphi_{A2}$, finally leading to extinction at $\varphi_{A3}$ [2–4]. These regimes, with different terminology of classification, can be found elsewhere [5–7]. In gasifier cookstoves, generally, low air supply rates are employed, within the oxygen limited regime, allowing for variations in the fuel consumption rates and the linked heat release by adjusting the air supply rate.

Especially in the oxygen-limited regime, the air supply has a defining influence on the fuel conversion, and many related parameters, such as the process temperature, the reaction front velocity and product composition [8]. The thermochemical conversion process is also dependent on a multitude of other input parameters, as follows: Smaller fuel particle sizes have been shown to increase the internal heat transfer in the bed due to a higher bed porosity [2, 5] and thus achieve higher reaction front propagation rates [5, 6]. A larger particle size leads to lower peak temperatures in the reaction front, but a wider range of air supply rates, before the process is cooled by convection [5, 6]. An increasing moisture content in the fuel has been shown to
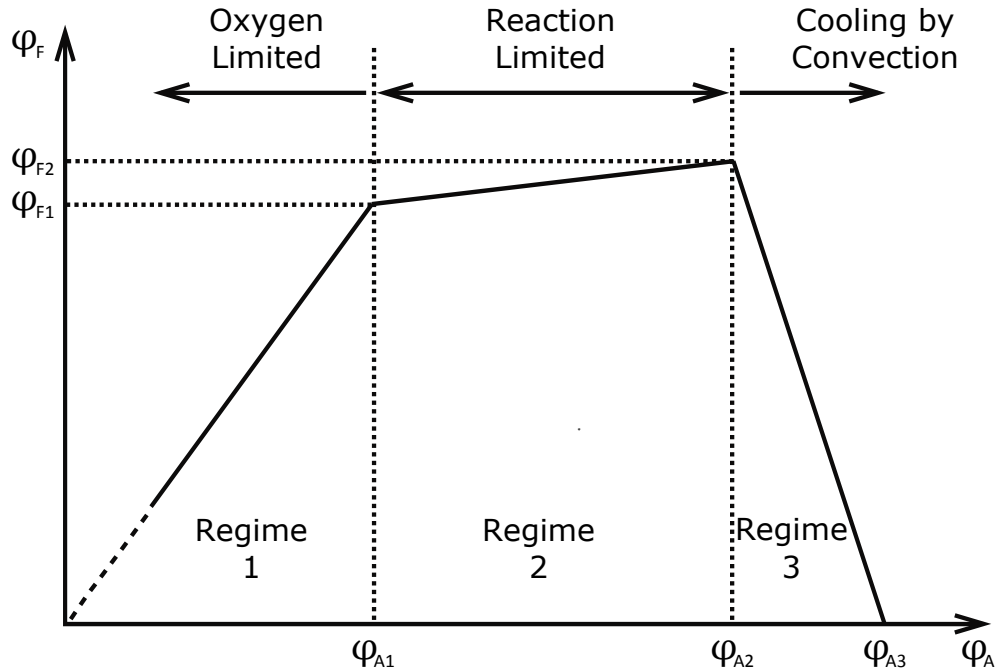
***Figure 3.1:*** Fuel consumption mass flux, $\varphi_F$ $(\text{kg}_{fuel}\cdot\text{m}^{-2}\text{s}^{-1})$, behaviour in the batch-fed reverse downdraft process as a function of the air mass flux, $\varphi_A$ $(\text{kg}_{air}\cdot\text{m}^{-2}\text{s}^{-1})$, adapted after [3].

influence the heat transfer [9], reduce the propagation rate and the reaction front thickness [10]. Greater moisture contents also extends the applicable air supply range and increases the char reactivity [10]. An increasing fuel ash content, up to 13% (g/g), has been shown to influence the fuel consumption and propagation rate of the reaction front [2]. Further impacts on the reaction front, especially from high ash content biomass fuels, such as manures, have yet to be investigated.

With a limited air supply, devolatilisation of the solid fuel in the reaction front (refer to Section 2.2.4) leads to a multitude of products, which can be divided into the three states: (1) a wide variety of gases (CO, $CO_2$, $H_2$, $CH_4$ $C_2H_2$, $C_2H_4$, $C_2H_6$, etc.) [11]; (2) liquid tars and water [12]; and (3) solid char (mainly carbon and ash) [13] (as described in Section 2.2).

### 3.1.2 Gaseous Products

The concentration of each gaseous product is dependent on a multitude of influences, including the type of feedstock, the elemental and chemical composition of the feedstock, the gasifying agent and its availability, as well as the kinetics of chemical reactions under specific process conditions [14]. Gaseous products are mainly produced within the reaction front, but can also be formed through the degradation of tars within the char layer downstream of the reaction front, which will be discussed in more detail in Section 3.1.3.2.

A wide range of the producer gas compositions can be found from gasifier stoves. Reported concentrations of mainly $CO$, $CO_2$, $CH_4$, $O_2$ and $H_2$ for a variety of fuels [15, 16] are presented in Table 3.1 [17–20]. The $N_2$ concentration is typically >50% and the producer gas heating value is in the range 3–6 MJ·m$^{-3}$. A deeper understanding of the decisive parameters that lead to the production of certain gases would be beneficial to enable an *a priori* prediction of the producer gas composition.

***Table 3.1:*** Producer gas compositions from gasifier stoves using a variety of fuels. Gas concentrations are provided on a molar basis.

| Fuel | $T_{Bed}$ (°C) | $H_2$ | CO | $CH_4$ | $CO_2$ | $O_2$ | Tar | |
|---|---|---|---|---|---|---|---|---|
| Wood chips | 723–933 | 1.6–7.5 | 8–13 | 1.5–2.5 | 18–20 | 0.8–2.8 | - | [17] |
| Corn cob chips | 600 | 0–2 | 9–12 | 0–1.5 | 12–20 | 0–5 | - | [18] |
| Eucalyptus chips | 750 | 0–4 | 8–21 | 0–3 | 8–15 | 0–8 | - | [18] |
| Douglas fir chips | 700 | 2–7 | 8–17 | 0–2 | 9–14 | 0–7 | - | [18] |
| Lodgepole pine pellets | 800 | 9–11 | 14–16 | 2 | 10–15 | 0–5 | - | [18] |
| Rice hulls | 700–850 | 2.8–4.4 | 14–16 | - | 12–13 | - | 3–17 (g/m$^3$) | [19] |
| Wood chips | 650–850 | 3.3–6.6 | 14–15 | - | 13–14 | - | 10–90 (g/m$^3$) | [19] |
| Wood chips | 700 | 13.8 | 17.6 | 4.1 | 16 | - | 8.5 (wt%) | [20] |

### 3.1.3 Liquid Products

#### 3.1.3.1 Tars from Biomass Conversion

The liquid product fraction from biomass decomposition consists of tars and water. Tar generally refers to a wide range of hydrocarbon compounds and many definitions, such as "all organic compounds with a molecular weight larger than benzene (excluding soot and char)" [21] exist. A widely accepted definition further classifies tars from biomass conversion into the categories: (1) Primary products: cellulose-derived products such as levoglucosan, hydroxy-acetaldehyde, and furfurals; analogous hemicellulose-derived products; and lignin-derived methoxyphenols; (2) Secondary products: phenolics and olefins; (3) Alkyl tertiary products: methyl derivatives of aromatics, such as methyl acenaphthylene, methylnaphthalene, toluene, and indene; (4) Condensed tertiary products, polycyclic aromatic hydrocarbons (PAH) without substituents: benzene, naphthalene, acenaphthylene, anthracene/phenanthrene and pyrene [12, 22]. The production of the different tar fractions is mainly dependent on the process temperature [23]. It has been found that while a wide range of products can be present, the primary and tertiary products are mutually exclusive in producer gas from the thermochemical conversion of biomass [12]. In Figure 3.2 the influence of the process temperature on the type and yield of the product is presented. It can be seen that with increasing process temperatures, the overall product yield of tars decreases. However, increasing temperatures also cause the complexity of products to increase until the formation of highly stable long chained PAHs at temperatures >900°C. Tars produced at lower temperatures can be decomposed at higher temperatures, through a process called thermal cracking (refer to Table 2.3). In any biomass conversion process, spatial inhomogeneities can lead to a wide variety of tars being produced and a case by case approach is currently necessary to investigate particular systems.

In autothermal reverse downdraft processes, the temperatures increase abruptly
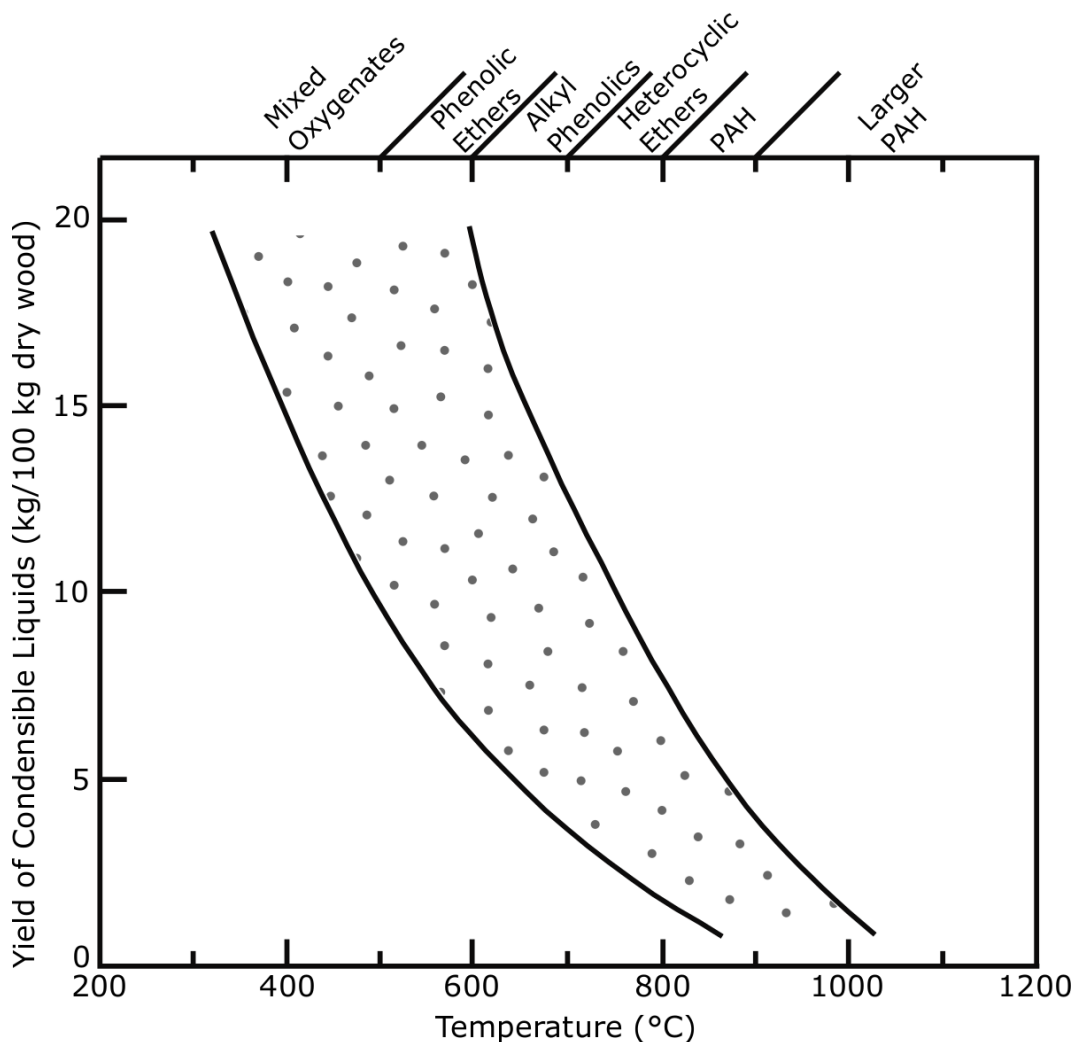
***Figure 3.2:*** Temperature dependence of biomass tar production, adapted from [12, 23].

in the reaction front, where devolatilisation occurs in a thin layer (refer to Section 2.2), as described previously. With a char layer at elevated temperatures downstream of the reaction front, further reactions may be occurring, but at lower temperatures than those in the reaction front. The peak process temperature in the reaction front and the temperature of the char layer are mainly dependent on the air supply. In a 150 mm high reactor with wood chips, increasing the air flow led to an increase in process temperatures from 650 to 850°C and a corresponding decrease

in tar content in the producer gas from 90 to 10 g·m$^{-3}$ [24]. In the same reactor, a variation in the particle size had no clear influence on the tar production, while an increasing moisture content led to a reduction of tars [16]. In a similar reactor, using four different species of wood chips, tar yields from 2–6% (g/g), at process temperatures of ≈800°C have also been reported [25]. Tars, if not combusted downstream may be released from the combustion system as volatile organic compounds. Further work will be necessary to identify the tar production from gasifier stoves at different temperatures using a variety of fuels to enable the analysis of their influence on the combustion process and the overall performance of the stove.

### 3.1.3.2   Tar Reduction Mechanisms

Tar production from biomass conversion has been identified as problematic for subsequent processes [26]. Tars are much more difficult to oxidise completely than combustible gases, leading to a multitude of difficulties in combustion applications. Tars can lead to the release of products from incomplete combustion and their reduction in the producer gas could contribute to more efficient combustion and thus process optimisation.

Tar reduction mechanisms can be classified as primary mechanisms, where measures are taken to reduce the amount released from the conversion process, and secondary mechanisms, which reduce the amount of tars in the producer gas downstream of the solid fuel bed [11]. Primary mechanisms rely on optimising the reactor design and the operating conditions, such as the temperature regime, pressure, oxidiser supply or additive catalysts. Secondary mechanisms can consist of a multitude of physical, mechanical or thermal methods, but these are not an option for gasifier stoves and are therefore beyond the scope of this thesis. An overview of primary and secondary mechanisms has previously been presented [27–29].

Primary mechanisms mainly take advantage of the decomposition characteristics of tars. Tars can crack when exposed to certain temperatures; reform in the presence

of $CO_2$ or $H_2O$, or oxidise, as per reactions R13 and R17–R19 in Table 2.3 [30–32]. These reactions can be influenced by the process conditions. For example, the presence of char can enhance the decomposition of tars [33–35]. The wide variety of products released from biomass conversion leads to such complexity that most studies on thermal or catalytic decomposition are being performed on model compounds. Extensive reviews of such studies have been conducted [36–38].

In the autothermal reverse downdraft process, higher primary air supplies lead to higher temperatures in the reaction front, as well as in the char layer downstream of the reaction front. For thermal cracking, it has been found that oxygen-containing compounds (such as phenol, cresol and naphthols) are converted at temperatures of 700–850°C, while non-oxygen-containing aromatic compounds, which are formed at higher temperatures, also decompose at higher temperatures, of >850°C [37] (refer also to Figure 3.2). Generally lower yields of tars and higher yields of gases [28] are accompanied by higher yields of larger 3- and 4-ring aromatics, which can be found at high process temperatures (>900°C). Increasing the residence time at consistently high temperatures can also reduce tar yields [39]. For example, tars from wood chip pyrolysis were decreased by 88% by passing them through a region of 900°C with 0.12 s residence time in this region [40]. Thus, increasing temperatures will decrease the tar yield, but increase the complexity of the tars, which could prove either beneficial or detrimental to the subsequent combustion process and requires further scrutiny.

When hot char is present, it has been suggested that it can catalyse or enhance the cracking of tars directly, as they are released within the biomass particle and once they have been released from the biomass particle [11, 41]. Char has been shown to catalyse not only cracking, but also isomerisation and aromatisation of aliphatic compounds (alkanes, alkenes, alkanoic acids, ketones, alcohols and amines) at temperatures between 300°C and 600°C [33] and is generally less effective for conversion of larger molecular compounds [34]. The addition of $CO_2$ or $H_2O$, upstream

of a char bed, has been found to increase the free radical content, such as OH and H, and the oxidation of tars from rice straw pyrolysis with those species [35]. The supply of $O_2$ causes oxidation and reduction of pyrolysis tar compounds, which can be further reduced if a char bed is present [30, 42]. The influence of the produced char in gasifier stoves on the release of tars has yet to be established.

In the autothermal reverse downdraft process, tars released during devolatilisation in the reaction front enter an atmosphere containing $CO_2$, $H_2O$ and possibly $O_2$ and then pass through a layer of char at elevated temperatures downstream, before being released from the fuel bed. It has been suggested that the extent of tar cracking due to the presence of char is limited in gasifier stoves because of the thin char layer thickness [17]. Furthermore, it is unclear if temperatures and residence times downstream of the reaction front are sufficient to affect tar concentrations.

### 3.1.4 Solid Products

#### 3.1.4.1 Char

Char is the solid carbonaceous residue obtained when biomass is exposed to heat under inert or oxygen-deficient conditions. It is called "biochar" if designated for use in environmental management [43]. It contains a large fraction of the fuel carbon and ash content. Biochar has potential as a soil amendment, for nutrient supply and conditioning [44]; it can be an income generator in resource-constrained communities; a waste management system, especially relevant for water treatment; and an opportunity for a carbon negative energy supply through carbon sequestration [13, 45–47]. The yield, composition and morphology of biochar depends significantly on the feedstock, as well as the conditions of the thermochemical conversion, particularly in terms of the process temperature [1, 48–51].

For comparability and classification of different grades of biochar, guidelines have been proposed in the European Biochar Certificate (EBC) by the European Biochar

Foundation [52] and the International Biochar Initiative (IBI) [53]. Both sets of guidelines require a molar $H/C_{org}$ ratio <0.7 (similar to coal, refer to Figure 2.1), a determination of the nutrient content, the pH value, the bulk density, the moisture content, the ash content, the PAH content, the heavy metal content and the specific surface area. The EBC also requires an $O/C_{org}$ of <0.4. While the EBC classifies biochars as either basic or premium grade, based on the PAH and heavy metal contents, the IBI distinguishes biochars on the basis of their organic carbon content (Class 1: $\geq$60%; Class 2: 30–60%; Class 3: 10–30%; minimum: 10%). The classification of chars produced in gasifier cookstoves is seldom performed [45, 54] and could provide further insights into the potential of the technology.

The production of char has many process implications. Primarily, it allows for the separation of devolatilisation/gasification and combustion dominated reaction zones and retains a large fraction of the ash within its solid structure. These influences on ongoing processes are not well understood, as, generally, when producing char, this is the sole process purpose and the conversion chemistry is of little importance or, as is the case in nearly all biomass applications, complete consumption of the feedstock is desired and char is simply a product of incomplete combustion. A more in-depth analysis of the combined production of producer gas and biochar in an autothermal reverse downdraft process would be beneficial to enable process optimisation.

### 3.1.4.2 Ash

Ash refers to the solid product from complete combustion. In biomass, a large number of elements and inorganic compounds are present in a wide range of concentrations. Two main fractions can be distinguished in fixed bed combustion systems, namely fly ash, which is volatilised in the process or entrained by the gas phase in the reactor, and bottom ash. The impact of both fractions on the combustion process is not yet fully understood, but overviews of current knowledge can be found in the literature [55–59].

Minor elements in biomass include N, Ca, K, Si, Mg, Al, S, Fe, P, Cl, Na, Mn and Ti [56]. These elements can occur in the form of various compounds, that can change over the thermochemical conversion process. A large fraction of the ash may be retained in the solid char structure, placing greater importance on the volatility of ash constituents, as well as the melting behaviour of solids, in gasifier stoves. Thermodynamic equilibrium calculations for wood, at 900°C in a fluidised bed and entrained flow reactor, suggest that ten elements (N, S, Cl, Zn, Hg, Cd, Pb, Se, F, Sb) volatilise completely, either in elemental (Zn, Hg, Cd, Pb), hydride, or oxihydride state [60]. However, five elements (Ca, Si, Al, P, Ti) remained as oxides in the condensed phase [60]. Ashing of biomass feedstock has shown that increasing the temperature between 450°C and 1000°C leads to lower ash yields, mainly due to the release of K and Na in the form of chlorides [61–63]. Based on the elemental composition, ash melting points of ≤900°C have been suggested for most biomass feedstock [58]. Devolatilisation and melting behaviour of ash constituents can substantially influence the performance of a combustion system [64, 65] and its overall impact, especially for the combined production of producer gas and char requires consideration.

In gasifier stoves, a large fraction of the ash constituents may be retained in the solid structure if char is produced, which could potentially mitigate detrimental impacts on the combustion process. The utilisation of high ash content fuels, such as agricultural residues or manures, can aggravate potential impacts that have yet to be investigated for the type of stove under consideration at different process conditions.

## 3.2 Combustion of Thermochemical Conversion Products

### 3.2.1 The Producer Gas Combustion Process

In gasifier cookstoves, the fuel at the secondary air inlet is provided by the producer gas released from the thermochemical conversion of the solid fuel (as presented in Figure 1.1). It contains the combustible gases CO, $H_2$, $CH_4$ and other hydrocarbon gases, as well as a wide variety of tars [66], as discussed in more detail in Sections 3.1.2 and 3.1.3. Other species, mainly $N_2$ from the air, and oxidised species such as $CO_2$ and $H_2O$ can also form a substantial fraction of the producer gas [67]. Traces of S, Cl, Na, K and other fuel ash constituents may also be present [67], as described in Section 3.1.4.2. The wide variability of combustible compounds released from the thermochemical conversion process, especially when varying the feedstock as presented in Table 3.1, poses a challenge for the identification of combustion mechanisms. This is necessary to generate an in-depth understanding of the interplay of various processes, as well as for efficient combustor design [68]. When investigating producer gas combustion, most studies focus on cleaned producer gas—tars and particulates are removed to achieve a pure gas mixture—from continuous coal gasification (also termed synthesis gas or syngas) [69]. Large discrepancies between models and measured values [68] underline that the reaction mechanisms, even in highly controlled systems, are not yet fully understood. In the present system, these difficulties are exacerbated by the presence of tar species and fuel ash constituents. Furthermore, most investigations focus on premixed combustion, while in the presented system non-premixed laminar combustion occurs in the secondary flame front.

Studies on producer gas combustion focus mainly on its application in engines and turbines, therefore, the focus is on premixed combustion in high pressure systems with controlled stoichiometry [70]. A vast amount of literature is available,

while only selected aspects are presented here, with detailed investigations provided elsewhere [69, 71]. It has been found that the combustion behaviour of gas mixtures can be markedly different from that of its constituents and small changes in mixture fractions can have a substantial influence [72]. The presence of H in a gas mixture in particular has been highlighted [72]. When H is present, the main oxidation mechanism is via $CO + OH \rightleftharpoons CO_2 + H$ (R20), which reacts much faster than the oxidation of CO alone (refer to R7 in Table 2.3) [72]. CO oxidation via OH then influences ignition and extinction limits, as well as flame propagation velocities [72]. The presence of small amounts of $NO_x$ has been recognised as providing an alternative route for $HO_2$ consumption and provision of OH, which can significantly increase the overall chemical reaction rates [69]. The presence of diluents $N_2$, $CO_2$ and $H_2O$ in the combustible gas mixture generally decreases the flame speed through a reduction in the reaction rates [73]. $N_2$ dilution, rather than $CO_2$ or $H_2O$, reduces the flame extinction strain rate [74]. Increasing concentrations of $CO_2$ have been identified as reducing flame speeds due to reverse reaction R20, which becomes especially influential in low $H_2$ gas mixtures [75]. Conversely, the absorption of radiation by $CO_2$ and $H_2O$ has been shown to increase flame speed and extend flammability limits [73, 76]. As the product composition from biomass conversion can vary throughout the process and small changes in the feedstock composition can change the mixture fractions, the producer gas composition should be identified as it may have a substantial impact on secondary combustion in gasifier cookstoves. Once the producer gas reaches the secondary air inlet in gasifier stoves, sufficient air may be supplied, and they can oxidise if an ignition source is present. The influence of the producer gas composition from various types of feedstock on the combustion process has yet to be established.

### 3.2.2 Gaseous Products

The products from complete hydrocarbon combustion are $H_2O$ and $CO_2$, typically in the gas phase, accompanied by incomplete combustion leading to the release of CO and $H_2$ as well as hydrocarbon gases [77], as per reactions R7–R19 in Table 2.3. As a result of gas-combustion, and compared with other cookstoves, the separation of the thermochemical conversion and producer gas combustion processes have been shown to produce low CO and particulate matter (PM) emissions under laboratory conditions [78, 79].

In combustion processes where air is the oxidiser, a significant pollutant stems from the oxidation of nitrogen ($NO_x$) [80, 81]. In a flame, thermal $NO_x$ is formed when temperatures >1600°C for seconds or >2000°C for only milliseconds are present [82]. Prompt $NO_x$ is formed when fuel-derived radicals react with $N_2$ [83]. In solid fuel combustion, $NO_x$ can also be derived from fuel bound N. During devolatilisation, N is mainly retained in the char, as in this process a C-N matrix is formed [83]. Subsequently when the char is combusted, $NO_x$ and the $NO_x$ precursors, HCN and $NH_3$, are released [83]. The impact of this mechanism may be reduced if the char is a product, but a detailed investigation of $NO_x$ emissions from gasifier cookstoves is outside the scope of this thesis.

Small amounts of S can also be present in the biomass feedstock, which leads to the formation $SO_2$. The concentrations of S in biomass are generally quite low, compared with coal or other fossil fuels, and its influence and contribution to the combustion process is therefore considered minor.

### 3.2.3   Particulate Matter

#### 3.2.3.1   Soot

Soot is widely defined as comprising of combustion-generated particulates whose main constituent is carbon [80]. It is also referred to as black carbon or carbon black, because of its light absorbing properties [84]. Soot is characterised by its form: small carbon spherules with strong absorption properties across the visible spectrum [84]. Furthermore, it has a very high vaporisation temperature which makes it stable at high temperatures and ensures its insolubility in other atmospheric aerosol components [84].

General requirements for soot formation are high temperatures, in the range of 1800–2800°C, sufficient oxygen availability for substantial combustion of the fuel and residence times in the order of a few milliseconds [85]. Formation of initial soot particles can occur via surface reaction mechanisms or through nucleation from collision and coalescence of PAH molecules [86]. It has been suggested that for low temperature flames, nucleation plays a significant role, while surface reactions are dominant at higher flame temperatures [86, 87]. Subsequently the formed particles can grow further, through the attachment of gaseous species to their surfaces or by coagulation, via coalescence, condensation or collision of particles [85]. Indications suggest that the surface growth rate is much larger than the coagulation rate [88].

Figure 3.3 provides a general overview of the organic products from incomplete combustion from biomass and coal combustion processes, with a focus on soot formation mechanisms. It can be seen that after the formation of gases and tars in the thermochemical conversion process (as described in Section 3.1), two main surface reaction mechanisms, namely H-abstraction-$C_2H_2$-addition (HACA) and reactions of cyclopent-adiene (CPD), are proposed as being of particular importance [89]. Polycyclic aromatic hydrocarbons (PAH) are considered to be the main soot precursors in biomass combustion. Soot can form from PAHs via two main pathways: (1) HACA

evolves through two principal steps: (i) abstraction of a hydrogen atom, mostly identified as being caused by a gaseous hydrogen atom, $A_i + H \rightarrow A_{i-} + H_2$, which causes the molecule to be activated to a radical, and enables further growth; (ii) a gaseous acetylene molecule is then added to the radical site, $A_{i-} + C_2H_2 \rightarrow$ to form the products [90–92]; (2) reactions with cyclopentadienyl (CPDyl = $C_5H_5$) in a combustion system result in the formation and growth of PAH products [93]. Intermediate volatile organic compounds (refer also to Section 3.1.3) may be co-emitted with soot and may condense on the soot carbon spherules, together with volatile ash constituents [83]. Further investigations of a variety of hydrocarbon fuels would provide a more in-depth understanding of soot formation pathways [94, 95], but this is outside the scope of this thesis. However, the above presented findings highlight the importance of tars in soot formation mechanisms. Therefore, an identification of tar reduction mechanisms from the thermochemical conversion process in the fuel bed of gasifier stoves could prove beneficial for soot reduction from producer gas combustion.
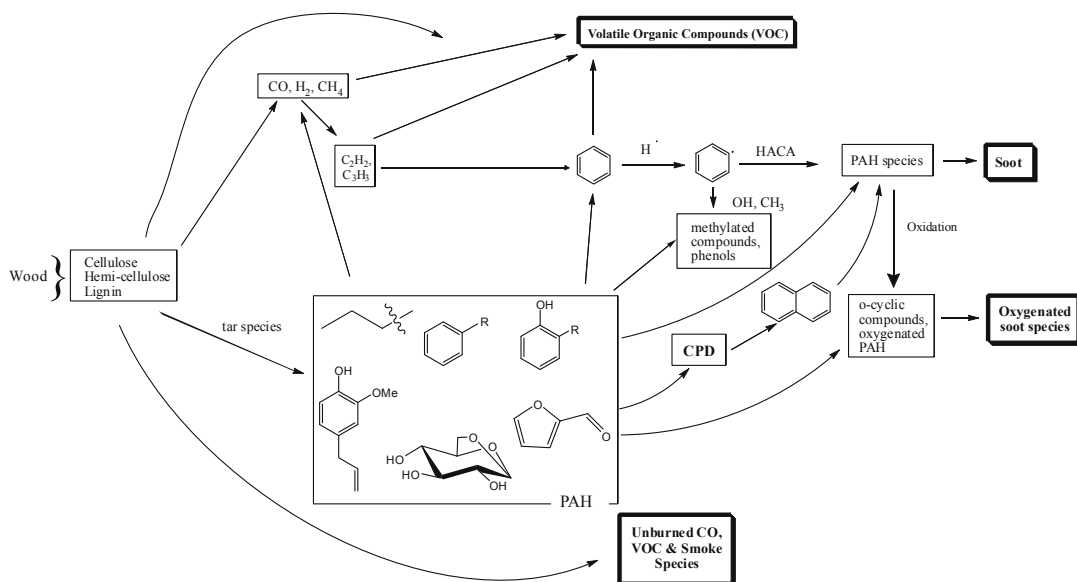


***Figure 3.3:*** Potential routes for the release of products from incomplete biomass combustion, adapted after [89].

The presented studies provide an overview of the influencing parameters and fundamental mechanisms of soot particle formation in hydrocarbon combustion. It is apparent that the formation of the soot of a homogeneous fuel under highly controlled conditions is extremely complex. The inhomogeneity of producer gas utilised in a simple atmospheric combustor will therefore not enable a detailed investigation of soot formation mechanisms. However, particulate matter measurements from the producer gas combustion could provide valuable information and enable combustion optimisation.

### 3.2.3.2 Ash Constituents

The ash constituents present in the secondary combustion region, also called fly ash in fixed bed combustion, will consist of devolatilised and entrained compounds, as described in Section 3.1.4.2. These compounds can influence the combustion chemistry and inhibit or catalyse oxidation reactions [96].

Figure 3.4 presents possible routes for the release of mainly K, Cl and S compounds from the solid fuel and indicates the interplay across released tars [55]. It can be seen that the release of ash constituents from the fuel evolves either within the organic tars, or through devolatilisation and the entrainment of ash constituents. Subsequent reactions then lead to the formation of larger fly ash particulates, to which aerosols can stick, or which may form furnace deposits. For different fuels, changing particulate emissions have been identified, for example for corn stover, two types of particles, (1) an agglomerate of soot with condensed organics and ash species (including potassium, chloride, sulfates and phosphates), and (2) a spherical organic particle, have been found [97]. Two mechanisms, (1) the entrainment of coarse ash particles ($>10$ $\mu$m) in the gas stream [98, 99] and (2) the vaporisation and nucleation of submicron-sized minerals [98, 100–103], have been shown to contribute to fly ash. It has also been found that during transient events organic compounds dominate the emissions, whilst during steady-state combustion inorganic compounds are of greater

importance [83].

It has been suggested that trace quantities of S, Cl, K or Na can affect the overall producer gas combustion process and have a significant impact on the formation of $SO_2$, HCl, $NO_x$, PAH, and soot [96]. Experiments using KCl-doped biomass have shown that Cl can interact with fuel methoxyl groups, leading to the formation of $CH_3Cl$ [104] and that HCl [105, 106] as well as $CH_3Cl$ [107], already at low concentrations, strongly inhibit the oxidation of CO. Phosphorous-containing compounds have shown strong flame-inhibiting characteristics [108, 109]. Furthermore, the addition of Fe (200 ppm) and Mn (140 ppm) to a laminar, sooting, premixed ethylene-oxygen-nitrogen flame has been shown to cause a potential threefold increase in soot [110]. The influence of specific ash constituents on a staged combustion process requires further scrutiny; however, this is outside the scope of the present investigation.

The impact of fuel ash constituents on the secondary combustion process and the particulate emissions is largely unknown. Due to the complexity and interaction of ongoing processes, an analysis of the particulate matter emissions from direct producer gas combustion could provide further insights into the influence of ash constituents.

## 3.3 Small-Scale Application in Cookstoves

### 3.3.1 Cookstove Development

In small-scale applications, emissions reduction can often only be performed through the optimisation of the combustion process itself. Downstream gas cleaning, which is generally performed in large-scale or high-tech applications, such as power plants or internal combustion engines may not be possible. In some small-scale devices a flue is used to transport the exhaust stream outside the building, but as these rely on buoyancy, implementing gas cleaning will be challenging. Therefore, a deeper
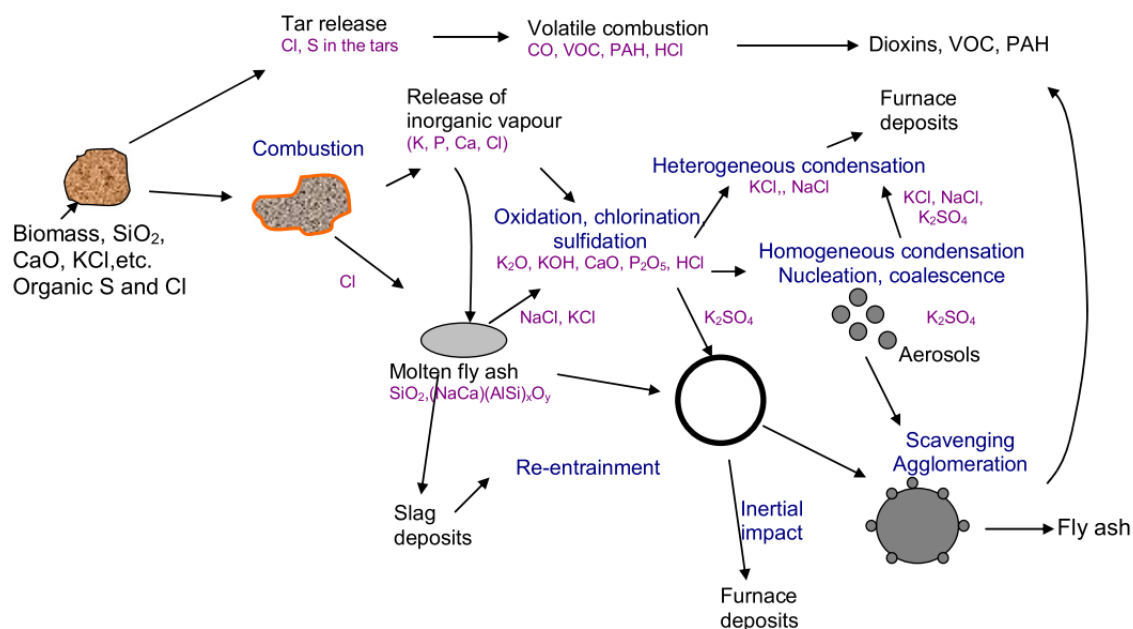
***Figure 3.4:*** Pathways leading to particulate emissions and emissions from incomplete combustion, with a focus on ash constituents [55].

understanding of the combustion process itself and measures that increase efficiency are necessary.

The air supply is a defining parameter. Its supply and regulation has a profound influence on performance. As mentioned previously, most cookstoves rely on natural draft for their air supply, which then depends on the buoyancy force, hence temperature differences and the reactor geometry. It has been suggested that already small ambient disturbances impact buoyancy-driven air supplies and can therefore affect the efficiency of cookstoves [111]. Shielding of the combustion region, as seen in many improved cookstoves [112–114], can mitigate this issue. Many natural draft stoves, especially gasifier or rocket type stoves (a stove that is continuously fed from the side and features conventional combustion), have shown clear improvements in comparison with three stone fires [78, 115]. The use of forced draft has been suggested to provide the potential for further emissions reductions. However, the feasibility of using forced draft is substantially limited by the requirement for electricity, which

results in a more complex and costly system [111]. Increasing emissions, as well as heat transfer efficiency [116], suggested for forced draft stoves, could compensate for the additional complexity due to the use of electric fans.

Air staging has also been shown to increase burn-out in many combustion systems and therefore reduce emissions from incomplete combustion [117]. In a rocket type stove, the introduction of air downstream of the fuel bed achieved a reduction in the emissions from incomplete combustion, but care must be taken as over-supply of air can lead to flame quenching and an increase in pollutant emissions [118]. The geometry of the air supply and its potential invasiveness into the combustion region can also be of importance and must be accounted for in design considerations [119]. A number of research articles have shown that a forced air supply leads to greater mixing of air and combustible species, and thus increased combustion performance [115, 120–124]. Conversely others have found no reduction of emissions from incomplete combustion when using forced draft [116]. Furthermore, transients at start-up, shut-down and refuelling, have a substantial impact on the total emissions [125] and may also be influenced by the air supply. A deeper understanding of combustion in small-scale atmospheric systems, and particularly the influence of the air supply, is necessary to ensure consistent emissions reductions.

Emissions from incomplete combustion from cookstoves are often related to the supplied fuel and, within the widely used biomass fuels, wood is generally regarded as a better fuel than agricultural residues, which in turn are regarded as better than manures, based on the experimental findings in the literature [126, 127]. The cause of the discrepancy between different biomass fuels is largely unknown and requires further investigation.

Additionally, emissions reductions can be achieved through processing of the fuel, for example through pelletisation [128, 129], retained heat cooking [130], or automation of the combustion process to reduce user influences [131]. User practice has been shown to be of substantial importance for the efficient utilisation of a

cookstove [120, 132–134]. Furthermore, mathematical modelling approaches can be used to better understand and complement experimental work [135–137]. Such topics also need further consideration but are outside the scope of the present investigation.

### 3.3.2 Gasifier Cookstoves

Research which focuses on the specific processes in reverse downdraft gasifier stoves is widely dispersed and can consist of scientific articles and theses [15, 138, 139], as well as there being much work presented in the grey literature [140]. A brief overview of the most relevant findings is presented here. This work provided the basis for the reactor design and the developmental framework of the present investigation.

A natural draft gasifier stove with a gas wick downstream of the secondary air inlet was used to investigate and describe the working principle of this type of stove by Reed et al. [141]. Further work was performed on the importance of the primary air supply using forced air [1] and tests were undertaken with a variety of fuels [50]. This work helped to establish the benefit of separating the combustion of volatiles and char, in the particular manner of gasifier stoves.

A forced draft Oorja gasifier stove, using wood as fuel, was investigated by Varunkumar et al. [7, 17, 142]. The influence of increasing the air supply and the classification of subsequent regimes of the solid fuel conversion process was examined. Based on the superficial velocity ($v_s$) (the mean velocity of the primary air within the reactor) two regimes were suggested: (1) "gasification dominated" for $v_s < 170$ mm·s$^{-1}$ and (2) "char oxidation dominated" for $v_s > 170$ mm·s$^{-1}$, corresponding with Figure 3.1. In this thesis, these regimes will be termed (1) oxygen-limited and (2) reaction-limited, as described in Section 3.1.1. The conversion behaviour was described: In the oxygen-limited regime, as similar to single particle conversion, where mainly volatile release and oxidation occurs. Simultaneously char is produced. Here, a thinning reaction front can be noticed with the increasing air supply. In the reaction limited regime, char and volatile oxidation occur concurrently as sufficient

oxygen availability overcomes the char conversion-limiting oxygen diffusion to the particle [7]. Furthermore, it has been shown that in the char combustion stage, within the oxygen-limited regime, the conversion depends largely on the char density [142]. During devolatilisation, the producer gas constituents were measured and the tars estimated to simulate secondary combustion and heat transfer to the vessel on top of the stove. It was shown that inducing swirl in the secondary combustion zone had no effect, but that the stove geometry and pot size influence the heat transfer properties strongly [17].

Tryner et al. studied a variety of natural draft stoves and a forced draft experimental reactor using multiple fuels [18, 143, 144]. A comparison of three modifications of the Jinqilin natural draft stove, a Philips HD 4008 natural draft stove, and a Peko Pe natural draft stove, with wood pellets and corn cobs as fuels, presented a wide variation in performance from small design differences [143]. The profound effect of the fuel type and test procedure on the release of emissions and especially the impact of transients, during start-up, re-fuelling and shut-down, is highlighted [143]. The forced draft experimental reactor was used with corn cob chips, eucalyptus chips, Douglas fir chips and lodgepole pine pellets as fuels. Multiple primary and secondary air supplies rates were investigated, with SA:PA ratios of 3–4 presenting low emissions from incomplete combustion during the devolatilisation of the solid fuel [18]. Other ratios of 1 to 3.1, 5.7, 6.2 [50] and 2.3 [145] have been reported, but no investigation of the related efficiency was performed. Confirming a ratio of primary to secondary air, which provides high performance would be a priority, as it could then underpin all emergent gasifier stove designs. Furthermore, a smaller hole size at the secondary air inlet led to a reduction of emissions, while the swirl of secondary air had a negligible impact [18]. The emissions of sub-micron particulate emissions from wood chip combustion in the forced draft experimental reactor showed a bimodal size distribution with peaks at 10 nm and 40 nm during normal operation, with a pot on the stove [144]. Once the pot was removed, only a unimodal peak at

10 nm was noted. This may indicate that the pot has an influence on the secondary combustion zone, most likely due to flame quenching. Flame quenching by the pot can potentially be mitigated through optimising the stove geometry to avoid contact between the flames and the cooking surface. Transient events, when refuelling and during shut-down, accounted for approximately 29% and 59%, respectively, of the total mass of released particulate matter [144].

When comparing the various investigations presented above, as well as related studies [45, 146], it can be noticed already that small variations in the stove geometry or the utilised fuel may have a significant impact on the stove's performance. Basic design principles, such as the air inlet ratios or the bed depth therefore require further attention to enable the design of more efficient stoves in the future, especially in terms of the use of a variety of fuels and their impact on the combustion process.

## 3.4 Research Gaps

For this thesis four specific research gaps have been identified:

**1. Research Gap:** In gasifier stoves the air supply is of central importance, but its influence is still not fully understood. While primary air sustains the thermo-chemical conversion, further complexity is added to the combustion process as the relationship between the two air stages must be considered. Complete combustion is a requirement only in the secondary combustion region.

- **Aim:** *Examine the influences of the air supply and distribution on the combustion processes.*

- **Objective:** Examine the influence of variations of the draft type (natural- or forced-draft), the amount of primary and secondary air supply, as well as their relationship and relative locations, in terms of the released gaseous emissions.

**2. Research Gap:** The presence of char, downstream of the reaction front, may influence the composition of the producer gas released from the thermochemical conversion of the solid fuel. It has been suggested that the char may facilitate the decomposition of tars but a verification of this mechanism in small-scale gasifier stoves and an investigation into the nature of such influences could be beneficial. Decomposition of tars to combustible gases within the solid fuel bed could provide desirable implications for the producer gas quality.

- **Aim:** *Investigate the impact of the char layer on the autothermal thermochemical conversion process.*

- **Objective:** Study the influence of an increasing fuel bed depth and the resulting increase of the char layer thickness during the conversion process on the release of products from the solid fuel conversion process.

**3. Research Gap:** In application, a wide variety of fuels are being combusted in cookstoves, while most research focuses on the use of woody biomass. A deeper understanding of the influence of different feedstocks, with a wide range of ash contents, on the thermochemical conversion process is of interest.

- **Aim:** *Investigate the impact of a variety of fuels with a wide range of ash contents on the autothermal thermochemical conversion process.*

- **Objective:** Investigate how different fuels and fuel compositions affect the process conditions. Analyse products from the thermochemical conversion process, with a particular focus on potential influences of the fuel ash content.

**4. Research Gap:** The producer gas released from the thermochemical conversion of the solid biomass provides the fuel for the secondary combustion process in gasifier stoves and its composition may vary widely in between different fuels. An analysis of the combustion products with more information about the producer

gas may provide a more in-depth understanding of the combustion processes and mechanisms that control the emissions.

- **Aim:** *Extend the understanding of the producer gas combustion process downstream of the fuel bed, particularly mechanisms that control the emissions.*

- **Objective:** Analyse how different fuels and fuel compositions affect the products from the secondary combustion process, downstream of the fuel bed.

These gaps are individually addressed in independent research articles. Each article forms one of the four main chapters of this thesis.

## 3.5   References

[1] T. Reed, R. Walt, S. Ellis, A. Das, and S. Deutch, "Superficial Velocity - The Key To Downdraft Gasification," in *4th Biomass Conference of the Americas*, (Oakland), 1999.

[2] J. Porteiro, D. Patiño, J. Collazo, E. Granada, J. Moran, and J. L. Miguez, "Experimental analysis of the ignition front propagation of several biomass fuels in a fixed-bed combustor," *Fuel*, vol. 89, no. 1, pp. 26–35, 2010.

[3] J. Porteiro, D. Patiño, J. Moran, and E. Granada, "Study of a fixed-bed biomass combustor: Influential parameters on ignition front propagation using parametric analysis," *Energy and Fuels*, vol. 24, no. 7, pp. 3890–3897, 2010.

[4] M. Fatehi and M. Kaviany, "Adiabatic reverse combustion in a packed bed," *Combustion and Flame*, vol. 99, pp. 1–17, 1994.

[5] M. Horttanainen, J. Saastamoinen, and P. Sarkomaa, "Operational limits of ignition front propagation against airflow in packed beds of different wood fuels," *Energy and Fuels*, vol. 16, no. 3, pp. 676–686, 2002.

[6] M. Rönnbäck, M. Axell, L. Gustavsson, H. Thunman, and B. Lecher, "Combustion processes in a biomass fuel bed - Experimental results," in *Progress in Thermochemical Biomass Conversion* (A. Bridgwater, ed.), ch. 59, pp. 743–757, Bodmin: Blackwell Science Ltd, 2001.

[7] S. Varunkumar, N. K. S. Rajan, and H. S. Mukunda, "Universal Flame Propagation Behavior in Packed Bed of Biomass," *Combustion Science and Technology*, vol. 185, no. 8, pp. 1241–1260, 2013.

[8] P. Garcia-Bacaicoa, R. Bilbao, J. Arauzo, and M. Luisa Salvador, "Scale-up of

downdraft moving bed gasifiers (25-300 kg/h) – Design, experimental aspects and results," *Bioresource Technology*, vol. 48, no. 3, pp. 229–235, 1994.

[9] E. A. T. Yuntenwi, N. A. MacCarty, D. Still, and J. Ertel, "Laboratory study of the effects of moisture content on heat transfer and combustion efficiency of three biomass cook stoves," *Energy for Sustainable Development*, vol. 12, no. 2, pp. 66–77, 2008.

[10] Y. B. Yang, V. N. Sharifi, and J. Swithenbank, "Effect of air flow rate and fuel moisture on the burning behaviours of biomass and simulated municipal solid wastes in packed beds," *Fuel*, vol. 83, no. 11-12, pp. 1553–1562, 2004.

[11] P. Basu, *Biomass Gasification and Pyrolysis and Torrefaction*. Elsevier, second ed., 2013.

[12] T. A. Milne, R. J. Evans, and N. Abatzoglou, "Biomass Gasifier "Tars": Their Nature, Formation, and Conversion," tech. rep., National Renewable Energy Laboratory, Golden, 1998.

[13] C. Brewer and R. Brown, "Biochar," in *Comprehensive Renewable Energy* (A. Sayigh, ed.), ch. 5, pp. 357–384, Elsevier Ltd., 2012.

[14] J. G. Speight, "Chemistry of Gasification," in *Gasification of Unconventional Feedstock*, ch. 2, pp. 135–152, Laramie: Elsevier Inc., 2014.

[15] S. Varunkumar, *Packed bed gasification-combustion in biomass based domestic stoves and combustion systems*. PhD thesis, Indian Institute of Science, 2012.

[16] A. M. James R, W. Yuan, and M. Boyette, "The Effect of Biomass Physical Properties on Top-Lit Updraft Gasification of Woodchips," *Energies*, vol. 9, no. 4, pp. 283–296, 2016.

63

[17] S. Varunkumar, N. K. S. Rajan, and H. S. Mukunda, "Experimental and computational studies on a gasifier based stove," *Energy Conversion and Management*, vol. 53, no. 1, pp. 135–141, 2012.

[18] J. Tryner, J. W. Tillotson, M. E. Baumgardner, J. T. Mohr, M. W. Defoort, and A. J. Marchese, "The Effects of Air Flow Rates, Secondary Air Inlet Geometry, Fuel Type, and Operating Mode on the Performance of Gasifier Cookstoves," *Environmental Science and Technology*, vol. 50, no. 17, pp. 9754–9763, 2016.

[19] A. M. James R, W. Yuan, M. D. Boyette, and D. Wang, "Airflow and insulation effects on simultaneous syngas and biochar production in a top-lit updraft biomass gasifier," *Renewable Energy*, vol. 117, pp. 116–124, 2018.

[20] E. Daouk, L. Van de Steene, F. Paviet, E. Martin, J. Valette, and S. Salvador, "Oxidative pyrolysis of wood chips and of wood pellets in a downdraft continuous fixed bed reactor," *Fuel*, vol. 196, pp. 408–418, 2017.

[21] J. Kiel, S. V. Paasen, and J. Neeft, "ECN-C–04-014: Primary measures to reduce tar formation in fluidised-bed biomass gasifiers," tech. rep., Energy Research Centre of the Netherlands, 2004.

[22] R. J. Evans and T. A. Milne, "Molecular Characterization of the Pyrolysis of Biomass. 2. Applications," *Energy and Fuels*, vol. 1, no. 4, pp. 311–319, 1987.

[23] E. Baker, M. Brown, D. C. Elliott, and L. Mudge, "Characterization and treatment of tars from biomass gasifiers," *AIChE 1988 Summer National Meeting*, 1988.

[24] A. James, W. Yuan, M. D. Boyette, D. Wang, and A. Kumar, "Characterization of Biochar from Rice Hulls and Wood Chips Produced in a Top-Lit Updraft

Biomass Gasifier," *Transactions of the ASABE*, vol. 59, no. 3, pp. 749–756, 2016.

[25] E. Díez, I. Gómez, and J. Pérez, "Mass, energy, and exergy analysis of top-lit updraft micro-gasification process: Effect of firewood type and forced primary air flow," *Sustainable Energy Technologies and Assessments*, vol. 29, pp. 82–91, 2018.

[26] T. Reed and A. Das, "Handbook of Biomass Downdraft Gasifier Engine Systems," tech. rep., Solar Energy Research Institute, Golden, 1988.

[27] L. Devi, K. J. Ptasinski, and F. J. J. G. Janssen, "A review of the primary measures for tar elimination in biomass gasification processes," *Biomass and Bioenergy*, vol. 24, no. 2, pp. 125–140, 2002.

[28] S. Anis and Z. A. Zainal, "Tar reduction in biomass producer gas via mechanical, catalytic and thermal methods : A review," *Renewable and Sustainable Energy Reviews*, vol. 15, no. 5, pp. 2355–2377, 2011.

[29] M. L. Valderrama Rios, A. M. González, E. E. S. Lora, and O. A. Almazán del Olmo, "Reduction of tar generated during biomass gasification: A review," *Biomass and Bioenergy*, vol. 108, pp. 345–370, 2018.

[30] S. Zhao, Y. Luo, Y. Zhang, and Y. Long, "Experimental investigation of the synergy effect of partial oxidation and bio-char on biomass tar reduction," *Journal of Analytical and Applied Pyrolysis*, vol. 112, pp. 262–269, 2015.

[31] J. Ahrenfeldt, H. Egsgaard, W. Stelte, T. Thomsen, and U. B. Henriksen, "The influence of partial oxidation mechanisms on tar destruction in TwoStage biomass gasification," *Fuel*, vol. 112, pp. 662–680, 2013.

[32] P. Gilbert, C. Ryu, V. Sharifi, and J. Swithenbank, "Tar reduction in pyrolysis

vapours from biomass over a hot char bed," *Bioresource Technology*, vol. 100, no. 23, pp. 6045–6051, 2009.

[33] R. A. Regtop, J. Ellis, P. T. Crisp, A. Ekstrom, and C. J. R. Fookes, "Pyrolysis of model compounds on spent oil shales, minerals and charcoal. Implications for shale oil composition," *Fuel*, vol. 64, no. 12, pp. 1640–1646, 1985.

[34] J. Park, Y. Lee, and C. Ryu, "Reduction of primary tar vapor from biomass by hot char particles in fixed bed gasification," *Biomass and Bioenergy*, vol. 90, pp. 114–121, 2016.

[35] W. G. Wu, Y. H. Luo, Y. Su, Y. L. Zhang, S. H. Zhao, and Y. Wang, "Nascent biomass tar evolution properties under homogeneous/heterogeneous decomposition conditions in a two-stage reactor," *Energy and Fuels*, vol. 25, no. 11, pp. 5394–5406, 2011.

[36] J. Han and H. Kim, "The reduction and control technology of tar during biomass gasification/pyrolysis: An overview," *Renewable and Sustainable Energy Reviews*, vol. 12, no. 2, pp. 397–416, 2008.

[37] R. Zwart and B. Vreugdenhil, "ECN-E–08-087: Tar formation in pyrolysis and gasification," tech. rep., Energy Research Centre of the Netherlands, 2009.

[38] Y. Shen, "Chars as carbonaceous adsorbents/catalysts for tar elimination during biomass pyrolysis or gasification," *Renewable and Sustainable Energy Reviews*, vol. 43, pp. 281–295, 2015.

[39] W. F. Fassinou, L. Van de Steene, S. Toure, G. Volle, and P. Girard, "Pyrolysis of Pinus pinaster in a two-stage gasifier: Influence of processing parameters and thermal cracking of tar," *Fuel Processing Technology*, vol. 90, no. 1, pp. 75–90, 2009.

[40] P. Morf, P. Hasler, and T. Nussbaumer, "Mechanisms and kinetics of homogeneous secondary reactions of tar from continuous pyrolysis of wood chips," *Fuel*, vol. 81, no. 7, pp. 843–853, 2002.

[41] A. S. Al-Rahbi, J. A. Onwudili, and P. T. Williams, "Thermal decomposition and gasification of biomass pyrolysis gases using a hot bed of waste derived pyrolysis char," *Bioresource Technology*, vol. 204, pp. 71–79, 2016.

[42] S. Hosokai, K. Norinaga, T. Kimura, M. Nakano, C. Z. Li, and J. I. Hayashi, "Reforming of volatiles from the biomass pyrolysis over charcoal in a sequence of coke deposition and steam gasification of coke," *Energy and Fuels*, vol. 25, no. 11, pp. 5387–5393, 2011.

[43] J. Lehmann and S. Joseph, eds., *Biochar for Environmental Management: science and technology.* London: VA : Earthscan, second ed., 2015.

[44] S. B. Liaw and H. Wu, "Tuning Biochar Properties via Partial Gasification: Facilitating Inorganic Nutrients Recycling and Altering Organic Matter Leaching," *Energy and Fuels*, vol. 29, no. 7, pp. 4407–4417, 2015.

[45] C. Birzer, P. Medwell, G. MacFarlane, M. Read, J. Wilkey, M. Higgins, and T. West, "A biochar-producing, dung-burning cookstove for humanitarian purposes," *Procedia Engineering*, vol. 78, pp. 243–249, 2014.

[46] E. Parparita, M. Brebu, M. Azhar Uddin, J. Yanik, and C. Vasile, "Pyrolysis behaviors of various biomasses," *Polymer Degradation and Stability*, vol. 100, no. 1, pp. 1–9, 2014.

[47] D. Woolf, J. Lehmann, E. M. Fisher, and L. T. Angenent, "Biofuels from pyrolysis in perspective: Trade-offs between energy yields and soil-carbon additions," *Environmental Science and Technology*, vol. 48, no. 11, pp. 6492–6499, 2014.

[48] M. J. Antal and M. Gronli, "The art, science, and technology of charcoal production," *Industrial and Engineering Chemistry Research*, vol. 42, pp. 1619–1640, 2003.

[49] H. Yibo, H. Li, X. Chen, C. Xue, C. Chen, and G. Liu, "Effects of moisture content in fuel on thermal performance and emission of biomass semi-gasified cookstove," *Energy for Sustainable Development*, vol. 21, no. 1, pp. 60–65, 2014.

[50] T. B. Reed, E. Anselmo, and K. Kircher, "Testing & Modeling the Wood-Gas Turbo Stove," in *Progress in Thermochemical Biomass Conversion Conference* (A. Bridgwater, ed.), (Bodmin), pp. 693–704, Blackwell Science Ltd, 2001.

[51] M. Indren, N. Cheruvu, C. Birzer, and P. Medwell, "Biochar production and characterisation - A field study," *GHTC 2017 Proceedings - IEEE Global Humanitarian Technology Conference*, 2017.

[52] EBC (2012), "European Biochar Certificate - Guidelines for a Sustainable Production of Biochar," tech. rep., European Biochar Foundation (EBC), Arbaz, Switzerland, 2017.

[53] IBI-STD-2.1, "Standardized Product Definition and Product Testing Guidelines for Biochar That Is Used in Soil," tech. rep., International Biochar Initiative, 2015.

[54] H. K. Nsamba, S. E. Hale, G. Cornelissen, and R. T. Bachmann, "Designing and Performance Evaluation of Biochar Production in a Top-Lit Updraft Upscaled Gasifier," *Journal of Sustainable Bioenergy Systems*, vol. 5, no. 2, pp. 41–55, 2015.

[55] A. Williams, J. Jones, L. Ma, and M. Pourkashanian, "Pollutants from the

combustion of solid biomass fuels," *Progress in Energy and Combustion Science*, vol. 38, no. 2, pp. 113–137, 2012.

[56] S. V. Vassilev, D. Baxter, L. K. Andersen, C. G. Vassileva, and T. J. Morgan, "An overview of the organic and inorganic phase composition of biomass," *Fuel*, vol. 94, pp. 1–33, 2012.

[57] S. V. Vassilev, D. Baxter, and C. G. Vassileva, "An overview of the behaviour of biomass during combustion: Part I. Phase-mineral transformations of organic and inorganic matter," *Fuel*, vol. 112, pp. 391–449, 2013.

[58] S. Du, H. Yang, K. Qian, X. Wang, and H. Chen, "Fusion and transformation properties of the inorganic components in biomass ash," *Fuel*, vol. 117, pp. 1281–1287, 2014.

[59] L. L. Baxter, "Ash deposition during biomass and coal combustion: A mechanistic approach," *Biomass and Bioenergy*, vol. 4, no. 2, pp. 85–102, 1993.

[60] K. Froment, F. Defoort, C. Bertrand, J. M. Seiler, J. Berjonneau, and J. Poirier, "Thermodynamic equilibrium calculations of the volatilization and condensation of inorganics during wood gasification," *Fuel*, vol. 107, pp. 269–281, 2013.

[61] X. Wei, U. Schnell, and K. R. G. Hein, "Behaviour of gaseous chlorine and alkali metals during biomass thermal utilisation," *Fuel*, vol. 84, pp. 841–848, 2005.

[62] Y. Huang, H. Liu, H. Yuan, X. Zhuang, S. Yuan, X. Yin, and C. Wu, "Release and Transformation Pathways of Various K Species during Thermal Conversion of Agricultural Straw. Part 1: Devolatilization Stage," *Energy and Fuels*, vol. 32, pp. 9605–9613, 2018.

[63] J. M. Johansen, J. G. Jakobsen, F. J. Frandsen, and P. Glarborg, "Release of K, Cl, and S during pyrolysis and combustion of high-chlorine biomass," *Energy and Fuels*, vol. 25, no. 11, pp. 4961–4971, 2011.

[64] L. Wang, G. Skjevrak, Ø. Skreiberg, H. Wu, H. K. Nielsen, and J. E. Hustad, "Investigation on Ash Slagging Characteristics during Combustion of Biomass Pellets and Effect of Additives," *Energy and Fuels*, vol. 32, no. 4, pp. 4442–4452, 2018.

[65] A. Burton and H. Wu, "Influence of biomass particle size on bed agglomeration during biomass pyrolysis in fluidised bed," *Proceedings of the Combustion Institute*, vol. 34, pp. 2199–2205, 2017.

[66] P. Raman, J. Murali, D. Sakthivadivel, and V. S. Vigneswaran, "Performance evaluation of three types of forced draft cook stoves using fuel wood and coconut shell," *Biomass and Bioenergy*, vol. 49, pp. 333–340, 2013.

[67] T. Nussbaumer, "Combustion and Co-combustion of Biomass: Fundamentals, Technologies, and Primary Measures for Emission Reduction," *Energy and Fuels*, vol. 17, no. 6, pp. 1510–1521, 2003.

[68] C. Olm, I. G. Zsély, T. Varga, H. J. Curran, and T. Turányi, "Comparison of the performance of several recent syngas combustion mechanisms," *Combustion and Flame*, vol. 162, no. 5, pp. 1793–1812, 2015.

[69] T. C. Lieuwen, V. Yang, and R. A. Yetter, eds., *Synthesis Gas*. Boca Raton: Taylor & Francis, 2009.

[70] L. Wang, C. L. Weller, D. D. Jones, and M. A. Hanna, "Contemporary issues in thermal gasification of biomass and its application to electricity and fuel production," *Biomass and Bioenergy*, vol. 32, no. 7, pp. 573–581, 2008.

[71] F. Battin-Leclerc, J. M. Simmie, and E. Blurock, *Cleaner Combustion - Developing Detailed Chemical Kinetic Models*. London: Springer, 2013.

[72] T. Lieuwen, V. McDonell, E. Petersen, and D. Santavicca, "Fuel Flexibility Influences on Premixed Combustor Blowout, Flashback, Autoignition, and Stability," *Journal of Engineering for Gas Turbines and Power*, vol. 130, pp. 011506–1 – 011506–10, 2008.

[73] Y. Ju, G. Masuya, and P. D. Ronney, "Effects of radiative emissions and absorption on the propagation and extinction of premixed gas flames," *Symposium (International) on Combustion*, pp. 2619–2626, 1998.

[74] O. Park and E. M. Fisher, "Effect of Oxycombustion Diluents on the Extinction of Nonpremixed Methane Opposed-Jet Flames," *Combustion Science and Technology*, vol. 188, no. 3, pp. 370–388, 2016.

[75] D. L. Zhu, F. N. Egolfopoulos, and C. K. Law, "Experimental and numerical determination of laminar flame speeds of methane/(Ar, N2, CO2)-air mixtures as function of stoichiometry, pressure, and flame temperature," *Symposium (International) on Combustion*, vol. 22, no. 1, pp. 1537–1545, 1989.

[76] Z. Chen, X. Qin, B. Xu, Y. Ju, and F. Liu, "Studies of radiation absorption on flame speed and flammability limit of CO2 diluted methane flames at elevated pressures," *Proceedings of the Combustion Institute*, vol. 31, pp. 2693–2700, 2007.

[77] Z. Tan, *Air Pollution and Greenhouse Gases - From Basic Concepts to Engineering Applications for Air Emission Control*. Singapore: Springer, 2014.

[78] J. Jetter, Y. Zhao, K. R. Smith, B. Khan, T. Yelverton, P. DeCarlo, and M. D. Hays, "Pollutant emissions and energy efficiency under controlled conditions for household biomass cookstoves and implications for metrics useful in setting

international test standards," *Environmental Science and Technology*, vol. 46, no. 19, pp. 10827–10834, 2012.

[79] J. J. Jetter and P. Kariher, "Solid-fuel household cook stoves: Characterization of performance and emissions," *Biomass and Bioenergy*, vol. 33, no. 2, pp. 294–305, 2009.

[80] I. Glassman, R. A. Yetter, and N. G. Glumac, "Combustion of nonvolatile fuels," in *Combustion*, ch. 9, pp. 495–551, Elsevier, fifth ed., 2015.

[81] P. Glarborg, J. A. Miller, B. Ruscic, and S. J. Klippenstein, "Modeling nitrogen chemistry in combustion," *Progress in Energy and Combustion Science*, vol. 67, pp. 31–68, 2018.

[82] J. A. Wünning and J. G. Wünning, "Flameless oxidation to reduce thermal NO-formation," *Progress in Energy and Combustion Science*, vol. 23, no. 1, pp. 81–94, 1997.

[83] J. M. Jones, A. R. Lea-Langton, L. Ma, M. Pourkashanian, and A. Williams, *Pollutants Generated by the Combustion of Solid Biomass Fuels*. London: Springer, 2014.

[84] T. C. Bond and R. W. Bergstrom, "Light Absorption by Carbonaceous Particles: An Investigative Review," *Aerosol Science and Technology*, vol. 40, no. 1, pp. 27–67, 2006.

[85] B. S. Haynes and H. G. Wagner, "Soot Formation," *Progress in Energy and Combustion Science*, vol. 7, pp. 229–273, 1981.

[86] G. Blanquart and H. Pitsch, "Analyzing the effects of temperature on soot formation with a joint volume-surface-hydrogen model," *Combustion and Flame*, vol. 156, no. 8, pp. 1614–1626, 2009.

[87] J. A. Koziński and R. Saade, "Effect of biomass burning on the formation of soot particles and heavy hydrocarbons. An experimental study," *Fuel*, vol. 77, no. 4, pp. 225–237, 1998.

[88] T. Kim and Y. Kim, "Interactive transient flamelet modeling for soot formation and oxidation processes in laminar non-premixed jet flames," *Combustion and Flame*, vol. 162, no. 5, pp. 1660–1678, 2015.

[89] E. M. Fitzpatrick, K. D. Bartle, M. L. Kubacki, J. M. Jones, M. Pourkashanian, A. B. Ross, A. Williams, and K. Kubica, "The mechanism of the formation of soot and other pollutants during the co-firing of coal and pine wood in a fixed bed combustor," *Fuel*, vol. 88, no. 12, pp. 2409–2417, 2009.

[90] M. Frenklach, D. W. Clary, W. C. Gardiner, and S. E. Stein, "Detailed kinetic modeling of soot formation in shock-tube pyrolysis of acetylene," *Symposium (International) on Combustion*, vol. 20, no. 1, pp. 887–901, 1985.

[91] M. Frenklach, "Reaction mechanism of soot formation in flames," *Physical Chemistry Chemical Physics*, vol. 4, no. 11, pp. 2028–2037, 2002.

[92] A. Indarto, A. Giordana, and G. Ghigo, "Formation of PAHs and soot platelets: multiconfiguration theoretical study of the key step in the ring closure – radical breeding polyyne-based mechanism," *Journal of Physical Organic Chemistry*, vol. 23, pp. 400–410, 2010.

[93] M. Lu and J. A. Mulholland, "PAH Growth from the pyrolysis of CPD, indene and naphthalene mixture," *Chemosphere*, vol. 55, no. 4, pp. 605–610, 2004.

[94] C. S. McEnally, L. D. Pfefferle, B. Atakan, and K. Kohse-Höinghaus, "Studies of aromatic hydrocarbon formation mechanisms in flames: Progress towards closing the fuel gap," *Progress in Energy and Combustion Science*, vol. 32, no. 3, pp. 247–294, 2006.

[95] J. M. Wilson, M. T. Baeza-Romero, J. M. Jones, M. Pourkashanian, A. Williams, A. R. Lea-Langton, A. B. Ross, and K. D. Bartle, "Soot Formation from the Combustion of Biomass Pyrolysis Products and a Hydrocarbon Fuel, n -Decane: An Aerosol Time Of Flight Mass Spectrometer (ATOFMS) Study," *Energy and Fuels*, vol. 27, no. 3, pp. 1668–1678, 2013.

[96] P. Glarborg, "Hidden interactions—Trace species governing combustion and emissions," *Proceedings of the Combustion Institute*, vol. 31, pp. 77–98, 2007.

[97] J. Pagels, D. D. Dutcher, M. R. Stolzenburg, P. H. Mcmurry, M. E. Gälli, and D. S. Gross, "Fine-particle emissions from solid biofuel combustion studied with single-particle mass spectrometry: Identification of markers for organics, soot, and ash components," *Journal of Geophysical Research Atmospheres*, vol. 118, no. 2, pp. 859–870, 2013.

[98] H. Wiinikka and R. Gebart, "Critical parameters for particle emissions in small-scale fixed-bed combustion of wood pellets," *Energy and Fuels*, vol. 18, no. 4, pp. 897–907, 2004.

[99] S. B. Liaw, X. Chen, Y. Yu, M. Costa, and H. Wu, "Effect of particle size on particulate matter emissions during biosolid char combustion under air and oxyfuel conditions," *Fuel*, vol. 232, pp. 251–256, 2018.

[100] S. B. Liaw, C. Deng, and H. Wu, "A Novel Two-Stage Alumina Reactor System for Burning Volatiles Generated in Situ from Biosolid: Effect of Pyrolysis Temperature and Combustion Conditions on PM1 Emission," *Energy and Fuels*, vol. 32, no. 9, pp. 9438–9447, 2018.

[101] S. B. Liaw and H. Wu, "High-Phosphorus Fuel Combustion: Effect of Oxyfuel Conditions on PM10 Emission from Homo- and Heterogeneous Phases," *Energy and Fuels*, vol. 31, no. 3, pp. 2317–2323, 2017.

[102] X. Chen, S. B. Liaw, and H. Wu, "Important role of volatile - char interactions in enhancing PM1 emission during the combustion of volatiles from biosolid," *Combustion and Flame*, vol. 182, pp. 90–101, 2017.

[103] C. Feng, M. Zhang, and H. Wu, "Trace Elements in Various Individual and Mixed Biofuels: Abundance and Release in Particulate Matter during Combustion," *Energy and Fuels*, vol. 32, no. 5, pp. 5978–5989, 2018.

[104] Y. Wang, H. Wu, Z. Sárossy, C. Dong, and P. Glarborg, "Release and transformation of chlorine and potassium during pyrolysis of KCl doped biomass," *Fuel*, vol. 197, pp. 422–432, 2017.

[105] J. F. Roesler, R. A. Yetter, and F. L. Dryer, "Detailed Kinetic Modeling of Moist CO Oxidation Inhibited by Trace Quantities of HCl," *Combustion Science and Technology*, vol. 85, pp. 1–22, 1992.

[106] J. F. Roesler, R. A. Yetter, and F. L. Dryer, "The Inhibition of the CO / H2O / O2 Reaction by Trace Quantities of HCl," *Combustion Science and Technology*, vol. 82, no. 1-6, pp. 87–100, 1992.

[107] J. F. Roesler, R. A. Yetter, and F. L. Dryer, "Perturbation of Moist CO Oxidation by Trace Quantities of CH3Cl," *Combustion Science and Technology*, vol. 101, pp. 199–229, 1994.

[108] M. A. MacDonald, *Inhibition of Non-Premixed Flames by Phosphorus-Containing Compounds*. PhD thesis, Cornell University, 2000.

[109] T. M. Jayaweera, E. M. Fisher, and J. W. Fleming, "Flame suppression by aerosols derived from aqueous solutions containing phosphorus," *Combustion and Flame*, vol. 141, no. 3, pp. 308–321, 2005.

[110] A. S. Feitelberg, J. P. Longwell, and A. F. Sarofim, "Metal enhanced soot and PAH formation," *Combustion and Flame*, vol. 92, no. 3, pp. 241–253, 1993.

[111] H. S. Mukunda, S. Dasappa, P. J. Paul, N. K. S. Rajan, M. Yagnaraman, D. Ravi Kumar, and M. Deogaonkar, "Gasifier stoves – science, technology and field outreach," *Current Science*, vol. 98, no. 5, pp. 627–638, 2010.

[112] S. Amrose, "Development and Testing of the Berkeley Darfur Stove," tech. rep., Lawrence Berkeley National Laboratory, 2008.

[113] N. A. MacCarty and K. M. Bryden, "A unified set of experimental data for cylindrical, natural draft, shielded, single pot, wood-fired cookstoves," *Energy for Sustainable Development*, vol. 26, pp. 62–71, 2015.

[114] N. A. MacCarty and K. M. Bryden, "An integrated systems model for energy services in rural developing communities," *Energy*, vol. 113, pp. 536–557, 2016.

[115] N. A. MacCarty, D. Ogle, D. Still, T. C. Bond, C. Roden, and B. Willson, "Laboratory comparison of the global-warming potential of six categories of biomass cooking stoves," tech. rep., Aprovecho Research Center, 2007.

[116] M. P. Kshirsagar and V. R. Kalamkar, "A comprehensive review on biomass cookstoves and a systematic approach for modern cookstove design," *Renewable and Sustainable Energy Reviews*, vol. 30, pp. 580–603, 2014.

[117] E. J. Leijenhorst, W. Wolters, B. Van De Beld, and W. Prins, "Staged Biomass Gasification by Autothermal Catalytic Reforming of Fast Pyrolysis Vapors," *Energy and Fuels*, vol. 29, no. 11, pp. 7395–7407, 2015.

[118] J. J. Caubel, V. H. Rapp, S. S. Chen, and A. J. Gadgil, "Optimization of Secondary Air Injection in a Wood-Burning Cookstove: an Experimental Study," *Environmental Science and Technology*, vol. 52, pp. 4449–4456, 2018.

[119] V. H. Rapp, J. J. Caubel, D. L. Wilson, and A. J. Gadgil, "Reducing Ultrafine Particle Emissions Using Air Injection in Wood-Burning Cookstoves," *Environmental Science and Technology*, vol. 50, no. 15, pp. 8368–8374, 2016.

[120] N. A. MacCarty, D. Still, D. Ogle, and T. Drouin, "Assessing Cook Stove Performance: Field and Lab Studies of Three Rocket Stoves Comparing the Open Fire and Traditional Stoves in Tamil Nadu, India on Measures of Time to Cook, Fuel Use, Total Emissions, and Indoor Air Pollution," tech. rep., Aprovecho Research Center, 2008.

[121] N. A. MacCarty, D. Still, and D. Ogle, "Fuel use and emissions performance of fifty cooking stoves in the laboratory and related benchmarks of performance," *Energy for Sustainable Development*, vol. 14, no. 3, pp. 161–171, 2010.

[122] D. Still, N. A. MacCarty, D. Ogle, T. Bond, and M. Bryden, "Test Results of Cook Stove Performance," tech. rep., Aprovecho Research Center, 2011.

[123] M. Kumar, S. Kumar, and S. K. Tyagi, "Design, development and technological advancement in the biomass cookstoves: A review," *Renewable and Sustainable Energy Reviews*, vol. 26, pp. 265–285, 2013.

[124] P. S. Arora and S. Jain, "Estimation of organic and elemental carbon emitted from wood burning in traditional and improved cookstoves using controlled cooking test," *Environmental Science and Technology Technology*, vol. 49, pp. 3958 – 3965, 2015.

[125] M. Deng, S. Zhang, M. Shan, J. Li, J. Baumgartner, E. Carter, and X. Yang, "The impact of cookstove operation on PM2.5 and CO emissions: A comparison of laboratory and field measurements," *Environmental Pollution*, vol. 243, pp. 1087–1095, 2018.

[126] C. Venkataraman and G. U. M. Rao, "Emission factors of carbon monoxide and size-resolved aerosols from biofuel combustion," *Environmental Science and Technology*, vol. 35, no. 10, pp. 2100–2107, 2001.

[127] K. R. Smith, R. Uma, V. V. N. Kishore, K. Lata, V. Joshi, J. Zhang, R. Rasmussen, and M. Khalil, "Greenhouse gases from small-scale combustion devices in developing countries: Phase IIA; Household Stoves in India," tech. rep., United States Environmental Protection Agency, Washington, 2000.

[128] G. Shen, S. Tao, S. Wei, Y. Zhang, R. Wang, B. Wang, W. Li, H. Shen, Y. Huang, Y. Chen, H. Chen, Y. Yang, W. Wang, W. Wei, X. Wang, W. Liu, X. Wang, and S. L. Simonich, "Reductions in emissions of carbonaceous particulate matter and polycyclic aromatic hydrocarbons from combustion of biomass pellets in comparison with raw fuel burning," *Environmental Science and Technology*, vol. 46, no. 11, pp. 6409–6416, 2012.

[129] Z. Zongxi, S. Zhenfeng, Z. Yinghua, D. Hongyan, Z. Yuguang, Y. X. Zhang, A. Riaz, C. Pemberton Pigott, and D. Renjie, "Effects of biomass pellet composition on the thermal and emissions performances of a TLUD cooking stove," *International Journal of Agricultural and Biological Engineering*, vol. 10, no. 4, pp. 189–197, 2017.

[130] D. K. Still, S. Bentson, N. Murray, J. Andres, Z. Yue, and N. A. MacCarty, "Laboratory experiments regarding the use of filtration and retained heat to reduce particulate matter emissions from biomass cooking," *Energy for Sustainable Development*, vol. 42, pp. 129–135, 2018.

[131] C. Schmidl, M. Luisser, E. Padouvas, L. Lasselsberger, M. Rzaca, C. Ramirez-Santa Cruz, M. Handler, G. Peng, H. Bauer, and H. Puxbaum, "Particulate and gaseous emissions from manually and automatically fired small scale combustion systems," *Atmospheric Environment*, vol. 45, no. 39, pp. 7443–7454, 2011.

[132] C. A. Roden, T. C. Bond, S. Conway, A. B. Osorto Pinel, N. A. MacCarty, and D. Still, "Laboratory and field investigations of particulate and carbon

monoxide emissions from traditional and improved cookstoves," *Atmospheric Environment*, vol. 43, no. 6, pp. 1170–1181, 2009.

[133] N. G. Johnson and K. M. Bryden, "The impact of cookstove adoption and replacement on fuelwood savings," *Proceedings - 2012 IEEE Global Humanitarian Technology Conference*, pp. 387–391, 2012.

[134] N. D. Moses, N. A. MacCarty, and M. H. Pakravan, "Development of a Practical Evaluation for Cookstove Usability," *Energy for Sustainable Development*, vol. 48, pp. 154–163, 2018.

[135] N. A. MacCarty and K. M. Bryden, "Modeling of household biomass cookstoves: A review," *Energy for Sustainable Development*, vol. 26, pp. 1–13, 2015.

[136] S. B. Kausley and A. B. Pandit, "Modelling of solid fuel stoves," *Fuel*, vol. 89, no. 3, pp. 782–791, 2010.

[137] I. Haberle, *Numerical simulation of transient behavior of wood log decomposition and combustion.* PhD thesis, Norwegian University of Science and Technology, 2018.

[138] J. Tryner, *Combustion Phenomena in Biomass Gasifier Cookstoves.* PhD thesis, Colorado State University, 2016.

[139] A. M. James R, *Simultaneous Biochar and Syngas Production in a Top-Lit Updraft Biomass Gasifier.* PhD thesis, North Carolina State University, 2015.

[140] C. Roth, "Micro-gasification : cooking with gas from dry biomass," tech. rep., GIZ - Deutsche Gesellschaft fuer Internationale Zusammenarbeit, Eschborn, 2014.

[141] T. B. Reed and R. Larson, "A wood-gas stove for developing countries," *Energy for Sustainable Development*, vol. 3, no. 2, pp. 34–37, 1996.

[142] S. Varunkumar, N. K. S. Rajan, and H. S. Mukunda, "Single Particle and Packed Bed Combustion in Modern Gasifier Stoves - Density Effects," *Combustion Science and Technology*, vol. 183, no. 11, pp. 1147–1163, 2011.

[143] J. Tryner, B. D. Willson, and A. J. Marchese, "The effects of fuel type and stove design on emissions and efficiency of natural-draft semi-gasifier biomass cookstoves," *Energy for Sustainable Development*, vol. 23, pp. 99–109, 2014.

[144] J. Tryner, J. Volckens, and A. J. Marchese, "Effects of operational mode on particle size and number emissions from a biomass gasifier cookstove," *Aerosol Science and Technology*, vol. 52, no. 1, pp. 87–97, 2018.

[145] P. Raman, N. K. Ram, and R. Gupta, "Development, design and performance analysis of a forced draft clean combustion cookstove powered by a thermo electric generator with multi-utility options," *Energy*, vol. 69, pp. 813–825, 2014.

[146] E. M. Carter, M. Shan, X. Yang, J. Li, and J. Baumgartner, "Pollutant emissions and energy efficiency of chinese gasifier cooking stoves and implications for future intervention studies," *Environmental Science and Technology*, vol. 48, no. 11, pp. 6461–6467, 2014.

# Chapter 4

---

# Influence of Primary and Secondary Air Supply on Gaseous Emissions from a Small-Scale Staged Solid Biomass Fuel Combustor

---

## Statement of Authorship

| | |
|---|---|
| Paper Title: | Influence of Primary and Secondary Air Supply on Gaseous Emissions from a Small-Scale Staged Solid Biomass Fuel Combustor |
| Status: | Published |
| Details: | *Energy & Fuels*, vol. 32, pp. 4212–4220<br><br>DOI: 10.1021/acs.energyfuels.7b03152 |

### Principal Author

| | |
|---|---|
| Name: | Thomas Kirch |
| Contribution: | Performed an extensive literature review. The particular application in resource constraints communities has an important influence that was considered from development of the research questions through the reactor design to the analysis of the performance, for potential optimisation of future cookstove designs. As this work deals with gaining a deeper understanding of the combustion processes, a clear focus is placed on these aspects. Multiple figures were developed to provide an in-depth description of the process, of the utilised combustor and of the analysis methods. The codes for data processing, as well as their analysis and interpretation were written. Developed, structured, wrote and edited the manuscript. Acted as corresponding author. |
| Contribution Percentage (%): | 70 |
| Certification: | This paper reports on original research I conducted during the period of my Higher Degree by Research candidature and is not subject to any obligations or contractual agreements with a third party that would constrain its inclusion in this thesis. I am the primary author of this paper. |
| Signature: | Date: **28.02.2019** |

**Co-Author Contributions**

By signing the Statement of Authorship, each author certifies that:

1. the candidate's stated contribution to the publication is accurate (as detailed above);

2. permission is granted for the candidate to include the publication in the thesis; and

3. the sum of all co-author contributions is equal to 100% less the candidates stated contribution.

| | |
|---|---|
| Name: | Cristian H. Birzer |
| Contribution Details: | Guided research direction. Supervised work development. Helped generate ideas for tests and edited manuscript. |
| Signature: | Date: **28 Feb 2019** |

| | |
|---|---|
| Name: | Philip J. van Eyk |
| Contribution Details: | Guided research direction. Supervised work development. Helped generate ideas for tests and edited manuscript. |
| Signature: | Date: *28 Feb 2019* |

| | |
|---|---|
| Name: | Paul R. Medwell |
| Contribution Details: | Guided research direction. Supervised work development. Helped generate ideas for tests and edited manuscript. |
| Signature: | Date: **28 Feb 2019** |

# Influence of Primary and Secondary Air Supply on Gaseous Emissions from a Small-Scale Staged Solid Biomass Fuel Combustor

Thomas Kirch,[*,†,‡] Cristian H. Birzer,[†,‡] Philip J. van Eyk,[‡,§] and Paul R. Medwell[†,‡]

[†]School of Mechanical Engineering, [§]School of Chemical Engineering, and [‡]Humanitarian and Development Solutions Initiative, The University of Adelaide, Adelaide, South Australia 5005, Australia

**ABSTRACT:** The emissions from traditional biomass combustion systems for cooking and heating are, globally, the main cause for premature mortality as a result of air pollution. A staged combustion process that separates the thermochemical conversion of the solid fuel and the combustion of the released products offers potential to reduce harmful emissions for solid fuel combustion and could, therefore, help mitigate the issue. In the present study, the fundamental combustion behavior of a small-scale staged combustor was investigated, with a focus on an independent systematic analysis of relevant parameters. Natural and forced draft conditions as well as a combination of both were tested. The relative location of primary to secondary air was also varied. When lighting the fuel, higher air flows lead to faster ignition and lower emissions. A steady-state combustion phase is achieved when gasification products are burned with secondary air, which occurs mainly while the solid fuel is being pyrolyzed. After the steady-state phase, char remains as the solid pyrolysis product. Gasification of the remaining char was found to release great amounts of CO, which are emitted from the combustor, in the case of natural draft secondary air (SA). With higher air flows of forced SA, an exceptionally high nominal combustion efficiency $[NCE = X_{CO_2}/(X_{CO} + X_{CO_2})]$ can be achieved in the steady-state phase. Forced SA flows cause a longer duration of the steady-state phase from the combustion of raw biomass gasification products into the combustion of char gasification products. This extension leads to a significant reduction of emissions of incomplete combustion. Additionally, smaller distances between the SA inlet and the fuel stack caused lower emissions of incomplete combustion. The combination of forced draft primary air and natural draft SA presented worse combustor performance than under natural draft conditions.

## 1. INTRODUCTION

Approximately 2.8 billion people currently rely on solid biomass fuel to satisfy their cooking and heating needs.[1] Globally, emissions caused by the use of traditional open fires or simple cookstoves are the main cause of premature mortality as a result of air pollution.[2] This includes 2.89 million and 2.93 million premature deaths annually related to household air pollution from solid fuels and ambient particulate matter (PM) pollution, respectively.[3] These findings illustrate the need for clean-burning cooking devices. A reduction of the amount of pollutant emissions released from incomplete combustion through traditional cooking methods could lead to not only health improvements but also social as well as environmental benefits.[4,5]

Staged combustors have demonstrated promising results as cookstoves in laboratory studies compared to other cookstoves. This type of combustor has been shown to produce low emissions of incomplete combustion, carbon monoxide (CO) and PM, in cooking applications.[6,7] Other emissions, such as nitric oxides (NO$_x$), can also be reduced through staged combustion.[8] The main feature that sets them apart from other types of combustors is the use of pyrolysis and gasification to transform the batch-fed solid biomass fuel into combustible gases, which are subsequently burned separately in time and location.[9] The measurement of gaseous combustion products can provide valuable information to gain a better understanding of the ongoing processes.

The two-staged combustion process is initiated by lighting the fuel from the top with the aid of a kindling material. Lighting has been identified as a major source of emissions of incomplete combustion, where the higher heating value of the kindling material and also the supply of forced air can be beneficial.[10] Lighting causes the combustion of the top layer of solid biomass and consumes oxygen in the combustor, creating a vitiated environment, leading to a so-called "migrating pyrolysis front" to establish, in which only partial oxidation occurs. This front moves opposite to the primary air (PA) flow, down the fuel stack. Simultaneously, the pyrolysis products are burned separately at a secondary air (SA) inlet.[11] This separation of pyrolysis and combustion processes is illustrated in Figure 1. The remaining char, which accounts for 20−30% of the initial mass,[12−14] can subsequently be burned or used for other purposes, such as soil amendment.[15] Three successive processes are most prominent in staged biomass combustors: the lighting of kindling material at the top of the fuel stack, the migrating pyrolysis, where the release and combustion of volatile compounds prevails, and the char gasification, where the remaining char is converted into CO and CO$_2$ through surface oxidation. A systematic analysis of each of these phases could aid in decoupling processes to analyze individual parameters in isolation.

The migrating pyrolysis front propagation and, thus, the fuel conversion as well as the heat release are controlled by the supply of PA.[12,16−23] It has been shown that forced air can lead to a reduction of emissions of incomplete combustion.[24−26] Con-
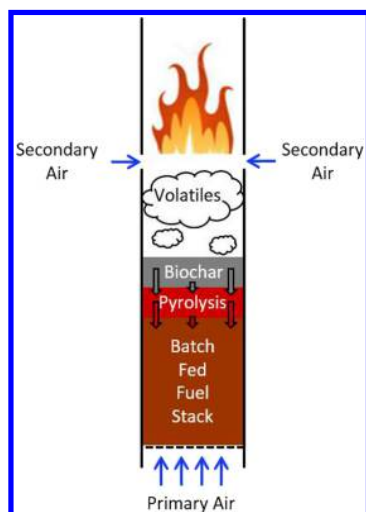
**Figure 1.** Schematic illustration of the combustion process in the staged combustor.

versely, in some cases, it is possible that forced air staged combustion stoves, although energy-efficient, may not necessarily reduce emissions.[27] These contradictory findings reinforce the need for a deeper understanding of the underlying processes to ensure emission efficiency of future stove designs.

There is widespread belief that forced air compared to natural draft leads to greater mixing and, thus, increased performance.[28,29] Many forced draft stoves are equipped with one single fan that supplies air to both the PA and SA inlets. The ratio of PA/SA is then fixed, dependent upon the stove geometry.[11] However, a few studies have been concerned with the influence of PA[28,30−32] or the ratio of PA/SA[28,29,31,32] on the combustion properties of the combustor. There is a paucity of scientific understanding of such systems and the parameters that control the emissions. In particular, the influence of SA flows as well as the relative location to the PA flow are poorly understood in small-scale staged combustion systems. In continuously fed domestic biomass boilers, iterative parametric investigation of the staged air supply has been found to provide means to decrease specific emissions[8,33,34] and could provide similar benefits for the studied combustion system.

The present parametric study was carried out in a research combustor to study and gain a deeper understanding of the ongoing fundamental processes in small-scale staged combustion devices. Preliminary tests under natural draft conditions set a baseline against which alterations can be compared. Subsequently a combination of forced PA and natural draft SA are tested. Because the required air supply will change throughout the different combustion phases, it might be advantageous to entrain the SA via natural draft. Further tests are conducted with a specified PA flow and variable SA flow, to study the influence of an increasing air flow on the emissions of the combustion process. The relative location of the SA inlet to the fuel stack is also considered. With a fixed location of the SA inlet, a varying distance of the air supply to the fuel might have an influence on the stove performance.

In most research on cooking devices that use biomass fuel, the overall stove efficiency is determined through tests that emulate user practices. This approach is dependent upon a multitude of variables, including the combustion and heat transfer properties as well as handling by the user, which has been shown to lead to high variability of results.[35,36] This paper focuses solely on the

fundamental combustion properties of a small-scale staged combustor, enabling a more independent analysis of relevant parameters. Specifically, the focus of the current work is on the role of the PA and SA supply and their locations relative to the fuel bed. A deeper understanding of the underlying combustion properties could enable future optimization of such devices, which is the motivation of this research.

## 2. EXPERIMENTAL DETAILS

**2.1. Staged Combustor.** The research combustor used in the current work has previously been presented[32,37] and shown in Figure 2.
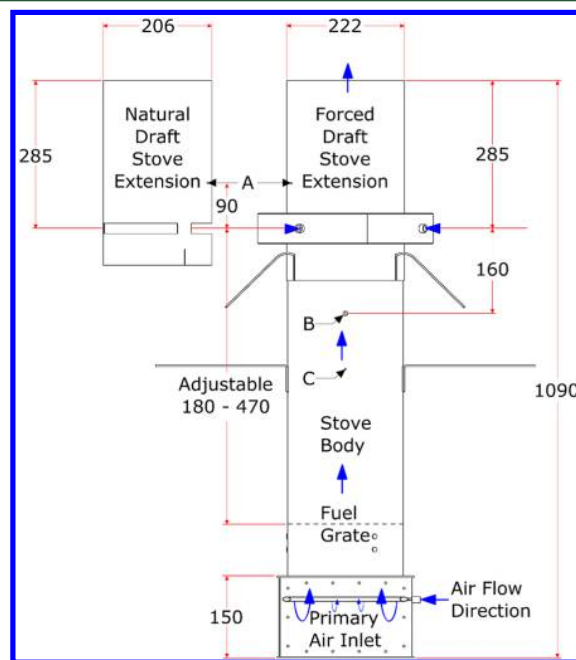


**Figure 2.** Schematic diagram of the combustor, with inlet locations for thermocouples (A and B) and measuring location of the outer combustor body temperature (C), with the air flow direction and all numeric values in millimeters.

It incorporates the principal features of a PA inlet at the bottom of the combustor and a lateral SA inlet in the upper region. Its dimensions were chosen to be slightly larger than many commercial products [e.g., the Champion top-lit up-draft (TLUD)[11]], especially the height. This increased size enables an investigation of scaling effects over a wider range of combustion-relevant parameters, such as the fuel grate (FG) location. Importantly, the large diameter of the vessel provides a nearly one-dimensional reactor to facilitate subsequent modeling. The research combustor has been designed to advance the fundamental-level understanding and to study the underlying physical processes. Thus, the combustor will be used to assess the combustion properties and not the cooking performance. It is important to recognize that the current system does not include a pot on top of the stove. If the secondary flame front was to interact with such a pot, localized quenching could occur and, subsequently, lead to an increase in the emission of the products of incomplete combustion. However, with proper design and operation of a stove, such effects would ideally not occur in an operational stove.

The steel cylinder combustor body has a diameter of 206 mm, a height of 600 mm, and a wall thickness of 8 mm. Inside the combustor body, the FG, on which the fuel is placed, is held via three hooks. These are attached to the rim of the combustor body; the FG location is variable by adjusting the length of these hooks between 50 and 570 mm below the SA inlet. The hooks enable the grate to be easily removable from the combustor for post-combustion analysis of the solid residual matter as well as cleaning. The grate is perforated with 3 mm diameter

holes, with an open-area ratio of 26%, which allows PA from beneath the grate to enter the fuel stack. The combustor body is placed on top of the PA inlet chamber.

*2.1.1. PA Configurations.* The PA inlet chamber (dimensions of 248 × 248 × 150 mm) is equipped with removable side walls. When the side walls are taken off, the air can enter freely over the whole combustor body diameter via natural draft, and if closed off, air can be applied through a controlled inlet. In the natural draft configuration, the amount of air that enters is determined by the buoyancy force as a result of the pressure difference over the combustor height during the combustion process. In the forced air configuration, the sides of the chamber are closed off and the inlet is connected to dry compressed air. The in-flow is controlled by a needle valve and a rotameter upstream of the inlet. Downstream of the inlet, air passes through a diffuser ring with ten 1 mm diameter holes. These holes in the diffuser are directed downward, which forces the air flow to be inverted before entering the combustor body. The inversion of the PA flow leads to less swirl and a more uniform air flow through the combustor body. Subsequently, the flow through the combustor body is influenced by the porous fuel bed. The air flow through the direction in the combustor is presented in Figure 2. In the present study, tests were performed in the natural draft as well as the forced air configuration.

*2.1.2. SA Configurations.* The SA enters the combustor through three 190 mm long, 20 mm high, lateral openings. These are located 285 mm below the top of the combustor extension and 55 mm above the exit plane of the combustor body. There are two different configurations that allow air to enter either via natural draft or forced by introducing compressed air. For the natural draft configuration, the three openings of the combustor extension, shown in Figure 2, are open to the surroundings. In the forced air configuration, the inlet is enclosed by a diffuser skirt. The forced air combustor extension has four inlets. All four inlets are connected by hoses of equal length to a manifold. The manifold is situated downstream of a needle valve and rotameter by which the inflow of dried compressed air is regulated. These measures were taken to ensure a uniform flow throughout the skirt to enter the combustor extension. In all forced air configurations, PA and SA are separately controlled via independent air supply lines.

**2.2. Data Collection.** The data collection setup consists of emission data being collected in one central location, while temperature data were constantly measured in two locations. The research combustor was placed under a fume hood, which was connected to an extraction duct and a fan to ensure that all emissions from the combustor were directed outside of the laboratory. The measuring probe of a Testo 350XL gas analyzer was placed 830 mm above the exit plane, along the central axis of the research combustor. This sampling location is at the interface of the fume hood and the extraction duct. The released gases from the research combustor will expand upon leaving the combustor, mix with the surrounding air, and enter into the fume hood. The hood acts as an aerodynamic contraction, reducing the 1060 mm intake down to a diameter of 185 mm at the point that the measurements are collected. The diameter of the fume hood intake compared to the research combustor diameter ensures that all emissions from the reactor are collected. The high contraction ratio of the fume hood promotes intense mixing of the gases, such that the emissions from the combustor are well-mixed by the time that they reach the measurement point. The gas analyzer was used to measure the CO, $CO_2$, and $H_2$ emissions at 1 Hz, on a dry basis. The resolution was 1 ppm for low emission levels (<2000 ppm) and 5 ppm for high emission levels (>2000 ppm) of CO measurements. The resolution for $CO_2$ measurements was 0.01%. For all measurements, unburned hydrocarbons (methane, propane, and butane) were below the detection limit, namely, 100 ppm. Temperature data were collected, at 1 Hz, via two K-type thermocouples inside the combustor body and the combustor extension, shown in Figure 2 at locations A and B, respectively. For procedural purposes, temperatures were measured in location C, when needed, via an infrared thermometer.

**2.3. Test Procedure.** The research combustor, with a wall thickness of 8 mm, has a higher thermal mass than usual cookstoves. It therefore was deemed necessary to ensure that only preheated tests were recorded, to minimize any influence on the combustion performance,

although the process can also be achieved with a cold start. After preheating the combustor, a new batch of fuel was introduced when the outer wall temperature in location C, shown in Figure 2, measured 150 °C. For kindling, 5 mL of methylated spirits (96% ethanol, CAS Registry Number 67-63-0) was poured over the fuel stack and ignited when the outer wall temperature reached 135 °C. The chosen starting wall temperature of 135 °C is below the temperature encountered later in the burn cycle. Therefore, thermal energy from the combustion goes toward increasing the body temperature. However, it is not possible to preheat to a higher temperature both for manual handling safety during the reload process and also to avoid volatilization of the biomass fuel, which starts at approximately 200 °C.[26]

The fuel for each test consisted of 700 g of dried locally sourced pine chips (*Pinus radiata*). The wood chips were obtained from various locations across the Mount Lofty ranges of South Australia. They were sourced in bulk, as pre-chipped material, and sieved through a 25 mm aperture, resulting in an average particle size of 24 × 8 × 3 mm (length × width × height). The bulk density of the dried pine chips is approximately 210 kg m⁻³. This density and amount of fuel used led to a fuel bed height of 100 mm and a test duration of approximately 600 s. While a greater amount of fuel would extend the time spend in the steady-state and char phases, it would not impact the findings. The proximate analysis of the pine chips provided a composition of 16.8% fixed carbon, 82.9% volatile matter, and 0.4% ash mass fractions on a dry basis. The ultimate analysis yielded mass fractions of 51.2% C, 6.2% H, 42.0% O, and 0.2% N on a dry basis. Pine chips were chosen as fuel because wood is the most commonly combusted biomass.[38] The influence of the moisture content has previously been studied[13] and is outside the scope of the presented research study. To avoid the influence of inconsistent moisture content on the burning rate and the emissions,[13] all of the chips were dried prior to testing. This was performed by keeping them for 16 h in a confined space at a constant temperature of 37 °C, created by an air conditioning unit. The drying process resulted in a fuel moisture content of approximately 7% determined via the ASTM D4442-92(2003) standard procedure.[39]

Four sets of tests were conducted with various different configurations presented in Table 1. The first set of tests are performed

**Table 1. Configurations of the Natural Draft (ND), Varying PA, Varying SA, and Varying FG Location below the SA Inlet Cases That Were Tested**

| | repetition | PA flow (L min⁻¹) | SA flow (L min⁻¹) | FG location (mm) | equivalence ratio (Φ) |
|---|---|---|---|---|---|
| both ND | 8 | ND | ND | 470 | |
| varying PA | 5 | 78 | ND | 470 | |
| | 4 | 98 | ND | 470 | |
| | 6 | 118 | ND | 470 | |
| | 6 | 138 | ND | 470 | |
| varying SA | 4 | 118 | 328 | 470 | 1.11 |
| | 3 | 118 | 410 | 470 | 0.94 |
| | 3 | 118 | 492 | 470 | 0.81 |
| | 3 | 118 | 574 | 470 | 0.71 |
| varying FG location | 4 | 118 | ND | 180 | |
| | 3 | 118 | ND | 270 | |
| | 3 | 118 | ND | 370 | |
| | 6 | 118 | ND | 470 | |

with both the PA and SA inlet in natural draft configuration. These natural draft tests can be considered as a baseline against which the various alterations of PA and SA flow can be compared. The following sections provide details about the respective variations within each set of tests.

*2.3.1. PA Testing.* The PA flow is varied, while SA is introduced through natural draft. The PA flow rates are 78, 98, 118, and 138 L min⁻¹, corresponding to 47.0, 59.0, 71.0, and 83.2 g m⁻² s⁻¹, respectively. The flow rates are reported at standard temperature and

pressure (STP) conditions, namely, 0 °C and $10^5$ Pa. These values were chosen in accordance with previous studies on fixed-bed reactors and provide an oxygen-limited environment for the migrating pyrolysis.[16−18,20,21] They are also similar to values and extending the range of a previous study on a similar combustor.[30]

*2.3.2. SA Testing.* For the SA tests, the PA flow was set to a value of 118 L min⁻¹, while SA flows of 328, 410, 492, and 574 L min⁻¹ were injected into the combustor extension. No previous studies have been found in which specified flow rates of SA were introduced into a staged combustor. Therefore, an approximation was performed on the basis of previous findings. It has been reported that, during the migrating pyrolysis, the PA to fuel (A/F) mass ratio settles at about 1.5 for different PA flow rates.[30] From the ultimate analysis, a mole fraction of $C_{1.00}H_{1.45}O_{0.62}$ can be derived for the pine chips, with a respective stoichiometric A/F mass ratio of 6.2 for complete combustion. Assuming an A/F mass ratio of 1.5 during the migrating pyrolysis,[30] the overall fuel equivalence ratio ($\phi$) would be 1.11, 0.94, 0.81, and 0.71 for the different SA air flows. Therefore, fuel-rich conditions can be expected for the 328 L min⁻¹ case, but fuel-lean conditions are expected for all other flow rates.

*2.3.3. Varying FG Location Testing.* The location of the fuel stack within the combustor was varied to change the residence time of the gases within the combustor body. The tests were performed with the FG at distances of 180, 270, 370, and 470 mm below the SA inlet, as presented in Figure 2. The PA flow was set to a constant value 118 L min⁻¹, and the natural draft combustor extension was attached to the combustor body.

**2.4. Data Processing.** To account for dilution and determine a quantitative value for the combustor efficiency, the measured emissions were normalized. This normalization was performed by relating the measured concentrations to all gaseous carbonaceous combustion products. This include the calculation of the nominal combustion efficiency $[NCE = X_{CO_2}/(X_{CO} + X_{CO_2})$, where $X$ is mole fraction], which has been previously established for the evaluation of cookstoves.[40] The only gaseous carbonaceous species that were considered in the normalization were CO and $CO_2$, because the hydrocarbon emissions were below the detection limit.

The three expected phases of operation are (1) the lighting phase, (2) the steady-state phase, and (3) the char phase. Rigorous analysis identified that all three phases could be identified on the basis of the transition between phases. A mathematical decision rule was used to separate the three phases, to be able to analyze each phase separately. When the temporal derivative of the normalized CO profile exceeded a value of ±0.002 s⁻¹, a change in phase was identified. This value was established to be a robust identifier of a change in phase. Figure 3
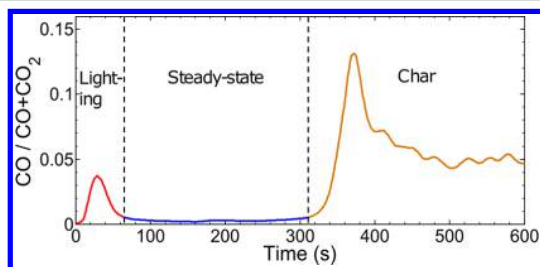


**Figure 3.** Normalized CO emission profile with separated phases by the mathematical decision rule. The phase change was identified when the temporal derivative of the normalized CO profile $[X_{CO}/(X_{CO} + X_{CO_2})]$ exceeded a value of ±0.002 s⁻¹.

presents an example emission profile, divided into the three phases by the mathematical decision rule. For each of the three phases, peak values or time-weighted-average (TWA) values were calculated. In the lighting phase, the average of the peak values over all repeat runs was calculated because this measure is best suited to the transient processes where peaks occur. For the steady-state phase, TWA values provide an average value for the steady emissions. For the char phase, both average peak

values and TWA values were calculated to account for multiple emission peaks experienced in this phase.

## 3. RESULTS

**3.1. Natural Draft.** Preliminary tests were conducted with the research combustor in its natural draft configuration. The results from these natural draft conditions are presented within the figures of the results from the other sets of tests, such that the natural draft case serves as a reference point. In this way, it is possible to see if changing operating parameters can enhance the performance and mitigate emissions of incomplete combustion.

The natural draft tests were used to identify the different combustion phases, the lighting phase, the steady-state phase, and the char phase (as previously described in detail[41]). In the lighting phase, the kindling material is lit on top of the fuel stack, leading to the combustion of the top layer of the solid biomass fuel. In this phase, high emissions of incomplete combustion, namely, CO and $H_2$, were detected, as seen in Figure 4. In the
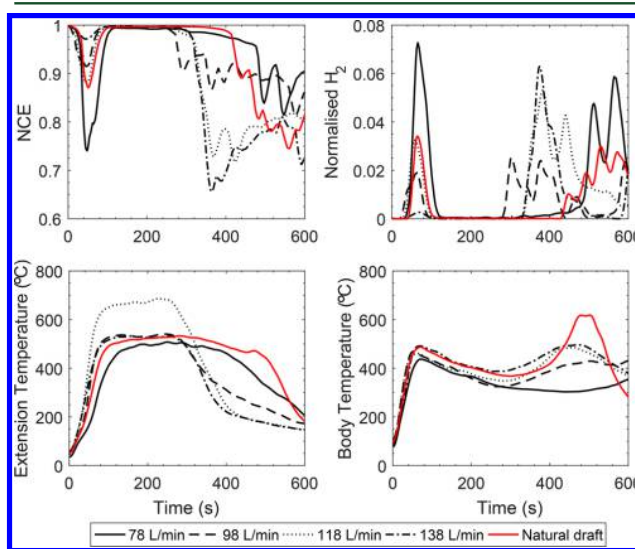


**Figure 4.** Average normalized emission profiles of $H_2$, the nominal combustion efficiency $[NCE = X_{CO_2}/(X_{CO} + X_{CO_2})]$, and measured gas-phase temperature profiles inside the combustor body and the combustor extension for various PA flows and the natural draft case.

steady-state phase, the NCE is very high, accompanied by low emissions of products of incomplete combustion. In the char phase, the NCE decreases significantly and the emissions of CO rise.

**3.2. Variation of PA.** The emissions and gas-phase temperature profiles with varying PA flows and natural draft SA flow are presented in Figure 4. As explained previously, the three combustion processes of lighting in the first 76−102 s, the steady-state combustion in the following 178−281 s, and after that the char gasification were identified. For the measured emissions, average peak values were calculated for the lighting phase and TWA values were calculated for the steady-state as well as char phases, as presented in Table 2.

It can be seen in Figure 4 that, in the lighting phase, the normalized peak NCE and the measured gas-phase temperature inside the combustor body rise, while the normalized $H_2$ emissions subside substantially with an increase in PA flow. This is consistent with a previous study,[10] which also showed that higher air flows lead to a higher rate of combustion. In the natural draft case, the emissions of products of incomplete combustion

**Table 2. Average Peak Emissions in the Lighting Phase and TWA Emissions in the Steady-State and Char Phases for All Four Investigated Cases, with the Standard Deviation in Parentheses**

| | natural draft | varying PA (L min⁻¹) | | | | varying SA (L min⁻¹) | | | | varying FG location (mm) | | | |
|---|---|---|---|---|---|---|---|---|---|---|---|---|---|
| | | 78 | 98 | 118 | 138 | 328 | 410 | 492 | 574 | 180 | 270 | 370 | 470 |
| | | | | | | **Lighting Phase** | | | | | | | |
| minimum NCE | 0.8404 (0.1659) | 0.6155 (0.1424) | 0.8639 (0.1233) | 0.8266 (0.1597) | 0.9631 (0.0124) | 0.9851 (0.0045) | 0.9868 (0.0004) | 0.9889 (0.0012) | 0.9920 (0.0019) | 0.9988 (0.0005) | 0.9988 (0.0011) | 0.9785 (0.0029) | 0.8267 (0.1597) |
| maximum H₂ peak | 0.0418 (0.0538) | 0.1044 (0.0513) | 0.0314 (0.0352) | 0.0447 (0.0466) | 0.0043 (0.0027) | 0.0007 (0.0007) | 0.001 (0.0005) | 0.00105 (0.0009) | 0.00023 (0.0004) | 0.0 (0.00000) | 0.00047 (0.00082) | 0.00179 (0.00057) | 0.0447 (0.04656) |
| | | | | | | **Steady-State Phase** | | | | | | | |
| time in phase | 285.4 (27.7) | 281.4 (121.3) | 224.5 (67.7) | 178.8 (19.8) | 213.7 (21.6) | 275.7 (20.6) | 263.0 (30.2) | 279.3 (15.0) | 242.7 (29.5) | 419.25 (29.3) | 398.0 (25.0) | 258.3 (17.0) | 178.8 (19.7) |
| TWA NCE | 0.9965 (0.0006) | 0.9931 (0.0024) | 0.9963 (0.0008) | 0.9970 (0.0007) | 0.9968 (0.0008) | 0.9938 (0.0016) | 0.9977 (0.0018) | 0.9989 (0.0004) | 0.9991 (0.0003) | 0.9951 (0.0016) | 0.9966 (0.0002) | 0.9970 (0.0004) | 0.9970 (0.0007) |
| TWA H₂ | 0.00013 (0.00015) | 0.00049 (0.0004) | 0.00021 (0.00017) | 0.0003 (0.00024) | 0.00005 (0.00005) | 0.0003 (0.00008) | 0.00013 (0.00021) | 0.00006 (0.00006) | 0.00001 (0.00001) | 0.00013 (0.00014) | 0.00020 (0.0002) | 0.00002 (0.00001) | 0.0003 (0.00024) |
| | | | | | | **Char Phase** | | | | | | | |
| TWA NCE | 0.8518 (0.0428) | 0.9271 (0.0348) | 0.8912 (0.0532) | 0.8303 (0.0182) | 0.7773 (0.0225) | 0.9277 (0.0356) | 0.9549 (0.0165) | 0.9590 (0.0156) | 0.9600 (0.0026) | 0.9089 (0.0105) | 0.8340 (0.0084) | 0.7788 (0.0156) | 0.8303 (0.0182) |
| TWA H₂ | 0.01368 (0.00727) | 0.01667 (0.01008) | 0.01026 (0.00286) | 0.01679 (0.00516) | 0.01343 (0.00396) | 0.00277 (0.00384) | 0.00078 (0.00073) | 0.00135 (0.00145) | 0.00003 (0.00003) | 0.00645 (0.00284) | 0.01536 (0.00397) | 0.01207 (0.00174) | 0.01679 (0.00516) |

are much higher than those in all of the forced air cases, except the 78 L min$^{-1}$ case. To start the process, the fuel is placed inside the combustor body and lit from the top. The initial combustion of kindling material and the top layer of biomass consume the surrounding oxygen inside the combustor body. In the forced draft cases, the air flow through the fuel bed provides necessary oxygen for further combustion, while in the natural draft case, the flow has to be established by the buoyancy force. Thus, to start a flow through the fuel stack, the buoyancy force has to exceed the pressure drop imposed by the fuel stack. This pressure drop could lead to a lower PA flow in the beginning, causing the high emissions in the lighting phase. A comparison of the natural draft and varying PA test results suggests that the average natural draft flow rate is close to 98 L min$^{-1}$.

Increasing the PA leads to a higher fuel conversion and a shorter time in the steady-state phase. This is supported by the increase of TWA NCE values up to 0.9968, while the time in this phase as well as normalized H$_2$ emissions decrease to 0.00005, as presented in Table 2. The gas-phase temperature profiles increase slightly with the PA compared to the natural draft case, except for the case of 118 L min$^{-1}$, in which the temperatures exceed all other measurements by approximately 150 °C. This increase in the temperature is related to the higher fuel conversion and the decrease of emissions of incomplete combustion, which will lead to a greater heat release in the system. Further addition of air leads to cooling as a result of air dilution.

As shown in Table 2, the TWA NCE values decrease from 0.9271 to 0.7773 in the char phase with higher PA flows. It is hypothesized that, with a higher air flow, the products of the gasification process, mainly CO, are not subsequently burned in flaming combustion on top of the fuel stack. The flames observed on top of the fuel stack in the gasification phase consume a higher proportion of the CO emissions in the natural draft case than with higher PA flows. The higher flow rates appear to allow for insufficient residence time for complete oxidation within the flaming region. This is supported by the gas-phase temperature profiles inside the combustor body. Temperatures increase with higher forced PA flow but are consistently much lower than in the natural draft case. In addition, it can be assumed that the higher velocity of the migrating pyrolysis front, with higher PA flow, results in a higher initial heating rate of the solid fuel.[20] The initial heating rate has been shown to be decisive for the reactivity of the char.[42,43] Therefore, the high CO emissions, especially at the beginning of the char phase, could be caused by a higher reactivity of the remaining char after the steady-state phase.

**3.3. Variation of SA.** Figure 5 presents the normalized emissions and temperature profiles with varying SA as well as the natural draft case. It can be seen that, in all phases, the emissions are reduced substantially and the NCE is, except for the lowest value of SA, consistently higher than in the natural draft case. The initial peak of emissions in the lighting phase is reduced, and the gas-phase temperatures inside the combustor body rise significantly.

In the steady-state phase, it can be seen that the flow rate of 328 L min$^{-1}$ leads to higher emissions than all of the other cases, including the natural draft case. Thus, it can be assumed that a flow rate of 328 L min$^{-1}$ provides, as expected from the calculations presented in section 2.3.2, fuel-rich conditions and insufficient oxygen for complete combustion of the pyrolysis products. NCE is consistently higher for all other air flows compared to the natural draft case. In accordance, the gas-phase temperature inside the combustor extension is consistently
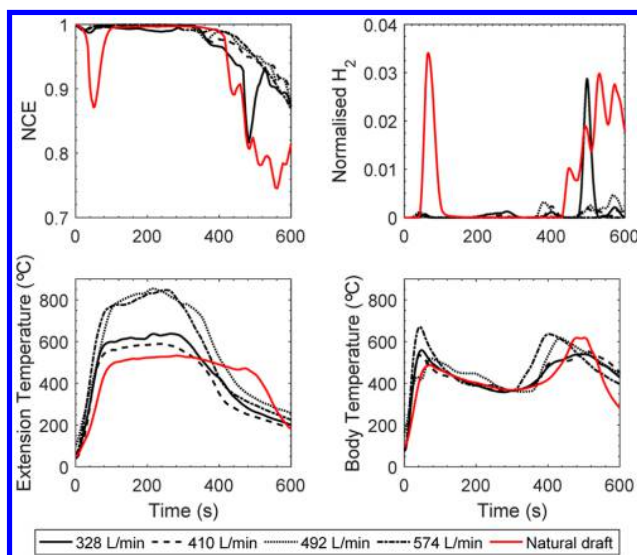


**Figure 5.** Average normalized emission profiles of H$_2$, nominal combustion efficiency [NCE = $X_{CO_2}/(X_{CO} + X_{CO_2})$], and measured gas-phase temperature profiles inside the combustor body and the combustor extension for various SA flows at 118 L min$^{-1}$ PA flow and the natural draft case.

higher. It should be highlighted that, with the forced SA flows of 492 and 574 L min$^{-1}$, up to approximately 300 °C higher temperatures can be measured.

In the char phase, the reduction of emissions is especially significant, in relation to the natural draft case. TWA NCE, as presented in Table 2, rises for all flow rates above 0.92 and up to 0.96, while the normalized H$_2$ value sinks as low as 0.00003. Values of such high efficiency had previously not been achieved in the char phase. This indicates that, with higher SA flow rates, a significantly greater proportion of CO emissions from the char gasification are oxidized. It should be stressed that, only in the case of the two higher air flow rates, the gas-phase temperatures inside the combustor body reach temperatures similar to the natural draft case. These high temperatures were only achieved with both air flows in natural draft configuration and with high SA flows, while temperatures with forced PA and natural draft SA were lower. Thus, it can be assumed that the higher SA flow rates lead to a higher heat release from combustion in this phase.

A noticeable increase in efficiency is noted between the flow rates of 328 and 492 L min$^{-1}$ but only a slight increase above that. This could mean that increasing the SA flow beyond a specified air/fuel ratio has only a marginal influence on the performance. It can be assumed that an optimal ratio of the PA/SA exists and that, for a specific PA flow, lower SA flow values might lead to insufficient mixing of combustible gases with air, while an oversupply might lead to cooling and potentially quenching of the flame front. A ratio of PA/SA flow of about 1:4 appears to achieve a very high combustion efficiency for this configuration. Previously ratios of 1 to 3.1, 5.7, 6.2,[28] and 2.3[44] have been reported, but no relationship to the efficiency was established. Ratios of 1:3 and 1:4 have also been reported to achieve low CO emissions in the steady-state phase, while the char phase has not been considered.[31] Further investigation coupling the combustion efficiency with the heat transfer efficiency would be helpful in finding an optimal PA/SA flow ratio.

**3.4. Variation of the FG Location.** The normalized emissions and temperature profiles of various FG locations are

presented in Figure 6. It can be seen that a reduction of the fuel stack distance to the SA inlet leads to higher measured
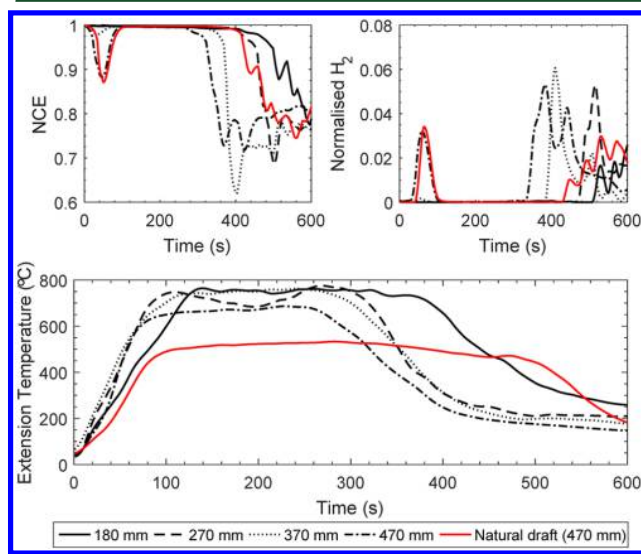


**Figure 6.** Average normalized emission profiles of $H_2$, nominal combustion efficiency $[NCE = X_{CO_2}/(X_{CO} + X_{CO_2})]$, and measured gas-phase temperature profiles inside the combustor extension for varying distances of the FG below the SA inlet at 118 L min$^{-1}$ PA flow and the natural draft case.

temperatures inside the combustor extension ranging from 150 to 250 °C above the natural draft case. The increased temperature compared to the natural draft case of about 150 °C with a FG distance of 470 mm can be attributed to the supply of forced PA. The further temperature increase can be assumed to be due to the smaller distances of the FG. With a smaller distance between the fuel and the SA inlet, there will be less heat loss of the gasification products before combustion, leading to an increase in the combustion temperature and, thus, efficiency. The higher temperatures will cause a greater buoyancy force at the SA inlet, increasing the amount of entering air, which, in turn, will affect the combustion efficiency. Decreasing emissions of products of incomplete combustion were recorded in the lighting and char phases, with smaller distances of the FG. FG locations of 180 and 270 mm provided a NCE value of 0.9988 in the lighting phase, which was the highest of all measured configurations. A smaller distance of the FG location also prolonged the high-efficiency steady-state phase significantly, with a minor reduction of the NCE. In the char phase, a smaller distance of the FG caused a higher NCE but only the lowest distance of 180 mm achieved a higher NCE than the natural draft configuration.

## 4. DISCUSSION

In comparison of the profiles, presented in Figures 4 and 5, it needs to be kept in mind that, in the set of varying SA flow rates, PA was fixed to the value of 118 L min$^{-1}$ and the FG location was at 470 mm below the SA inlet. Of special interest when relating these profiles to one another is that, with higher SA flows, the steady-state phase is longer and the emissions of incomplete combustion in the char phase are extensively mitigated, as seen in Table 2.

It has been established that the migrating pyrolysis is primarily governed by the PA flow.[12] Direct influence of SA on the fuel

stack is highly unlikely, even at the highest air flows, because of the large distance between the SA inlet and the fuel stack. This leads to the assertion that, with a specified PA flow, the migrating pyrolysis is of similar intensity and length. This raises the question of how the introduction of forced SA prolongs the steady-state phase. From the temperature profiles and NCE profiles in Figure 4, it can be deduced that the flame front at the SA inlet cannot be sustained at the end of the migrating pyrolysis; it extinguishes, and subsequently, high proportions of CO are emitted in the configuration in which SA is introduced by natural draft. In the forced SA cases, if the migrating pyrolysis is assumed to be of similar length as in the natural draft SA and 118 L min$^{-1}$ PA configuration, the flame does not extinguish at the end of this phase. With a flame present at the SA inlet, the CO emissions, which were emitted in the natural draft SA case, are oxidized further. Therefore, it appears that, with forced SA flow, sufficient mixing of entering air and combustible gases, in conjunction with much higher temperatures in the combustor extension, can be achieved to sustain a flame at the SA inlet. With a flame present at the SA inlet, a greater part of the CO emissions produced by the gasification process of char is burned in steady-state combustion, as seen in Figure 5. The combustion of CO from char gasification with increased SA at the SA inlet presents an extension of the steady-state combustion at this location, which was previously achieved only during the migrating pyrolysis.

A similar trend as with higher SA flows can be observed with smaller distances of the FG in the steady-state phase. The steady-state phase lasts much longer, for 419 s, with the lowest distance of the FG, as compared to 179 s with the greatest distance. Similar to the forced SA air cases, much higher gas-phase temperatures were also measured in the combustor extension. In Figure 6, it can be seen that the measured gas temperature inside the combustor extension is approximately 100 °C higher with a FG distance of 180 mm compared to 470 mm. When the gas temperature is higher, there is an increase in buoyancy-induced flow as a result of the greater density difference between the gases inside the combustor extension and the cold SA. Accordingly, the higher air flow, with a smaller distance of the FG, in conjunction with the higher temperatures appears to keep a flame present at the SA inlet during the combustion of gasification products from mainly raw biomass and into the combustion of mainly CO from char gasification. This extension of the steady-state combustion, to include combustion of char gasification products, seems to be the reason for a longer duration of this phase and a reduction of overall CO emissions.

In the char phase, the reduction of emissions, especially CO, with the higher SA flow is a result of a combination of the longer steady-state phase and the influence of SA on the air flow inside the combustor body. A higher efficiency and the combustion of char gasification products at the end of the steady-state phase will lead to a much lower amount of char remaining after this phase. The lower amount of remaining char alone cannot explain the much higher NCE in the char phase with increasing SA flow. Therefore, SA must also have an influence on the flow field inside the combustor body. The increasing amount of forced SA being introduced will lead to better mixing and more complete combustion in the secondary flame front. Future studies of the influence of SA on the flow field inside staged combustors could provide deeper insights.

The direct application of the current findings in cookstoves is primarily limited by the chosen research approach, which is focused specifically on the combustion science of the thermochemical process. In this study, measurements were

carried out without emulating user practice or performing cooking tasks. Therefore, the influence of a cooking pot on top of the stove on the combustion performance is unknown. Similarly, with a smaller diameter reactor, the influence of quenching by the cold walls may become more pronounced. In an optimized system, it is aspirational for combustion to be completed before contact with the cooking surface or walls. The heat transfer to the pot would then be exclusively achieved by hot flue gases. Hence, in such a system, the combustion properties would be independent of the cooking performance. To achieve such a system, further fundamental research on the gasification and combustion behaviors of staged combustors, using different fuels and air supply conditions, as well as the heat transfer properties would be beneficial.

## 5. CONCLUSIONS

The present study investigates the influence of PA and SA with natural draft as well as forced draft in various relations to each other on the combustion process in a staged combustor. The location of fuel within the combustor was modified to simulate the variation of the relative position of the PA and SA inlet to the fuel stack. This study presents general insights into the combustion processes in small-scale staged combustion devices. The combustor used for this research was custom-made for the purpose of studying the ongoing combustion processes and is not being used for cooking, which limits the comparability to commercial products, which are usually tested while performing certain cooking tasks.

In the lighting phase, emissions of incomplete combustion can be significantly reduced by providing a sufficient air supply. This can be achieved by either ensuring that the top of the fuel stack is always as close as possible to the SA inlet, which achieves the highest efficiency, or introducing SA by forced draft. When using forced draft, the peak NCE rises by increasing the PA flow, from 0.84 with natural draft up to 0.96, but even more so by increasing the SA flow, up to 0.99.

The migrating pyrolysis is governed by the PA flow, with higher flows increasing the heat release. During the migrating pyrolysis, the products are oxidized in steady-state combustion at the SA inlet. When using a combination of forced PA supply and natural draft SA, an increase of PA leads to a shorter time in this steady-state phase with higher combustion temperatures and a higher NCE. Introducing forced SA in combination with forced PA leads to longer steady-state combustion, extending it from primarily combustion of volatile pyrolysis products to combustion of primarily carbon monoxide from char gasification. This provides a drastic reduction of products of incomplete combustion and a significant increase in efficiency. A considerable increase in combustion efficiency was identified for PA/SA flow ratios of up to 1:4 for the wood chips fuel. Reducing the distance between the SA inlet and the fuel stack, with SA introduced by natural draft, had a similar effect to increasing SA via forced draft. Therefore, an adjustable FG, to be able to use a variable amount of fuel without increasing the release of emissions of incomplete combustion, should be considered for any staged combustor design. Future work including the influence of the fuel stack depth on the combustion process would be beneficial.

In the char phase, increasing the PA flow produced significantly more emissions of incomplete combustion. With the addition of an increased amount of forced SA, these emissions could be burned cleanly.

In the present study, different air requirements for the three phases of lighting, steady-state, and char have been identified. The application of dynamic air control rather than a constant air supply to suit each phase could be the topic of future research. Furthermore, it could be shown that forced PA in combination with natural draft SA is not a beneficial option. To achieve low emissions in this configuration, it would require attentive handling to reduce the PA flow after the steady-state phase. Forced draft for the PA as well as SA flow increases the controllability and efficiency in all phases. To achieve low emissions of incomplete combustion, fuel-lean conditions must be ensured in the secondary flame front. The combustion efficiency is also greater with a smaller distance between the fuel and the SA inlet.

## ■ AUTHOR INFORMATION

**Corresponding Author**
*E-mail: thomas.kirch@adelaide.edu.au.

**ORCID** 
Thomas Kirch: 0000-0002-6288-7466

**Notes**
The authors declare no competing financial interest.

## ■ ACKNOWLEDGMENTS

## ■ REFERENCES

(1) Bonjour, S.; Adair-Rohani, H.; Wolf, J.; Bruce, N. G.; Mehta, S.; Prüss-Ustün, A.; Lahiff, M.; Rehfuess, E. A.; Mishra, V.; Smith, K. R. Solid fuel use for household cooking: Country and regional estimates for 1980−2010. *Environ. Health Perspect.* **2013**, *121*, 784−790.

(2) Lelieveld, J.; Evans, J. S.; Fnais, M.; Giannadaki, D.; Pozzer, a. The contribution of outdoor air pollution sources to premature mortality on a global scale. *Nature* **2015**, *525*, 367−71.

(3) Murray, C. J. L.; Forouzanfar, M. H.; Alexander, L.; Anderson, H. R.; Bachman, V. F.; et al. Global, regional and national comparative risk assessment of 79 behavioural, environmental/occupational and metabolic risks or clusters of risks in 188 countries 1990−2013: A systematic analysis for the Global Burden of Disease Study 2013. *Lancet* **2015**, *386*, 2287−2323.

(4) Sovacool, B. K. The political economy of energy poverty: A review of key challenges. *Energy Sustainable Dev.* **2012**, *16*, 272−282.

(5) Anenberg, S. C.; Balakrishnan, K.; Jetter, J.; Masera, O.; Mehta, S.; Moss, J.; Ramanathan, V. Cleaner cooking solutions to achieve health, climate, and economic cobenefits. *Environ. Sci. Technol.* **2013**, *47*, 3944−3952.

(6) Jetter, J.; Zhao, Y.; Smith, K. R.; Khan, B.; Yelverton, T.; DeCarlo, P.; Hays, M. D. Pollutant emissions and energy efficiency under controlled conditions for household biomass cookstoves and implications for metrics useful in setting international test standards. *Environ. Sci. Technol.* **2012**, *46*, 10827−10834.

(7) Jetter, J. J.; Kariher, P. Solid-fuel household cook stoves: Characterization of performance and emissions. *Biomass Bioenergy* **2009**, *33*, 294−305.

(8) Houshfar, E.; Skreiberg, Ø.; Løvås, T.; Todorović, D.; Sørum, L. Effect of excess air ratio and temperature on NOx emission from grate combustion of biomass in the staged air combustion scenario. *Energy Fuels* **2011**, *25*, 4643−4654.

(9) Reed, T. B.; Larson, R. A wood-gas stove for developing countries. *Energy Sustainable Dev.* **1996**, *3*, 34−37.

(10) Arora, P.; Das, P.; Jain, S.; Kishore, V. V. N. A laboratory based comparative study of Indian biomass cookstove testing protocol and Water Boiling Test. *Energy Sustainable Dev.* **2014**, *21*, 81−88.

(11) Roth, C. *Micro-gasification: Cooking with Gas from Dry Biomass*; Deutsche Gesellschaft für Internationale Zusammenarbeit (GIZ): Eschborn, Germany, 2014; http://www.giz.de/fachexpertise/downloads/giz2014-en-micro-gasification-manual-hera.pdf.

(12) Reed, T.; Walt, R.; Ellis, S.; Das, A.; Deutch, S. Superficial Velocity—The Key to Downdraft Gasification. *Proceedings of the 4th Biomass Conference of the Americas*; Oakland, CA, Aug 29−Sept 2, 1999; pp 1−8.

(13) Yibo, H.; Li, H.; Chen, X.; Xue, C.; Chen, C.; Liu, G. Effects of moisture content in fuel on thermal performance and emission of biomass semi-gasified cookstove. *Energy Sustainable Dev.* **2014**, *21*, 60−65.

(14) Branca, C.; Di Blasi, C. Global Kinetics of Wood Char Devolatilization and Combustion. *Energy Fuels* **2003**, *17*, 1609−1615.

(15) Birzer, C.; Medwell, P.; MacFarlane, G.; Read, M.; Wilkey, J.; Higgins, M.; West, T. A Biochar-producing, Dung-burning Cookstove for Humanitarian Purposes. *Procedia Eng.* **2014**, *78*, 243−249.

(16) Fatehi, M.; Kaviany, M. Adiabatic reverse combustion in a packed bed. *Combust. Flame* **1994**, *99*, 1−17.

(17) Rönnbäck, M.; Axell, M.; Gustavsson, L.; Thunman, H.; Lecher, B. Combustion Processes in a Biomass Fuel Bed-Experimental Results. In *Progress in Thermochemical Biomass Conversion*; Bridgwater, A., Ed.; Blackwell Science, Ltd.: Oxford, U.K., 2001; Chapter 59, pp 743−757, DOI: 10.1002/9780470694954.ch59.

(18) Horttanainen, M.; Saastamoinen, J.; Sarkomaa, P. Operational limits of ignition front propagation against airflow in packed beds of different wood fuels. *Energy Fuels* **2002**, *16*, 676−686.

(19) Yang, Y. B.; Sharifi, V. N.; Swithenbank, J. Effect of air flow rate and fuel moisture on the burning behaviours of biomass and simulated municipal solid wastes in packed beds. *Fuel* **2004**, *83*, 1553−1562.

(20) Porteiro, J.; Patiño, D.; Collazo, J.; Granada, E.; Moran, J.; Miguez, J. L. Experimental analysis of the ignition front propagation of several biomass fuels in a fixed-bed combustor. *Fuel* **2010**, *89*, 26−35.

(21) Porteiro, J.; Patiño, D.; Moran, J.; Granada, E. Study of a fixed-bed biomass combustor: Influential parameters on ignition front propagation using parametric analysis. *Energy Fuels* **2010**, *24*, 3890−3897.

(22) Buchmayr, M.; Gruber, J.; Hargassner, M.; Hochenauer, C. Experimental investigation of the primary combustion zone during staged combustion of wood-chips in a commercial small-scale boiler. *Biomass Bioenergy* **2015**, *81*, 356−363.

(23) Kuo, J. T.; Hsu, W.-S.; Yo, T.-C. Effect of Air Distribution on Solid Fuel Bed Combustion. *J. Energy Resour. Technol.* **1997**, *119*, 120.

(24) MacCarty, N.; Still, D.; Ogle, D. Fuel use and emissions performance of fifty cooking stoves in the laboratory and related benchmarks of performance. *Energy Sustainable Dev.* **2010**, *14*, 161−171.

(25) Aprovecho Research Center. *Test Results of Cook Stove Performance*; Aprovecho Research Center: Cottage Grove, OR, 2011; http://aprovecho.org/publications-3/.

(26) Kumar, M.; Kumar, S.; Tyagi, S. Design, development and technological advancement in the biomass cookstoves: A review. *Renewable Sustainable Energy Rev.* **2013**, *26*, 265−285.

(27) Kshirsagar, M. P.; Kalamkar, V. R. A comprehensive review on biomass cookstoves and a systematic approach for modern cookstove design. *Renewable Sustainable Energy Rev.* **2014**, *30*, 580−603.

(28) Reed, T. B.; Anselmo, E.; Kirchef, K. Testing & Modeling the Wood-Gas Turbo Stove. In *Progresss in Thermochemical Biomass Conversion Conference*; Bridgwater, A., Ed.; Blackwell Science, Ltd.: Oxford, U.K., 2001; Chapter 55, pp 693−704, DOI: 10.1002/9780470694954.ch55.

(29) Mukunda, H. S.; Dasappa, S.; Paul, P. J.; Rajan, N. K. S.; Yagnaraman, M.; Ravi Kumar, D.; Deogaonkar, M. Gasifier stoves—Science, technology and field outreach. *Curr. Sci.* **2010**, *98*, 627−638.

(30) Varunkumar, S.; Rajan, N. K. S.; Mukunda, H. S. Experimental and computational studies on a gasifier based stove. *Energy Convers. Manage.* **2012**, *53*, 135−141.

(31) Tryner, J.; Tillotson, J. W.; Baumgardner, M. E.; Mohr, J. T.; Defoort, M. W.; Marchese, A. J. The effects of fuel properties, air flow rates, secondary air inlet geometry, and operating mode on the performance of TLUD semi-gasifier cookstoves. *Environ. Sci. Technol.* **2016**, *50*, 9754−9763.

(32) Kirch, T.; Medwell, P. R.; Birzer, C. H. Natural draft and forced primary air combustion properties of a top-lit up-draft research furnace. *Biomass Bioenergy* **2016**, *91*, 108−115.

(33) Eskilsson, D.; Rönnbäck, M.; Samuelsson, J.; Tullin, C. Optimisation of efficiency and emissions in pellet burners. *Biomass Bioenergy* **2004**, *27*, 541−546.

(34) Carroll, J. P.; Finnan, J. M.; Biedermann, F.; Brunner, T.; Obernberger, I. Air staging to reduce emissions from energy crop combustion in small scale applications. *Fuel* **2015**, *155*, 37−43.

(35) Lombardi, F.; Riva, F.; Bonamini, G.; Barbieri, J.; Colombo, E. Laboratory protocols for testing of Improved Cooking Stoves (ICSs): A review of state-of-the-art and further developments. *Biomass Bioenergy* **2017**, *98*, 321−335.

(36) Birzer, C.; Medwell, P.; Wilkey, J.; West, T.; Higgins, M.; Macfarlane, G.; Read, M. An analysis of combustion from a top-lit up-draft (TLUD) cookstove. *J. Humanitarian Eng.* **2013**, *2*, 1−8.

(37) Kirch, T.; Birzer, C. H.; Medwell, P. R.; Holden, L. The role fo primary and secondary air on wood combustion in cookstoves. *Int. J. Sustainable Energy* **2017**, 1−10.

(38) Yevich, R.; Logan, J. A. An assessment of biofuel use and burning of agricultural waste in the developing world. *Global Biogeochem. Cycles* **2003**, *17*, 1095.

(39) ASTM International. *ASTM D4442-92(2003): Standard Test Methods for Direct Moisture Content Measurement of Wood and Wood-Based Materials*; ASTM International: West Conshohocken, PA, 2003.

(40) Johnson, M.; Edwards, R.; Berrueta, V.; Masera, O. New approaches to performance testing of improved cookstoves. *Environ. Sci. Technol.* **2010**, *44*, 368−374.

(41) Kirch, T.; Medwell, P. R.; Birzer, C. H. Assessment of natural draft combustion properties of top-lit up-draft research furnace. *Proceedings of the Australian Combustion Symposium 2015*; Melbourne, Victoria, Australia, Dec 7−9, 2015.

(42) Janse, A. M. C.; de Jonge, H. G.; Prins, W.; van Swaaij, W. P. M. Combustion Kinetics of Char Obtained by Flash Pyrolysis of Pine Wood. *Ind. Eng. Chem. Res.* **1998**, *37*, 3909−3918.

(43) Dall'Ora, M.; Jensen, P. A.; Jensen, A. D. Suspension combustion of wood: Influence of pyrolysis conditions on char yield, morphology, and reactivity. *Energy Fuels* **2008**, *22*, 2955−2962.

(44) Raman, P.; Ram, N. K.; Gupta, R. Development, design and performance analysis of a forced draft clean combustion cookstove powered by a thermo electric generator with multi-utility options. *Energy* **2014**, *69*, 813−825.

# Chapter 5

---

# Influences of Fuel Bed Depth and Air Supply on Small-Scale Batch-Fed Reverse Downdraft Biomass Conversion

---

## Statement of Authorship

| | |
|---|---|
| Paper Title: | Influences of Fuel Bed Depth and Air Supply on Small-Scale Batch-Fed Reverse Downdraft Biomass Conversion |
| Status: | Published |
| Details: | *Energy & Fuels*, vol. 32, pp. 8507–8518 |
| | DOI: 10.1021/acs.energyfuels.8b01699 |

## Principal Author

| | |
|---|---|
| Name: | Thomas Kirch |
| Contribution: | Performed the literature review., with a particular focus on hydrocarbon chemistry and the use of char to convert pyrolysis products. Developed aims and objectives of the research study. Designed the experimental reactor. Constructed and set-up experimental facilities and analytical methods. In particular, the producer gas extraction and gas cleaning of all non-gaseous constituents had to be performed to enable the measurement of the product gas composition. Obtained biomass fuel, wood pellets. Designed experimental matrix and performed experimental work. Performed solid composition analyses, proximate analysis, and calorific value determination of the biomass fuel and produced chars. Wrote codes for data analysis. Performed data analysis and transferred to appropriate figures for visualisation. Structured, wrote and edited the research article. Acted as corresponding author. |
| Contribution Percentage (%): | 70 |
| Certification: | This paper reports on original research I conducted during the period of my Higher Degree by Research candidature and is not subject to any obligations or contractual agreements with a third party that would constrain its inclusion in this thesis. I am the primary author of this paper. |
| Signature: | Date: **28.02.2019** |

**Co-Author Contributions**

By signing the Statement of Authorship, each author certifies that:

1. the candidate's stated contribution to the publication is accurate (as detailed above);

2. permission is granted for the candidate to include the publication in the thesis; and

3. the sum of all co-author contributions is equal to 100% less the candidates stated contribution.

| | |
|---|---|
| Name: | Paul R. Medwell |
| Contribution Details: | Guided research direction. Supervised work development. Helped generate ideas for tests and edited manuscript. |
| Signature: | Date: 28 Feb 2019 |

| | |
|---|---|
| Name: | Cristian H. Birzer |
| Contribution Details: | Guided research direction. Supervised work development. Helped generate ideas for tests and edited manuscript. |
| Signature: | Date: 28 Feb 2019 |

| | |
|---|---|
| Name: | Philip J. van Eyk |
| Contribution Details: | Guided research direction. Supervised work development. Helped generate ideas for tests and edited manuscript. |
| Signature: | Date: 28 Feb 2019 |

# Influences of Fuel Bed Depth and Air Supply on Small-Scale Batch-Fed Reverse Downdraft Biomass Conversion

Thomas Kirch,[*,†,‡] Paul R. Medwell,[†,‡] Cristian H. Birzer,[†,‡] and Philip J. van Eyk[§,‡]

[†]School of Mechanical Engineering, The University of Adelaide, Adelaide, SA 5000, Australia

[‡]Humanitarian and Development Solutions Initiative, The University of Adelaide, Adelaide, SA 5005, Australia

[§]School of Chemical Engineering, The University of Adelaide, Adelaide, SA 5005, Australia

**S** Supporting Information

**ABSTRACT:** The producer gas composition and the thermochemical conversion process of a small-scale reverse downdraft reactor has been investigated under ten operating conditions with different fuel bed depths and air supply rates. The operating principle of this research reactor is a batch-fed reverse downdraft process, using wood pellets as the solid biomass fuel. The oxygen-limited regime, where the fuel consumption increases nearly linearly with the air supply, has been identified, and four flow rates over the range of this regime have been investigated. The fuel bed depth was varied between one and four reactor diameters (1D (100 mm)−4D (400 mm)). The results demonstrate that increasing the primary air mass flux leads to both greater fuel consumption and higher temperatures as well as heating rates in the reaction front. Greater air supply rates and the resulting higher temperatures lead to a substantial increase in fuel conversion into permanent gases, rather than tars or char, and a rise in the cold gas efficiency (CGE) from 33% to 73%, from the lowest to highest air flow rate at a 4D fuel bed depth. However, the temporal producer gas heating value is similar in all configurations. With increasing depth, it is evident that $H_2$ production is promoted by the char layer downstream of the reaction front and that a certain layer thickness is necessary to achieve the potential near steady-state product flow at a specific flow rate. Interestingly, a greater fuel bed depth enhances the hydrogen conversion rate to permanent gases by more than 20% and the CGE from 48% to 53%, while the fuel consumption and temperature profiles remain similar. A general trend of increasing performance was identified at the 3D and 4D depths, when compared with the 1D and 2D fuel bed depths. The produced char exhibits a high fixed and elemental carbon content. Therefore, the conversion efficiency of this process can be increased both through increasing the fuel bed depth and, even more, through adjusting the air supply, promoting the yield of permanent gases and the conversion of produced tars.

## 1. INTRODUCTION

Solid biomass fuels provide the majority of renewable energy worldwide[1] and are often used in small-scale devices for localized heat generation. Unfortunately, current small-scale devices typically have low efficiency and high emissions from incomplete combustion.[2] An alternative reactor type features reverse downdraft, whereby the thermochemical conversion process of the solid biomass fuel is separated in time and location from the combustion of the product gas. These types of reactors achieve lower emissions of incomplete combustion[3] and show potential for small-scale heat and power generation.[4,5] However, despite the potential applications, a deeper understanding of the ongoing thermochemical conversion processes in such systems is needed for the systematic improvement of future designs.[6]

Packed-bed reverse downdraft reactors are lit from the top, which leads to the ignition of the surface of the solid fuel, while air is supplied from underneath the fuel bed.[7] Subsequently, a reaction front propagates against the air flow and down the fuel bed, causing the release of volatile matter and leaving a solid layer of char.[8] The devolatilisation process in the reaction front is sustained by heat from partial oxidation of the volatile gases with the limited air supply and is therefore called an autothermal process.[9] The gaseous products (producer gas) rise through the solid layer of hot char, leave the fuel bed, and can subsequently be burned with secondary air.[10,11] Once the

reaction front reaches the bottom of the fuel bed, the majority of the volatile matter has been released, and char, consisting mainly of fixed carbon, is left as a solid product.[12] At this stage, the process can be quenched and the char can be collected. If the process is not quenched, an updraft process starts where the char is oxidized, with the air supply from underneath. This can release high concentrations of CO. The process continues until only the ash is left behind as a solid product. If the process is quenched before the updraft process starts, the char product can be collected and used for other purposes, depending on its properties. In order to increase the quality, quantity, and range of application of the char, it is necessary to further develop understanding and optimization of the process for producer gas as well as char production.[13]

For batch-fed systems, three combustion regimes have been identified, with increasing air supply: (1) an oxygen-limited regime, where the fuel consumption is nearly linearly dependent on the oxidizer supply; (2) a reaction-limited regime, where the solid fuel mass loss is independent of the air flow rate; and (3) a regime where the process is cooled by convection and finally quenched.[14] The limits of these regimes are fuel dependent and are influenced by characteristics such as

the fuel moisture content and particle size.[15−18] In the oxygen-limited regime, the conversion process is controlled by the air supply, thereby enabling the heat release via this parameter. Small-scale reverse downdraft reactors mostly operate in the oxygen-limited regime, but limited research has been concerned with the products of the thermochemical conversion process released under these conditions; instead the focus has primarily been on the air supply and the overall system performance, including the subsequent combustion process.[3]

With limited air supply, the products of the devolatilisation process are (1) a wide variety of gases (CO, $CO_2$, $H_2$, $CH_4$ $C_2H_2$, $C_2H_4$, $C_2H_6$, $C_6H_6$, etc.);[19] (2) liquid tars, heavier hydrocarbons, and water; and (3) solid char (mostly carbon and ash). The producer gas composition (on a volumetric basis) of batch-fed autothermal gasification has been reported in the range of 1−9% $H_2$, 8−13% CO, 11−20% $CO_2$, and 1−3% $CH_4$.[20,21] The main factors influencing producer gas composition are the air supply, heating rate, final temperature, and the type of initial biomass fuel,[22] coupled with the design and pressure of the reactor.[9] The fuel bed depth as a design parameter is not well understood and could be influential on the producer gas composition.

While the gaseous and solid devolatilisation products are desired, the liquid products, and especially the tars, are generally not desired, since these hydrocarbon compounds have been identified as soot precursors.[23] In the reverse downdraft configuration, the hot temperatures and catalytic properties of char downstream of the reaction front can influence those products that are released from the devolatilisation process. While maximum reaction temperatures are dependent on the air supply, the char layer thickness above the reaction front increases as the reaction propagates down the fuel bed. Thermal cracking (decomposition) reactions of tars released from biomass pyrolysis have been shown to increase with temperature[24,25] and can achieve 80−90% tar reduction at temperatures above 1000 °C.[26] Primary and secondary tars have been reduced at temperatures over 1100 °C, due to cracking reactions, although more tertiary tars are formed.[26−28] Thermal tar cracking reactions are expected to increase the production of CO and $H_2$.[28] These reactions can be enhanced in the presence of char,[19,29−31] which can lead to a further reduction of tar after the released products pass through a hot char bed.[32] The maximum char layer thickness is dependent on the initial fuel bed depth as it increases with the propagation of the reaction front. It has been suggested that cracking processes due to the presence of char are limited in small-scale reverse downdraft reactors because of the limited thickness of the char layer.[33] A variation of the air supply and the fuel bed depth can therefore yield further insights into the effects of thermal cracking and the presence of a hot char layer on the composition of the producer gas in reverse downdraft reactors.

This research article aims to contribute to a deeper understanding and further classification of the ongoing processes in small-scale batch-fed reverse downdraft reactors. Two parameters, the fuel bed depth and the air supply rate, are investigated. While the air flow rate has previously been identified as reaction limiting at low supply rates, the influence of the fuel bed depth has not yet been extensively studied, and further information can be gained from an in depth analysis of the products released from the thermochemical conversion process. A combined study of both parameters allows a

comparison and determination of the degree to which the fuel bed depth and the air supply influence the released products. Producer gas, as well as solid char, are considered as products, and their properties are investigated through an analysis of their composition. The findings of this work could provide alternative means by which to analyze reactor designs in terms of process optimization for the combined production of producer gas and char.

## 2. EXPERIMENTAL SETUP

**2.1. Reactor.** A schematic diagram of the batch-fed reactor is presented in Figure 1. Fuel was loaded from the top and placed on a
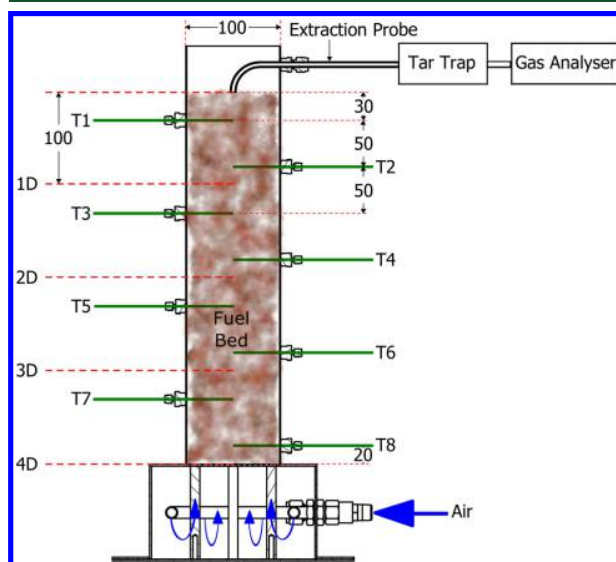


**Figure 1.** Schematic diagram of the reactor and measuring equipment setup. All distances in millimeters.

grate mounted above an air plenum. For this arrangement, the air entering from the bottom was purposely insufficient to oxidize all of the producer gas within the length of the reactor. A small portion of the released gases from the devolatilisation process were extracted from the reactor, and the remainder were subsequently combusted in a non-premixed flame immediately above the exit plane of the reactor. It is important to note that the measurements are sampled from within the potential core of the jet, upstream of the flame, and are not influenced by the secondary combustion process.

The supply of dry compressed air was regulated through a flow meter and introduced into the reactor via a distribution ring, with its nozzles facing downward to create an even flow pattern. Based on preliminary experiments to span the combustion regimes of interest, air mass fluxes of 0.025, 0.050, 0.075, and 0.125 kg m$^{-2}$ s$^{-1}$ were chosen for the present study. For simplicity, these flow rates will be referred to as FR025, FR050, FR075, and FR125, respectively, from here on.

Up to eight K-type thermocouples (labeled T1−T8) are inserted into the fuel. Thermocouple 1 was mounted at a distance of 30 mm beneath the initial top of the fuel bed, with distances of 50 mm between each of the subsequent thermocouples, while the last thermocouple was placed at 20 mm above the fuel grate. The reactor was mounted on a weighing scale (Radwag WLC 20/A2) with a maximum capacity of 20.0 kg and a readability and repeatability of $10^{-4}$ kg.

The reactor has an inner diameter of 98 mm. The external wall was covered with 25 mm-thick thermal insulation. The grate has a 67.2% open area and adjustable feet, so that its location can be adjusted within the reactor to accommodate diverse fuel bed heights between

100 and 400 mm. In all cases, the top of the fuel stack was always initially at the entrance plane of the extraction probe.

An extraction probe, for sampling the released devolatilisation products, was situated at the top of the fuel bed. The probe was curved with a 90° bend to penetrate the reactor wall, where it is then led into a heated line which was subsequently introduced into a cooled tar trap. The tar trap was used for the retention of all nongaseous products. A feasible method for the gravimetric measurement of the produced tars could not be established in the research facilities. Downstream of the tar trap, an adjustable flow rate vacuum pump regulated the flow of sample extraction and was manually set to correspond to the gas analyzer flow rate. Subsequently, the flow was passed through the gas analyzer (Section 2.2).

**2.2. Gas Analyzer.** The gas analyzer downstream of the tar trap was an MRU Vario Plus Industrial Analyzer, which measures volumetric composition on a dry basis. $CO_2$, CO, and $C_xH_y$, reported as a $CH_4$ equivalent, were measured using NDIR sensors with a range up to 30% (v/v) and an accuracy ±3% of the reading. $O_2$ and $H_2$ were measured using an electrochemical sensor with a range up to 21% and an accuracy of ±0.2% of the absolute value and a range up to 100% and an accuracy ±0.02% of the reading. $CO_2$, CO, $CH_4$, $H_2$, and $O_2$ were measured by the analyzer, with $N_2$ determined by subtraction. Calibration of the gas analyzer was performed daily. Measurements were recorded continuously at a rate of 0.5 Hz.

**2.3. Fuel.** Cylindrical wood pellets, with a nominal diameter of 6.5 mm and nominal length of 40 mm (resulting in 5−40 mm length), produced from timber waste in multiple timber mills around Australia, were used as fuel. The pellets consisted of hammer-milled wood shavings, from multiple wood species, to which pine saw dust was added before compression, resulting in a bulk density of approximately 700 kg m$^{-3}$. Pellet Heaters Australia manufacture the product which was purchased from Barbeques Galore (Adelaide, Australia). The proximate analysis of the pellets yielded a dry-basis mass composition of 76.5% volatile matter, 17.6% char, and 5.9% ash. The moisture content of the raw fuel was 4.3% (g/g), using an established method.[34] The mass-based ultimate analysis resulted in 47.4% C, 6.4% H, and 0.1% N, and the higher heating value of the fuel was 17.6 MJ kg$^{-1}$, as determined in a bomb calorimeter.

**2.4. Procedure.** Two main parameters, the air mass flux and the fuel bed depth, were controlled in the present study, as presented in Table 1. To avoid any influence from the thermal mass of the reactor

**Table 1. Experimental Configurations, Number of Repetitions Performed, and Experimental Code**

| fuel bed depth (mm) | fuel mass (kg) | air mass flux (kg m$^{-2}$ s$^{-1}$) | repetitions | code |
|---|---|---|---|---|
| 100 | 0.525 | 0.025 | 3 | 1D FR025 |
| | | 0.050 | 3 | 1D FR050 |
| | | 0.075 | 5 | 1D FR075 |
| | | 0.125 | 3 | 1D FR125 |
| 200 | 1.05 | 0.075 | 6 | 2D FR025 |
| 300 | 1.575 | 0.075 | 5 | 3D FR025 |
| 400 | 2.1 | 0.025 | 5 | 4D FR025 |
| | | 0.050 | 6 | 4D FR050 |
| | | 0.075 | 5 | 4D FR075 |
| | | 0.125 | 7 | 4D FR125 |

(cold start) on the process, it was preheated prior to use. Fuel was introduced into the reactor at inner reactor temperatures <100 °C to avoid effects from fuel drying. For each experiment, the preweighed fuel batch was placed into the reactor and the air mass flux was preset on the flow meters. The top of the fuel bed was lit, with the aid of 10 mL of methylated spirits (96% ethanol, CAS 64-17-5) and one paper towel for ignition, when the outer reactor wall was approximately 50 °C.

The experiment was stopped when the reaction front reached the fuel grate. The end time was determined by calculating the average reaction front velocity (the distance over time between the thermocouples reaching 600 °C) for each configuration and extrapolating from the time after thermocouple T8 measured 600 °C. The process was then stopped by shutting off the air supply and introducing one-third of the estimated char mass as iced water into the reactor, to rapidly cool the process. To further quench all reactions, nitrogen (>99.99% $N_2$) was supplied through the air inlet at the bottom of the reactor and passed over the char layer.

Four fuel bed depths and four flow rates were tested, with each configuration being repeated multiple times, as presented in Table 1. The fuel bed depths of 100, 200, 300, and 400 mm are set in relation to the inner diameter of the reactor, 98 mm, and are referred to as 1D, 2D, 3D, and 4D, respectively, hereafter. At 1D and 4D four air flow rates were used, while all four depths were tested at 0.075 kg m$^{-2}$ s$^{-1}$. The clear trend established at 1D and 4D is consistent, and therefore, it was not necessary to repeat measurements at 2D and 3D for all four flow rates.

After each test the remaining char, as the solid product of the process, was extracted from the reactor. In the case of the 4D fuel bed depth, the remaining char was extracted in three distinct portions. The three portions describe the top, middle, and bottom third of the char bed in the reactor.

**2.5. Analysis.** A weighing scale was used to measure the fuel mass loss, which was expected to present a linear profile over time.[33] The measured weight loss confirmed the linear profile, and a linear fit of the fuel mass flux was determined by the mass loss over time in relation to the cross-sectional area of the reactor. Preliminary data were gathered at the 1D fuel depth (0.525 kg of fuel) to establish the limits of the oxygen-limited air mass flux regime for the utilized fuel. The flow rates were increased into the reaction-limited regime to establish the limits of the oxygen-limited regime and the subsequent transition into the reaction-limited regime. In these preliminary experiments only weight loss data and temperature measurements were recorded. These results are compared with values from the literature.[14] It should be kept in mind that the values found in the literature[14,16] were calculated based on thermocouple data, represented by the reaction front velocity and the fuel bulk density ($\dot{m}_{fuel} = v_{front} \times \rho_{fuel}$) because the fuel mass loss was not measured. In this approximation, the remaining char was not considered and will therefore lead to an overestimation of the fuel mass flux, when compared with direct measurement of the fuel mass loss, as performed here.

A total of eight thermocouples, situated along the center of the reactor, were measured via a thermocouple data logger. Mean maximum temperatures are determined as an average of the highest temperatures of the thermocouples used in the experiment. Maximum temperature measurements of the lowest thermocouple (20 mm from the fuel grate) were disregarded, since an influence of the temperature due to proximity to the fuel grate was identified. For each thermocouple, the heating rate was calculated based on the time taken for the thermocouple to be heated from 100 °C to 70% of the maximum temperature. The mean heating rate for each test was calculated from the heating rates of all the used thermocouples, and the value reported for each configuration was the mean of all the repeat tests.

The producer gas composition was measured for the four different air mass flux rates at 1D and 4D, as well as for FR075 at 2D and 3D. Figure 2 presents a representative plot of one experiment (4D FR125), with the start and end points of the considered measurements. A uniform starting point had to be chosen, after which the profiles of multiple experiments provided similar trends. This enables the calculation of an average value for each time point after the starting point, leading to one average plot for each configuration. The $O_2$ concentration was chosen to determine the beginning and end points of the producer gas measurements. A threshold of 0.75% (v/v) $O_2$ was established as a reliable value. The start and end points of the measurement duration were determined when the $O_2$ concentration initially and at the end of the process passed this threshold, as shown
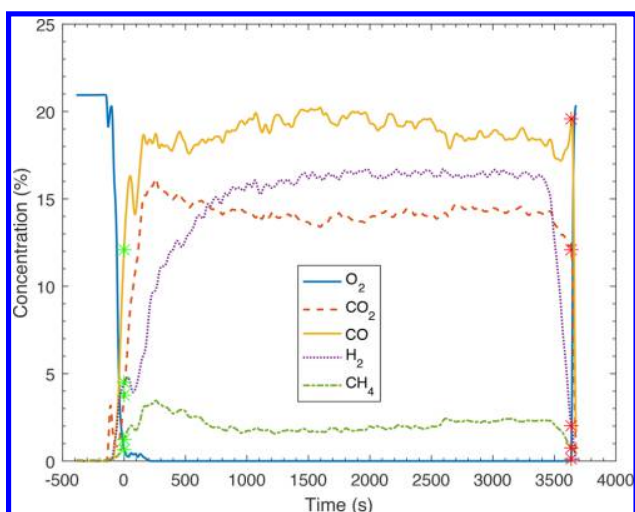
**Figure 2.** Example of volumetric concentration profiles of the continuous measurement of gaseous devolatilisation products at 4D FR125, with start and stop points marked by stars.

in Figure 2. Mean values of the average plot for each configuration are calculated, resulting in an average producer gas composition. The heating value of the producer gas was calculated on the basis of the higher heating value of the constituents. To calculate the product flow of gaseous species, $N_2$ was considered to be conserved. This takes into account that, since the amount of $N_2$ in the air supply and the concentration of $N_2$ in the producer gas was known, the amount of each gas species can be calculated from the molecular balance, as performed previously.[35] The continuous flow of products was calculated via eq 1.

$$\dot{n}_{gas} = \frac{x_{gas}}{x_{N_2 measured}} \times \dot{n}_{N_2 air} \tag{1}$$

For the calculation of the fuel constituent conversion in the thermochemical conversion process, the supply of $N_2$ via air was considered to be conserved. The conversion of carbon and hydrogen from the fuel into the gas phase, as well as into specific gas species, was determined by eqs 2 and 3.

$$C_{gas} = \frac{m_{air}\omega_{N_{air}}/M_{N_2}(x_{CO_2} + x_{CO} + x_{CH_4})/x_{N_2}}{m_{fuel}\omega_C/M_C} \tag{2}$$

$$H_{2-gas} = \frac{m_{air} \times 0.767/M_{N_2} \times (x_{H_2} + 2x_{CH_4})/x_{N_2}}{m_{fuel}\omega_H/M_H} \tag{3}$$

The cold gas efficiency, which describes the energy content of the producer gas relative to the energy content of the converted fuel, was calculated using eq 4. This provides a measure of the loss of energy within the system, specifically the energy to sustain the autothermal process, heat loss from the reactor, and latent heat of the products. As the energy contained in the char is not lost and is available for subsequent processes, it is subtracted from the energy of the provided fuel. The energy content of the producer gas was calculated based on the measured gas concentrations, while other hydrocarbon compounds, which are condensed in the tar trap and have not been quantified, were not included. The higher heating values (HHV) of the fuel and the char were measured using a bomb calorimeter, and those of the producer gas species were determined based on the composition measurements and using values reported in the literature.[36]

$$CGE = \frac{V_{N_2-air}/x_{N_2-measured} \times (12.6x_{CO} + 39.8x_{CH_4} + 12.8x_{H_2})}{HHV_{pellets}m_{fuel} - HHV_{char}m_{char}} \tag{4}$$

The biomass, along with the char samples from each configuration, were tested for their ultimate analysis (CHN composition), proximate analysis (moisture (M), volatile matter (VM), fixed carbon (FC), and ash content), and their HHV. The proximate analysis, using thermogravimetric analysis techniques, was based on a method previously reported.[34]

## 3. RESULTS AND DISCUSSION

**3.1. Mass Flux.** The results of the mean fuel consumption rate as a function of the air supply are presented in Figure 3;
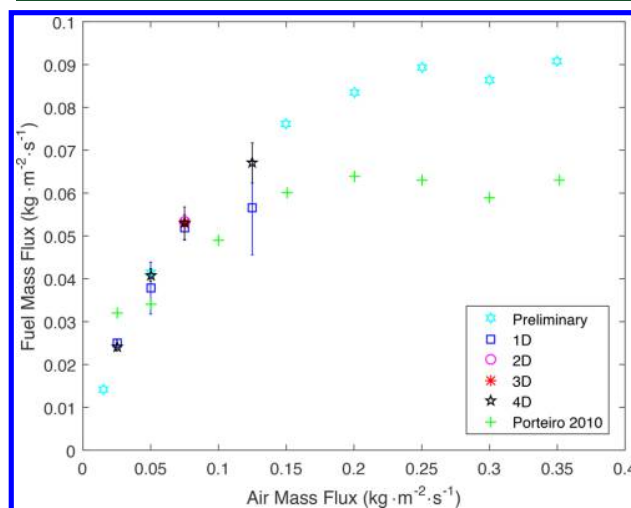


**Figure 3.** Fuel mass flux versus air mass flux for different experimental configurations, preliminary data, and data found in the literature.[14] Error bars display the standard error of the mean.

both parameters are reported on a mass flux basis, herein referred to as the fuel mass flux and the air mass flux. The error bars in Figure 3, as well as in all following figures, display the standard error of the mean.[37] As outlined in Section 1, in this type of reactor, the three fuel mass flux regimes can be defined as a function of the air mass flux. The focus of the current work is on the oxygen-limited regime. Preliminary experiments were performed at one fuel bed depth (1D). Only the weight loss and temperature measurements were recorded in order to identify the upper-limit of the air mass flux (as described in Section 2.5) and are shown in Figure 3, where they are compared with those values reported in the literature.[14] More detailed experiments were performed at other fuel bed depths (1D−4D), and the gaseous product composition data were also collected and are presented in Figure 3. Further information on the stoichiometry of the process is provided in the Supporting Information.

In the oxygen-limited regime, the fuel mass flux increases linearly with the air mass flux, which Figure 3 indicates is for an air mass flux of $\lesssim 0.1$ kg m$^{-2}$ s$^{-1}$ (up to approximately FR100). This range is in agreement with the literature for wood pellets.[14,16,38,39] Also apparent from Figure 3 is that the linear relationship between air and fuel mass flux is independent of the fuel stack depth (between 1D and 4D). A transition from the oxygen-limited to the reaction-limited regime is apparent around FR125, beyond which the fuel mass flux is nearly independent of the additional air supply. In the present study, the air mass flux was not further increased into the third regime (cooling), since in small-scale applications low air supplies are
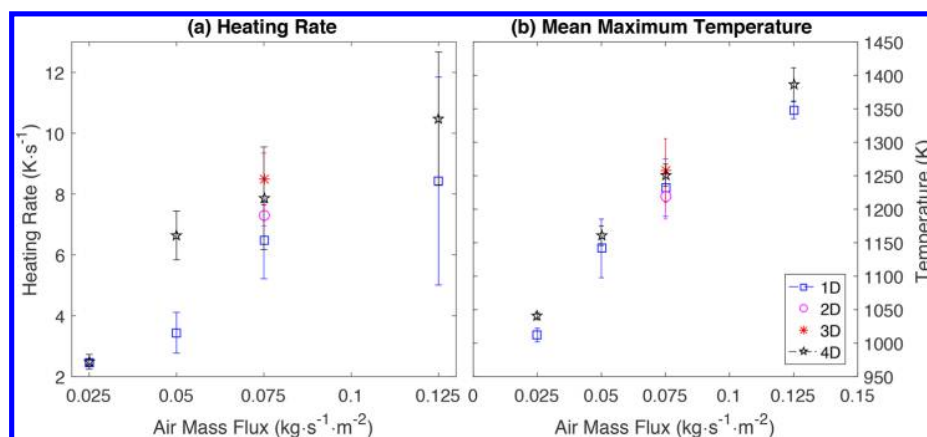
**Figure 4.** Heating rate (a) and mean maximum temperature (b) over the air mass flux. Error bars indicate the standard error of the mean.
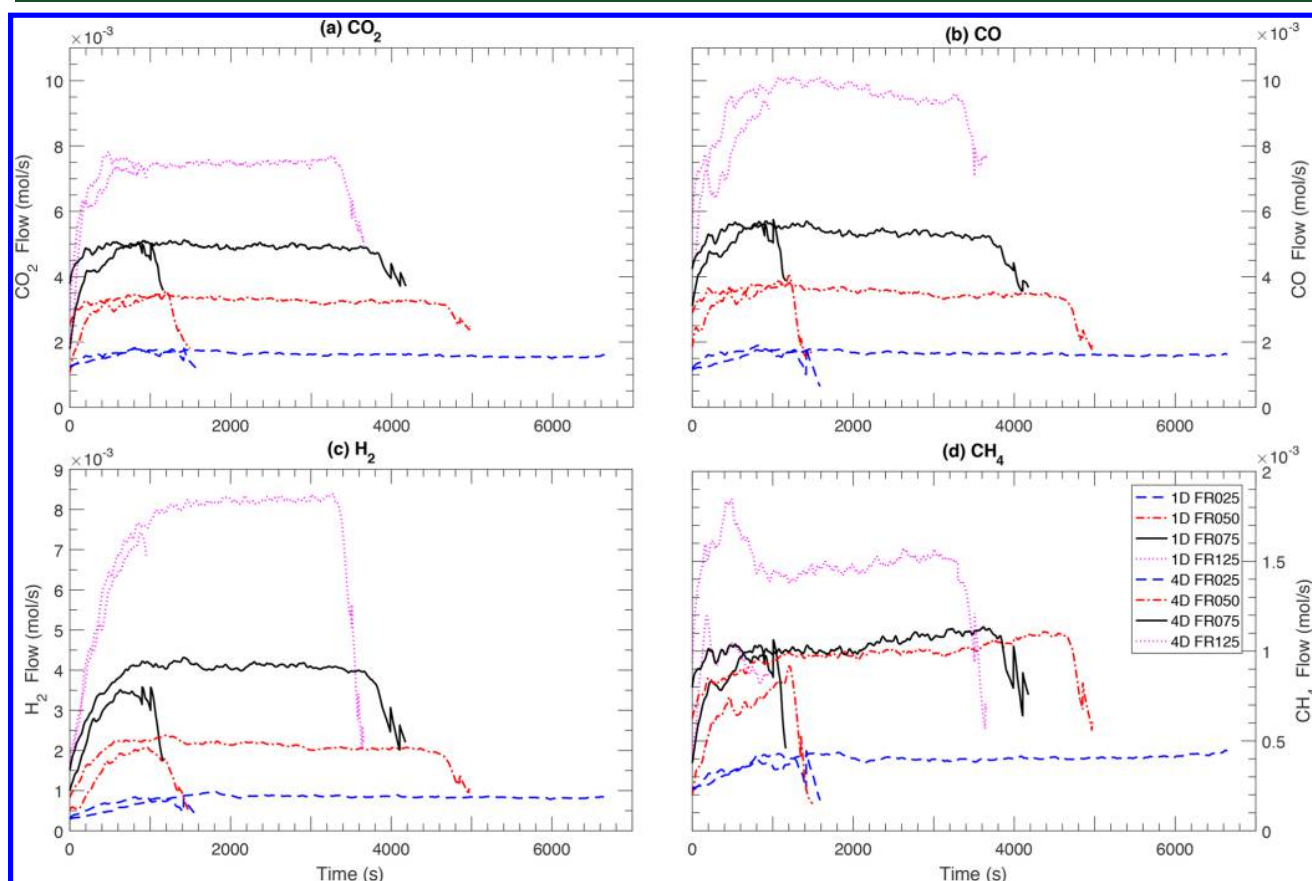


**Figure 5.** Flow of gaseous devolatilisation products over the period under consideration.

dominant. The ability to control the conversion process and heat release via the air supply is of particular interest here.

**3.2. Reactor Temperature.** The heating rate and the maximum reaction front temperature of the packed bed at the center of the reactor are presented in Figure 4 (calculated as presented in Section 2.5). In this figure the greater heat release at larger air supply rates is confirmed, as the mean maximum temperature and the heating rate increase with the air mass flux. A nearly linear increase of the mean maximum temperature of approximately 35% is noted over the 5-fold increase in air mass flux, while the heating rate more than quadruples. As with the mass loss data (Section 3.1), the mean

maximum temperature increases linearly for the air flow rates FR025–FR075.

Increasing temperatures have multiple influences on the process, as presented in Section 1. At temperatures greater than 1000 °C, low tar yields are generally expected.[40] It has previously been described that particles undergoing devolatilisation have a slightly lower temperature than that measured in the backed bed, because oxidation of the volatiles occurs in the gas phase surrounding the particles.[41,42] Therefore, the heating rate of the embedded thermocouples presented in Figure 4 is that of the packed bed, which will be similar to that of the particle itself. Therefore, the higher temperatures and

heating rates in Figure 4 occur with the higher air flux cases FR075 and FR125, and thus these cases are expected to have lower tar yields.

**3.3. Influence of Air Supply.** *3.3.1. Gaseous Products.* In autothermal reactors the fuel mass flux, the temperature profiles and the producer gas composition are coupled and dependent on the supplied air mass flux. In Figure 5 the molecular flow of the measured gaseous products ($CO_2$, CO, $H_2$, and $CH_4$) released over the duration of the process is presented. These products result from reactions in the reaction front and downstream before the extraction probe is reached. Possible reactions are presented in Table 2. In the reaction

**Table 2. Process Reactions[43,44]**

| | | |
|---|---|---|
| heterogeneous | $C + 0.5O_2 \rightarrow CO$ | R1 |
| | $C + CO_2 \leftrightharpoons 2CO$ | R2 |
| | $C + H_2O \leftrightharpoons CO + H_2$ | R3 |
| | $C + H_2 \leftrightharpoons CH_4$ | R4 |
| homogeneous | $CO + 0.5O_2 \leftrightharpoons CO_2$ | R5 |
| | $H_2 + 0.5O_2 \leftrightharpoons H_2O$ | R6 |
| | $CH_4 + 0.5O_2 \leftrightharpoons CO + 2H_2$ | R7 |
| | $CO + H_2O \leftrightharpoons CO_2 + H_2$ | R8 |
| | $CO_2 + 4H_2 \rightarrow CH_4 + H_2O$ | R9 |
| | $CH_4 + H_2O \leftrightharpoons CO + 3H_2$ | R10 |
| | $2CO + 2H_2 \rightarrow CH_4 + CO_2$ | R11 |
| tar cracking | $tars \rightarrow C + C_nH_m + gases$ | R12 |
| tar reforming | $C_nH_m + nH_2O \rightarrow nCO + (n + 0.5m)H_2$ | R13 |
| | $C_nH_m + nCO_2 \rightarrow 2nCO + (0.5m)H_2$ | R14 |
| | $C_nH_m + 2nH_2O \rightarrow nCO_2 + (0.5m + 2n)H_2$ | R15 |

front, while oxygen is available, exothermic reactions R1−R7 will be most influential and lead to substantial heat release. Once the oxygen is consumed and higher concentrations of $CO_2$ and $H_2O$ (from combustion and fuel drying) are present,

reactions R8−R15 will have a greater impact and the gas composition exiting the reaction front will depend on the thermochemical interaction between the presented reactions at the process temperature. As the reaction front moves down the fuel bed, along the temporal axis, more char is accumulated downstream of the front. While the devolatilisation products are released from the biomass and char is formed, the solid weight decreases, but there is only minimal change in the occupied volume in the reactor. Therefore, for example, when half the duration of the process has passed, the products from the reaction front move through approximately half the initial fuel bed depth of char. Thus, changes over time of released products can be related to an increasing char layer thickness, downstream of the reaction front, and ongoing reactions in this char layer. In Figure 5 the two main influences investigated in this article—the fuel bed depth and the air mass flux—are presented with all the flow rates for 1D and 4D cases. The plot for each configuration is an average of multiple repetitions of the experiment, as described in Section 2.5.

When changing the flow rates, FR025−FR125, at 1D and 4D depths, a complex influence on the different gaseous products is identified, as shown in Figure 5. In all cases it can be seen that the flow of the measured gaseous species increases initially until it reaches a near steady-state flow. There is a gradual increase of product flow with increasing air flow. The well-known increasing of the $CO/CO_2$ primary product ratio with increasing temperatures[45] can be noticed in the oxygen-limited regime (FR025−FR075) and is much more defined in the transition to the reaction-limited regime (FR125).

The release of $CH_4$ does not seem to follow the clear trend of increasing flow at higher air supplies. There is no notable flow increase between FR050−FR075, which suggests that with higher temperatures in the range of 1150−1250 K, an increase in the reaction rates of $CH_4$ producing reactions is
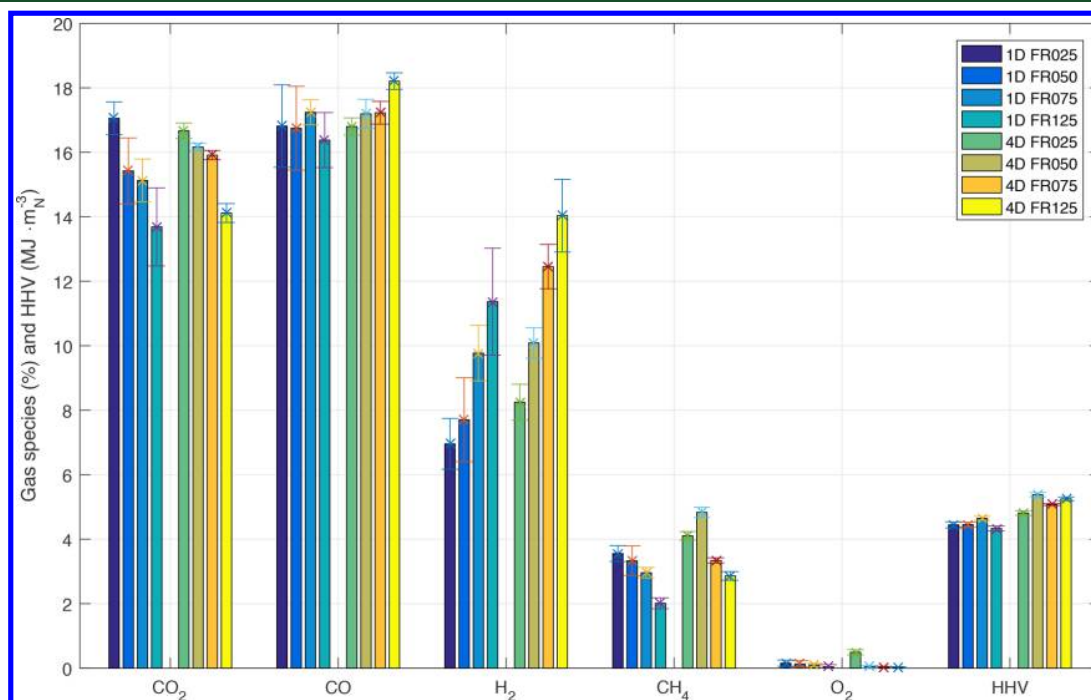
**Figure 6.** Time-weighted volumetric average concentrations (% v/v) of gaseous devolatilisation products at fuel bed depths of 1D and 4D for the different air mass fluxes, as well as the higher heating values of the gas (MJ $m_N^{-3}$). Error bars indicate the standard error of the mean.

compensated by increasing consuming reactions. Importantly, in all the 4D cases the $CH_4$ flow increases as a function of time, suggesting that a greater char layer thickness affects the $CH_4$ production, via methanation or tar cracking reactions (R9−R12).

For the $H_2$ concentration, it takes between 1000 and 2000 s to reach a near steady-state concentration. Increasing the air mass flux and, thus, the process temperature does not reduce the time but does increase the value of the near steady-state concentration substantially, mainly influenced by reactions R7 and R8 as well as R12−R15. This initial time suggests that a certain char layer thickness is necessary to promote the release of $H_2$. Increasing $H_2$ values at higher flow rates and fuel bed depth suggest that increasing amounts of char downstream of the reaction front as well as higher temperatures increase the release of this product.

The volumetric time-weighted average producer gas constituent concentrations and the calculated HHV of the producer gas at the four different air mass flux configurations for 1D and 4D depths are shown in Figure 6. Very low oxygen concentrations were measured in all cases, confirming that the oxygen supply is a reaction limiting variable. All concentrations are notably influenced by the air supply and the fuel bed depth.

The mean concentrations (Figure 6) reflect and clarify the results presented in Figure 5. Although the produced flow of the gaseous products increases, mean $CO_2$ and $CH_4$ concentrations decrease in the producer gas with increasing air mass flux but increase with the fuel bed depth (with the exception of $CH_4$ in the FR050). At 1D, the CO concentration is similar for all air mass fluxes, while at 4D it increases with the air supply, suggesting an influence of the greater fuel bed depth. The $H_2$ concentration increases with the air flow for both depths, by as much as 8−14% (v/v) at 4D. The trends of both the CO and $H_2$ concentrations, the main products of tar cracking and reforming reactions, for R12−R15, show the combined influence of increasing process temperatures and a greater char layer.

Similar systems have been studied previously with comparable fuels.[20,21] The producer gas composition for similar air mass fluxes has been found to be quite different. Lodgepole pine pellets and Douglas fir chips were tested at 1.6D fuel bed depths. Compared with the results presented here, both fuels produced similar CO and $CO_2$ concentrations, but lower $CH_4$ and $H_2$ concentrations, at an air mass flux of 0.052 kg m$^{-2}$ s$^{-1}$.[21] Wood pellets have also been tested in a 1D depth reactor at air mass fluxes of 0.032 and 0.051 kg m$^{-2}$ s$^{-1}$. Much lower CO and $H_2$ concentrations of 8.0% and 1.6%, respectively, were found at FR032,[20] compared with 16.8% and 7.0%, respectively, at FR025 1D, as seen in Figure 6. In both cases no thermal insulation of the reactor was used; a resultant 10−20% lower reaction front temperature could be the cause of this discrepancy. Conversely, pine bark chips were tested at higher flow rates and higher reaction temperatures but also exhibited lower concentrations of all gaseous products.[17] A moisture content of >10%, compared with <5% in the used pellets here, will have an influence on this difference in concentrations, as the moisture evaporation will consume released energy and the greater steam concentration will influence ongoing reactions. Very similar conditions and gaseous concentrations were achieved using Casuarina (*Casuarina equisetifolia*) wood in a thermally insulated reactor.[46] These wide variations in measurements show that small differences in the reactor design or fuel composition can

have a significant influence on the producer gas composition and that deeper insights into the batch-fed autothermal conversion process are necessary for efficient reactor design.

*3.3.2. Biomass Conversion.* Figure 7 presents the molar conversion of biomass carbon (C) into the different products,
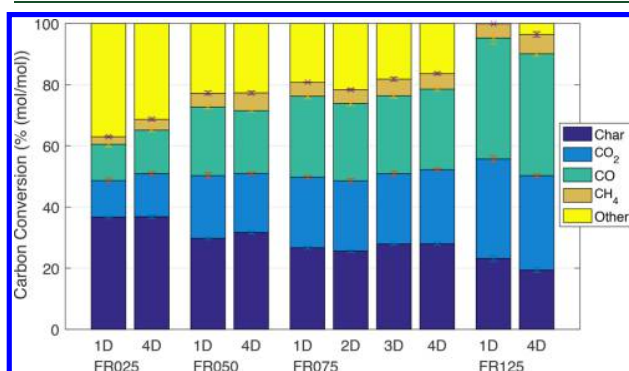


**Figure 7.** Conversion of initial carbon in the biomass into the different products for increasing flow rates, FR025−FR125, for 1D and 4D fuel bed depths and at FR075 for 2D and 3D fuel bed depths. Error bars indicate the standard error of the mean.

$CO_2$, CO, $CH_4$, and char, with increasing flow rates for both the 1D and 4D cases. "Other" is determined by subtraction and accounts mainly for hydrocarbons (tars) and carbonaceous particles, which were not measured. The amount of carbon converted to "Other" decreases from 34 ± 3% at FR025 to 1.8 ± 1.8% at FR125. This decrease of "Other" products provides an indication of increased tar cracking occurring with a greater air supply and the resulting higher temperatures (Section 3.2).

At 4D, a greater air supply results in increasing $CO_2$ and CO yields from 14.2 ± 0.1% to 35.5 ± 4.5%. The increase in the $CO/CO_2$ product ratio at higher air supply rates can be related to carbon oxidation at higher temperatures[45] (see Section 3.3.1). Furthermore, the char yield decreases by nearly half in the 4D configuration. The increase in the CO and $CO_2$ yield reflects increasing heterogeneous char gasification (R1−R4) and thus a reduction in char yield. Tar cracking reactions (R12) will also contribute to the increase in gaseous carbonaceous products, mainly of CO.

The conversion to $CH_4$ shows lower values at FR025 and FR075, and higher at FR050, but the peak value is reached at FR125. A higher air mass flux leads to an increase of the $CH_4$ and CO gas yields which are the desired species for further gas-phase combustion. This increase in conversion will most likely be the result of increasing tar cracking reactions due to higher process temperatures with the air supply, as suggested in Section 3.2.

Figure 8 presents the molar conversion of hydrogen (H) from the biomass into the different hydrogen-containing products. "Other" accounts primarily for water and tars. The $H_2$ and $CH_4$ yield increases with the air mass flux. With the air mass flux, the $H_2$ yield rises from 7.4 ± 1.4% to 35.7 ± 2.7%, from FR025 to FR125. Increasing yields of $CH_4$ as well as $H_2$ with rising temperatures are expected (see Section 3.3.1), due to tar cracking reactions (R12−R15).[28] A trend of increasing hydrogen conversion is visible with the greater fuel bed depth and higher flow rates.

*3.3.3. Cold Gas Efficiency.* Gasification systems can be evaluated by their cold gas efficiency (CGE), which describes the energy content of the producer gas relative to the energy
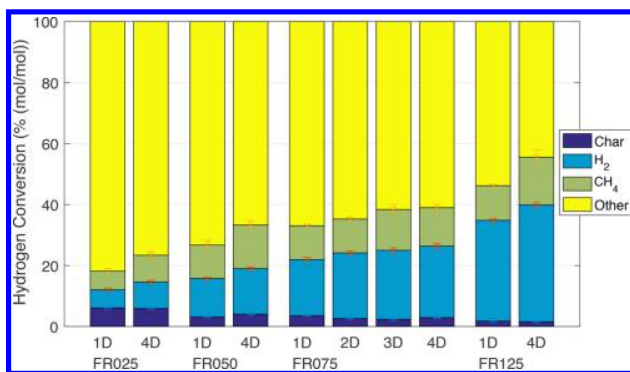
**Figure 8.** Conversion of the fuel hydrogen into the different products. Error bars indicate the standard error of the mean.

released from the converted fuel,[47] as per eq 4. Here, only the measured gases ($CO$, $CO_2$, $H_2$, and $CH_4$) are considered in the calculation of the CGE; other hydrocarbon species, which have not been quantified in this study, notably tars, are not included. Statistical analysis suggests a significant difference between FR025−FR050 and FR075−FR125, but between FR050 and FR075 a lower statistical difference was apparent.

The increased conversion yields of permanent gases, presented in Section 3.3.2, are mirrored in the CGE as presented in Figure 9. The CGE increases nearly linearly from
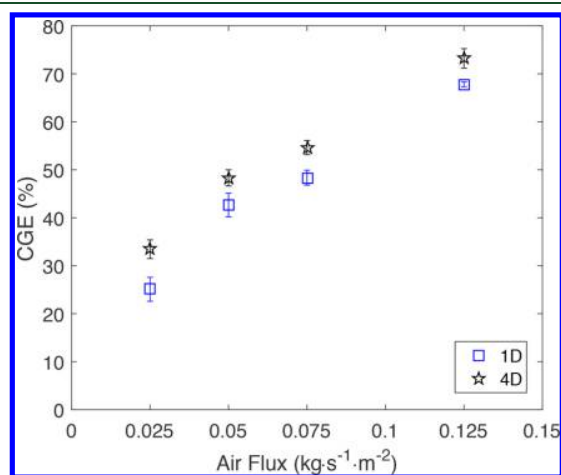


**Figure 9.** Cold gas efficiency (CGE) as a function the air mass flux for two fuel bed depths. Error bars indicate the standard error of the mean.

$29.3 \pm 4.2\%$ to $70.5 \pm 2.7\%$ between FR025 and FR125, for 1D and 4D. The low values of the CGE at FR025 can be explained by the high tar content, while at FR125 a large fraction of tars, as well as char, are converted into permanent gases that contribute to the CGE.

Different shapes of *Jacaranda Copaia* wood were used in a similar reactor at air supply rates approximately 10% lower than FR125, achieving CGE values between 31−38% which are much lower than the results presented here.[42] In that work it was not stated if char was produced, or also consumed in the process, and how the CGE was calculated, making a direct comparison difficult. In a similarly sized continuous downdraft gasifier, a CGE over 70% was reported, at an air supply comparable with FR050.[48] Although, the peak process temperature and the producer gas composition appear similar, the tar

yield here seems much higher and the CGE is more than 20% lower.

**3.4. Influence of Fuel Bed Depth.** *3.4.1. Gaseous Products.* Figure 10 presents the temporal evolution of gaseous products for varying fuel bed depths (the average producer gas composition is provided in the Supporting Information). The profiles at 4D and 3D achieve more steady profiles, rather than at 2D and 1D. It is evident that at greater fuel bed depths, the steady propagation of the reaction front occupies a larger part of the process, while at lower fuel bed depths, the effects of transients at start-up and shut-down are more prominent.

In all cases the flow of $CH_4$ increases as a function of time, suggesting increasing methanation or tar cracking reactions (R9−R12) with a greater char layer thickness (see also Section 3.3.1). The value of $H_2$ of the near steady-state flow does not change notably between 2D and 4D. In the 1D configuration the flow remains much lower in the limited time of the process. The time to reach the near steady concentration occupies a larger proportion of the process duration at lower depth. This indicates that a depth greater than 1D is necessary to reach the potential of the $H_2$ release in this process.

*3.4.2. Biomass Conversion.* Figure 7 presents the molar conversion of carbon (C) in the biomass into the different products. When comparing the yields with the concentrations, it should be noted that conversion yields consider the species concentration, the process duration, and the amount of produced gases, as explained in more detail in Sections 2.5 and 3.3.2. The amount of carbon converted to "Other", mainly tars, decreases from $19.2 \pm 1.6\%$ to $16.4 \pm 1\%$ between 1D and 4D fuel bed depths, at FR075. This provides an indication of increased tar cracking with greater char layer thickness. A general trend of greater conversion yields of permanent gases and char can be seen at 3D and 4D, when compared with 1D and 2D.

Figure 8 presents the molar conversion of hydrogen (H) in the biomass into the different products. The "Other" species, mainly water and tars, are reduced from 67.0% to 61.0% between 1D and 4D. With depth, there is a change in $H_2$ yield from 1D to 2D of 18.7% to 21.5%, while it further increases to 23.5% (mol/mol) at 4D. The increase with depth can be related to the temporal profiles, as discussed previously and presented in Figure 5. Cracking of tars will have an influence on the increase of $H_2$.

*3.4.3. Cold Gas Efficiency.* The CGE with increasing fuel bed depth is presented in Figure 11. It can be seen that the CGE increases from 48.4% to 54.6% from 1D to 4D, at FR075. Generally higher efficiencies are achieved at 3D and 4D. These higher efficiencies are the result of greater conversion to combustible permanent gases in the presence of a larger char layer thickness in the system. Statistical analysis confirmed a very low statistic difference between 1D−2D and 3D−4D, with a much higher difference when comparing 1D and 2D with 3D and 4D.

In the conversion yields in Figure 8 (and in the Supporting Information), where only $H_2$ shows a substantial increase, the influence of the fuel stack depth seems to have a rather negligible impact on the process. However, the cold gas efficiency in Figure 11 confirms that 1D and 2D are not sufficient and that a quite substantial 10% increase can be achieved when increasing the depth to 3D or 4D.

**3.5. Char Layer.** Tables 3 and 4 present the mass-based proximate and ultimate analyses, the H/C and O/C ratios, the char product yield, and the higher heating value of the
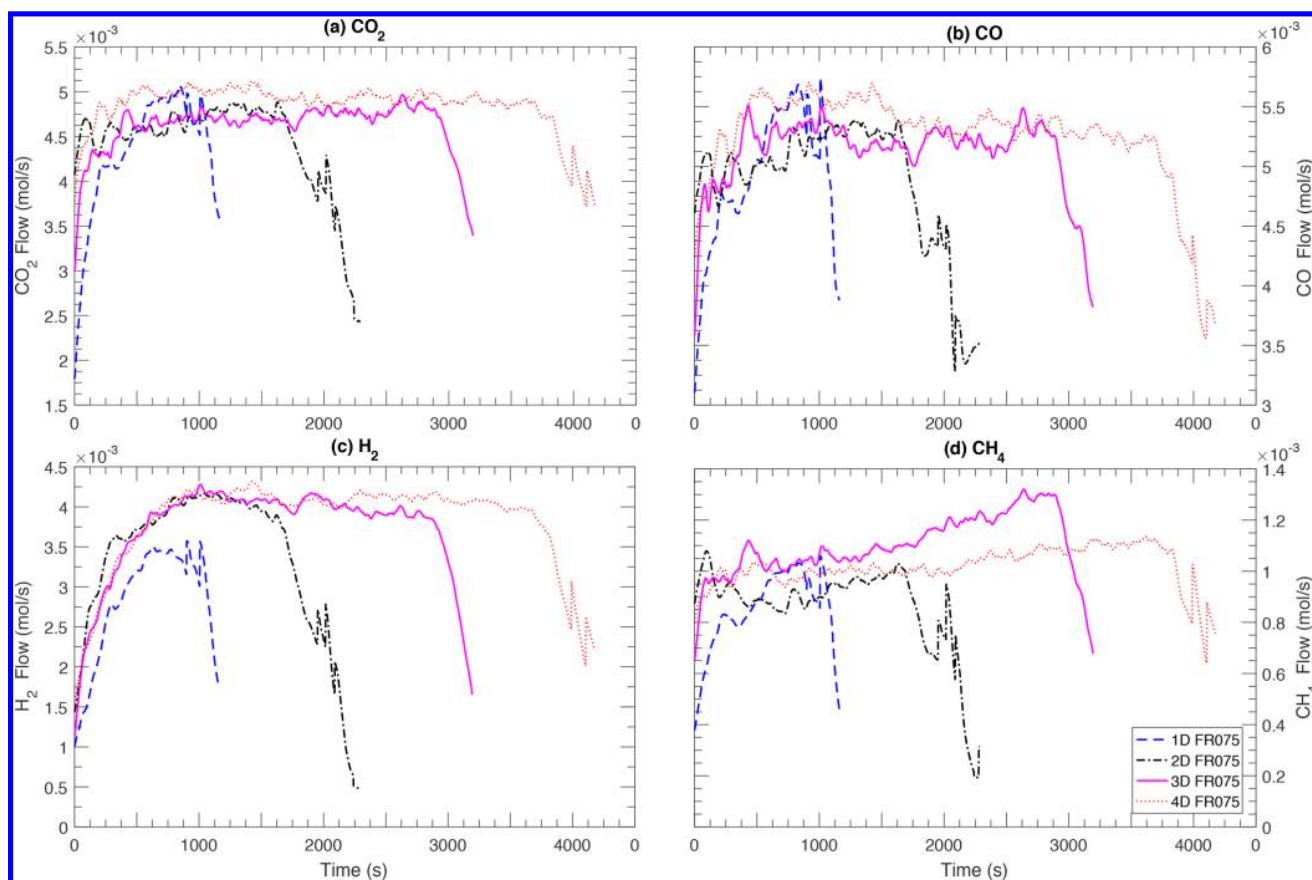
**Figure 10.** Flow of gaseous devolatilisation products over the period under consideration.
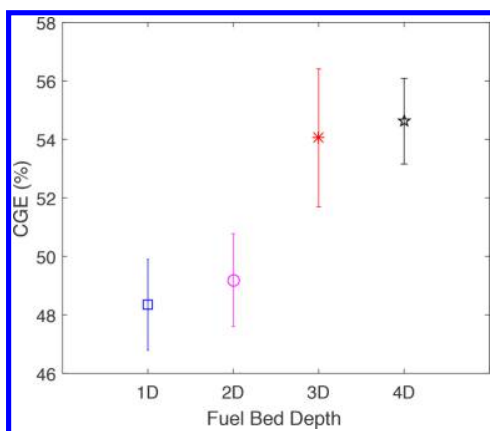


**Figure 11.** Cold gas efficiency (CGE) over the fuel bed depth at FR075. Error bars indicate the standard error of the mean.

**Table 3. Proximate and Ultimate Analyses Results for the Wood Pellet Fuel and Chars from the Different Test Configurations, in Addition to H/C Mass Ratios, O/C Mass Ratios, Char Yield with Standard Error (SE), and HHV Values**

| Configuration | FC | VM | Ash | H:C | Yield | HHV |
|---|---|---|---|---|---|---|
|  | C | H | N | O:C | SE | MJ/kg |
| Wood Pellets | 17.8 | 71.5 | 4.8 |  |  | 17.6 |
|  | 47.4 | 6.4 | 0.1 |  |  |  |
| 1D FR025 | 93.7 | 5.4 | 0.9 | 0.3 | 18.6 | 32.9 |
|  | 90.3 | 2.0 | 0.2 | 0.06 | ( 0.1) |  |
| 1D FR050 | 94.7 | 4.5 | 0.8 | 0.2 | 15.0 | 32.1 |
|  | 91.2 | 1.3 | 0.3 | 0.06 | ( 0.1) |  |
| 1D FR075 | 93.9 | 3.4 | 2.8 | 0.2 | 13.8 | 30.5 |
|  | 88.4 | 1.6 | 0.2 | 0.08 | ( 0.2) |  |
| 1D FR125 | 95.0 | 4.2 | 0.9 | 0.1 | 11.9 | 31.8 |
|  | 92.0 | 1.0 | 0.3 | 0.05 | ( 0.5) |  |
| 2D FR075 | 95.8 | 3.6 | 0.6 | 0.2 | 13.9 | 30.5 |
|  | 87.7 | 1.2 | 0.3 | 0.09 | ( 0.2) |  |
| 3D FR075 | 85.4 | 0.7 | 13.9 | 0.1 | 14.3 | 32.1 |
|  | 93.3 | 1.1 | 0.2 | 0.04 | ( 0.1) |  |

produced chars for all configurations. The chars are separated into the top, middle, and bottom of the bed for the 4D cases, as explained in Section 2.4. In all cases, the fixed carbon (FC) and the elemental carbon content are very similar, with changing depths and flow rates. All produced chars exhibit a high carbon content, with values greater than 92% for FC and 84% for C.

The volatile matter (VM) and elemental hydrogen content decrease with increasing flow rates, as well as fuel bed depths. This trend of reducing elemental hydrogen and hydrogen compounds can be explained by the longer exposure to high

temperatures and higher maximum reaction temperatures. A similar behavior has been established for pyrolysis processes.[49]

In the conversion process the mass-based char yield, as well as the carbon and hydrogen bound in the char, decreases with increasing air mass flux. With increasing fuel bed depth, the char yield generally increases, which also suggests that char downstream of the reaction front does not participate in subsequent reactions. At 4DFR025, nearly all FC is retained in the char, while at FR125, only about half is retained.

Table 4. Proximate and Ultimate Analyses Results for Chars from the Different Test Configurations, in Addition to the H/C and O/C Mass Ratios, Char Yield with Standard Error (SE), and HHV Values

| Configuration | FC / C | VM / H | Ash / N | FC / C | VM / H | Ash / N | FC / C | VM / H | Ash / N | H:C / O:C | Yield SE | HHV MJ/kg |
|---|---|---|---|---|---|---|---|---|---|---|---|---|
| | Bottom | | | Middle | | | Top | | | | | |
| 4D FR025 | 94.1 | 4.6 | 1.3 | 94.3 | 3.7 | 2.0 | 94.1 | 4.1 | 1.8 | 0.3 | 19.9 | 32.5 |
| | 88.7 | 1.9 | 0.2 | 90.2 | 1.8 | 0.2 | 87.5 | 2.1 | 0.2 | 0.08 | ( 0.2) | |
| 4D FR050 | 95.1 | 3.5 | 1.4 | 94.9 | 2.9 | 2.2 | 96.0 | 2.5 | 1.4 | 0.2 | 16.6 | 32.0 |
| | 89.4 | 1.5 | 0.3 | 92.3 | 1.3 | 0.2 | 85.2 | 1.8 | 0.3 | 0.08 | ( 0.3) | |
| 4D FR075 | 93.3 | 2.7 | 4.0 | 92.7 | 4.2 | 3.1 | 93.1 | 3.7 | 3.2 | 0.2 | 14.4 | 31.2 |
| | 94.3 | 1.1 | 0.3 | 91.6 | 1.2 | 0.2 | 84.7 | 1.5 | 0.2 | 0.07 | ( 0.3) | |
| 4D FR125 | 94.0 | 2.4 | 3.6 | 85.2 | 1.9 | 12.9 | 88.8 | 2.8 | 8.4 | 0.1 | 10.1 | 31.6 |
| | 89.7 | 0.9 | 0.3 | 93.3 | 0.9 | 0.2 | 86.0 | 1.2 | 0.3 | 0.07 | ( 0.3) | |

All produced chars would be regarded as Class 1 biochars based on their CHNO composition if used as a soil amendment. In all cases the H/C and O/C ratios are much lower than the thresholds proposed by the European Biochar Foundation of 0.7 and 0.4, respectively.[50,51] Generally these ratios are calculated on the basis of the organic carbon (OC) fraction in the char, but because of the high temperatures in this particular conversion process and a carbon fraction of >84% (g/g) for all configurations, all elemental carbon can be assumed to be OC.

**3.6. Discussion.** The autothermal process in the studied reactor displays an interrelationship of many parameters, such as the air supply, fuel consumption, composition of released products, subsequent exothermic or endothermic reactions of released products, and the process temperature. In this process the composition of released products, for a specific fuel, depends not only on the supply of the oxidizer but also on the internal heat transfer in the fuel as well as the external heat loss from the reactor. This complex interrelationship leads to great difficulty in isolating specific influences on the final producer gas composition. Multiple indicators for particular trends in the presented study need further discussion.

When trying to isolate the impact of different influences, it has been observed here that heterogeneous reactions do not seem to occur downstream of the reaction front. The indications for the absence of heterogeneous reactions found in this study are that toward the end of the process, when the char layer thickness is greatest, the flow of carbonaceous products does not increase and greater fuel bed depths lead to a greater yield of char, except at the highest flow rate. The exception of the highest flow rate supports the argument made in Section 3.1 that this flow rate is a transition between the oxygen- and reaction-limited regimes. Char gasification with $CO_2$ or $H_2O$, downstream of the reaction front, requires high reactant concentrations as well as high temperatures,[22] which seem to be present only at the highest flow rate. Figure 12 presents the temperature profile in the reactor, from the top (T1) to the bottom (T8) (see Figure 1), for the 4D cases at the time when thermocouple T7 (70 mm above the fuel grate) reached the maximum temperature. Downstream of the reaction front it can be seen that, while for FR125 four thermocouples exceed 800 °C, which is considered within the range of gasification processes,[47] this is only the case for one thermocouple for FR075 and none at lower air flow rates. These relatively low temperatures downstream of the reaction front will lead to low reaction rates of char gasification.[45] Furthermore, even at FR125, where the highest temperatures are achieved downstream of the reaction front, it is possible that the increase in heterogeneous reactions of the char are due to gasification in the reaction front with oxygen, rather than
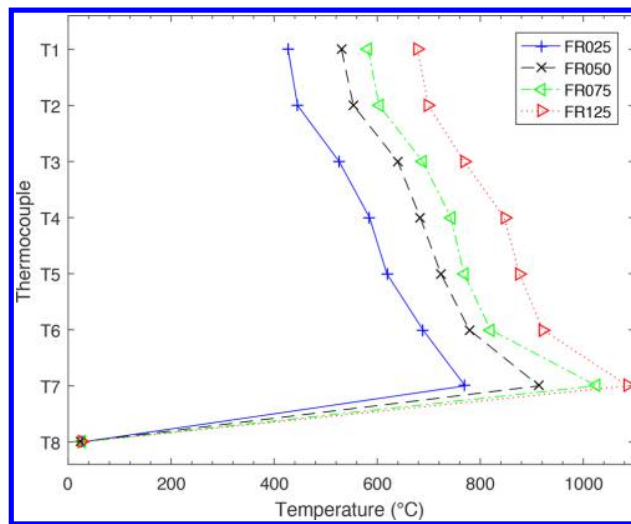


**Figure 12.** Reactor temperature profile for the 4D cases when thermocouple T7 reached the maximum temperature.

downstream with $CO_2$ or $H_2O$. Therefore, heterogeneous reactions (R1−R4 in Table 2) downstream of the reaction front can be neglected as possible contributors to increasing conversion yields to permanent gases with depth.

It can be shown that the conditions in the reaction front do not vary with depth and that heterogeneous reactions do not influence the release of producer gas components downstream. Therefore, the varying producer gas composition and yield with depth could relate to ongoing subsequent processes downstream of the reaction front. Possible downstream reactions, R5−R15, are presented in Table 2. Higher temperatures, as achieved at higher air flow rates, will favor reactants of the exothermic water gas shift and homogeneous methanation reactions, R8−R11, in accordance with Le Chatelier's principle, while higher reaction rates for the tar degradation and reforming reactions, R12−R15, are achieved.[52] It can be assumed that the presence of char promotes tar cracking reactions.[44] A greater residence time in the char bed at elevated temperatures (see Figure 12), which results from the propagation of the reaction front down the fuel bed over time, will influence these subsequent reactions. The increase of $CH_4$ flow, representing all gaseous hydrocarbon species along the temporal axis as noted in all configurations (see Figures 5 and 10), supports the assertion of increasing tar cracking reactions in the char layer as it increases in depth. A combination of the reactions, presented in Table 2, will lead to the notable increase in the conversion products $H_2$, $CH_4$, and CO, while tar cracking and reforming

reactions are most likely to have the greatest influence. Future work on gravimetric determination of the amount of tars and an analysis of the produced species could provide further information.

Experimental investigations on the degradation of tars are generally performed at similar or higher temperatures than the conversion temperature at which the tars are produced. In the present system, thermochemical conversion occurs at the maximum temperature in the reaction front, while degradation is assumed to occur downstream in the char bed at elevated temperatures. The high temperatures in the reaction front will lead to the formation of products that are more thermally stable at these temperatures.[53] Therefore, the limited increase in conversion to permanent gases with increasing fuel bed depths could be partially due to tar cracking downstream of the reaction front, occurring at lower temperatures than those at which the tars are produced.

One possible application of the new knowledge from this study is in small-scale domestic stoves. In this application, a fuel bed depth of 3D and 4D is expected to lead to a more steady conversion process, with lower tar yields and greater conversion to permanent gases. Tar and permanent gas yields could be influenced by tar cracking reactions in the char bed downstream of the reaction. Furthermore, with a greater fuel bed depth, a longer time is spent in the steady-state propagation of the reaction front, while lower depths are more strongly affected by transients at start-up and shut-down. This could be of particular interest since typically commercial[8] as well as experimental designs of this type of reactor are in the range 1D−2D fuel bed depths, while this research suggests that increasing this parameter has a beneficial effect on the conversion process.

## 4. CONCLUSIONS

The presented study investigates the influence of the air supply and the fuel bed depth on the conversion process in a small-scale batch-fed reverse downdraft reactor. Four flow rates, from 0.025−0.125 kg m$^{-2}$ s$^{-1}$, and fuel bed depths, from 100−400 mm (1D−4D), were used in the experiments.

Increasing the air supply also increases the fuel consumption, the temperature, and the conversion processes to permanent gases in the reaction front. Substantially higher combustible gas yields and cold gas efficiencies (CGE) are achieved with higher temperatures at greater air supply levels. With higher temperatures, the increase in combustible gas yields can be explained by greater rates of tar conversion reactions and an increase in the $CO/CO_2$ product ratio.

When increasing the fuel bed depth, the conditions in the reaction front, such as the fuel consumption and temperatures, are not affected; however, it needs to be kept in mind that, as the reaction front moves down the fuel bed, a char layer, of increasing depth, accumulates downstream. It was confirmed that this char layer downstream of the reaction front does not participate in heterogeneous gasification reactions with the gaseous products released from the reaction front. However, conversion of tars appears to be enhanced by a hot char layer which leads to increasing concentrations and yields of permanent gases, especially of CO and $H_2$, with increasing fuel bed depth. For all gaseous products, transients at start-up and shut-down of the process are more dominant at lower fuel bed depths, and generally higher conversion to permanent gases can be noted at 3D and 4D, rather than at 1D and 2D fuel bed depths. The increase in the permanent gas yield with

greater fuel bed depths provides a strong indication that there is a reduction in the release of tars.

The CGE can therefore be improved by increasing the fuel bed depth and improved even more by providing a greater air supply, or a combination of both. A higher producer gas quality for subsequent combustion applications is achieved with increasing CGE.

For applications in cookstoves, the increase in efficiency with greater fuel depth, larger than one reactor diameter, could provide a simple tool for optimization without compromising on the simplicity of the system. The high efficiency of the investigated process and the potential for further optimization, in combination with the opportunity for the production of high quality biochar, make this process especially attractive.

## ■ ASSOCIATED CONTENT

### Ⓢ Supporting Information

The Supporting Information is available free of charge on the ACS Publications website at DOI: 10.1021/acs.energy-fuels.8b01699.

>  Additional information regarding the experimental setup, stoichiometry, and influence of fuel bed depth (PDF)

## ■ AUTHOR INFORMATION

### Corresponding Author

*E-mail: thomas.kirch@adelaide.edu.au.

### ORCID Ⓘ

Thomas Kirch: 0000-0002-6288-7466

Philip J. van Eyk: 0000-0003-3768-2044

### Notes

The authors declare no competing financial interest.

## ■ ACKNOWLEDGMENTS

## ■ REFERENCES

(1) WEC. *World Energy Resources: 2013 Survey*; World Energy Council: 2013; pp 11.

(2) Arora, P.; Jain, S. A review of chronological development in cookstove assessment methods: Challenges and way forward. *Renewable Sustainable Energy Rev.* **2016**, *55*, 203−220.

(3) Sutar, K. B.; Kohli, S.; Ravi, M. R.; Ray, A. Biomass cookstoves: A review of technical aspects. *Renewable Sustainable Energy Rev.* **2015**, *41*, 1128−1166.

(4) Reed, T.; Das, A. Handbook of Biomass Downdraft Gasifier Engine Systems. *Solar Energy Research Institute* **1988**, 140.

(5) Martinez, J. D.; Mahkamov, K.; Andrade, R. V.; Silva Lora, E. E. Syngas production in downdraft biomass gasifiers and its application using internal combustion engines. *Renewable Energy* **2012**, *38*, 1−9.

(6) Molino, A.; Chianese, S.; Musmarra, D. Biomass gasification technology: The state of the art overview. *J. Energy Chem.* **2016**, *25*, 10−25.

(7) Reed, T. B.; Larson, R. A wood-gas stove for developing countries. *Energy Sustainable Dev.* **1996**, *3*, 34−37.

(8) Roth, C. An introduction to concepts and applications of wood-gas burning technologies for cooking. *Micro-gasification: cooking with*

*gas from dry biomass*, 2nd ed.; Deutsche Gesellschaft für Internationale Zusammenarbeit (GIZ) GmbH: 2014; http://www.giz.de/fachexpertise/downloads/giz2014-en-micro-gasification-manual-hera.pdf.

(9) Karellas, S. Chapter 4. In *Biofuels and Biorefineries*; Fang, Z., Ed.; Springer: Dordrecht, Germany, 2015; Vol. *5*, pp 97−117.

(10) Kirch, T.; Medwell, P. R.; Birzer, C. H. Natural draft and forced primary air combustion properties of a top-lit up-draft research furnace. *Biomass Bioenergy* **2016**, *91*, 108−115.

(11) Kirch, T.; Birzer, C. H.; van Eyk, P. J.; Medwell, P. R. Influence of Primary and Secondary Air Supply on Gaseous Emissions from a Small-Scale Staged Solid Biomass Fuel Combustor. *Energy Fuels* **2018**, *32*, 4212−4220.

(12) Birzer, C.; Medwell, P.; MacFarlane, G.; Read, M.; Wilkey, J.; Higgins, M.; West, T. A Biochar-producing, Dung-burning Cookstove for Humanitarian Purposes. *Procedia Eng.* **2014**, *78*, 243−249.

(13) Brewer, C.; Brown, R. Chapter 5. In *Comprehensive Renewable Energy*; Sayigh, A., Ed.; Elsevier Ltd.: 2012; pp 357−384.

(14) Porteiro, J.; Patiño, D.; Moran, J.; Granada, E. Study of a fixed-bed biomass combustor: Influential parameters on ignition front propagation using parametric analysis. *Energy Fuels* **2010**, *24*, 3890−3897.

(15) Horttanainen, M.; Saastamoinen, J.; Sarkomaa, P. Operational limits of ignition front propagation against airflow in packed beds of different wood fuels. *Energy Fuels* **2002**, *16*, 676−686.

(16) Porteiro, J.; Patiño, D.; Collazo, J.; Granada, E.; Moran, J.; Miguez, J. L. Experimental analysis of the ignition front propagation of several biomass fuels in a fixed-bed combustor. *Fuel* **2010**, *89*, 26−35.

(17) Pérez, J. F.; Melgar, A.; Benjumea, P. N. Effect of operating and design parameters on the gasification/combustion process of waste biomass in fixed bed downdraft reactors: An experimental study. *Fuel* **2012**, *96*, 487−496.

(18) Lu, H.; Ip, E.; Scott, J.; Foster, P.; Vickers, M.; Baxter, L. L. Effects of particle shape and size on devolatilization of biomass particle. *Fuel* **2010**, *89*, 1156−1168.

(19) Basu, P. *Biomass Gasification, Pyrolysis, and Torrefaction* **2013**, 1.

(20) Varunkumar, S. Packed bed gasification-combustion in biomass based domestic stoves and combustion systems. Ph.D. Thesis, Indian Institute of Science, 2012.

(21) Tryner, J.; Tillotson, J. W.; Baumgardner, M. E.; Mohr, J. T.; Defoort, M. W.; Marchese, A. J. The effects of fuel properties, air flow rates, secondary air inlet geometry, and operating mode on the performance of TLUD semi-gasifier cookstoves. *Environ. Sci. Technol.* **2016**, *50*, 9754−9763.

(22) Speight, J. G. Chapter 2. In *Gasification of Unconventional Feedstock*; Elsevier Inc.: Laramie, WY, 2014; pp 135−152.

(23) Fitzpatrick, E. M.; Bartle, K. D.; Kubacki, M. L.; Jones, J. M.; Pourkashanian, M.; Ross, A. B.; Williams, A.; Kubica, K. The mechanism of the formation of soot and other pollutants during the co-firing of coal and pine wood in a fixed bed combustor. *Fuel* **2009**, *88*, 2409−2417.

(24) Zhang, Y.; Kajitani, S.; Ashizawa, M.; Miura, K. Peculiarities of rapid pyrolysis of biomass covering medium- and high-temperature ranges. *Energy Fuels* **2006**, *20*, 2705−2712.

(25) Yu, Q.; Brage, C.; Chen, G.; Sjöström, K. Temperature impact on the formation of tar from biomass pyrolysis in a free-fall reactor. *J. Anal. Appl. Pyrolysis* **1997**, *40−41*, 481−489.

(26) Kaltschmitt, M.; Hartmann, H.; Hofbauer, H. *Energie aus Biomasse* **2009**, 1.

(27) Basu, P. Chapter 6. In *Biomass Gasification and Pyrolysis*, 2nd ed.; Elsevier Inc.: 2013; pp 177−198.

(28) Milne, T. A.; Evans, R. J.; Abatzaglou, N. Biomass Gasifier "Tars": Their Nature, Formation, and Conversion. *National Technical Information Service (NTIS)* **1998**, 1−68.

(29) Regtop, R. A.; Ellis, J.; Crisp, P. T.; Ekstrom, A.; Fookes, C. J. R. Pyrolysis of model compounds on spent oil shales, minerals and charcoal. Implications for shale oil composition. *Fuel* **1985**, *64*, 1640−1646.

(30) Park, J.; Lee, Y.; Ryu, C. Reduction of primary tar vapor from biomass by hot char particles in fixed bed gasification. *Biomass Bioenergy* **2016**, *90*, 114−121.

(31) Wu, W. G.; Luo, Y. H.; Su, Y.; Zhang, Y. L.; Zhao, S. H.; Wang, Y. Nascent biomass tar evolution properties under homogeneous/heterogeneous decomposition conditions in a two-stage reactor. *Energy Fuels* **2011**, *25*, 5394−5406.

(32) Brandt, P.; Larsen, E.; Henriksen, U. High tar reduction in a two-stage gasifier. *Energy Fuels* **2000**, *14*, 816−819.

(33) Varunkumar, S.; Rajan, N. K. S.; Mukunda, H. S. Experimental and computational studies on a gasifier based stove. *Energy Convers. Manage.* **2012**, *53*, 135−141.

(34) Saldarriaga, J. F.; Aguado, R.; Pablos, A.; Amutio, M.; Olazar, M.; Bilbao, J. Fast characterization of biomass fuels by thermogravimetric analysis (TGA). *Fuel* **2015**, *140*, 744−751.

(35) Lenis, Y. A.; Pérez, J. F.; Melgar, A. Fixed bed gasification of Jacaranda Copaia wood: Effect of packing factor and oxygen enriched air. *Ind. Crops Prod.* **2016**, *84*, 166−175.

(36) Waldheim, L.; Nilsson, T. Heating value of gases from biomass gasification. *IEA Bioenergy Agreement, Task 20 - Thermal Gasification of Biomass*; International Energy Agency: 2001; pp 61.

(37) Bondy, W. H.; Zlot, W. The Standard Error of the Mean and the Difference between Means for Finite Populations. *Am. Stat.* **1976**, *30*, 96−97.

(38) Mehta, Y.; Richards, C. Gasification Performance of a Top-Lit Updraft Cook Stove. *Energies* **2017**, *10*, 1529.

(39) Rönnbäck, M.; Axell, M.; Gustavsson, L.; Thunman, H.; Lecher, B.; Bridgwater, A. *Progress in Thermochemical Biomass Conversion* **2001**, 743−757.

(40) Baker, E.; Brown, M.; Elliott, D. C.; Mudge, L. Characterization and treatment of tars from biomass gasifiers. *AIChE 1988 Summer National Meeting*; American Institute of Chemical Engineers: 1988; pp 11.

(41) Varunkumar, S.; Rajan, N. K. S.; Mukunda, H. S. Universal Flame Propagation Behavior in Packed Bed of Biomass. *Combust. Sci. Technol.* **2013**, *185*, 1241−1260.

(42) González, W. A.; Pérez, J. F.; Chapela, S.; Porteiro, J. Numerical analysis of wood biomass packing factor in a fixed-bed gasification process. *Renewable Energy* **2018**, *121*, 579−589.

(43) Basu, P. Chapter 7. In *Biomass Gasification, Pyrolysis and Torrefaction*; Elsevier Inc.: 2013; pp 199−248.

(44) Shen, Y. Chars as carbonaceous adsorbents/catalysts for tar elimination during biomass pyrolysis or gasification. *Renewable Sustainable Energy Rev.* **2015**, *43*, 281−295.

(45) Laurendeau, N. M. Heterogeneous kinetics of coal char gasification and combustion. *Prog. Energy Combust. Sci.* **1978**, *4*, 221−270.

(46) Mahapatra, S.; Kumar, S.; Dasappa, S. Gasification of wood particles in a co-current packed bed: Experiments and model analysis. *Fuel Process. Technol.* **2016**, *145*, 76−89.

(47) Higman, C.; Van der Burgt, M. Chapter 2. In *Gasification*; Elsevier Inc.: 2008; pp 11−31.

(48) Kihedu, J. H.; Yoshiie, R.; Nunome, Y.; Ueki, Y.; Naruse, I. Counter-flow air gasification of woody biomass pellets in the auto-thermal packed bed reactor. *Fuel* **2014**, *117*, 1242−1247.

(49) Williams, P. T.; Besler, S. The Influence of Temperature and Heating Rate on the Slow Pyrolysis of Biomass. *Renewable Energy* **1996**, *7*, 233−250.

(50) IBI (International Biochar Initiative). *Standardized Product Definition and Product Testing Guidelines for Biochar That Is Used in Soil*; International Biochar Initiative: 2015; pp 61.

(51) Schmidt, H.-P. *European Biochar Certificate − Guidelines for a Sustainable Production of Biochar*; European Biochar Foundation (EBC): Arbaz, Switzerland, 2016; pp 1−22

(52) Morf, P.; Hasler, P.; Nussbaumer, T. Mechanisms and kinetics of homogeneous secondary reactions of tar from continuous pyrolysis of wood chips. *Fuel* **2002**, *81*, 843−853.

(53) Evans, R. J.; Milne, T. A. Molecular characterization of pyrolysis of biomass. 1. Fundamentals. *Energy Fuels* **1987**, *1*, 123−138.

# Supporting Information:

# Influences of fuel bed depth and air supply on small–scale batch-fed reverse downdraft biomass conversion

Thomas Kirch,[*,†,‡] Paul R. Medwell,[†,‡] Cristian H. Birzer,[†,‡] and Philip J. van Eyk[¶,‡]

†School of Mechanical Engineering, The University of Adelaide, Australia

‡Humanitarian and Development Solutions Initiative, The University of Adelaide, Australia

¶School of Chemical Engineering, The University of Adelaide, Australia

E-mail: thomas.kirch@adelaide.edu.au

# 1 Experimental Setup

## 1.1 Analysis

As in any combustion device, the relationship between the fuel consumption and the oxidiser supply, here air, is of central importance. This relationship can be presented in the form of; the air-to-fuel ratio (A/F = $m_{air}/m_{fuel}$), fuel-air equivalence ratio ($\Phi = \frac{(m_{fuel}/m_{O_2})}{(m_{fuel}/m_{O_2})_{st}}$) or air-fuel equivalence ratio ($\Lambda = \frac{(m_{O_2}/m_{fuel})}{(m_{O_2}/m_{fuel})_{st}}$). Equivalence ratios $\Phi$ and $\Lambda$ relate the oxygen and fuel consumption to the stoichiometric value. Traditionally, in continuously-fed gasifier literature, these values are calculated by the supplied air flow rate and the biomass mass flow rate. For the batch-fed systems presented here, it has been calculated using the supplied biomass less the produced char, thus the volatile fraction of the biomass, is used as the fuel input. Since the char was a desired product that was extracted at the end of the experiment, and was not intended to participate in the combustion process, taking all the supplied biomass as fuel would provide a misrepresentation, especially when considering the stoichiometric oxygen requirements. Therefore, $\Phi$ was calculated using the volatile matter: determined by subtracting the char (Ch) composition from the supplied biomass (B) as fuel is shown below in Equation 1. It should be noted that the subtraction of char from the global equivalence ratio was not related to any efficiency calculations.

$$\Phi = \frac{(m_{C_B} \cdot \omega_{C_B} + m_{H_B} \cdot \omega_{H_B} - m_{C_{Ch}} \cdot \omega_{C_{Ch}} - m_{H_{Ch}} \cdot \omega_{H_{Ch}})/(m_{O_{supply}} + m_{O_B} \cdot \omega_{O_B})}{(m_{C_B} \cdot \omega_{C_B} + m_{H_B} \cdot \omega_{H_B} - m_{C_{Ch}} \cdot \omega_{C_{Ch}} - m_{H_{Ch}} \cdot \omega_{H_{Ch}})/m_{O_{stoichiometric}}} \quad (1)$$

# 2 Results

## 2.1 Stoichiometry

Figure 1 presents the equivalence ratio ($\Phi$), calculated using Equation 1, as a function of the supplied air mass flux. In this context, $\Phi$ represents the factor by which the oxygen supply needs to be multiplied to completely combust all products released from the supplied biomass. In the presented process the stoichiometry is not actively regulated, as is the case in most thermochemical conversion and combustion processes, but a result of the autothermal reverse downdraft process. It can be seen in Figure 1 that $\Phi$ decreases with an increasing air mass flux. This shows that as more air is supplied, relatively less biomass is converted to volatile matter, and that the oxygen supply approaches its stoichiometric value for the combustion of the released volatile matter. Therefore, a relative increase in conversion to oxidised products can be expected at greater air flow rates, since more oxygen is consumed per unit of volatile matter released. This assertion would infer a greater heat release occurs, as well as a greater yield of products of the exothermic oxidation reactions (*viz.* $CO$, $CO_2$ and $H_2O$).
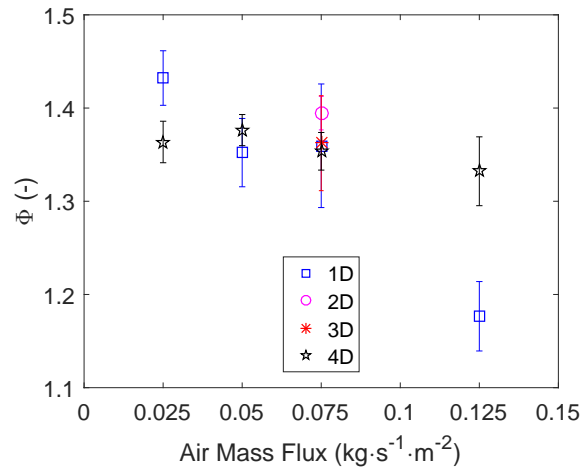


Figure 1: Equivalence ratio, at all measured configurations. Error bars indicate the standard error of the mean.

## 2.2 Influence of Fuel Bed Depth - mean producer gas composition

The volumetric time-weighted average producer gas composition at the different fuel bed depths, with constant air supply, is presented in Figure 2. A minor increase in the $CO_2$ concentration is noted above 2D, while the CO level is similar at all fuel bed depths. The mean $H_2$ value increases more than 20% with greater fuel bed depths, from 9.8% at 1D to 12.3% at 3D. The concentrations of hydrogen-containing molecules, $H_2$ and $CH_4$, are most significantly influenced by an increasing char layer thickness, providing an indication that these are affected by the presence of char. Overall, it can be seen that increasing the fuel bed depth increases the quality and HHV of the producer gas.
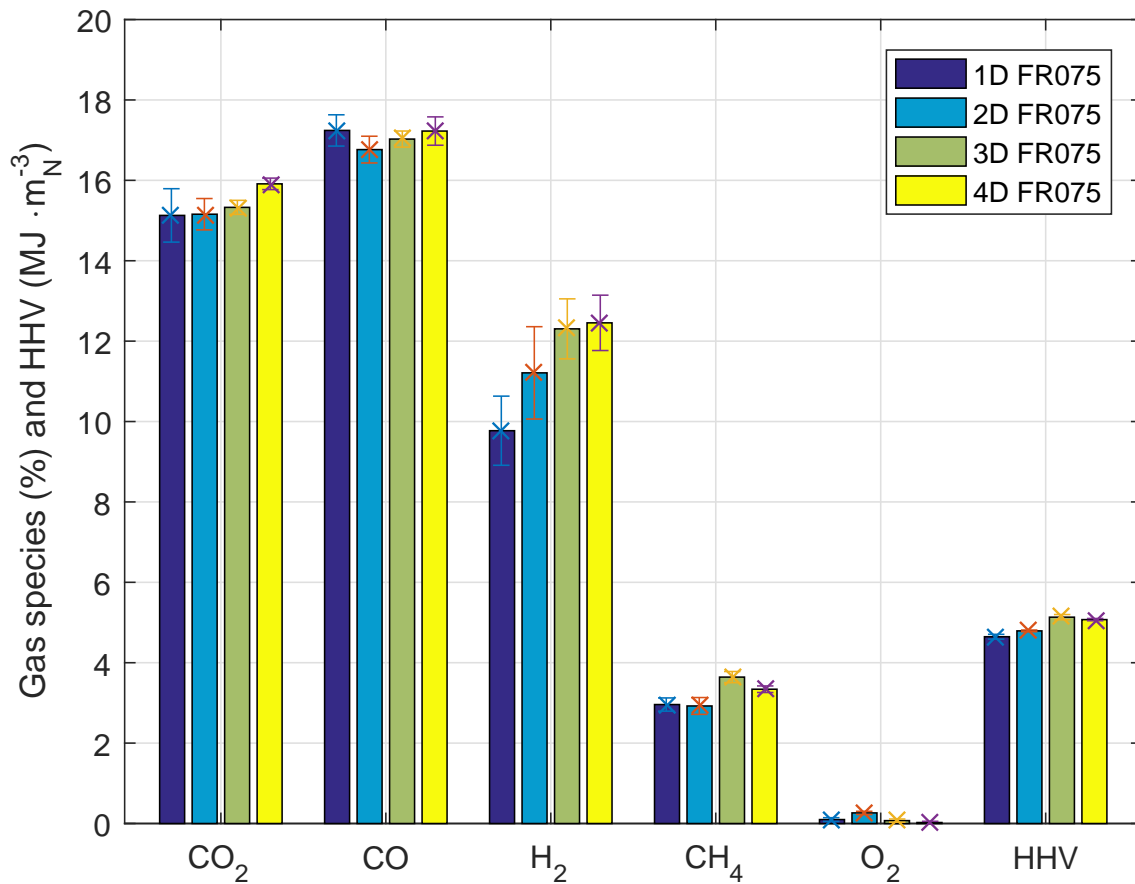


Figure 2: Time-weighted volumetric concentration (% vol/vol) of gaseous devolatilisation products at the different fuel bed depths, as well as the higher heating values of the gas (MJ·$m_N^{-3}$). Error bars indicate the standard error of the mean.

This page intentionally left mostly blank.

# Chapter 6

## Small-Scale Autothermal Thermochemical Conversion of Multiple Solid Biomass Feedstock

## Statement of Authorship

| | |
|---|---|
| Paper Title: | Small-Scale Autothermal Thermochemical Conversion of Multiple Solid Biomass Feedstock |
| Status: | Submitted |
| Details: | Renewable Energy |

### Principal Author

| | |
|---|---|
| Name: | Thomas Kirch |
| Contribution: | Performed the literature review and developed aims and objectives of the research study. Obtained biomass fuels, wheat straw, sheep manure and cow manure. Performed preliminary experiments to ensure process feasibility of the stated fuels. Hand processed cow manure into corresponding size distribution to sheep manure. Performed fuel size distribution measurements. Designed experimental matrix and performed experimental work. Performed solid composition analyses: proximate analysis using TGA with multiple repetitions of each sample; and calorific value determination using a bomb calorimeter. All biomass fuels as well as produced chars from each tested configuration were analysed. Wrote Matlab codes for data analysis. Performed data analysis and transferred to appropriate figures for visualisation. Structured, wrote and edited the research article. While the key findings are presented in the research article, supporting information ensure all findings are presented. Acted as corresponding author. |
| Contribution Percentage (%): | 70 |
| Certification: | This paper reports on original research I conducted during the period of my Higher Degree by Research candidature and is not subject to any obligations or contractual agreements with a third party that would constrain its inclusion in this thesis. I am the primary author of this paper. |
| Signature: | Date: 28.02.2019 |

114

**Co-Author Contributions**

By signing the Statement of Authorship, each author certifies that:

1. the candidate's stated contribution to the publication is accurate (as detailed above);

2. permission is granted for the candidate to include the publication in the thesis; and

3. the sum of all co-author contributions is equal to 100% less the candidates stated contribution.

| | |
|---|---|
| Name: | Paul R. Medwell |
| Contribution Details: | Guided research direction. Supervised work development. Helped generate ideas for tests and edited manuscript. |
| Signature: | Date: 28 Feb 2019 |

| | |
|---|---|
| Name: | Cristian H. Birzer |
| Contribution Details: | Guided research direction. Supervised work development. Helped generate ideas for tests and edited manuscript. |
| Signature: | Date: 28 Feb 2019 |

| | |
|---|---|
| Name: | Philip J. van Eyk |
| Contribution Details: | Guided research direction. Supervised work development. Helped generate ideas for tests and edited manuscript. |
| Signature: | Date: 28 Feb 2019 |

# Small-Scale Autothermal Thermochemical Conversion of Multiple Solid Biomass Feedstock

Thomas Kirch[a,c,*], Paul R. Medwell[a,c], Cristian H. Birzer[a,c], Philip J. van Eyk[b,c]

[a]*School of Mechanical Engineering, The University of Adelaide, S.A. 5005, Australia*
[b]*School of Chemical Engineering, The University of Adelaide, S.A. 5005, Australia*
[c]*Humanitarian and Development Solutions Initiative, The University of Adelaide, South Australia 5005, Australia*

**Abstract**

The thermochemical conversion of four types of biomass in a batch-fed reverse downdraft process for heat generation in cookstoves is investigated. Fuel switching is widely considered inefficient because many combustion devices do not respond well to changes in fuel. Here, the use of agricultural by-products, represented by wheat straw, sheep manure, cow manure, and wood pellets is addressed. Two air supply rates within the oxygen-limited regime, where the fuel consumption is linearly dependent on the air supply, are investigated. At higher air supply rates, in the reaction-limited regime, low carbon yields lead to the exposure of the ash fraction to high temperatures, such that the resultant ash melting has detrimental effects on the process. Generally, no detrimental impact of the ash content on the conversion process within the oxygen-limited regime could be identified. The release of gaseous products, evaluated through cold gas efficiency, increases linearly from 24–54% with higher air flow, corresponding to increasing process temperatures from 690–980°C, and is largely fuel type independent. The char produced from all feedstocks fall within the highest classification for biochars. This emphasises the potential of the investigated process for a combined production of producer gas and biochar from a variety of low-value biomass feedstocks.

*Keywords:*

Thermochemical conversion, Pyrolysis, Biomass, Gasification, Cookstove

Declarations of interest: none

---

*Corresponding author
Email address:* `thomas.kirch@adelaide.edu.au` (Thomas Kirch )

## 1. Introduction

The difficulty with achieving fuel flexibility in any combustion system is evident even in highly advanced systems, such as internal combustion engines [30] and gas turbines [49]. These need to be adapted significantly to achieve acceptable efficiency when switching between different homogeneous fuels. This inherent difficulty is much more pronounced when using inhomogeneous solid fuels. However, it remains common practice for users of small-scale domestic combustion systems for cooking and heating to alternate their fuel source according to availability and/or season [63]. This includes nearly half the world's population who rely on such systems for basic survival [9]. In order to minimise adverse health and environmental implications of incomplete combustion, a deeper understanding of the combustion properties of a wide range of utilised fuels is necessary to enable more efficient combustor design for small-scale solid fuel systems.

Small-scale combustion systems that use a batch-fed autothermal reverse downdraft process, called gasifer stoves, have been shown to exhibit high potential to reduce emissions of incomplete combustion, compared with similar sized conventional systems [34, 48]. In these improved systems, the fuel batch is lit on its top surface, leading to the formation of a reaction front that moves in the opposite direction from the air supply down the fuel bed [12, 39]. The propagation velocity of the reaction front for a specific fuel is mainly dependent on the air supply. Three regimes are identified, dependent on the air flux, namely; the oxygen-limited regime, the reaction-limited regime, and the regime where the process is cooled by convection [17, 44, 21, 40, 41, 38, 56]. Increasing the air supply rate results in increasing process temperatures, which in turn influences the product composition of the thermochemical conversion in the reaction front. The products are a complex mixture of gases, liquids (forming an aerosol with the gases, called producer gas) and solid char, with increasing yields of gases and decreasing yields of liquids and char, at higher temperatures [16]. The aerosol which is produced is subsequently burned with secondary air for heat generation, while the char can be extracted at the end of the process [28, 29]. This process is widely used with limited understanding of the biomass conversion process and especially the influence of using various fuels with different compositions. Previously wood fuels and rice hulls have been studied [22, 23, 50, 54], however, a more comprehensive investigation with a variety of fuels is needed to provide insight of the key parameters and to influence future designs.

The need for an assessment of fuel types and characteristics for small-scale applications has previously been identified [53]. However, most previous investigations in comparable systems

have focussed on woody biomass [27, 23, 50, 51, 35, 32, 19, 33]. Other widely used fuels in practice include agricultural residues and animal manures, which are burned in great quantities per household in countries such as India [37], but have not been studied extensively. Generally, the appropriacy of manure as fuel is debatable since it reduces its availability as a fertiliser. In the autothermal reverse downdraft reactor, this effect is minimised because biochar is produced which can be used as an alternative soil amendment. Few studies have focussed on the use of manure as fuel [59, 3, 7]. High emissions have been reported for direct combustion [52], while the thermochemical conversion process has not specifically been addressed. Continuous downdraft gasification of cow manure has not been found feasible, because of the low heating value of the product gas and a satisfactory process could only be achieved when mixed with sawdust [45]. The use of agricultural residues, such as wheat straw, which are often disposed of by field burning [63, 43] could provide another widely available fuel source. Continuous gasification of straw has been indicated to only be possible with pelletised fuel, as chopped straw led to air blockages [20]. The main difference between woody biomass, agricultural residues and animal manures are the bulk density (depending on particle size and density), the ash content and the related energy density. While wood has a low ash content, it is greater in agricultural residues and is generally much higher in manure. The main topics discussed when dealing with high ash content fuels are melting, fusing and slag formation [61, 24]. It has been suggested that the high K and Si concentrations in straw ash could lead to slag formation [25], but when producing char the high unburned carbon concentrations and the integrity of the initial particle structures could minimise these possible effects. Therefore, general concerns with the use of high ash content fuels in thermochemical conversion processes do not necessarily apply to the presented system. The influence of a high ash content in fuels on the thermochemical conversion process and the quality and efficiency of combustible gas production is not well understood.

The combined production of char and clean-burning combustible gases could provide beneficial implications for the process as well as the environment. Not only can the solid char lower the concentration of tars in the producer gas and retain a large fraction of the ash [29] to reduce particulate emissions, the biochar is also a product that can be used for a variety of subsequent applications. The specific characteristics of the biochar, such as surface area and high carbon content, make it a particularly valuable for soil amendment purposes [62]. Biochar is widely produced in a variety of systems, such as earth pits or rotary kilns, where only a portion of the released volatile

3

products from the biomass feedstock are utilised to sustain the thermochemical conversion process and the remainder vented [10]. A process that combines the production of biochar with the full utilisation of the volatiles for heat generation could substantially increase the efficiency of the system. The quality of char produced from small-scale reverse downdraft gasification is seldom assessed though and needs further investigation for the application as a soil amendment, especially when utilising unconventional non-woody biomass feedstock.

The focus of this article is to assess various value biomass feedstocks for the combined production of producer gas and solid char in small-scale applications. Four fuels, namely wood pellets, wheat straw, sheep manure and cow manure, have been investigated at two air supply rates. Novel insights into the batch-fed autothermal reverse downdraft conversion process when utilising high ash content fuels are gained. The products and product distribution are investigated through the continuous measurement of the produced gases, in combination with main constituent identification of the supplied fuel and produced char. These measurements enable an in-depth process analysis of the thermochemical conversion process, the release of combustible products as well as the quality of produced char, for multiple fuels representing a wide range of ash-contents. The resultant deeper understanding of the influence of biomass fuel composition, especially the ash content, on the autothermal thermochemical conversion process and its products, may additionally provide valuable information for downstream applications of the producer gas, as well as the char.

## 2. Materials and Methods

### 2.1. Reactor

The utilized small-scale thermochemical conversion and combustion reactor has been described previously [29]. Its main features, in the order of air flow are: an air supply chamber, a fuel grate on which the fuel rests, a reactor with ports for inserting thermocouples into the fuel bed, and a probe for the extraction of products above the fuel bed. Volatile products are combusted in a non-premixed flame, open to the environment, downstream of the extraction probe, however, the combustion process is not considered in this study.

Air is delivered at a constant flow rate during each of the experiments, resulting in the air mass flux specified in Table 1. The grate on which the fuel bed rests has 67.2% open area. The inner

4

diameter of the reactor is 98 mm and is insulated with a 25-mm-thick thermal blanket. Eight K-type thermocouples (T1–T8) are situated along the length of the reactor. The entire device is placed on a weighing scale, Radwag WLC 20/A2, with a readability as well as repeatability of $10^{-4}$ kg and a maximum capacity of 20.0 kg.

The probe used to extract volatile products is situated at the top of the initial fuel bed. This probe is connected to a tar trap, which is used for the retention of all non-gaseous products. Subsequently, the gas sample is analysed, described in §2.2.

### 2.2. Gas Analyser

The gas stream was sampled with a MRU Vario Plus analyser. It measures $CO_2$, CO and $CH_4$ up to 30% (vol./vol.) and an accuracy $\pm 3\%$ of the reading, using NDIR sensors. The measurements of $O_2$ and $H_2$ are measured with electrochemical sensors with a range up to 21% (vol./vol.) and an accuracy $\pm 0.2\%$ of the absolute value, and a range up to 100% (vol./vol.) and an accuracy $\pm 0.02\%$ of the reading, respectively. $N_2$ is determined by subtraction. The analyser was calibrated on a daily basis.

### 2.3. Fuels

Wood pellets, wheat straw, sheep manure and cow manure were tested in the present study. The results of the proximate and ultimate analyses for all fuels are presented in Figure 1. The ternary plots each enable the presentation of three constituents: (a) volatile matter (VM), fixed carbon (FC) and ash; and the three main elements: (b) carbon (C), hydrogen (H) and oxygen (O). Further information about the fuel and the tabulated values of the proximate and ultimate analyses are available in the Supplementary Material in Section S1.2. Due to the fuels bulk density 2.1 kg of wood pellets, 0.5 kg of wheat straw and 0.9 kg of manure were used for individual experiments.

### 2.4. Procedure

Prior to performing the experiments, the reactor was preheated and subsequent tests were started at inner reactor temperatures of <100 °C. Preheating was performed to avoid an influence from the large thermal mass of the reactor and reactor temperatures of <100 °C were chosen to minimise the influence of moisture evaporation when re-fuelling. Fuel was supplied in batches and the air mass flux was pre-set on the flow meters, prior to each experiment. Lighting was performed with the aid of 10 mL of methylated spirits (96% ethanol, CAS # 64-17-5) and a paper
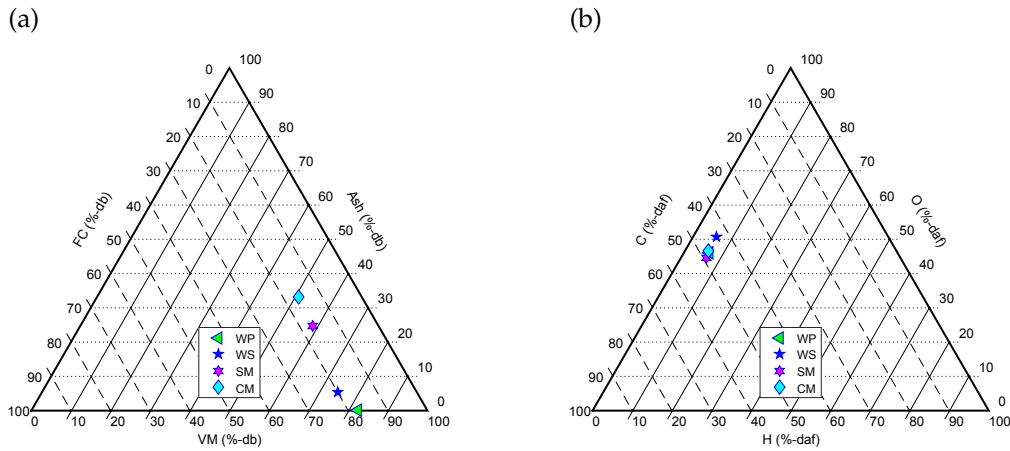
Figure 1: The fuel composition in terms of proximate analysis on a dry basis and ultimate analysis on a dry ash-free basis. The fuel types are: wood pellets (WP), wheat straw (WS), sheep manure (SM) and cow manure (CW). Axes show the three constituents of (a) the proximate analysis, fixed carbon (FC), ash, and volatile matter (VM), and (b) the ultimate analysis, carbon (C), oxygen (O), and hydrogen (H).

towel supplied to the top surface of the fuel bed. The temperature within the fuel bed was recorded throughout the process. The reaction front velocity for each configuration was determined in preliminary experiments (determined by the time taken between subsequent thermocouples reaching 600 °C) and the process was quenched once the reaction front reached the grate at the bottom of the fuel bed. Quenching was achieved by introducing ice water into the reactor from the top and by the provision of nitrogen (>99.99% $N_2$) instead of air to cool and prevent reactions inside the fuel bed. The remaining char was subsequently extracted. Multiple repeats for each tested fuel were performed at the two air supply rates, as presented in Figure 1. Air supply rates of 0.025 kg·m$^{-2}$·s$^{-1}$, for wood pellets, wheat straw and cow manure, and of 0.03 kg·m$^{-2}$·s$^{-1}$ for sheep manure, will be referred to herein as "low" and for all fuels 0.075 kg·m$^{-2}$·s$^{-1}$ as "high". These two air supply rates were chosen on the basis of preliminary experiments and a previous study [29], which have shown that these represent a high and low value within the oxygen limited regime. The exception of 0.030 kg·m$^{-2}$·s$^{-1}$ had to be made for sheep manure, since at lower flow rates no gaseous product measurements were possible, because excessive release of tar lead to repeated clogging of the tar trap.

Table 1: Experimental configurations, the number of repetitions performed and the experimental code.

| Fuel type | Air Mass Flux $(kg \cdot m^{-2} \cdot s^{-1})$ | Repetitions | Code |
|---|---|---|---|
| Wood pellets | 0.025 | 5 | WP-L |
| | 0.075 | 5 | WP-H |
| Wheat straw | 0.025 | 4 | WS-L |
| | 0.075 | 4 | WS-H |
| Sheep manure | 0.030 | 4 | SM-L |
| | 0.075 | 5 | SM-H |
| Cow manure | 0.025 | 3 | CM-L |
| | 0.075 | 4 | CM-H |

*2.5. Analysis*

For each experiment, the reactor is placed on a weighing scale to measure the fuel mass loss during the conversion process. The fuel mass loss was expected to display a linear profile with changes to air supply, based on previous research [40, 55]. The two air supplies at the focus of this study are 0.025 and 0.075 $kg \cdot m^{-2} \cdot s^{-1}$. These two flow rates were chosen on the basis of air supply regimes determined from mass loss measurements during preliminary experiments in the range 0.010–0.200 $kg \cdot m^{-2} \cdot s^{-1}$. Only mass loss was measured during the preliminary experiments, whilst gas sampling was performed during all subsequent tests. It should to be noted that comparable values found in the literature [41] are not based on weight measurements but calculated on the basis of thermocouple data, represented by the reaction front velocity and the fuel bulk density ($\dot{m}_{Fuel} = v_{Front} \cdot \rho_{Fuel}$). All figures presenting measured values include error bars that display the standard error of the mean [8].

Eight thermocouples recorded the gas phase temperature within the reactor. Mean maximum temperatures are determined as an average of the highest temperatures of the thermocouples T1–T7 and the value reported for each configuration was the mean of all repeat tests. Measurements of the lowest thermocouple T8 (at 20 mm from the fuel grate) were disregarded, since an increase of temperature due to the proximity to the fuel grate was observed.

An elemental balance was performed for carbon (C) and hydrogen (H) in the thermochemical conversion. The supply of $N_2$ via air was considered to be conserved, allowing the calculation of molecular C and H in the measured gas via the relationship between the supplied $N_2$ and the analysed $N_2$, as per Equation 1. Equations 2 and 3 present the overall calculation of molecular C and H in the measured gas, while the equations can be adapted for individual gas species. The

content of tars and water in the producer gas was not measured.

$$\dot{n}_{gas} = \frac{x_{gas}}{x_{N_2 measured}} \cdot \dot{n}_{N_2 air} \tag{1}$$

$$C_{gas} = \frac{m_{air} \cdot \omega_{N_{air}} / M_{N_2} \cdot (x_{CO_2} + x_{CO} + x_{CH_4}) / x_{N_2}}{(m_{fuel-daf} \cdot \omega_C - m_{char-af} \cdot \omega_C) / M_C} \tag{2}$$

$$H_{2_{gas}} = \frac{m_{air} \cdot \omega_{N_{air}} / M_{N_2} \cdot (x_{H_2} + 2 \cdot x_{CH_4}) / x_{N_2}}{(m_{fuel-daf} \cdot \omega_H - m_{char-af} \cdot \omega_H) / M_H} \tag{3}$$

Where $\dot{n}$ is the molecular gas flow and $x$ is the molecular gas concentration. The provided or product mass is represented by $m$, the mass fraction by $\omega$ and the molecular mass by $M$.

To evaluate the process performance, the cold gas efficiency (CGE) was calculated on the basis of the energy content of the produced gases relative to the energy content of the converted fuel, as presented in Equation 4. The measured gas concentrations are considered as the energy content of the producer gas, while other hydrocarbon compounds and carbonaceous particles that might be released from the fuel bed are not included. The higher heating value (HHV) of the fuel and the char were measured using a bomb calorimeter and that of the gaseous species were based on well characterised values found in the literature [60].

$$CGE = \frac{V_{N2-air} / x_{N2} \cdot (x_{CO} \cdot 12.6 + x_{CH_4} \cdot 39.8 + x_{H_2} \cdot 12.8)}{HHV_{fuel} \cdot m_{fuel} - HHV_{char} \cdot m_{char}} \tag{4}$$

Fuels, as well as produced char samples from each configuration, were analysed for their ultimate (CHN), proximate (moisture (M), volatile matter (VM), fixed carbon (FC) and ash content) composition and their HHV. The proximate analysis was performed via thermogravimetric analysis (TGA), using a previously established method [47]. For both fuel and char samples, the ash content was also determined following ISO 18122:2015 [1] and the moisture content following ASTM D4442-92(2003) [4]. The reported proximate analyses therefore consist of the moisture content, via the ASTM standard, the VM fraction, via TGA analysis, the ash content, via the ISO standard, and the fixed carbon fraction is calculated via subtraction.

## 3. Results

### 3.1. Mass Flux and Process Temperature

Figure 2 shows the fuel mass flux—the consumption of fuel per time and reactor area—as a function of the supplied air mass flux, for each of the fuels considered in this study. Preliminary experiments were performed over a wide range of conditions, where only one repetition was performed. Also shown are the experimental results at the two air supply rates used for the majority of this work, as well as values found in the literature [41] for wood pellets. Previous research has shown that with increasing air flow, under sub-stoichiometric conditions, the fuel consumption increases initially linearly (oxygen-limited regime), then less severely until a further increase does not change the fuel consumption (reaction-limited regime) and at super-stoichiometric air supply, leads to cooling of the process until extinction (refer to §1). Cookstoves generally operate in the initial regime, where the fuel mass flux is linearly dependent on the air mass flux, and this regime is therefore the focus of the present study.

All fuels investigated behave similarly and the fuel mass flux increases linearly in the oxygen-limited regime in Figure 2 up to an air supply rate of $\approx$0.1 kg·m$^{-2}$·s$^{-1}$. In this regime, the value of the fuel mass flux (WP>WS>CM>SM) is notably lower when the fuel contains a high amount of ash. This lower fuel mass flux can be explained by a lower oxidiser-fuel contact, lower diffusion of gas species and the lower energy content of the bed, due to the high ash content, as hypothesised previously [40]. The lower fuel mass flux at a given air mass flux also results in a higher air to fuel ratio (A/F), which has previously been found to be similar for various biomass types with lower ash content [56]. This shows that the high ash content in manures has an impact on the conversion speed, but also that the conversion regimes are dependent on the superficial velocity (air mass flux / air density) and thus the oxygen availability as well as residence time.

For WP and WS, increasing the air mass flux to >0.1 kg·m$^{-2}$·s$^{-1}$ leads to a transition to the reaction-limited regime and the fuel mass flux increases less rapidly with increasing air mass flux, until it reaches a plateau. For SM and CM, higher air flows exceeding >0.125 kg·m$^{-2}$·s$^{-1}$ lead to a slight decrease in the fuel mass flux. This decrease is caused by a variety of factors including ash melting, which substantially alters the fuel bed properties. At such high air supply rates little to no char is produced. Therefore, the utilisation of this type of system outside the oxygen-limited regime is not advisable, as further discussed in Sections 3.3 and 3.4.
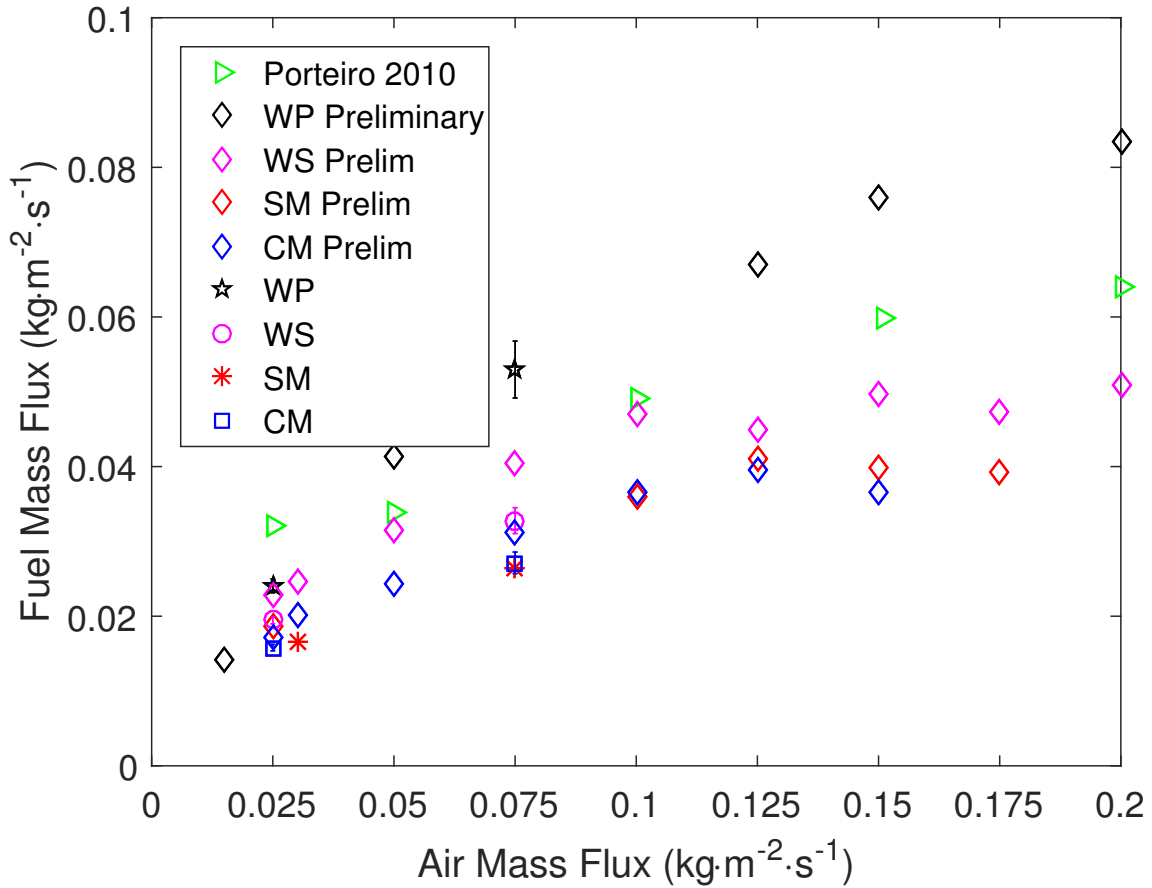
9

Figure 2: The fuel mass flux, the fuel consumption per time and reactor area, is presented as a function of the air mass flux for different experimental configurations, preliminary data and data found in the literature [41]. The error bars display the standard error of the mean.

The relationship between the mean peak temperature and the bulk density of the fuel bed is shown in Figure 3. The peak temperature is recorded at the centre of the fuel bed. It can be seen that there is a slight bulk density dependence of the mean peak temperature, similar to previous studies [40, 46]. With a lower bulk density, the total heat release per reactor volume is much lower and the thermal mass of the reactor wall and volume will have a greater influence on the peak temperature, compared with fuels with higher bulk density. Previously a higher bulk density has been related to a decreasing reaction front propagation velocity through the fuel bed [40], which also corresponds with a higher heat release per reactor volume. Here, no influence of other potentially related parameters, such as ash content, volatile matter content or particle size was
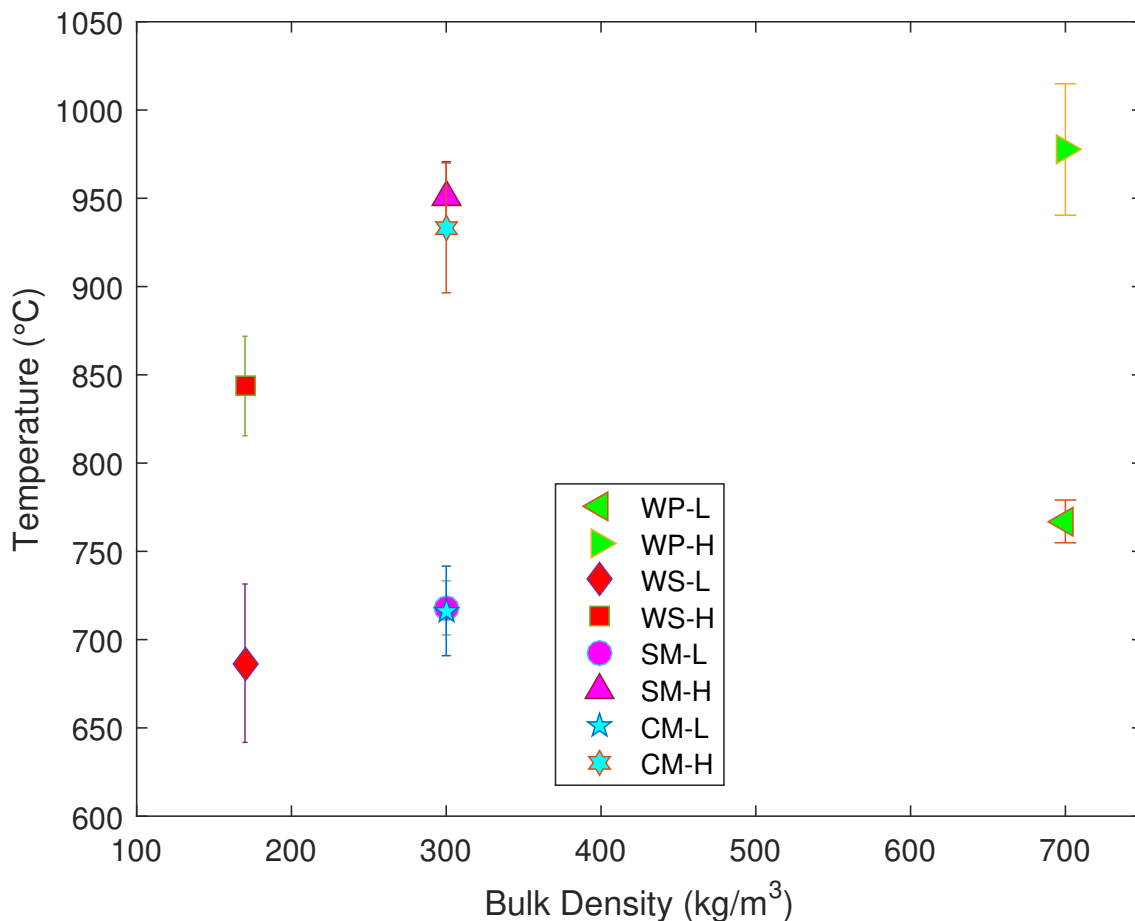
found.



Figure 3: The mean peak conversion temperature at the reactor centre is presented in relation to the initial bulk density of the fuel. The error bars display the standard error of the mean.

### 3.2. Gaseous Products

The time-weighted average species concentration over the duration of the experiment, as well as the calculated HHV of the producer gases (refer to §2.5) are presented in Figure 4. The mean volumetric concentration of the main product species from the thermochemical conversion process and $O_2$ are shown for all four fuels at high and low air supply. It can be noted that for each configuration, the $O_2$ concentration is low and re-evaluation of the concentrations on a 0% $O_2$ basis did not change the trends in between configurations. In terms of application in small-scale

11

combustion systems, it needs to be kept in mind that the producer gas presented here is the fuel for the subsequent combustion process.

In Figure 4 it can be seen that increasing the air supply has contrary effects for $CO_2$ and $CO$. At higher air supply rates, less $CO_2$ and more $CO$ is produced, which may be explained by a shift in the biomass conversion chemistry to an increasing primary product ratio of $CO/CO_2$ with increasing process temperatures [31]. Furthermore, previous research suggests that higher process temperatures [5] as well as higher temperatures in the char layer downstream of the reaction front [29] promote the conversion of tars (hydrocarbon compounds with higher boiling points than benzene [36]) to form mainly $CO$ and $H_2$ (via reactions R13–R16, presented in the Supplementary Material in Table S3). This conversion of tars contributes to an increasing $CO$ yield with greater air supply. As the combustible gases are more easily burned completely than the tars, greater conversion yields of these products may be beneficial for subsequent combustion.

Similar to the $CO$ and $CO_2$ results, the hydrogen-containing species, $H_2$ and $CH_4$, also follow contrary trends with increased air flow rate. The mean $H_2$ concentration is higher with increasing air supply and process temperatures, while the $CH_4$ concentration decreases. This trend can be explained by a combination of the decomposition of hydrocarbon compounds at higher temperatures (R13–R16, see Supplementary Material in Table S3) and the interplay of homogeneous gasification reactions (R7–R12, see Supplementary Material in Table S3).

When comparing the different fuels with one another it can be seen that the highest concentrations of all combustible species is released from the WP, hence also exhibiting the highest HHV. CM exhibits the lowest HHV, while WS and SM are quite similar. Therefore, WP provides the highest quality gas for subsequent combustion. Whilst this supports the previous work that has focussed on woody biomass as a feedstock, it also highlights the challenges associated with the use of lower-grade fuels that are widely used.

In a previous study, wheat straw had been tested at an air supply of approximately $0.065 \mathrm{kg \cdot m^{-2} \cdot s^{-1}}$ and it was found that it exhibited a similar process temperature, but higher peak $CO$ and $CO_2$ concentrations [25]. Although the previous system [25] is very similar to the one presented here, the comparison is limited because the char was consumed, leading to a higher prevalence of heterogeneous gasification reactions (R2–R5) and higher carbon oxide fractions in the producer gas. Similarly, higher temperatures and higher concentrations of all combustible gaseous products ($CO$, $H_2$ and $CH_4$), have been found with complete wheat straw fuel conversion elsewhere [61]. In

a similar, but continuous process, with char production, higher $H_2$ and CO concentrations were achieved with a simultaneous decrease in tars when using wood chips and wood pellets as fuel at 0.022 kg·m$^{-2}$·s$^{-1}$ [11]. In this continuous reactor the product gas passed through a constant layer of char at elevated temperatures [11], where tar cracking may occur, while here the char layer thickness increases as the reaction front propagates down the fuel bed and initially no char is present.
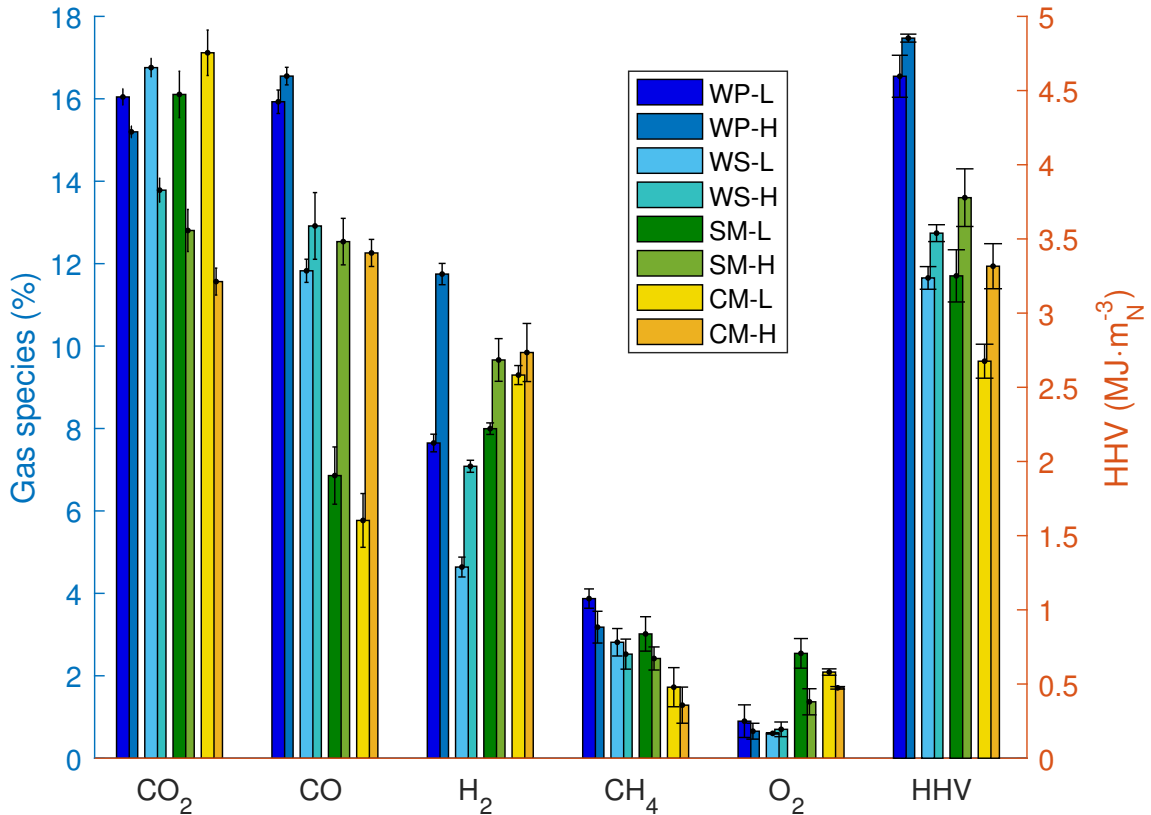


Figure 4: The time-weighted average volumetric producer gas composition, over the duration of the conversion process, as a mean of all replicates and the resulting HHV, of the gaseous products, are presented. The error bars display the standard error of the mean.

### 3.3. Biomass Conversion

The molecular conversion balance of carbon from the different fuels into the gaseous products, solid char and "other" (accounting mainly for tars and released particles) are presented in Figure 5. With increasing air flow, a general trend of increasing gaseous products accompanied by a

13

reduction of tars and char can be seen. This trend can be explained by higher process temperatures and has been well documented for biomass conversion processes [16, 6].

Focussing on a comparison of the conversion to permanent gases it can be seen that the combined yield of $CO_2$, CO and $CH_4$, at low flow rate follows the relation of WP > WS > CM > SM. At high air supply, the relation changes to CM > SM > WP > WS. The release of combustible gases, CO and $CH_4$, from the manures are particularly sensitive to changes in the air supply: from <40% at low air supply to >50% at high air supply. The higher increase of gas yield for the manures appears to be due to greater conversion of the fixed carbon fraction, with a simultaneous reduction of the char yield. For WP and WS both the char and other yields change more similarly, between low and high air supply. When considering that all fuels have a very similar carbon content, on a dry ash free basis (see Figure 1), the larger ash content in the manures appears to facilitate a greater conversion of fixed carbon to gaseous products at high air supply.

The char-carbon yield is lowest for the manures with high air flow. Thus, there will be less carbon available to form the structure of the char. This will be even more pronounced when further increasing the air supply, as described in Section 3.1. As char is a desired product of this process, a further increase of the air supply is not suitable for its production, especially when using manures as fuel—however, the higher proportion of producer gas in the high air supply case is advantageous.

The "other" fraction primarily includes tars, which are generally considered an undesirable product because they have been identified as a soot precursor for the subsequent combustion [18]. The fraction of tars is notably highest in SM, therefore explaining why this fuel was prone to clogging of the sampling line at $0.025\,\text{kg·m}^{-2}\text{·s}^{-1}$ and instead required an air supply of $0.030\,\text{kg·m}^{-2}\text{·s}^{-1}$ to ameliorate this issue (as described in §2.4). The lowest yields are achieved from WS, supporting the potential of this widely wasted fuel in this type of thermochemical conversion process.

Figure 6 presents the molecular balance of the supplied hydrogen in the fuel, into the measured gases and solid char, as well as "other", which accounts for mainly tars and water. For both air supply rates, WS presents the lowest conversion to gaseous products. It can be assumed that the low gas yield is due to lower peak process temperatures, when compared with the other fuels (see Figure 3). For both low and high air supply, it should also be noted that while the gas yields are similar for WP and SM, they are highest for CM. This trend cannot be explained by a temperature influence, as WP achieved the highest process temperature. Similar to the conversion
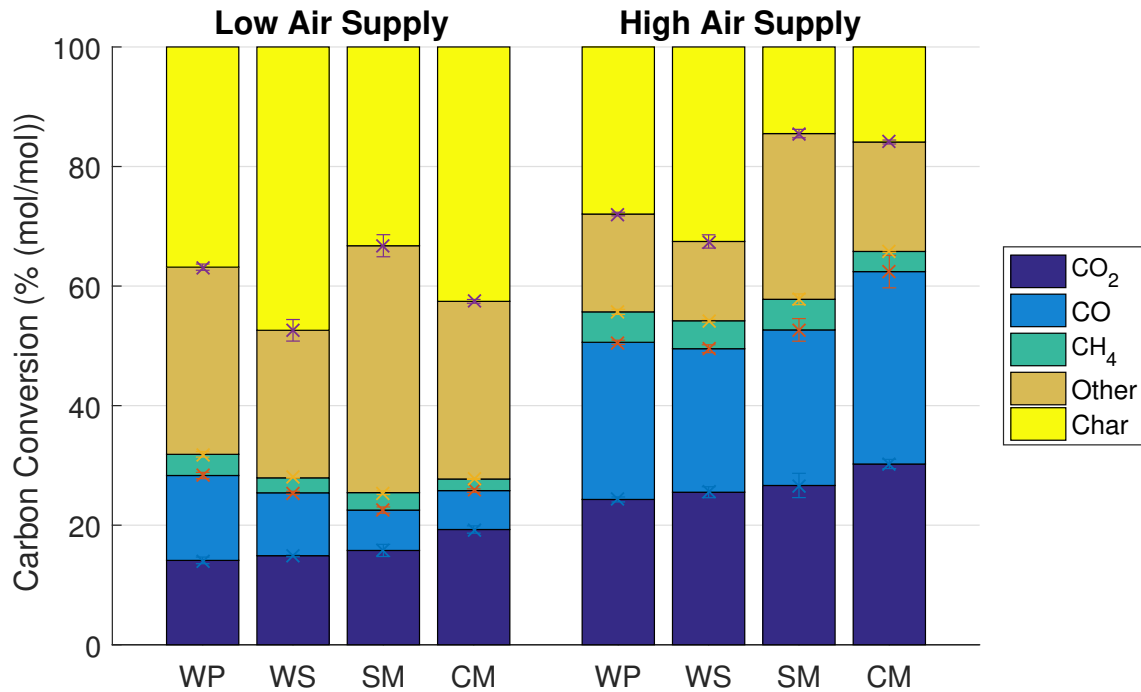
14

Figure 5: Conversion of fuel carbon to the gaseous products, $CO_2$, CO and $CH_4$, "other", accounting mainly for tars but also for carbonaceous particles that could be ejected from the fuel bed, and the solid char. The error bars display the standard error of the mean.

of carbon, the relatively high conversion yield of hydrogen-containing gases from the manures could be caused by the influence of the ash constituents. While the release of $CH_4$ appears to be consistent in between fuels at low and high air supply, the release of $H_2$ seems fuel dependent. This could be due to the presence of ash, since $H_2$ is highest in the manures.

The thermochemical conversion process can be evaluated through the cold gas efficiency (CGE), which provides a measure of the energy in the produced gas relative to that consumed from the supplied fuel (see §2.5). In Figure 7 the CGE is presented in relation to the mean peak process temperature. The efficiency appears to have a near-linear response with temperature, irrespective of fuel type.

In a similar-sized continuous downdraft gasifier using woody biomass pellets, at an air supply rate of $\approx 0.050$ kg·m$^{-2}$·s$^{-1}$, a CGE of over 70% was reported [26]. Although, the peak process temperature is higher at 0.075 kg·m$^{-2}$·s$^{-1}$ here and the producer gas composition appears similar, the CGE is more than 20% lower. Complete conversion of the char and a larger fraction of tars to
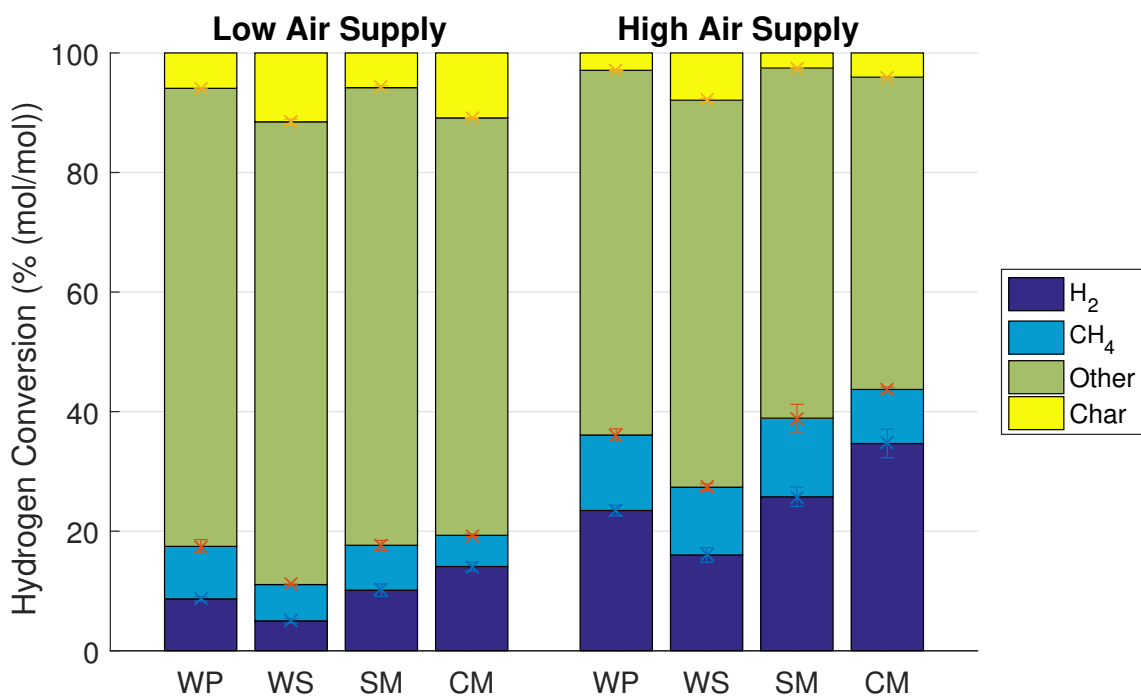
Figure 6: Conversion of fuel hydrogen to the gaseous products, $H_2$ and $CH_4$, "other", accounting mainly for water and tars, and the solid char. The error bars display the standard error of the mean.

producer gas in the continuous gasifier will contribute to this higher CGE.

### 3.4. Biochar

In Figure 8(a) the proximate-, and in 8(b) the ultimate-, analyses of the produced chars are shown as ternary plots (the respective values are provided in the Supplementary Material in Tables S4 and S5). The ternary plots enable the presentation of (a) the three constituents; volatile matter (VM), fixed carbon (FC) and ash; and (b) the three main elements: carbon (C), hydrogen (H) and oxygen (O).

The largest differences between the fuels can be seen in (a) along the fixed carbon and ash axes and in (b) along the carbon and oxygen axes. It can be noted that the carbon and the fixed carbon fractions generally decrease when increasing the air supply and are especially low for the manures. At 0.075 kg·m$^{-2}$·s$^{-1}$ only approximately 10% and 20% of fixed carbon remain in the char for CM and SM, respectively. At higher flow rates, the fixed carbon fraction is too low to retain a carbon structure, which is the basis of the char. Without the supporting carbon structure
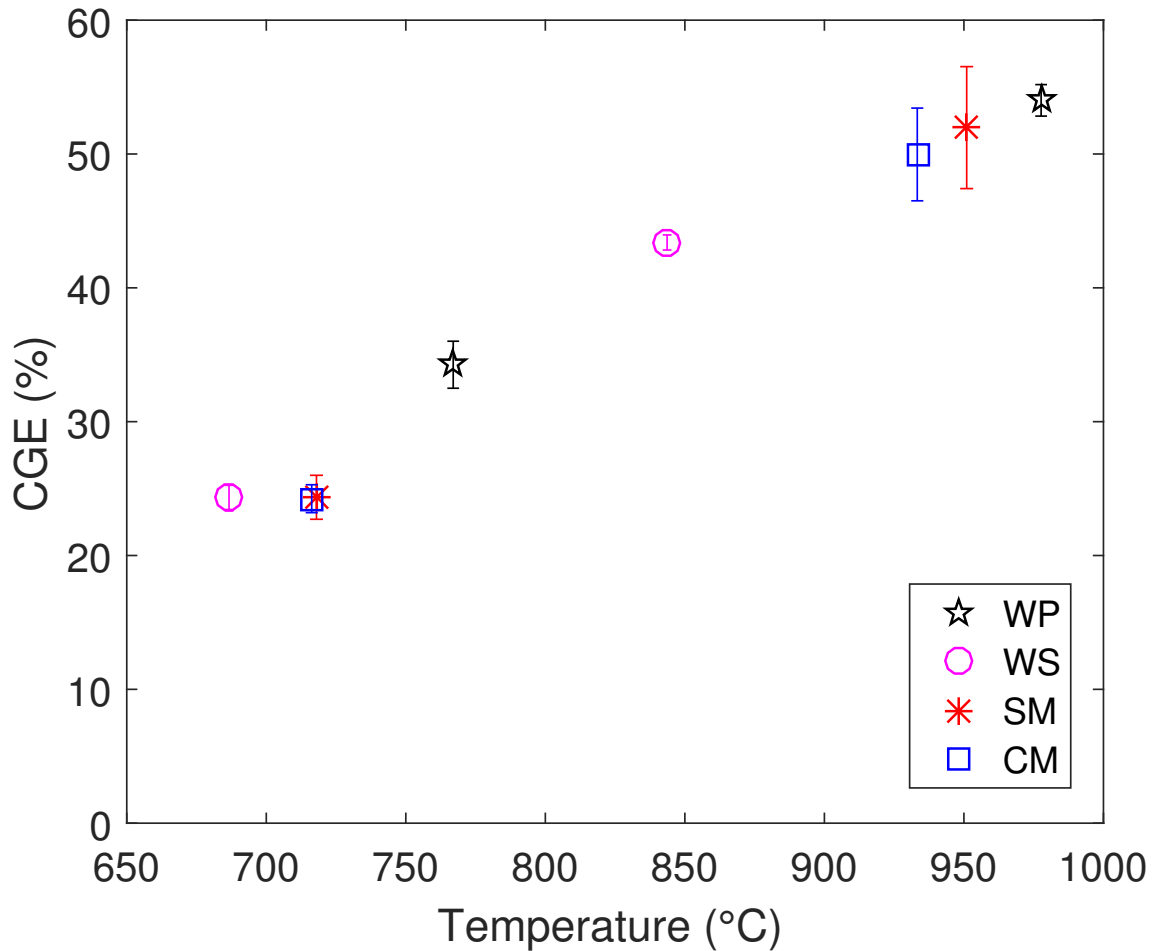
16

Figure 7: The cold gas efficiency (CGE) versus the mean peak temperature in the reaction front for all tested configurations. The error bars display the standard error of the mean.

and temperatures in excess of 900 °C (refer to Figure 3), ash melting occurs, which substantially alters the porous structure of the fuel bed and has negative process implications (refer to § 1). The impact of ash melting on the solid product can be seen in photographs which are included in the Supplementary Material in Figures S5 and S6.

Table 2 presents the higher heating value, the weight-based yield and the energy yield of the char. At low air supply for wood pellets, the char yield is 20% and the energy yield is 37%, which agree well with literature values under pyrolysis conditions of $\gtrsim$20% and $\gtrsim$40%, respectively [16, 62]. Similarly, wheat straw under low air supply conditions gives $\gtrsim$30% char yield and $\gtrsim$40%
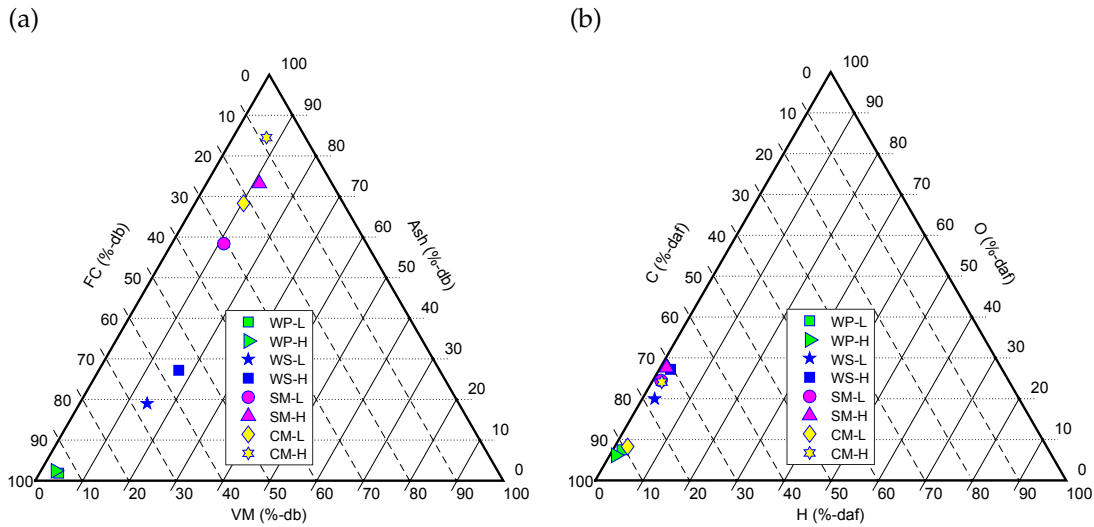
Figure 8: In (a) the proximate analyses, on a dry basis (db), and in (b) the ultimate analyses, on a dry ash free basis (daf), are presented. All values are on a mass basis.

energy yield in both Table 2 and pyrolysis literature [16, 62]. Therefore, the results indicate that at low air supply, pyrolysis conditions of temperatures >700°C are approached. In contrast, at higher air supply, the yields of both char and energy are lower by nearly a factor of two. Generally, it can be seen that increasing the air supply leads to a reduction in yields as well as heating value, because of the increasing ash fraction in the char.

Table 2: The mass yield (g/g), the energy yield (MJ/MJ) and the bulk calorific value (MJ/kg) of the produced char.

| Air supply | WP | WS | SM | CM |
|---|---|---|---|---|
| Mass yield (g/g) | | | | |
| low | 0.20 | 0.32 | 0.40 | 0.50 |
| high | 0.14 | 0.24 | 0.31 | 0.37 |
| Energy yield (MJ/MJ) | | | | |
| low | 0.37 | 0.44 | 0.33 | 0.39 |
| high | 0.26 | 0.27 | 0.21 | 0.12 |
| HHV (MJ/kg) | | | | |
| low | 32.5 | 22.6 | 11.1 | 9.8 |
| high | 31.2 | 18.2 | 9.2 | 3.9 |

When considering a molecular balance, rather than a mass balance as presented by the proximate and ultimate analyses, generally a decrease of both the molecular H:C and O:C ratios has previously been identified with increasing process temperature, for woody biomass as well as

18

wheat straw [62] (H:C and O:C ratios for produced chars as well as the fuels are presented in the Supplementary Material in Figure S7). This trend can also be found in the present study and similarly applies to the SM and CM chars. The difference in O:C ratio, between the fuel and the char, is less severe in the case of the manures, as oxygen can be expected to be present within the ash [58]. All produced chars fall within the category of Class 1 biochars, based on their molecular composition, with H:C and O:C ratios lower than 0.7 and 0.4 respectively, as proposed by the European Biochar Foundation [2, 15] . Therefore, even the high ash content chars could attain the highest classification biochars for soil amendment purposes, but future work regarding further classification criteria will address this issue in more depth.

## 4. Discussion

As mentioned in Section 1, three regimes have been identified for the thermochemical conversion of many biomass materials with increasing air supply, namely: oxygen-limited, where the fuel conversion is linearly dependent on the air supply; reaction-limited, where the fuel conversion plateaus with respect to increasing air supply; and the regime where the process is cooled by convection. The present study focusses on the oxygen-limited regime, since char is mainly produced in this regime, however, preliminary experiments were also performed in the reaction-limited regime and the findings may aid in defining ongoing processes in these regimes more clearly.

When little oxygen is supplied to the ignited fuel, the conversion of the solid biomass is dominated by devolatilisation, leading to the formation of solid char (as defined by reaction R1 in the Supplementary Material in Table S3) with a lower influence of heterogeneous gasification reactions R2–R5 of the resultant char. When the air supply is increased, there is a general rise in fuel consumption, accompanied by higher process temperatures (see §3.1), higher yields of permanent gases and a reduction of the tar (see §3.3) and char yield (see §3.4), caused by a stronger influence of reactions R2–R5 (refer to the Supplementary Material in Table S3). This is supported by a comparison with the relevant literature reporting pyrolysis experiments [16, 62] (see §3.4), where similar char yields have been reported at comparable process temperatures for low air supply, while higher yields are reported at high air supply, when heterogeneous gasification reactions are more prominent if oxygen is supplied to the conversion process.

19

At low air supply, it should be noted that the molecular yield of C and H in the char is somewhat similar (interestingly WP and SM, and WS and CM, exhibit similar yields) while the reduction of yields at high air supply is more severe in the manures (see §3.3) compared with the lignocellulose fuels (WP and WS). Previously, it has been suggested that a higher lignin content, the most stable lignocellulose component, promotes the formation of char during pyrolysis [13]. While this will contribute to a similar carbon conversion yield of char for WP and WS, which generally have a similar lignin content [57], the fraction in manures is generally very low [42]. Furthermore, it is shown that the duration of the conversion per unit mass of supplied fuel was very similar for all fuels, although in the case of the high ash content fuels, much less dry ash-free fuel is available (see §3.2). This shows that the dry ash-free conversion process occurs more slowly in high ash content fuels but a larger fraction of the FC is consumed, leading to nearly complete conversion of FC under oxygen-limited conditions.

In the manure and WS chars for high and low air supply rates, more than 50% and 20% (g/g), respectively, of the product is ash. This ash is retained in the solid structure which minimises the influence of elutriation or ash melting, from these high ash containing fuels. In all cases, even for CM at high air supply where the char contains only 10% (g/g) FC (see §3.4), the carbon structure largely remains but loose ash can be noticed on the char surface (refer to the Supplementary Material in Figure S5). This shows that through the production of the char, not only is a valuable solid (see §3.4) created, but also beneficial process implications are achieved. Furthermore, the clear separation of a devolatilisation and a char conversion phase, which becomes less pronounced as lower char yields are achieved, will cease at higher air supply rates for high ash content fuels.

The high ash content in the manures does not appear to have a negative influence on the conversion to permanent gases, within the oxygen-limited regime (see §3.3). The presence of char has previously been shown to increase tar conversion to permanent gases [29] (as per reactions R13–R16, see Supplementary Material in Table S3). While this influence has not specifically been studied for chars with a high ash content, it can be assumed to be influential on the release of gaseous products. Overall, the molecular conversion to permanent gases and its evaluation through the CGE, appears to be mostly process temperature dependent, while the fuel type plays a secondary role.

In the reaction-limited regime, the conversion reactions of biomass devolatilisation and heterogeneous gasification of the produced char body (R1–R5, see Supplementary Material in Table S3)

20

occur more concurrently. This leads to a more simultaneous conversion and release of the volatile matter and fixed carbon fractions from the fuel batch. For all fuels, this causes a substantial reduction in the char yield and a change in bed morphology. The absence of the char structure at high air supplies leads to ash either being expelled in the form of fly-ash or exposed to high process temperatures exceeding the ash melting point [14] leading to product melting and particle fusing, which alters the fuel bed properties and causes problems within the reactor (refer to the Supplementary Material in Figures S5 and S6). This is of little importance for low-ash fuels but can be detrimental to high-ash fuels, such as manures. Problems occurring in the reactor include channel forming, which changes the combustion characteristic from a near homogeneous reaction front to locally differing conversion conditions, or ash fusing to walls. Furthermore, the plateau of the fuel conversion with a simultaneous increase of the air supply, in the reaction-limited regime, leads to increased dilution of combustible products.

## 5. Conclusions

The presented study investigates the conversion behaviour of four different biomass fuels in an autothermal reverse downdraft process, which is often used in gasifier cookstoves. The influence of two air supplies on the biomass conversion within the oxygen-limited regime, where the fuel conversion is linearly dependent on the air supply, is the focus of this study. Process implications of higher air supplies are also addressed.

- The conversion behaviour is similar for all fuels, irrespective of the ash-content, but the fuel conversion is inversely proportional to the ash-content.

- With increasing air supply and increasing process temperatures more fuel carbon is consumed and the possibility of ash-melting increases. By limiting the air supply, where more char is produced and peak temperatures are lower, ash-melting can be avoided.

- The fuel conversion to gaseous products in the oxygen-limited regime is mainly temperature dependent and independent of fuel type. Thus gaseous product estimation from this process could be based on the peak process temperatures.

- All produced chars achieve the highest classification, through international protocols, for soil amendment purposes, based on their elemental composition.

Overall it is shown that the thermochemical conversion of a high value biomass fuel, wood pellets, exhibit the best performance, but similar results can be achieved even with the lowest value biomass fuels, manures, and the agricultural by-product, wheat straw. The issue of ash melting and fusing, which is often detrimental to traditional combustion of high ash-content fuels can be avoided here through limitation of the air supply and the production of char. This highlights the potential for utilisation of low value fuels in the presented system for a combined production of producer gas for heat generation and biochar for soil amendment applications.

## 6. Acknowledgements

## 7. References

[1] , 2015. ISO 18122:2015 Solid biofuels - Determination of ash content.

[2] , 2015. Standardized Product Definition and Product Testing Guidelines for Biochar That Is Used in Soil. International Biochar Initiative, 61.

[3] Abeliotis, K., Pakula, C., 2013. Reducing health impacts of biomass burning for cooking-the need for cookstove performance testing. Energy Efficiency 6 (3), 585–594.

[4] American Society for Testing and Materials, 2003. ASTM D4442-92(2003): Standard Test Methods for Direct Moisture Content Measurement of Wood and Wood-based Materials.

[5] Baker, E., Brown, M., Elliott, D. C., Mudge, L., 1988. Characterization and treatment of tars from biomass gasifiers. AIChE 1988 Summer National Meeting, 11.

[6] Basu, P., 2013. Gasification Theory. In: Biomass Gasification, Pyrolysis and Torrefaction. Elsevier Inc., Ch. 7, pp. 199–248.

[7] Birzer, C., Medwell, P., MacFarlane, G., Read, M., Wilkey, J., Higgins, M., West, T., 2014. A Biochar-producing, Dung-burning Cookstove for Humanitarian Purposes. Procedia Engineering 78, 243–249.

[8] Bondy, W. H., Zlot, W., 1976. The Standard Error of the Mean and the Difference between Means for Finite Populations. The American Statistician 30 (2), 96–97.

[9] Bonjour, S., Adair-Rohani, H., Wolf, J., Bruce, N. G., Mehta, S., Prüss-Ustün, A., Lahiff, M., Rehfuess, E. A., Mishra, V., Smith, K. R., 2013. Solid fuel use for household cooking: Country and regional estimates for 1980-2010. Environmental Health Perspectives 121 (7), 784–790.

[10] Brewer, C. E., Brown, R. C., 2012. Biochar. In: Comprehensive Renewable Energy. Elsevier Ltd., Ch. 5, pp. 357–384.

[11] Daouk, E., Van de Steene, L., Paviet, F., Martin, E., Valette, J., Salvador, S., 2017. Oxidative pyrolysis of wood chips and of wood pellets in a downdraft continuous fixed bed reactor. Fuel 196, 408–418.

[12] Dasappa, S., 2014. Thermochemical Conversion of Biomass. In: Hornung, A. (Ed.), Transformation of Biomass: Theory to Practice. JohnWiley & Sons, Ltd, Ch. 6, pp. 133–157.

[13] Dorez, G., Ferry, L., Sonnier, R., Taguet, A., Lopez-Cuesta, J. M., 2014. Effect of cellulose, hemicellulose and lignin contents on pyrolysis and combustion of natural fibers. Journal of Analytical and Applied Pyrolysis 107, 323–331.

[14] Du, S., Yang, H., Qian, K., Wang, X., Chen, H., 2014. Fusion and transformation properties of the inorganic components in biomass ash. Fuel 117, 1281–1287.

[15] EBC (2012), 2017. European Biochar Certificate - GuidelinesGuidelines for a Sustainable Production of Biochar. Tech. rep., European Biochar Foundation (EBC), Arbaz, Switzerland.

[16] Fagbemi, L., Khezami, L., Capart, R., 2001. Pyrolysis products from different biomasses. Applied Energy 69 (4), 293–306.

[17] Fatehi, M., Kaviany, M., 1994. Adiabatic reverse combustion in a packed bed. Combustion and Flame 99 (1), 1–17.

[18] Fitzpatrick, E. M., Bartle, K. D., Kubacki, M. L., Jones, J. M., Pourkashanian, M., Ross, A. B., Williams, A., Kubica, K., 2009. The mechanism of the formation of soot and other pollutants during the co-firing of coal and pine wood in a fixed bed combustor. Fuel 88 (12), 2409–2417.

[19] González, W. A., Pérez, J. F., Chapela, S., Porteiro, J., 2018. Numerical analysis of wood biomass packing factor in a fixed-bed gasification process. Renewable Energy 121, 579–589.

[20] Henrich, E., Dinjus, E., Rumpel, S., Stahl, R., 2001. A Two-Stage Pyrolysis/Gasification Process for Herbaceous Waste Biomass from Agriculture. In: Bridgwater, A. (Ed.), Progress in Thermochemical Biomass Conversion. Blackwell Science Ltd, Bodmin, pp. 221–236.

[21] Horttanainen, M., Saastamoinen, J., Sarkomaa, P., 2002. Operational limits of ignition front propagation against airflow in packed beds of different wood fuels. Energy & Fuels 16 (3), 676–686.

[22] James R., A., Yuan, W., Boyette, M., 2016. The Effect of Biomass Physical Properties on Top-Lit Updraft Gasification of Woodchips. Energies 9 (4), 283.

[23] James R, A. M., Yuan, W., Boyette, M. D., Wang, D., 2018. Airflow and insulation effects on simultaneous syngas and biochar production in a top-lit updraft biomass gasifier. Renewable Energy 117, 116–124.

[24] Jones, J. M., Lea-Langton, A. R., Ma, L., Pourkashanian, M., Williams, A., 2014. Pollutants Generated by the Combustion of Solid Biomass Fuels. Springer London Heidelberg New York Dordrecht.

[25] Khor, A., Ryu, C., bin Yang, Y., Sharifi, V. N., Swithenbank, J., 2007. Straw combustion in a fixed bed combustor. Fuel 86 (1-2), 152–160.

[26] Kihedu, J. H., Yoshiie, R., Nunome, Y., Ueki, Y., Naruse, I., 2014. Counter-flow air gasification of woody biomass pellets in the auto-thermal packed bed reactor. Fuel 117, 1242–1247.

[27] Kirch, T., Birzer, C. H., Eyk, P. J. V., Medwell, P. R., 2018. Influence of Primary and Secondary Air Supply on Gaseous Emissions from a Small-Scale Staged Solid Biomass Fuel Combustor. Energy & Fuels 32, 4212–4220.

[28] Kirch, T., Medwell, P. R., Birzer, C. H., 2016. Natural draft and forced primary air combustion properties of a top-lit up-draft research furnace. Biomass and Bioenergy 91, 108–115.

[29] Kirch, T., Medwell, P. R., Birzer, C. H., Van Eyk, P. J., 2018. Influences of fuel bed depth and air supply on small-scale batch-fed reverse downdraft biomass conversion. Energy & Fuels 32, 8507–8518.

[30] Klimstra, J., 2015. Fuel flexibility with dual-fuel engines. In: Oakey, J. (Ed.), Fuel Flexible Energy Generation: Solid, Liquid and Gaseous Fuels. Elsevier Ltd, pp. 293–304.

[31] Laurendeau, N. M., 1978. Heterogeneous kinetics of coal char gasification and combustion. Progress in Energy and Combustion Science 4 (4), 221–270.

[32] Lenis, Y. A., Osorio, L. F., Pérez, J. F., 2013. Fixed bed gasification of wood species with potential as energy crops in Colombia: The effect of the physicochemical properties. Energy Sources, Part A: Recovery, Utilization and Environmental Effects 35 (17), 1608–1617.

[33] Lenis, Y. A., Pérez, J. F., Melgar, A., 2016. Fixed bed gasification of Jacaranda Copaia wood: Effect of packing factor and oxygen enriched air. Industrial Crops and Products 84, 166–175.

[34] MacCarty, N., Still, D., Ogle, D., 2010. Fuel use and emissions performance of fifty cooking stoves in the laboratory and related benchmarks of performance. Energy for Sustainable Development 14 (3), 161–171.

[35] Mahapatra, S., Kumar, S., Dasappa, S., 2016. Gasification of wood particles in a co-current packed bed: Experiments and model analysis. Fuel Processing Technology 145, 76–89.

[36] Milne, T. A., Evans, R. J., Abatzoglou, N., 1998. Biomass Gasifier "Tars": Their Nature , Formation , and Conversion. National Technical Information Service (NTIS), 1–68.

[37] Mukunda, H. S., Dasappa, S., Paul, P. J., Rajan, N. K. S., Yagnaraman, M., Ravi Kumar, D., Deogaonkar, M., 2010. Gasifier stoves - science, technology and field outreach. Current Science 98 (5), 627–638.

[38] Pérez, J. F., Melgar, A., Benjumea, P. N., 2012. Effect of operating and design parameters on the gasification/combustion process of waste biomass in fixed bed downdraft reactors: An experimental study. Fuel 96, 487–496.

[39] Pham, X. H., Piriou, B., Salvador, S., Valette, J., Van de Steene, L., 2018. Oxidative pyrolysis of pine wood, wheat straw and miscanthus pellets in a fixed bed. Fuel Processing Technology 178 (June), 226–235.

[40] Porteiro, J., Patiño, D., Collazo, J., Granada, E., Moran, J., Miguez, J. L., 2010. Experimental analysis of the ignition front propagation of several biomass fuels in a fixed-bed combustor. Fuel 89 (1), 26–35.

[41] Porteiro, J., Patiño, D., Moran, J., Granada, E., 2010. Study of a fixed-bed biomass combustor: Influential parameters on ignition front propagation using parametric analysis. Energy & Fuels 24 (7), 3890–3897.

[42] Prasad, S., Singh, A., Joshi, H. C., 2007. Ethanol as an alternative fuel from agricultural, industrial and urban residues. Resources, Conservation and Recycling 50 (1), 1–39.

[43] Rajput, P., Sarin, M. M., 2014. Polar and non-polar organic aerosols from large-scale agricultural-waste burning emissions in Northern India: Implications to organic mass-to-organic carbon ratio. Chemosphere 103, 74–79.

[44] Rönnbäck, M., Axell, M., Gustavsson, L., Thunman, H., Lecher, B., 2001. Combustion processes in a biomass fuel bed - Experimental results. In: Bridgwater, A. (Ed.), Progress in Thermochemical Biomass Conversion. Blackwell Science Ltd, Bodmin, Ch. 59, pp. 743–757.

[45] Roy, P. C., Datta, A., Chakraborty, N., 2010. Assessment of cow dung as a supplementary fuel in a downdraft biomass gasifier. Renewable Energy 35 (2), 379–386.

[46] Sakthivadivel, D., Iniyan, S., 2017. Combustion characteristics of biomass fuels in a fixed bed micro-gasifier cook stove. Journal of Mechanical Science and Technology 31 (2), 995–1002.

[47] Saldarriaga, J. F., Aguado, R., Pablos, A., Amutio, M., Olazar, M., Bilbao, J., 2015. Fast characterization of biomass fuels by thermogravimetric analysis (TGA). Fuel 140, 744–751.

[48] Sutar, K. B., Kohli, S., Ravi, M. R., Ray, A., 2015. Biomass cookstoves : A review of technical aspects. Renewable and Sustainable Energy Reviews 41, 1128–1166.

[49] Taamallah, S., Vogiatzaki, K., Alzahrani, F. M., Mokheimer, E. M. A., Habib, M. A., Ghoniem, A. F., 2015. Fuel flexibility , stability and emissions in premixed hydrogen-rich gas turbine combustion : Technology , fundamentals , and numerical simulations. Applied Energy 154, 1020–1047.

[50] Tryner, J., Tillotson, J. W., Baumgardner, M. E., Mohr, J. T., Defoort, M. W., Marchese, A. J., Mohr, T., Defoort, M. W., Marchese, A. J., 2016. The Effects of Air Flow Rates, Secondary Air Inlet Geometry, Fuel Type, and Operating Mode on the Performance of Gasifier Cookstoves. Environmental Science and Technology 50 (17), 9754–9763.

[51] Tryner, J., Willson, B. D., Marchese, A. J., 2014. The effects of fuel type and stove design on emissions and efficiency of natural-draft semi-gasifier biomass cookstoves. Energy for Sustainable Development 23, 99–109.

[52] Urmee, T., Gyamfi, S., may 2014. A review of improved Cookstove technologies and programs. Renewable and Sustainable Energy Reviews 33, 625–635.

[53] U.S. Department of Energy, 2011. Biomass Cookstoves Technical Meeting: Summary Report.

[54] Varunkumar, S., Rajan, N. K. S., Mukunda, H. S., 2011. Single Particle and Packed Bed Combustion in Modern Gasifier Stoves - Density Effects. Combustion Science and Technology 183 (11), 1147–1163.

[55] Varunkumar, S., Rajan, N. K. S., Mukunda, H. S., 2012. Experimental and computational studies on a gasifier based stove. Energy Conversion and Management 53 (1), 135–141.

[56] Varunkumar, S., Rajan, N. K. S., Mukunda, H. S., 2013. Universal Flame Propagation Behavior in Packed Bed of Biomass. Combustion Science and Technology 185 (8), 1241–1260.

[57] Vassilev, S. V., Baxter, D., Andersen, L. K., Vassileva, C. G., Morgan, T. J., 2012. An overview of the organic and inorganic phase composition of biomass. Fuel 94, 1–33.

[58] Vassilev, S. V., Baxter, D., Vassileva, C. G., 2013. An overview of the behaviour of biomass during combustion: Part I. Phase-mineral transformations of organic and inorganic matter. Fuel 112, 391–449.

[59] Venkataraman, C., Rao, G. U. M., 2001. Emission factors of carbon monoxide and size-resolved aerosols from biofuel combustion. Environmental Science and Technology 35 (10), 2100–2107.

[60] Waldheim, L. Nilsson, T., 2001. Heating value of gases from biomass gasification. IEA Bioenergy Agreement, Task 20 - Thermal Gasification of Biomass, 61.

[61] Wang, G., Silva, R. B., Azevedo, J. L., Martins-Dias, S., Costa, M., 2014. Evaluation of the combustion behaviour and ash characteristics of biomass waste derived fuels, pine and coal in a drop tube furnace. Fuel 117 (PART A), 809–824.

[62] Weber, K., Quicker, P., 2018. Properties of biochar. Fuel 217, 240–261.

[63] Yevich, R., Logan, J. A., 2003. An assessment of biofuel use and burning of agricultural waste in the developing world. Global Biogeochemical Cycles 17 (4), 6.1–6.21.

# Supplementary material:
# Small-Scale Autothermal Thermochemical Conversion of Multiple Solid Biomass Feedstock

Thomas Kirch[a,b,*], Paul R. Medwell[a,b], Cristian H. Birzer[a,b], Philip J. van Eyk[c]

*[a]School of Mechanical Engineering, The University of Adelaide, S.A. 5005, Australia*
*[b]Humanitarian and Development Solutions Initiative, The University of Adelaide, South Australia 5005, Australia*
*[c]School of Chemical Engineering, The University of Adelaide, S.A. 5005, Australia*

## S1. Materials and Methods

### S1.1. Reactor

Figure S1 presents a schematic diagram of the 98 mm inner diameter reactor used in the presented investigation. In this reactor air is supplied from below the fuel bed, through an air plenum. Air is provided by dry compressed air, which passes through a downwards facing distribution ring to achieve homogeneous flow characteristics when entering the fuel bed. Eight thermocouples (T1–T8) are mounted within the fuel bed at equidistance of 50 mm from one another. The fuel bed extends over a heights of 400 mm. Aerosol samples are extracted at the top of the fuel bed and are subsequently passed through a heated line ($> 250°C$) into a tar trap. All non-gaseous constituents are retained in the tar trap, before the clean gas enters the gas analyser.

### S1.2. Fuels

Four fuels, namely wood pellets (WP), wheat straw (WS), sheep manure (SM) and cow manure (CM), were utilised in the present investigation. Pictures of these four fuels are presented in Figure S2. The particle size distribution is shown in Table S1. The particle size distribution was established by thieving 500 g of the WS, SM and CM, and by measuring the length of the WP with a nominal diameter of 6.5 mm. The results of the proximate as well as ultimate analyses are presented in Table S2.

The wood pellets, with a nominal diameter of 6.5 mm and length of 40 mm, were produced from timber waste from multiple timber mills around Australia. The pellets consist of hammer-milled wood shavings, to which pine and saw dust were added before being compressed. Pellet Heaters Australia is the manufacturer of the product, which was purchased from Barbeques Galore (Adelaide, Australia).

The wheat straw was harvested in the third week of November 2017 by Belvedere Ridge in Reynolds, South Australia, Australia. It was air dried in the field for 10 to 14 days and steam cut to a nominal length of 5 to 10 mm. In the steam cutting process by Belvedere Ridge, the straw is heated and moist by the steam before cutting and subsequently dried and cooled. Preliminary
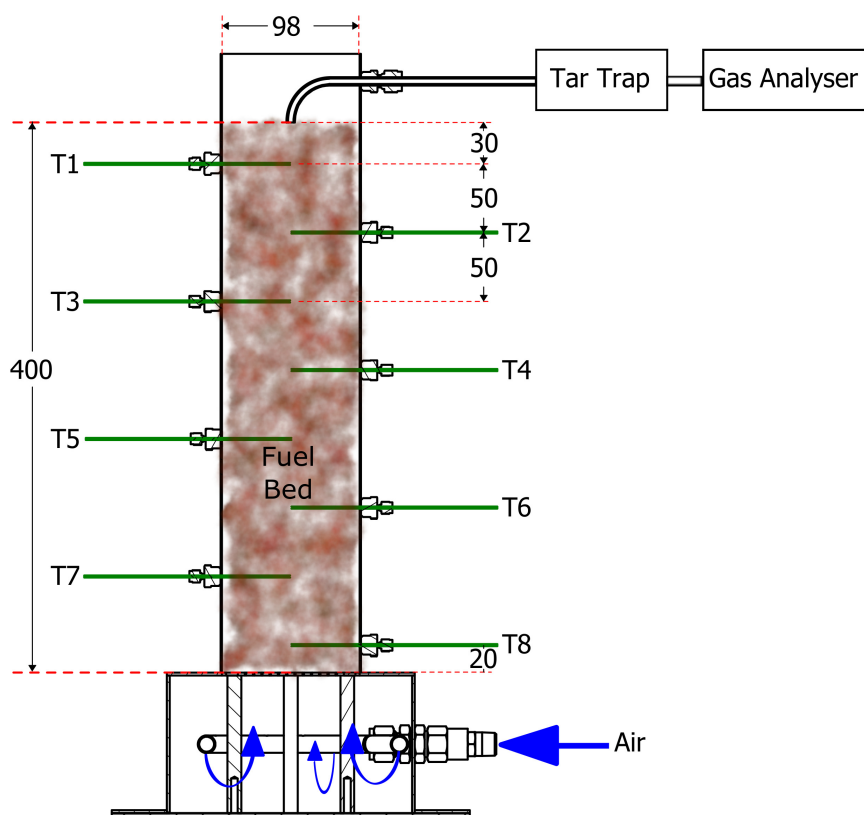
---

*Corresponding author

Figure S1: Schematic diagram of the research reactor, all measurements in (mm).

experiments using initial length material, as well as a previous study [1], have shown increased channel forming and an influence on steady reaction front propagation derive from this feedstock. When uncut material is used, the conversion process will propagate more quickly along individual stalks than in between stalks, leading to a discrepancy where some parts of a horizontal fuel bed plane consist of horizontally aligned stalks, while other parts consist of vertically aligned stalks. Therefore, the cut material was chosen as fuel.

The sheep manure was collected from grazing animals at a shearing station near Mallala, South Australia, Australia. No bedding material was used and contamination with soil was low. The natural particle size of the manure was used in the experiments. The particle size distribution of all fuels is presented in the Supplementary Material.

Cow manure was provided by the Minko North Dairy Farm at Korunye, South Australia, Australia. The manure was manually processed to achieve a similar size distribution as the sheep manure to reduce differences in particle size and enable closer comparability. The dairy cows were fed a daily diet of 4.5 kg wheat/canola meal, 10.8 kg potatoes, 4.5 kg lucerne hay, 14.25 kg brewers grain, 3 kg mill run, 13.66 kg faba bean silage, 1 kg of oaten hay and 2 kg of dairy grain. Hay was used as bedding material.

Both manures were dried at 105 °C overnight, before being stored for the experiments. By uni-

formly drying the fuels, the effects of moisture content were eliminated." The resulting moisture content of all fuels was within 7.2±2.1 % (g/g).
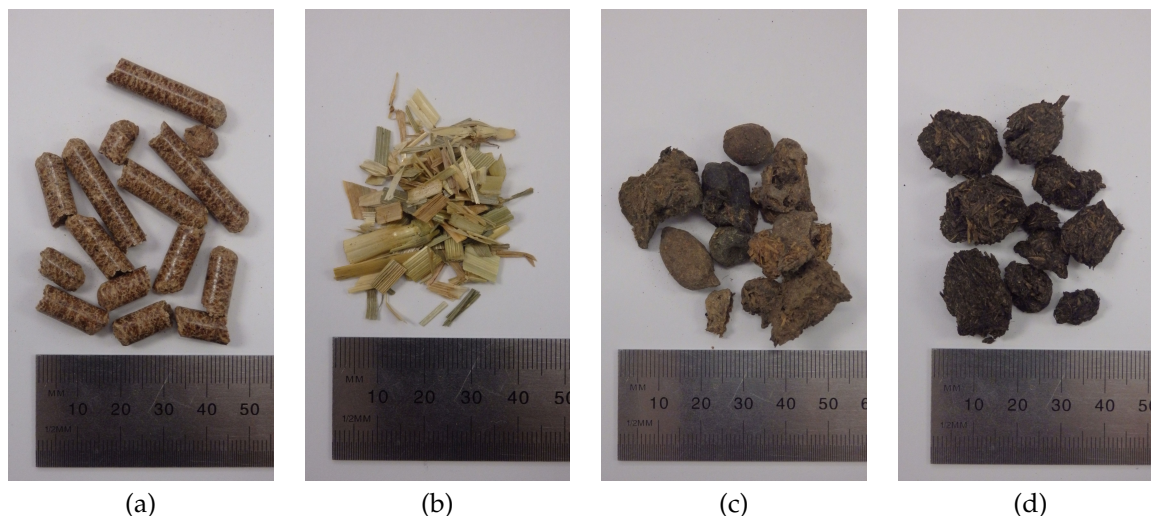


Figure S2: Pictures of the four fuels, wood pellets (a), wheat straw (b), sheep manure (c) and cow manure (d) as used in the experiments, with a ruler as reference (mm).

Table S1: Fuel size distribution.

| Fuel | Particle size (mm) | | | | | | | | Bulk density |
|---|---|---|---|---|---|---|---|---|---|
| | $< 0.5$ | 0.5 - 1.0 | 1.0 - 2.0 | 2.0 - 4.0 | 4.0 - 6.7 | 6.7 - 9.5 | 9.5 - 26.7 | $> 26.7$ | $(kg \cdot m^{-3})$ |
| Wood Pellets | 0.6 | 7.4 | 44.9 | 45.8 | 1.4 | 0.0 | 0.0 | 0.0 | 696.0 |
| Sheep Manure | 1.3 | 0.8 | 2.4 | 4.3 | 4.9 | 26.5 | 58.6 | 1.2 | 166.0 |
| Cow Manure | 0.4 | 0.3 | 1.2 | 5.1 | 10.6 | 23.8 | 58.6 | 0.0 | 300.0 |
| Wheat Straw | 0.2 | 1.3 | 8.8 | 58.9 | 29.6 | 1.2 | 0.0 | 0.0 | 300.0 |

*S1.3. Reactions*

In Table S3 the basic chemical reactions that occur in the utilised reactor are presented. These reactions provide the basis for the process discussed in the main article.

## S2. Results

*S2.1. Gaseous Products*

Figure S3 presents the molar flow of the produced gaseous products, $CO_2$, $CO$, $H_2$ and $CH_4$, over the duration of the process. It can be seen that for all fuels at low air supply, a steady release of each gaseous species is achieved, apart from transients at start-up and shut-down. At high air supply the release is much more variable, suggesting more variation of conversion conditions within the reaction front.

Table S2: Proximate and ultimate analyses results and the calorific value of the fuels. All measurements reported on a mass basis and volatile matter (VM), fixed carbon (FC) and ash reported on a dry basis. The ultimate analysis (CHNO) and the higher heating value (HHV) are reported on a dry ash free basis.

| Fuel | Moisture | VM | FC | Ash | HHV |
|---|---|---|---|---|---|
| | O | H | C | N | MJ/kg |
| Wood Pellets | $7.1 \pm 0.3$ | $82.4 \pm 1.2$ | $17.3 \pm 0.5$ | $0.3 \pm 0.0$ | 18.8 |
| | 45.9 | $6.4 \pm 0.1$ | $47.5 \pm 0.0$ | $0.1 \pm 0.0$ | |
| Wheat Straw | $7.9 \pm 0.3$ | $74.7 \pm 3.1$ | $20.0 \pm 2.8$ | $5.3 \pm 0.4$ | 20.1 |
| | 45.9 | $6.4 \pm 0.1$ | $43.5 \pm 0.4$ | $1.5 \pm 0.1$ | |
| Sheep Manure | $8.3 \pm 0.5$ | $58.6 \pm 0.7$ | $16.8 \pm 0.3$ | $24.6 \pm 0.6$ | 21.1 |
| | 41.3 | $6.3 \pm 0.1$ | $49.0 \pm 0.5$ | $3.3 \pm 0.0$ | |
| Cow Manure | $6.2 \pm 0.4$ | $50.8 \pm 0.9$ | $15.8 \pm 0.3$ | $33.3 \pm 2.3$ | 20.6 |
| | 42.5 | $5.9 \pm 0.0$ | $47.5 \pm 0.1$ | $4.1 \pm 0.0$ | |

Table S3: Process reactions [2, 3].

| | Reaction | |
|---|---|---|
| Devolatilisation | Biomass $\rightarrow C_n + C_xH_yO_z + C_aH_b + CO_2 + CO + H_2 + H_2O$ | R1 |
| Heterogeneous gasification | $C + 0.5 \cdot O_2 \rightarrow CO$ | R2 |
| | $C + CO_2 \leftrightharpoons 2 \cdot CO$ | R3 |
| | $C + H_2O \leftrightharpoons CO + H_2$ | R4 |
| | $C + H_2 \leftrightharpoons CH_4$ | R5 |
| Homogeneous gasification | $CO + 0.5 \cdot O_2 \rightarrow CO_2$ | R6 |
| | $H_2 + 0.5 \cdot O_2 \rightarrow H_2O$ | R7 |
| | $CH_4 + 0.5 \cdot O_2 \rightarrow CO + 2 \cdot H_2$ | R8 |
| | $CO + H_2O \leftrightharpoons CO_2 + H_2$ | R9 |
| | $CO_2 + 4 \cdot H_2 \rightarrow CH_4 + H_2O$ | R10 |
| | $CH_4 + H_2O \leftrightharpoons CO + 3 \cdot H_2$ | R11 |
| | $2 \cdot CO + 2 \cdot H_2 \rightarrow CH_4 + CO_2$ | R12 |
| Tar Cracking | Tars $\rightarrow C + C_nH_m +$ gases | R13 |
| Tar Reforming | $C_nH_m + n \cdot H_2O \rightarrow n \cdot CO + (n + 0.5 \cdot m) \cdot H_2$ | R14 |
| | $C_nH_m + n \cdot CO_2 \rightarrow 2 \cdot n \cdot CO + (0.5 \cdot m) \cdot H_2$ | R15 |
| | $C_nH_m + 2 \cdot n \cdot H_2O \rightarrow n \cdot CO_2 + (0.5 \cdot m + 2 \cdot n) \cdot H_2$ | R16 |
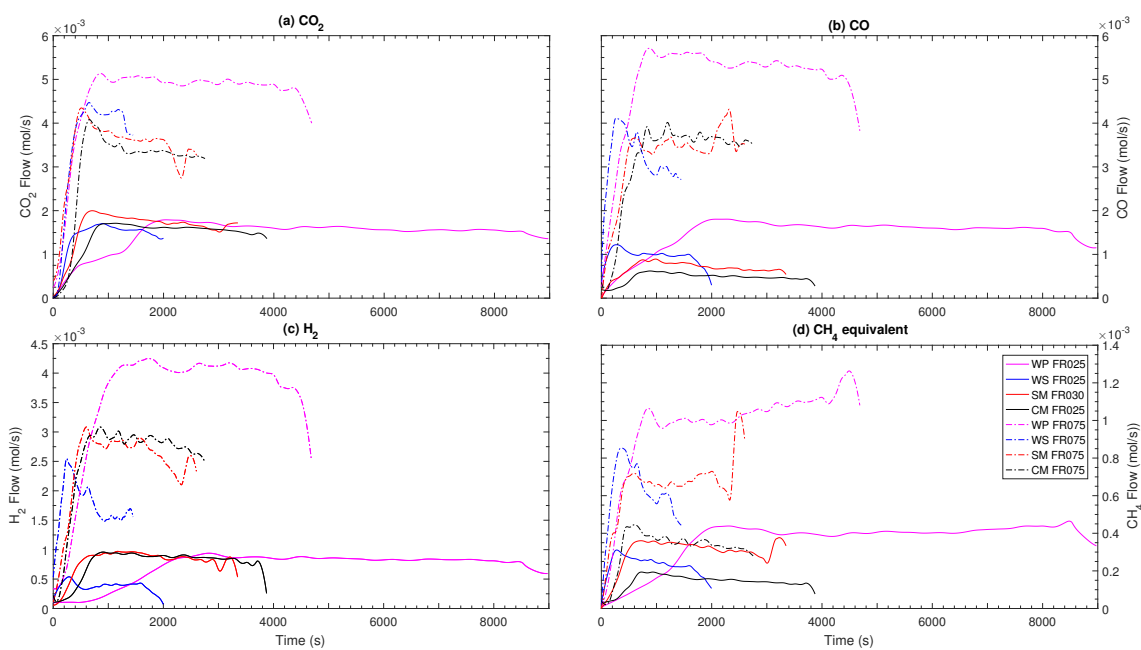
Figure S3: Molar flow of the main gas species, $CO_2$, $CO$, $H_2$ and $CH_4$, released from the thermichemical conversion process, over the process duration (s).

Figure S4 presents the molecular balance of the product yields of gaseous, solid and liquid fractions over the mean peak process temperature. It can be seen that there is a dependence of increasing gas, with simultaneous decreasing solid and liquid, production at higher temperatures. Especially the gas yield appears nearly linearly dependent of the process temperature. This trend has previously been identified [4].

*S2.2. Biochar*

Figure S5 presents pictures of the chars of all four utilised fuels at the two air supply rates under investigation. It can be seen that for the lignocellulosic fuels, WP and WS (Figures S5(a)–(d)), chars from both air supply rates appear quite similar. In the case of the manures, greater ash built-up on the particle surface is visible in Figures S5(e)–(h) and supported by lower yields of fixed carbon in the particle at high air supply, as discussed in the article. While for CM, at high air supply in Figure S5(h), only more ash can be noticed on the surface, for SM in Figure S5(f) indications of ash melting and fusing of particles can be seen. For all fuels a comparison between the initial fuel and the char shows that the particle structure is largely retained throughout the process.

Figure S6 displays selected chars from preliminary experiments performed at higher air supply rates. These chars show the result of ash melting and particle fusing. At higher air supply rates a larger fraction of the fixed carbon is consumed, leaving chars with higher ash content as a result. This effect increases with increasing ash content in the fuel. For WP, ash melting was not noticed within the investigated air supply rates. WS exhibited ash melting behaviour at 0.175 $kg \cdot m^{-2} \cdot s^{-1}$ (Figure S6(a)) but only for a limited amount of the produced char. As described in the previous paragraph, for SM, indications of ash melting can already be identified
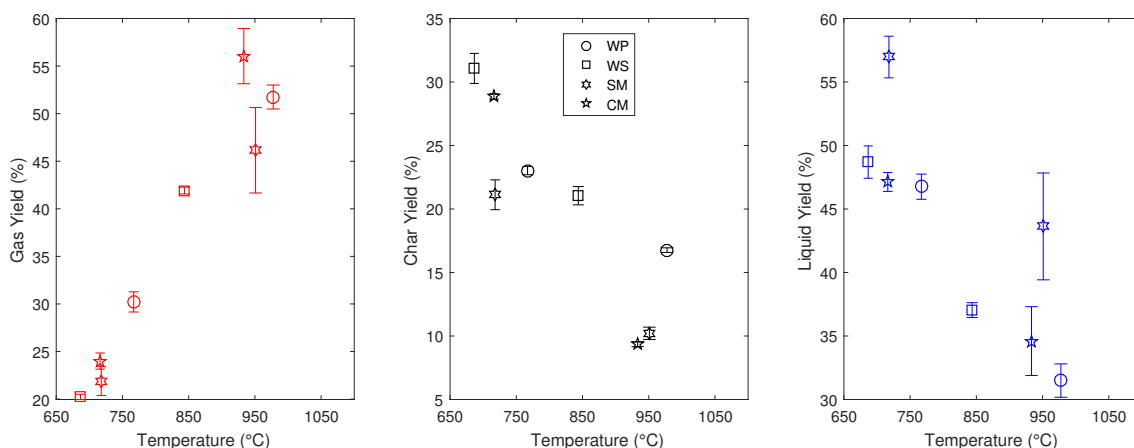
Figure S4: Molar conversion yields of the three product fractions, gases, char and liquids, over the mean peak process temperature.

at 0.75 kg·m$^{-2}$·s$^{-1}$ and for both CM and SM these became more prominent at 0.1 kg·m$^{-2}$·s$^{-1}$, as seen in Figure S6(b). At 0.15 kg·m$^{-2}$·s$^{-1}$ mainly ash is produced and nearly all of the solid product extracted at the end of the process exhibited ash melting and fusing characteristics, as seen in Figures S6(c) and S6(d).

Figure S7 presents the molar H:C over the O:C ratios of all produced chars and fuels. Interestingly when comparing the WP char values to results for biochar from woody biomass produced via slow pyrolysis they are more similar than those of biochars produced from gasification [5]. The mass based results of the proximate analyses are presented in Table S4 and those of the ultimate analyses in Table S5.

Table S4: Proximate of the produced chars. All measurements reported on a mass basis and volatile matter (VM), fixed carbon (FC) and ash reported on a dry basis.

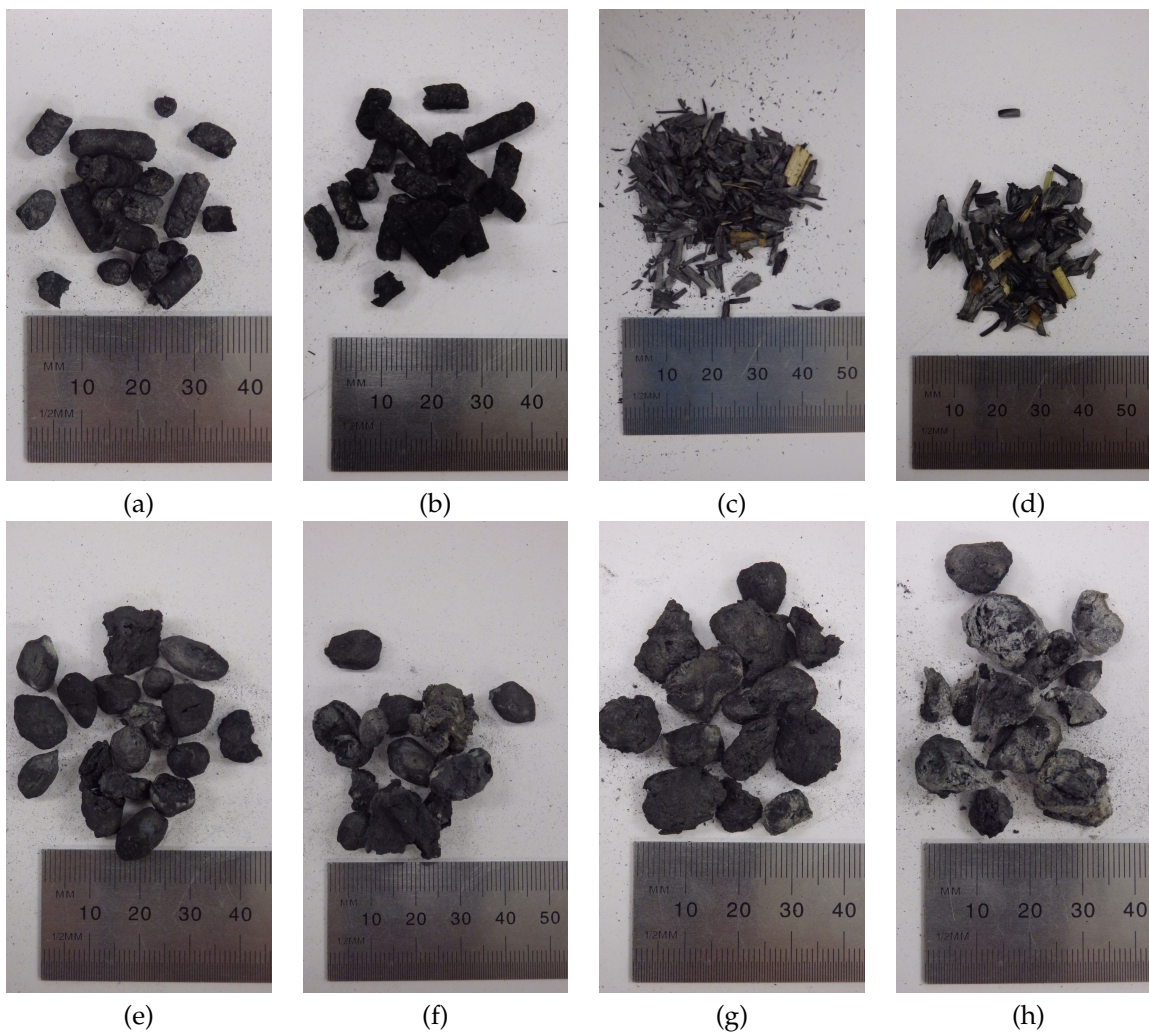| Code | VM | FC | Ash |
|---|---|---|---|
| WP025 | $4.1 \pm 0.0$ | $94.0 \pm 0.0$ | $1.9 \pm 0.1$ |
| WP075 | $3.1 \pm 0.4$ | $94.4 \pm 1.3$ | $2.5 \pm 0.1$ |
| WS025 | $14.4 \pm 2.1$ | $66.6 \pm 3.6$ | $18.9 \pm 0.4$ |
| WS075 | $17.1 \pm 0.8$ | $55.7 \pm 3.0$ | $27.2 \pm 1.3$ |
| SM025 | $11.2 \pm 0.5$ | $30.5 \pm 1.9$ | $58.4 \pm 0.9$ |
| SM075 | $11.4 \pm 2.6$ | $15.5 \pm 4.3$ | $73.1 \pm 1.6$ |
| CM025 | $10.4 \pm 1.2$ | $21.3 \pm 0.3$ | $68.3 \pm 0.3$ |
| CM075 | $7.2 \pm 0.6$ | $8.4 \pm 1.5$ | $84.4 \pm 3.1$ |

Figure S5: Pictures of the chars from each fuel at low and high air supply, WP025 (a), WP075 (b), WS025 (c), WS075 (d), SM030 (e), SM075 (f), CM025 (g) and CM075 (h), with a ruler as reference (mm).

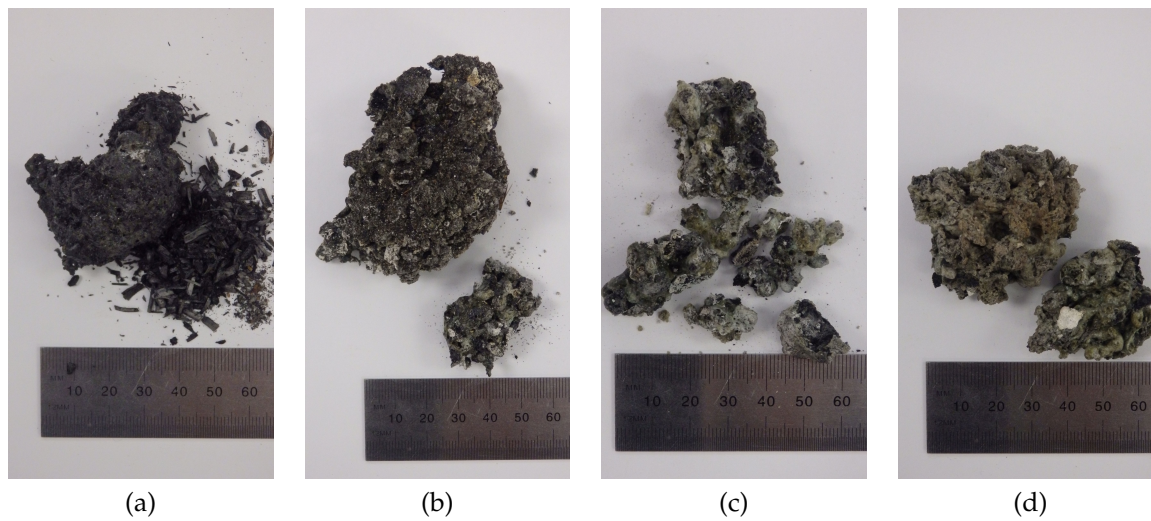(a)          (b)          (c)          (d)

Figure S6: Selected pictures of the chars at higher air supply rates, WS175 (a), SM100 (b), SM150 (c) and CM150, with a ruler as reference (mm).

Table S5: Ultimate analyses results of the produced chars. The ultimate analysis (CHNO) is reported on a dry ash free basis.

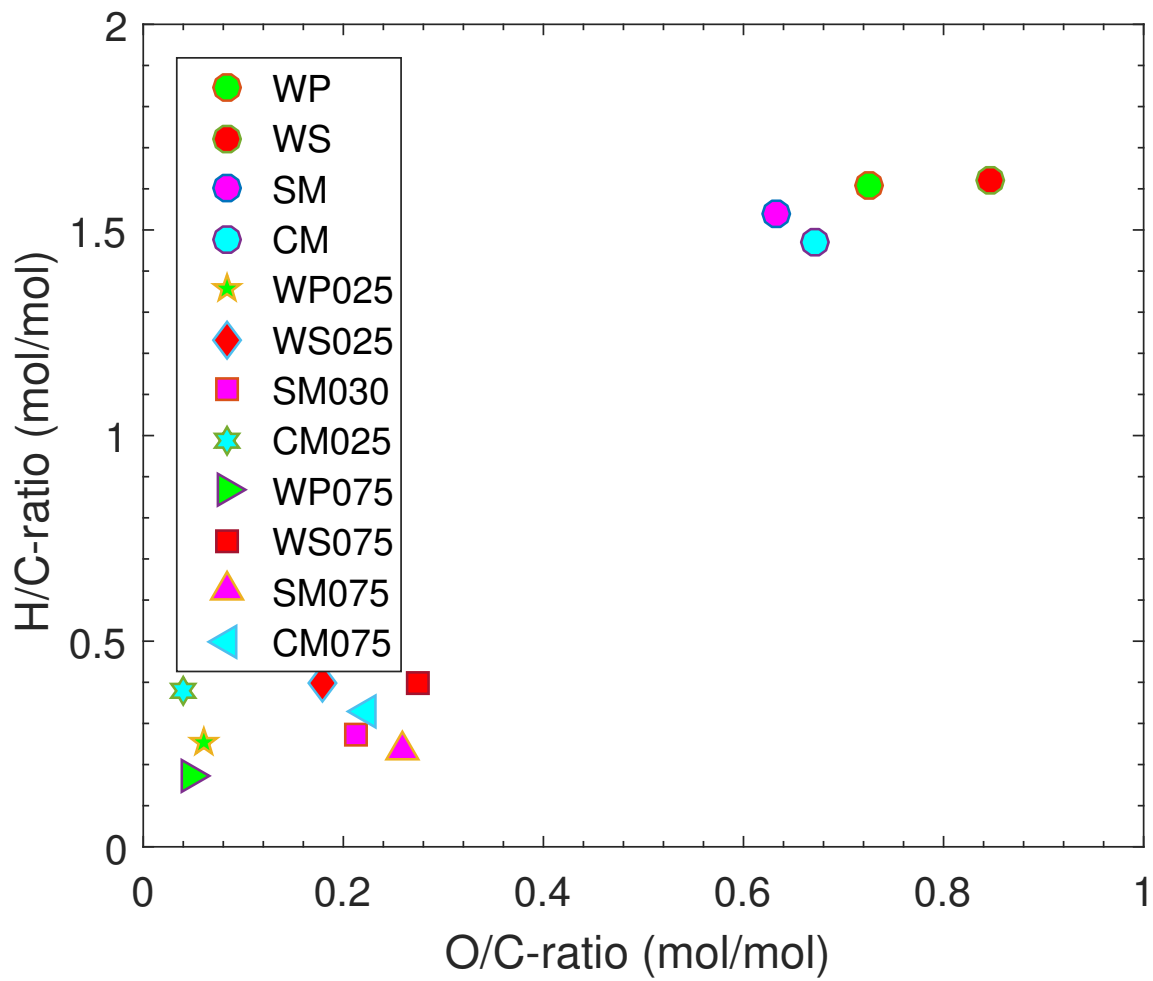| Code | C | H | N | O |
|---|---|---|---|---|
| WP025 | 90.5 | 1.9 | 0.2 | 7.3 |
| WP075 | 92.5 | 1.3 | 0.2 | 6.0 |
| WS025 | 77.4 | 2.6 | 1.5 | 18.5 |
| WP075 | 70.5 | 2.3 | 1.5 | 25.7 |
| SM025 | 73.8 | 1.7 | 3.5 | 21.0 |
| SM075 | 71.1 | 1.4 | 3.1 | 24.4 |
| CM025 | 88.9 | 2.8 | 3.5 | 4.8 |
| CM075 | 73.8 | 2.1 | 2.3 | 21.8 |

Figure S7: The H/C over the O/C molar ratio.

## S3. References

[1] A. Khor, C. Ryu, Y. bin Yang, V. N. Sharifi, J. Swithenbank, Straw combustion in a fixed bed combustor, Fuel 86 (1-2) (2007) 152–160. `doi:10.1016/j.fuel.2006.07.006`.

[2] P. Basu, Gasification Theory, in: Biomass Gasification, Pyrolysis and Torrefaction, Elsevier Inc., 2013, Ch. 7, pp. 199–248. `doi:10.1016/B978-0-12-396488-5.00007-1`.
URL `http://www.sciencedirect.com/science/article/pii/B9780123964885000071`

[3] Y. Shen, Chars as carbonaceous adsorbents/catalysts for tar elimination during biomass pyrolysis or gasification, Renewable and Sustainable Energy Reviews 43 (2015) 281–295. `doi:10.1016/j.rser.2014.11.061`.
URL `http://dx.doi.org/10.1016/j.rser.2014.11.061`

[4] M. Rönnbäck, M. Axell, L. Gustavsson, H. Thunman, B. Lecher, Combustion processes in a biomass fuel bed - Experimental results, in: A. Bridgwater (Ed.), Progress in Thermochemical Biomass Conversion, Blackwell Science Ltd, Bodmin, 2001, Ch. 59, pp. 743–757. `doi:10.1002/9780470694954.ch59`.

[5] C. E. Brewer, R. C. Brown, Biochar, in: Comprehensive Renewable Energy, 2012, Ch. 5, pp. 357–384. `doi:10.1016/B978-0-08-087872-0.00524-2`.

This page intentionally left mostly blank.

# Chapter 7

---

# Feedstock Dependence of Emissions from Reverse Downdraft Gasifier Cookstove

---

## Statement of Authorship

| | |
|---|---|
| Paper Title: | Feedstock Dependence of Emissions from Reverse Downdraft Gasifier Cookstove |
| Status: | Submitted |
| Details: | Environmental Science & Technology |

### Principal Author

| | |
|---|---|
| Name: | Thomas Kirch |
| Contribution: | Performed the literature review focussing specifically on the secondary combustion process and established mechanisms that influence the emissions. Developed aims and objectives of the research study. Designed experimental facilities including hood structure and extraction system. Designed, set-up and ran CFD simulations to ensure the validity of measurements taken in these facilities. Partially constructed and set-up the experimental facilities. Developed analytical methods for gaseous and particulate product measurements. Designed experimental matrix and performed experimental work. Performed gravimetric pre- and post-experimental measurements of filter papers for particulate measurements. Wrote codes for data analysis. Performed data analysis and transferred to appropriate figures for visualisation. Structured, wrote and edited the research article. While the key findings are presented in the research article, provided supporting information ensure all findings are presented. Acted as corresponding author. |
| Contribution Percentage (%): | 70 |
| Certification: | This paper reports on original research I conducted during the period of my Higher Degree by Research candidature and is not subject to any obligations or contractual agreements with a third party that would constrain its inclusion in this thesis. I am the primary author of this paper. |
| Signature: | Date: **28.02.2019** |

**Co-Author Contributions**

By signing the Statement of Authorship, each author certifies that:

1. the candidate's stated contribution to the publication is accurate (as detailed above);

2. permission is granted for the candidate to include the publication in the thesis; and

3. the sum of all co-author contributions is equal to 100% less the candidates stated contribution.

| | |
|---|---|
| Name: | Paul R. Medwell |
| Contribution Details: | Guided research direction. Supervised work development. Helped generate ideas for tests and edited manuscript. |
| Signature: | Date: **28 Feb 2019** |

| | |
|---|---|
| Name: | Cristian H. Birzer |
| Contribution Details: | Guided research direction. Supervised work development. Helped generate ideas for tests and edited manuscript. |
| Signature: | Date: **28 Feb 2019** |

| | |
|---|---|
| Name: | Philip J. van Eyk |
| Contribution Details: | Guided research direction. Supervised work development. Helped generate ideas for tests and edited manuscript. |
| Signature: | Date: *28 Feb 2019* |

# Feedstock Dependence of Emissions from a Reverse-Downdraft Gasifier Cookstove

Thomas Kirch[a,b,*], Paul R. Medwell[a,b], Cristian H. Birzer[a,b], Philip J. van Eyk[c]

[a]*School of Mechanical Engineering, The University of Adelaide, S.A. 5005, Australia*
[b]*Humanitarian and Development Solutions Initiative, The University of Adelaide, South Australia 5005, Australia*
[c]*School of Chemical Engineering, The University of Adelaide, S.A. 5005, Australia*

## Abstract

The present study investigates the combustion process of the producer gas from a gasifier cookstove, for four solid biomass fuels: wood pellets (WP), wheat straw (WS), sheep manure (SM) and cow manure (CM). It was found that a higher primary air supply and/or a deeper fuel bed reduces tars in the producer gas and increases the combustion efficiency, especially from low-ash-containing WP. At higher air supply rates, indications of a strong influence from the fuel ash content on the emissions were found. Although more combustible gases and fewer tars are produced in the conversion process, a substantial increase in particulate matter (PM) emissions is noted. At low air supply rates, the emissions of particulates with a nominal diameter <2.5 $\mu$m (PM$_{2.5}$) released from the combustion process are in the range of 6–30 mg·MJ$^{-1}_{released}$ (WP<WS<SM<CM), low when compared with similar devices. However, when the air supply is increased by a factor of three, the PM$_{2.5}$ emissions almost double for WP and increase more than ten fold for CM. At lower air supply rates, low emissions of both PM and CO are achieved. This is likely due to lower peak temperatures (reducing ash devolatilisation) and larger char yields (to retain ash particulates) from the thermochemical solid biomass conversion process. This shows that low air supply rates and the combined production of heat, for cooking, and char, for subsequent application, may achieve substantial benefits for the emissions of pollutants from gasifer cookstoves.

*Keywords:*
Combustion, Emissions, Biomass, Particulate Matter, Cookstove

Declarations of interest: none

*Corresponding author
Email address:* thomas.kirch@adelaide.edu.au (Thomas Kirch )

## 1. Introduction

The emissions from cookstoves burning solid biomass contribute considerably to anthropogenic emissions, causing a multitude of adverse effects on the present-day climate [1] as well as human health [2, 3]. These effects are mainly caused by products from incomplete combustion. Variation in feedstock has been linked to increasing emissions from incomplete combustion, with animal manures tending to be higher than agricultural residues and woody biomass [4]. These feedstocks are widely being used to fuel cookstoves, and are known to produce high levels of pollutant emissions. Therefore, investigating approaches to mitigate pollutant emissions when using a variety of fuels is an important area to improved combustion performance.

One particular type of cookstove, called gasifier stoves, is recognised as having potential for efficient and fuel flexible applications [5, 6]. In this type of stove, the thermochemical conversion of the solid fuel is separated from the combustion process of the released products. They tend to be batch-fed systems, where the fuel bed is lit on its top surface, while limited air is supplied from beneath the bed. This leads to the formation of a reaction front in which an autothermal reverse downdraft process converts the solid biomass to form gases and liquids, which are released from the bed as producer gas, leaving solid char as residue [7]. The producer gas is combusted with additional air downstream of the fuel bed. Many studies have investigated the overall efficiency of particular stoves while emulating user practices (i.e. performing cooking tasks) [8, 9, 10, 5, 11, 12, 6, 13, 14, 15]. When emulating user practices, the analysis of the combustion process itself is limited as there are additional influences on the process, such as flame quenching on the surface of the pot or inconsistent user fire tending, which impede the study of the underlying combustion process and their quantification is problematic [16]. Whilst such testing methodologies are critical for establishing the suitability of a particular stove for practical application, fundamental studies using well-controlled environments and conditions are needed to provide a deeper understanding of the combustion processes in such systems. In particular, by focusing only on the thermochemical conversion and combustion processes [17].

Investigations of the thermochemical conversion process within the fuel bed have shown that small changes of process parameters, such as reactor diameter or air supply, and fuel, including wood, miscanthus or rice hulls, can lead to a large variation in the producer gas composition [18, 19, 20, 21]. The influence of the fuel bed depth or the utilisation of high ash content fuels, such as manures, has yet to be performed. The complexity of producer gas combustion in small-scale applications stems from the presence of a multitude of chemical compounds, including gases, complex organic compounds (tars) and ash constituents, in the thermochemical conversion products [22, 23, 24, 25, 26]. The combustion process of such producer gas from biomass fuels is highly complex, particularly due to the presence of a wide variety of tars, which have also been identified as soot precursors [27], and due to ash, which can have an influence on the combustion chemistry [28]. To enable cookstove improvement, establishing a possible relationship between the producer gas combustion products and organic compounds in the producer gas, as well as ash constituents in the fuel, is necessary.

Previous work by the authors has investigated the thermochemical conversion process and product composition for wood pellets [29] as well as wheat straw, and sheep and cow manure [30] as fuels, in a particular research gasifier cookstove. The air supply was varied for all fuels and additionally the fuel bed depth for the wood pellets. The release of producer gas was the specific focus in those studies. In gasifier cookstoves the producer gas released from the thermochemical conversion process provides the fuel for secondary combustion process, which occurs in the form of a non-premixed jet flame when secondary air is added. In the present study the focus of the

2

analysis is placed on the secondary combustion process of the products from the thermochemical conversion process.

The emissions released from the combustion process from a small-scale gasifier stove are analysed in this study. Four biomass fuels, with a wide range of ash contents, up to four air supply configurations and for one fuel also four fuel bed depth are investigated. The main focus is on CO and particulate matter emissions, because of their particular interest for human health and environmental pollution. A deeper understanding of the producer gas combustion process and the influence of gaseous, organic and ash constituents and their contribution to the combustion emissions is the aim of this study. The influence of the combined production of heat, for cooking, and biochar, for subsequent utilisation, on the combustion emissions when utilising a variety of biomass fuels is investigated. The novelty of this work consists of the analysis of the secondary combustion process while considering the composition of the combusted producer gas as well as the produced char.

## 2. Materials and Methods

### 2.1. Fuels

Four biomass fuels, were utilised in the present investigation, namely wood pellets, wheat straw, sheep manure and cow manure. These have previously been analysed and described in detail [29, 30]. The proximate and ultimate analyses of all fuels, as well as their calorific value are provided in Table 1.

Wood pellets (WP), with a nominal diameter of 6.5 mm and length of 40 mm, were produced by Pellet Heaters Australia and were purchased from Barbeques Galore (Adelaide, Australia). These pellets consist of compressed hammer-milled wood shavings and saw dust. The wheat straw (WS) was from Reynolds, South Australia, Australia, and had been cut to a nominal length of 5 to 7 mm. Sheep manure (SM) was collected at a shearing station at Mallala, South Australia, Australia. Cow manure (CM) was provided by the Minko North Dairy Farm at Korunye, South Australia, Australia. Prior to testing, both manures were dried at 105 °C overnight, before being stored for the experiments, to achieve a comparable low moisture content.

Table 1: Proximate and ultimate analyses results and the calorific value of the fuels. All measurements are reported on a mass basis and volatile matter (VM), fixed carbon (FC) and ash reported on a dry basis. The ultimate analysis (CHNO) and the higher heating value (HHV) are reported on a dry ash free basis. For the proximate and ultimate analyses the standard error of the mean is provided. The mean bulk density is also included.

| Fuel | Moisture | VM | FC | Ash | HHV | Bulk Density |
| --- | --- | --- | --- | --- | --- | --- |
| | O | H | C | N | (MJ·kg$^{-1}$) | (kg·m$^{-3}$) |
| Wood Pellets | $7.1 \pm 0.3$ | $82.4 \pm 1.2$ | $17.3 \pm 0.5$ | $0.3 \pm 0.0$ | 18.8 | 696 |
| | 45.9 | $6.4 \pm 0.1$ | $47.5 \pm 0.0$ | $0.1 \pm 0.0$ | | |
| Wheat Straw | $7.9 \pm 0.3$ | $74.7 \pm 3.1$ | $20.0 \pm 2.8$ | $5.3 \pm 0.4$ | 20.1 | 166 |
| | 45.9 | $6.4 \pm 0.1$ | $43.5 \pm 0.4$ | $1.5 \pm 0.1$ | | |
| Sheep Manure | $8.3 \pm 0.5$ | $58.6 \pm 0.7$ | $16.8 \pm 0.3$ | $24.6 \pm 0.6$ | 21.1 | 300 |
| | 41.3 | $6.3 \pm 0.1$ | $49.0 \pm 0.5$ | $3.3 \pm 0.0$ | | |
| Cow Manure | $6.2 \pm 0.4$ | $50.8 \pm 0.9$ | $15.8 \pm 0.3$ | $33.3 \pm 2.3$ | 20.6 | 300 |
| | 42.5 | $5.9 \pm 0.0$ | $47.5 \pm 0.1$ | $4.1 \pm 0.0$ | | |

## 2.2. Test-facilities

Figure 1(a) shows an outline of the facilities, consisting of a square enclosure of 600 mm by 600 mm with a height of 1800 mm, and a 45° inclined hood that contracts into a 150 mm diameter duct in which two baffles are inserted. Isokinetic sample extraction was performed at 12 diameters (1800 mm) downstream of the second baffle. These facilities adhere to specifications provided in ISO 19867-1: 2018. The validity of gaseous measurements at the measurement location has been investigated using computational fluid dynamics and shown to be accurate in the current configuration [31].
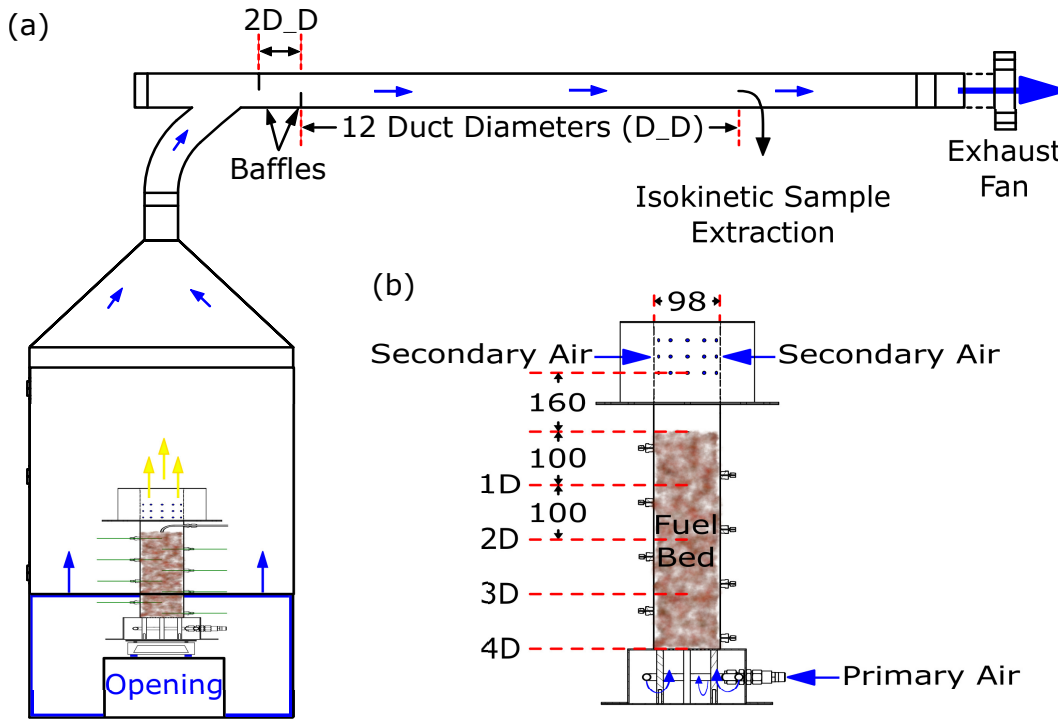


Figure 1: (a) The schematic diagram of the exhaust system is presented, including the emissions monitoring set-up. Distances in the exhaust system are provided in relation to the duct diameter

## 2.3. Reactor

The reactor is presented in Figure 1(b) and has previously been described, by Kirch *et al.*, in detail [29]. It has an inner diameter of 98 mm (1D) and a variable fuel bed height of 100–400 mm (1D–4D). A primary air flow is provided from below and secondary air is supplied downstream of the fuel bed, by dry compressed air. The secondary air inlet consists of a total of $36 \times 6$-mm diameter holes, evenly spaced around the circumference in three vertically-aligned rows 30 mm apart. Previous studies [30, 29] have presented measurements upstream of the secondary air inlets, to focus on the characterisation of the producer gas only.

4

## 2.4. Analysis Equipment

The gas analyser utilised was a Testo 350XL. This analyser uses an infra-red sensor, with a resolution of 0.01%, for the measurement of $CO_2$. CO is measured via an electrochemical sensor with a resolution of 1 ppm for low emission levels (<2000 ppm) and 5 ppm for high emission levels (>2000 ppm). Both CO and $CO_2$ emissions concentrations were recorded at 1 Hz, on a dry basis. The analyser was calibrated daily.

Optical particulate concentration measurements of the fraction with an aerodynamic diameter (d) 0.1<d<2.5 $\mu$m were performed using a TSI DustTrak II aerosol monitor model 8531. This provides real-time particulate concentrations in the exhaust flow at 1 Hz, with a readability of 0.001 mg·m$^{-3}$, a resolution of 0.1% of the reading and a range <400 mg·m$^{-3}$. Blank measurements showed a time-weighted average ambient particle concentration of 0.031 mg·m$^{-3}$ and real-time concentration measurements were calibrated to the gravimetric particle measurement (more details are provided in Section S 1.1 in the Supporting Information).

## 2.5. Gravimetric Particulate Measurements

Gravimetric measurements of all particulates and the fraction with an aerodynimc diameter $\leq$2.5 $\mu$m were performed. Sample extraction occurred isokinetically at 12 duct diameters downstream of the second baffle, as indicated in Figure 1(a). An external filter holder upstream of the Testo 350XL gas analyser was used to collect all particulates, while an internal filter holder in the DustTrak II provided the fraction $\leq$2.5 $\mu$m. In both cases, PTFE membrane filters with a pore size of 0.22 $\mu$m and a diameter of 37 mm were used. The filter media was desiccated and weighed with a readability of 0.01 mg. After the experiment, the filter media was desiccated for >24 h, weighed, returned to the desiccator for >24 h and weighed again. If the second measurement was within $\pm$0.05 mg of the first, the first measurement was accepted, in accordance with ISO-19867-1:2018. Blank measurements of the ambient particle concentration were performed and the measurements were found to be below the gravimetric limit of detection of 0.01 mg.

## 2.6. Procedure

The test procedure has been described previously [29] and is only briefly outlined here. To avoid influences from the large thermal mass of the reactor when performing replicate tests, the reactor was initially preheated and all tests where started with reactor wall temperatures <100 °C. Fuel was supplied to the reactor in batches. To ignite the fuel batch, 10 mL of methylated spirits (96 % ethanol, CAS # 64-17-5) and a paper towel were supplied to the top of the fuel bed. When the entire fuel batch was converted to char, the process was quenched by adding water ice from the top of the reactor and nitrogen (>99.99 % $N_2$), instead of air, from below the fuel bed to cool the process and end all ongoing reactions. Multiple repeats for each tested fuel were performed at two to four air supply mass flux and multiple fuel bed depths in the case of wood pellets, as presented in Table 2.

## 2.7. Analysis

The total amount of CO released was calculated on the basis of the concentration and the total duct flow rate. The total amount of CO released as well as the gravimetric PM measurements are mean values of all replicate tests (refer to Table 2) and were normalised to the amount of energy released from the fuel ($E_{released} = E_{fuel} - E_{char}$), as described previously [29, 30]. Gravimetric measurements of $PM_{2.5}$ and total PM were collected and $PM_{>2.5}$ was calculated as the difference of the two measurements.

Table 2: Experimental configurations: the fuel type, the fuel bed depth (BD, reported in (mm) and in relation to the reactor diameter (D)), the primary air supply (PA), the secondary air supply (SA), the total air supply (A), the number of repetitions performed.

| Fuel type | BD | | PA | SA | A | Repetitions |
|---|---|---|---|---|---|---|
| (Abbreviation) | (mm) | (D) | $(kg \cdot m^{-2} \cdot s^{-1})$ | $(kg \cdot m^{-2} \cdot s^{-1})$ | $(kg \cdot m^{-2} \cdot s^{-1})$ | |
| Wood pellets | 100 | 1 | 0.025 | 0.100 | 0.125 | 2 |
| (WP) | 100 | 1 | 0.050 | 0.200 | 0.250 | 3 |
| | 100 | 1 | 0.075 | 0.300 | 0.375 | 8 |
| | 100 | 1 | 0.125 | 0.500 | 0.625 | 4 |
| | 200 | 2 | 0.075 | 0.300 | 0.375 | 5 |
| | 300 | 3 | 0.075 | 0.300 | 0.375 | 4 |
| | 400 | 4 | 0.025 | 0.100 | 0.125 | 6 |
| | 400 | 4 | 0.050 | 0.200 | 0.250 | 7 |
| | 400 | 4 | 0.075 | 0.300 | 0.375 | 6 |
| | 400 | 4 | 0.125 | 0.500 | 0.625 | 7 |
| Wheat straw | 400 | 4 | 0.025 | 0.100 | 0.125 | 4 |
| (WS) | 400 | 4 | 0.075 | 0.300 | 0.375 | 4 |
| Sheep manure | 400 | 4 | 0.025 | 0.100 | 0.125 | 4 |
| (SM) | 400 | 4 | 0.075 | 0.300 | 0.375 | 7 |
| Cow manure | 400 | 4 | 0.025 | 0.100 | 0.125 | 3 |
| (CM) | 400 | 4 | 0.075 | 0.300 | 0.375 | 4 |

To account for dilution in the exhaust system and determine a quantitative value for the combustor efficiency, the measured gaseous emissions were normalised. The utilised normalisation relates the carbonaceous products of complete combustion to all gaseous carbonaceous combustion products. It must be considered that the only gaseous carbonaceous species considered in the normalisation were CO and $CO_2$, because the hydrocarbon emissions were below the detection limit of 100 ppm. The nominal combustion efficiency has been previously established for the evaluation of cookstoves [32] and was calculated using the mole fraction ($x$) of CO and $CO_2$ via Equation 1:

$$NCE = \frac{x_{CO_2}}{x_{CO_2} + x_{CO}} \tag{1}$$

Average profiles of the NCE for each configuration were calculated. To achieve this, real time NCE values for each individual test were calculated over the duration of the process and mean values established for each configuration. The NCE results are presented in the Supporting Information.

## 3. Results

### 3.1. Particulate Emissions

Figure 2 reports profiles of the $PM_{2.5}$ mass concentration in the exhaust stream over the duration of the experiments, for a range of fuels and primary air supply flux. A representative plot of one experiment for each configuration is shown, although all cases were repeated multiple times

(refer to Table 2). The $PM_{2.5}$ mass concentration ($mg \cdot m^{-3}$) in the exhaust gas flow is presented as a function of time for the four fuels in (a) WP, (b) WS, (c) SM and (d) CM. Measurements of multiple primary air supply mass flux, 0.025–0.125 $kg \cdot m^{-2} \cdot s^{-1}$, are shown as indicated in the respective legends. The air supply mass flux is provided on the basis of the reactor cross sectional area.

For wood pellets (WP), the $PM_{2.5}$ concentration decreases as a function of time for all air supply flux. Previously reported findings of the thermochemical conversion process in the solid fuel bed have shown that as the reaction front propagates down the bed and char accumulates downstream of the reaction front, the produced tars can crack [29]. This transforms tars into simpler combustible gases upstream of the secondary air inlet as the reaction front moves down the bed over time. Therefore, the noticeable decrease of $PM_{2.5}$ emissions along the temporal axis could be due to lower tar concentrations in the producer gas. Increasing primary air supply flux have been shown to lead to greater conversion temperatures throughout the fuel bed and a reduction in the overall tar yield [29]. Simultaneously higher temperatures will also cause a change in the composition of tar constituents. It is well understood that the tar fractions which have been identified as a soot precursor are polycyclic aromatic hydrocarbons (PAH) [33, 27, 34]. PAHs are formed within the solid fuel bed at temperatures of $>800°C$ with increasing complexity at higher temperatures [35]. For all fuels investigated these temperatures only occur at air supply flux of $>0.050$ $kg \cdot m^{-2} \cdot s^{-1}$[29, 30]. Therefore, the similar real-time concentrations of $PM_{2.5}$ at 0.025 $kg \cdot m^{-2} \cdot s^{-1}$and 0.050 $kg \cdot m^{-2} \cdot s^{-1}$and the subsequent slight increases may be related to an increasing PAH concentration in the producer gas.

Wheat straw (WS) exhibits a slightly different profile in Figure 2, compared with WP. While at 0.025 $kg \cdot m^{-2} \cdot s^{-1}$primary air supply, similar to WP, a reduction of the $PM_{2.5}$ over time can be noticed, which is not the case at 0.075 $kg \cdot m^{-2} \cdot s^{-1}$. This suggests that either tar cracking in the char bed occurs only at low primary air supply flux or more likely that at high air supply, other influences, such as the fuel ash content, become more influential.

For both manures, sheep (SM) and cow (CM), the trends appear similar in Figure 2. There is no reduction of the $PM_{2.5}$ concentration over time at 0.025 $kg \cdot m^{-2} \cdot s^{-1}$, which suggests that tar cracking with an increasing char layer downstream of the reaction does not notably influence the emissions. Similarly to WS this suggests that other influences, such as the fuel ash content, are more influential. The overall trend of lower $PM_{2.5}$ concentrations over time at all flow rates for WP, lower $PM_{2.5}$ concentrations over time only at low primary air supply flux for WS and no reduction in $PM_{2.5}$ concentration for the manures, suggests that an increasing ash content (CM>SM>WS>WP) has a greater influence on the emissions than the combustion of tars, or potentially the ash could inhibit tar cracking in the produced char layer. It must be considered that with increasing ash content in the fuel, the conversion of fuel carbon to char decreases substantially when increasing the air supply, as presented previously [30]. This leads to a rapid decrease of the fixed carbon content of the produced char. It is possible that either or both mechanisms may influence tar cracking in the char layer, but this is beyond the current scope of work.

Figure 3 presents the mean gravimetric measurements of: (a) $PM_{2.5}$ and (b) total PM for each configuration under investigation. For each configuration, the quantity of particulates released has been normalised to the mean energy released from the fuel ($E_{released}$ = $E_{fuel}$ - $E_{char}$) for each configuration. A logarithmic representation of the normalised particulate emissions was chosen to accommodate large variations in between configurations (numerical values are provided in the Supporting Information in Table S1).

In Figure 3(a), the $PM_{2.5}$ emissions from WP are similar at one diameter fuel bed depth (1D) with an increasing air supply flux, while they increase at 4D. The discrepancy of $PM_{2.5}$ between
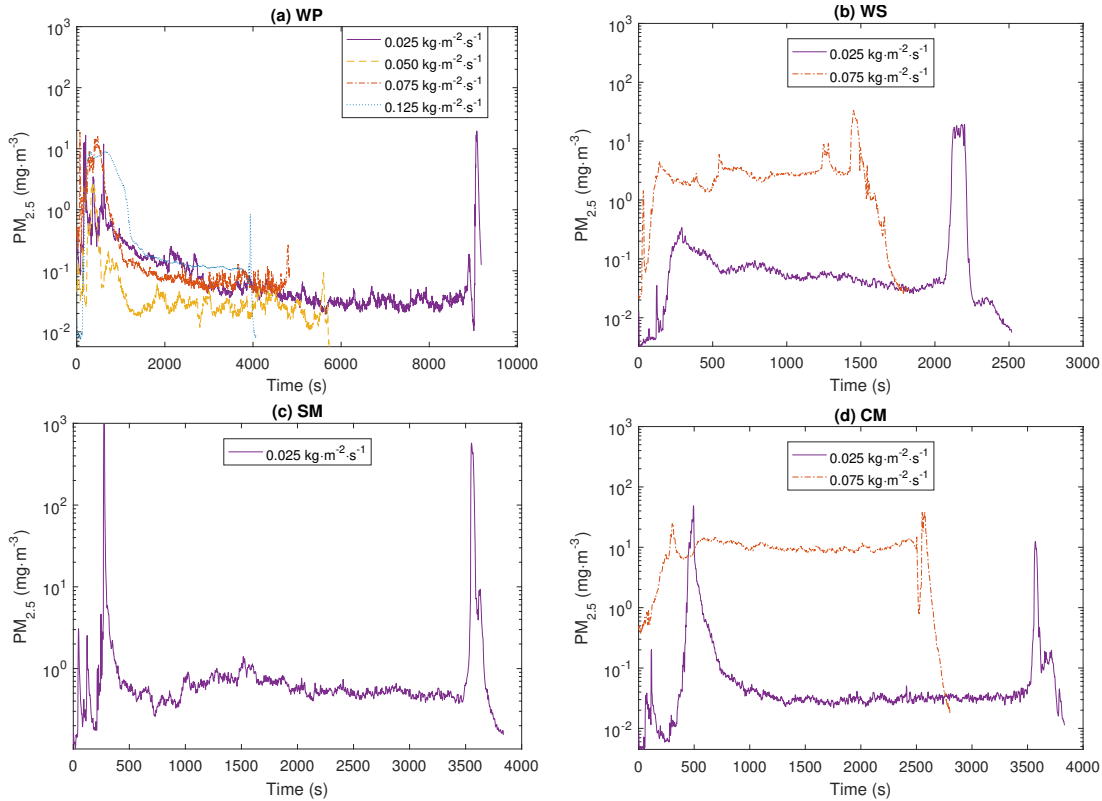
7

Figure 2: Temporal concentration of $PM_{2.5}$ mass in the exhaust gas stream, for all fuels: (a) wood pellets, (b) wheat straw, (c) sheep manure and (d) cow manure. The fuel bed depth is 4D. Air supply flux of 0.025–0.125 $kg \cdot m^{-2} \cdot s^{-1}$ are indicated in the respective legends.

1D and 4D could be due to a lower influence of transients, during lighting and quenching. With only 1D, transients are particularly influential due to the short length of the overall duration of the process (refer to Table S1), leading to a greater effect on the total emissions. Previous research has also found that during transient events, organic compounds dominate the emissions, while during steady-state combustion, inorganic compounds are of greater importance [36]. At 4D, the increase in the $PM_{2.5}$ emissions from WP with increasing air flow rate could be related to soot formation (which contributes mainly to $PM_{2.5}$ rather than larger particulates). Soot formation could be the result of an increasing PAH content in the producer gas, as discussed earlier in this section. The results also suggest that mechanisms apart from soot influence the $PM_{2.5}$ emissions. Similar trends have previously been observed for incomplete combustion emissions from biomass fuels, such as CO and soot [37]. It can be seen that for WP the release of CO decreases while the related nominal combustion efficiency (refer to Figure S1) increases with the increasing air supply, as described in more detail in the subsequent section. Thus more complete combustion, leading to less CO and soot, would be expected, as discussed in more detail in the following section. Therefore, the increase in PM emissions with the air supply could be due to influences other than incomplete combustion. Two mechanisms, namely the entrainment of ash particles in the gas
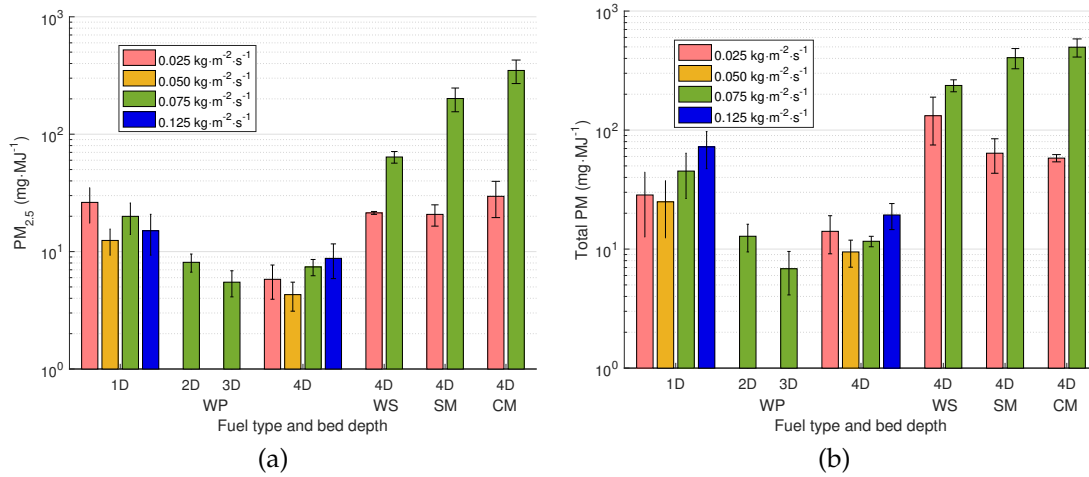
Figure 3: The gravimetric particulate emissions of (a) the $PM_{2.5}$ and (b) the total PM, normalised to the energy released from the fuel, are presented on a logarithmic scale for all investigated configurations and fuels. The error bars present the standard error of the mean.

stream and increasing devolatilisation of fuel ash constituents, could be influential [38]. Especially at high air supply flux, when little fixed carbon remains in the char product, ash constituents will become loose on the particle surface, as described previously [30]. These loose ash particles can be entrained more easily by the surrounding gas flow, for which the velocity also increases with the amount of air supplied. Furthermore, an increasing air supply leads to increasing fuel bed temperatures which will cause an enhanced devolatilisation of fuel ash constituents [39, 40, 41].

For WS, SM and CM a more substantial increase in the PM emissions can be noted with an increasing primary air supply. In Figure 4 the $PM_{2.5}$ and $PM_{>2.5}$ emissions are presented as a function of the fuel ash content. At high air supply, the overall trend of $PM_{2.5}$ can be related to the fuel ash content and follows the relationship WP<WS<SM<CM. As stated previously, ash constituents can be entrained in the gas stream or devolatilised from the fuel bed. Previously it has been suggested that especially S, Cl, K and Na, which are typically contained in many biomass fuels, even if present only in trace amounts in a combustion process, can have an impact on the formation of emissions, including CO and PM [42, 28]. The effects of certain compounds on the combustion chemistry, especially on producer gas combustion are largely unknown. Therefore, an increasing amount of ash in the fuel may lead to higher concentrations of ash constituents participating in the combustion process, which may contribute to the increasing $PM_{2.5}$ emissions.

The trends of the total PM in Figure 3(b) appear only slightly different, in comparison with $PM_{2.5}$. For all fuels a higher air supply flux leads to greater emissions. This increase in total PM emissions can also be related to greater entrainment of coarse fly ash ($>10\mu m$) particles with higher gas stream velocities. This contribution to total PM has previously been demonstrated for fixed-bed wood pellet combustion at similar primary air supply flux [43] and could affect the results here similarly. In Figure 4 for the $PM_{>2.5}$ emissions it can be noticed that while they are very similar for all non-woody biomass fuels at 0.075 $kg \cdot m^{-2} \cdot s^{-1}$ air supply, WS exhibits the largest emissions at 0.025 $kg \cdot m^{-2} \cdot s^{-1}$.

Overall, it can be noticed that low air supply flux lead to very efficient combustion and low
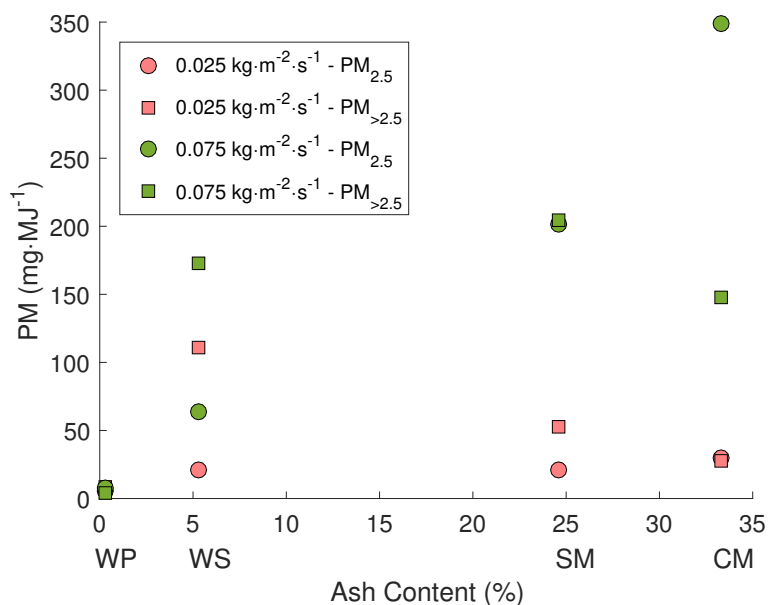
9

Figure 4: The mean $PM_{2.5}$ and $PM_{>2.5}$, normalised to the energy released from the fuel, as a function of the fuel ash content are presented.

emissions of PM from all fuels. The production of char and the retention of a large fraction of the ash in its structure appears to enable the much cleaner combustion of high ash-content fuels compared with high air supply flux [17, 29]. Therefore, it would be beneficial to design cookstoves to utilise a low air supply flux, while providing sufficient fire power for cooking, by adjusting the cross sectional area and to aim at producing char as a solid product rather than combusting it.

### 3.2. Gaseous Emissions

Figure 5 presents the accumulated CO emissions, normalised by the energy released from the fuel, for all investigated fuels and process configurations. CO is the main gaseous emission from incomplete combustion and a significant health concern for users. An analysis of real-time gaseous emissions measurements and their relationship to the efficiency of the combustion process is provided in the Supporting Information in Section S2.

Increasing the air supply flux for WP leads to a reduction in CO, however, the opposite trend is apparent for the manures, and no clear trend is measured for WS. Extremely low CO emissions can be seen in all cases for WP, especially when increasing primary air supply flux $>0.025\,\mathrm{kg\cdot m^{-2}\cdot s^{-1}}$, as well as with increasing fuel bed depths. A lower tar fraction from the conversion process before secondary combustion and higher cold gas efficiencies with increasing air supply flux as well as fuel bed depths, have been presented previously [30] and the resultant higher gas quality for combustion, leading to lower CO emissions, corroborates those findings here.

The trend of greater CO emissions with increasing air supply flux for the manures, and to some degree for WS, is similar to the PM emissions (refer to Figure 3). This suggests that particulate matter constituents, presumably ash constituents, influence the combustion process and the release of CO emissions. In regard to the producer gas composition, all fuels have been shown to

behave similarly, with lower tar yields and higher gas quality at higher primary air supply flux [30]. This strengthens the argument that fuel ash constituents influence the formation of emissions from incomplete combustion. When focusing on the manures, it can be seen that especially low CO emissions are released at 0.025 kg·m$^{-2}$·s$^{-1}$ from SM but higher emissions are released from CM, while at high air supply flux the values are similar for both manures. The particularly low emissions at low air supply flux highlight the potentially high efficiency of the combustion process, even when utilising high ash content fuels.
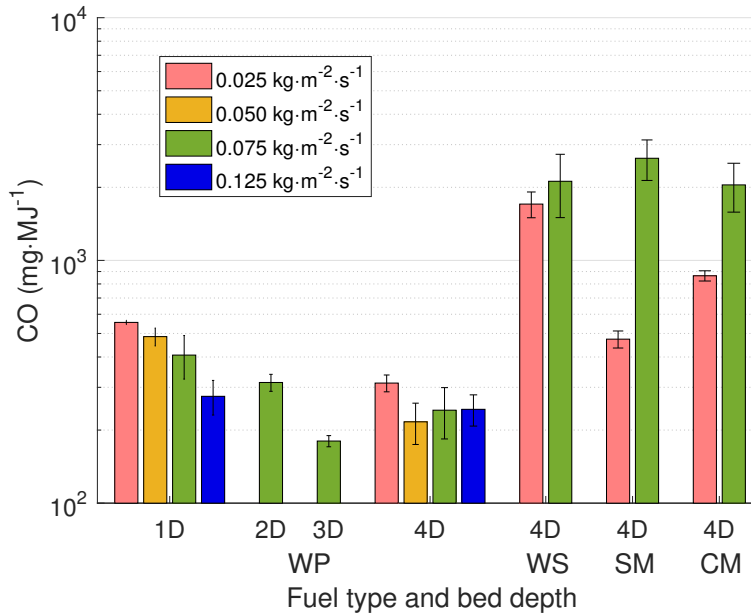


Figure 5: The emissions of CO normalised to the energy released from the fuel are presented on a logarithmic scale for all investigated configurations and fuels. The error bars present the standard error of the mean.

## 4. Discussion

The three mechanisms for PM emissions discussed here are; (1) incomplete combustion, leading to carbonaceous products, and release of ash constituents via (2) devolatilisation, and (3) entrainment. To achieve a reduction in PM emissions, each must be considered as individual but interconnected mechanisms. Different approaches are necessary for their mitigation, while currently the main approach for emissions reduction from cookstoves is to achieve more complete hydrocarbon combustion, while often disregarding the influence of ash constituents. As noticed here, a higher primary air supply can reduce tars in the producer gas and reduce incomplete combustion leading to lower CO emissions, notably from low ash content wood pellets. Simultaneously, the emissions of PM in all cases and CO for the higher ash content non-woody biomass fuels increase with the air supply, which can be related to the fuel ash content.

A previous investigation of multiple wood species, crop residues and cow manure, completely combusted in a traditional Indian stove [44], has shown that an elemental analysis of the PM$_{2.5}$

emissions could account for ≈50% of the total mass (the rest is assumed to be oxygen). These ≈50% were made up about half by C—lowest from cow manure—and ash constituents, mainly ions, K and Cl as well as ammonia—all highest from cow manure [44]. This demonstrates the significance of ash constituents in the PM emissions, especially from manures, while their influence on the combustion process [28], as well as their total contribution for a particular fuel, are largely unknown. This fraction of the PM, containing ash constituents, cannot be addressed through an increase in efficiency of the combustion process [45], but necessitates alternative approaches and considerations. Alternative approaches may include air control or the production of char, as investigated here, but also others such as fuel additives or the integration of advanced materials or even filters into the stove design. Here low air supply flux lead to very efficient combustion and low emissions of CO and PM for all fuels. Adapting the reactor cross sectional to accommodate low air supply flux, while still providing sufficient fire power for cooking, could be an approach to reduce pollutant emissions. This would lead a larger reactor diameter, while the height might need to be reduced. As it has also been shown here that a greater reactor height leads to lower emissions, its reduction might be a drawback. Additionally, the reactor dimensions would then only be adapted to a specific fuel. A modular cookstove design where multiple reactor sizes may be utilised could be a solution, but would substantially increase the systems complexity. Furthermore, it has been shown here that the production of char and the retention of a large fraction of the ash in its structure enables much cleaner combustion of high ash-content fuels. Since the char contains large amounts of energy it might not be in the user will need a clear incentive, most likely a economic benefit, for the production of char. More rigorous investigation and in-depth discussion of the fate of ash constituents in biomass combustion and mechanisms for their mitigation are therefore of importance.

To demonstrate the benefits of avoiding flame quenching by the pot and of the production of solid char in the presented gasifier cookstove these results are compared with values found in the literature from similar gasifier cookstoves, which were tested while performing cooking tasks. Figure 6 presents a comparison of the CO and $PM_{2.5}$ emissions of the present investigation and results found in the literature from similar devices with similar fuels. One study investigated the combustion process in a medium-size gasifier stove and reports the emissions on the basis of energy released from the fuel [46], similar to the present study. The remaining studies utilise standardised test protocols to evaluate the stove performance, either through the international [11, 47, 48, 5] or the Chinese [10, 9, 12] Water Boiling Test, where the emissions are reported on the basis of energy delivered to a cooking vessel contents. For better comparability, a moderate heat transfer efficiency of 35% [47] is applied to the results from the present investigation.

It can be seen in Figure 6 that very low emissions of PM and CO are only reached with wood fuels in literature, mostly pelletised, while here this can also be achieved using non-woody biomass. Lowest emissions are achieved in stoves specifically designed for experimental purposes with >1D fuel bed depth. Very consistent conditions in the experimental stoves and a reduction of the influence of transients, due to the larger depth, will contribute to their better performance. Furthermore, the present investigation is the only case where insulation material surrounds the combustion chamber, leading to lower heat loss and presumably higher efficiency of the thermochemical conversion. The apparent direct relationship between the $PM_{2.5}$ and CO emissions, as they increase simultaneously and not independently, in Figure ■ should be noted. This further suggests that both CO and PM emissions cannot only be related to incomplete combustion of the carbonaceous fuel, but also that CO emissions may be influenced by the same mechanisms that lead to the release of particulates, as described in the Gaseous Emissions Section. Additionally, two
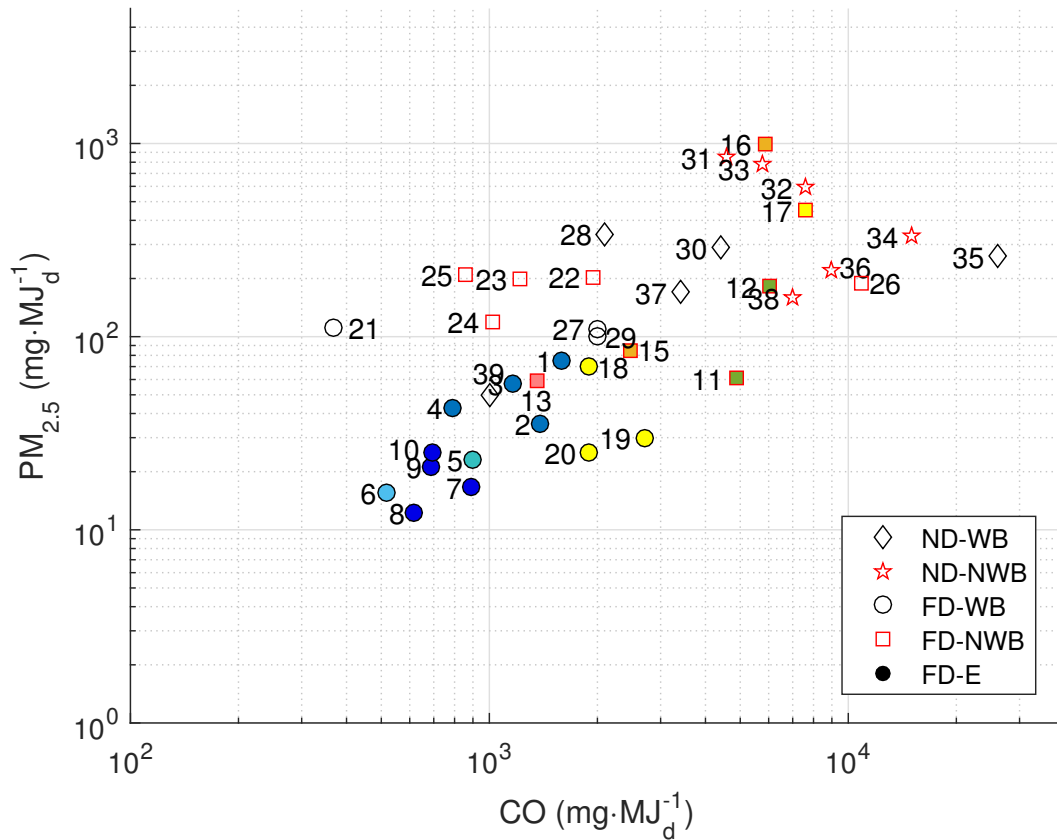
12

Figure 6: Results from the present investigation, under the assumption of a moderate thermal efficiency of 35%, as well as values found in the literature for $PM_{2.5}$ and CO emissions normalised to the energy delivered to the cooking vessel contents are presented. Three types of gasifier stoves: forced draft stoves (FD), forced draft experimental reactors (FD-E) and natural draft stoves (ND), using woody biomass (WB) or non-woody biomass (NWB) are included. Multiple stoves and fuels are investigated: Present investigation, (1–4) 1D, wood pellets (WP); (5) 2D, WP; (6) 3D, WP; (7–10) 4D, WP; (11–12) 4D, wheat straw; (13–14) 4D, sheep manure; (15–16) 4D, cow manure; (17–20) [11]; (21–22) [46]; (23–25) [10]; (26–27) [47]; (28–29) [48]; (30) [9]; (31–33) [12]; (34–39) [5].

general trends can be noticed in Figure 6: (1) forced draft stoves perform better in terms of emissions than natural draft stoves and (2) woody biomass achieves lower emissions than non-woody biomass.

For both CO and PM emissions, better results are achieved using forced draft, particularly in well-controlled experimental stoves. Similar to previous studies, this suggests that a constant, rather than buoyancy driven, air supply achieves better mixing of air with the combustible gases to aid more complete combustion [17]. While the emissions of PM can be due to multiple influences, as discussed earlier in this section, CO is released as a result of inefficiency of the combustion process. Lower emissions achieved in the present study (Figure 6 1–16), when compared with investigations emulating user practices (Figure 6 17–22 and 26–39), could also be due to the absence of a pot in the secondary combustion zone. In theory, the combustion process should be completed upstream of a pot and only hot gases would get in contact with the pot. If at any time

the secondary combustion zone extends to the surface of the pot, local flame quenching will occur leading to the release of increasing products from incomplete combustion, which is avoided in the present investigation.

When considering the difference between woody and non-woody biomass, especially the very low ash content of woody biomass in comparison with other biomass fuels, must be considered. As the influence of ash constituents on the combustion process is still largely unknown, as described above, this adds complexity to the discussion of fuels with increasing ash content. Many more parameters, such as bulk density, moisture content or fuel particle size could be of influence, but their discussion is outside the scope of this work. It is shown here, though, that in highly controlled conditions, very low emissions may be achieved with all investigated fuels, including the manures and wheat straw at low primary air supply flux. This demonstrates that a high fuel ash content is not necessarily a problem, but it appears that the production of char to retain a large fraction of the ash will be required to achieve low emissions from such fuels. It needs to be stressed that the results from the present study show that low value agricultural residues and even manures can be burned almost as cleanly as high quality wood pellets under controlled conditions in gasifier cookstoves. Therefore, gasifier cookstove designs should endeavour to accommodate low primary air flow rates, maximum reactor heights and promote the production of solid char, which have been shown as effective measures for emissions reduction.

## 5. Conclusions

The present study investigates the secondary combustion process in a small-scale batch fed cookstove. Multiple fuels, namely wood pellets, wheat straw, sheep manure and cow manure, have been tested, while the producer gas composition upstream of the secondary combustion zone has previously been reported. The products of the combustion process are analysed in light of the fuel, producer gas, and char product composition.

- Low tar concentrations in the producer gas from wood pellets reduces the emissions of CO. This is achieved with increasing air supply flux or greater fuel bed depth.

- Interestingly the previous trend does not extend to the PM emissions. Generally higher PM emissions have been found with increasing air supply, presumably due to the influence of the fuel ash constituents.

- Low air supply flux lead to very efficient combustion and low emissions of CO and PM for all fuels, in comparison with values found in the literature. Low primary air flow rates are therefore desired to minimise pollutant emissions.

- From all non-woody biomass fuels, the higher ash content, leads to increasing emissions of CO as well as PM with increasing air supply.

- A large fraction of CO and PM emissions is released during transient events at start-up and shut-down. In application PM emissions released at shut-down could be avoided by an isolated quenching method. Generally the reduction of emissions during transient events needs further scrutiny.

The strong influence of the ash fraction of the fuel is apparent. Especially at high air supply the influence of devolatilised and entrained particles leads to much greater emissions of PM for all

fuels and of CO in case of the non-woody biomass. It was shown that a larger yield of carbon in the produced char retains a greater fraction of the ash and substantially improves the combustion performance. It appears that the production of char, or other measures to retain the ash in the bed, will be necessary to achieve low emissions from cookstoves, especially when using high ash content fuels.

## 6. Acknowledgements

## 7. Supporting Information

Additional information, supplementing results and numerical values of the presented results

[1] T. C. Bond, S. J. Doherty, D. W. Fahey, P. M. Forster, T. Berntsen, B. J. Deangelo, M. G. Flanner, S. Ghan, B. Kärcher, D. Koch, S. Kinne, Y. Kondo, P. K. Quinn, M. C. Sarofim, M. G. Schultz, M. Schulz, C. Venkataraman, H. Zhang, S. Zhang, N. Bellouin, S. K. Guttikunda, P. K. Hopke, M. Z. Jacobson, J. W. Kaiser, Z. Klimont, U. Lohmann, J. P. Schwarz, D. Shindell, T. Storelvmo, S. G. Warren, C. S. Zender, Bounding the role of black carbon in the climate system: A scientific assessment, Journal of Geophysical Research: Atmospheres 118 (11) (2013) 5380–5552. `doi:10.1002/jgrd.50171`.

[2] S. Bonjour, H. Adair-Rohani, J. Wolf, N. G. Bruce, S. Mehta, A. Prüss-Ustün, M. Lahiff, E. A. Rehfuess, V. Mishra, K. R. Smith, Solid fuel use for household cooking: Country and regional estimates for 1980-2010, Environmental Health Perspectives 121 (7) (2013) 784–790. `doi:10.1289/ehp.1205987`.

[3] B. N. Young, M. L. Clark, S. Rajkumar, M. L. Benka-Coker, A. Bachand, R. D. Brook, T. L. Nelson, J. Volckens, S. J. Reynolds, C. L'Orange, N. Good, K. Koehler, S. Africano, A. B. Osorto Pinel, J. L. Peel, Exposure to household air pollution from biomass cookstoves and blood pressure among women in rural Honduras: A cross-sectional study, Indoor Air (April 2018) (2018) 130–142. `doi:10.1111/ina.12507`.

[4] H. S. Mukunda, S. Dasappa, P. J. Paul, N. K. S. Rajan, M. Yagnaraman, D. Ravi Kumar, M. Deogaonkar, Gasifier stoves – science, technology and field outreach, Current Science 98 (5) (2010) 627–638.

[5] J. Tryner, B. D. Willson, A. J. Marchese, The effects of fuel type and stove design on emissions and efficiency of natural-draft semi-gasifier biomass cookstoves, Energy for Sustainable Development 23 (2014) 99–109. `doi:10.1016/j.esd.2014.07.009`.
URL `http://linkinghub.elsevier.com/retrieve/pii/S0973082614000817`

[6] L. Deng, D. Torres-Rojas, M. Burford, T. H. Whitlow, J. Lehmann, E. M. Fisher, Fuel sensitivity of biomass cookstove performance, Applied Energy 215 (2018) 13–20. `doi:10.1016/j.apenergy.2018.01.091`.
URL `https://doi.org/10.1016/j.apenergy.2018.01.091`

[7] T. B. Reed, R. Larson, A wood-gas stove for developing countries, Energy for Sustainable Development 3 (2) (1996) 34–37. `doi:10.1016/S0973-0826(08)60589-X`.
URL `http://dx.doi.org/10.1016/S0973-0826(08)60589-X`

[8] T. B. Reed, E. Anselmo, K. Kircher, Testing & Modeling the Wood-Gas Turbo Stove, in: A. Bridgwater (Ed.), Progress in Thermochemical Biomass Conversion Conference, Blackwell Science Ltd, Bodmin, 2001, pp. 693–704.

[9] H. Yibo, H. Li, X. Chen, C. Xue, C. Chen, G. Liu, Effects of moisture content in fuel on thermal performance and emission of biomass semi-gasified cookstove, Energy for Sustainable Development 21 (1) (2014) 60–65. `doi:10.1016/j.esd.2014.05.007`.
URL `http://dx.doi.org/10.1016/j.esd.2014.05.007http://linkinghub.elsevier.com/retrieve/pii/S0973082614000490`

[10] Y. Chen, G. Shen, S. Su, W. Du, Y. Huangfu, G. Liu, X. Wang, B. Xing, K. R. Smith, S. Tao, Efficiencies and pollutant emissions from forced-draft biomass-pellet semi-gasifier stoves:

Comparison of International and Chinese water boiling test protocols, Energy for Sustainable Development 32 (2016) 22–30. `doi:10.1016/j.esd.2016.02.008`.
URL `http://linkinghub.elsevier.com/retrieve/pii/S0973082616000089`

[11] J. Tryner, J. W. Tillotson, M. E. Baumgardner, J. T. Mohr, M. W. Defoort, A. J. Marchese, The Effects of Air Flow Rates, Secondary Air Inlet Geometry, Fuel Type, and Operating Mode on the Performance of Gasifier Cookstoves, Environmental Science and Technology 50 (17) (2016) 9754–9763. `doi:10.1021/acs.est.6b00440`.

[12] Z. Zongxi, S. Zhenfeng, Z. Yinghua, D. Hongyan, Z. Yuguang, Y. X. Zhang, A. Riaz, C. Pemberton Pigott, D. Renjie, Effects of biomass pellet composition on the thermal and emissions performances of a TLUD cooking stove, International Journal of Agricultural and Biological Engineering 10 (4) (2017) 189–197. `doi:10.25165/j.ijabe.20171004.2963`.

[13] Z. Zhang, Y. Zhang, Y. Zhou, R. Ahmad, C. Pemberton-Pigott, H. Annegarn, R. Dong, Systematic and conceptual errors in standards and protocols for thermal performance of biomass stoves, Renewable and Sustainable Energy Reviews 72 (17) (2017) 1343–1354. `doi:10.1016/j.rser.2016.10.037`.
URL `http://dx.doi.org/10.1016/j.rser.2016.10.037`

[14] C. Birzer, P. Medwell, J. Wilkey, T. West, M. Higgins, G. Macfarlane, M. Read, An analysis of combustion from a top-lit up-draft ( TLUD ) cookstove, Journal of Humanitarian Engineering 2 (1) (2013) 1–8.

[15] J. Tryner, J. Volckens, A. J. Marchese, Effects of operational mode on particle size and number emissions from a biomass gasifier cookstove, Aerosol Science and Technology 52 (1) (2018) 87–97. `doi:10.1080/02786826.2017.1380779`.
URL `https://doi.org/10.1080/02786826.2017.1380779`

[16] C. A. Roden, T. C. Bond, S. Conway, A. B. Osorto Pinel, N. A. MacCarty, D. Still, Laboratory and field investigations of particulate and carbon monoxide emissions from traditional and improved cookstoves, Atmospheric Environment 43 (6) (2009) 1170–1181. `doi:10.1016/j.atmosenv.2008.05.041`.
URL `http://dx.doi.org/10.1016/j.atmosenv.2008.05.041`

[17] T. Kirch, C. H. Birzer, P. J. V. Eyk, P. R. Medwell, P. J. van Eyk, P. R. Medwell, Influence of Primary and Secondary Air Supply on Gaseous Emissions from a Small-Scale Staged Solid Biomass Fuel Combustor, Energy and Fuels 32 (2018) 4212–4220. `doi:10.1021/acs.energyfuels.7b03152`.
URL `http://pubs.acs.org/doi/10.1021/acs.energyfuels.7b03152`

[18] A. M. James R, W. Yuan, M. Boyette, The Effect of Biomass Physical Properties on Top-Lit Updraft Gasification of Woodchips, Energies 9 (4) (2016) 283–296. `doi:10.3390/en9040283`.
URL `http://www.mdpi.com1996-1073/9/4/283`

[19] A. M. James R, W. Yuan, M. D. Boyette, D. Wang, Airflow and insulation effects on simultaneous syngas and biochar production in a top-lit updraft biomass gasifier, Renewable Energy 117 (2018) 116–124. `doi:10.1016/j.renene.2017.10.034`.
URL `http://linkinghub.elsevier.com/retrieve/pii/S0960148117309965`

[20] Y. Mehta, C. Richards, Gasification Performance of a Top-Lit Updraft Cook Stove, Energies 10 (10) (2017) 1529. `doi:10.3390/en10101529`.
URL `http://www.mdpi.com/1996-1073/10/10/1529`

[21] X. H. Pham, B. Piriou, S. Salvador, J. Valette, L. Van de Steene, Oxidative pyrolysis of pine wood, wheat straw and miscanthus pellets in a fixed bed, Fuel Processing Technology 178 (June) (2018) 226–235. `doi:10.1016/j.fuproc.2018.05.029`.
URL `https://doi.org/10.1016/j.fuproc.2018.05.029`

[22] T. C. Lieuwen, V. Yang, R. A. Yetter (Eds.), Synthesis Gas, Taylor & Francis, Boca Raton, 2009.

[23] M. Fischer, X. Jiang, An assessment of chemical kinetics for bio-syngas combustion, Fuel 137 (2014) 293–305. `doi:10.1016/j.fuel.2014.07.081`.
URL `http://dx.doi.org/10.1016/j.fuel.2014.07.081`

[24] M. Fischer, X. Jiang, A chemical kinetic modelling study of the combustion of CH4 - CO - H2 - CO2 fuel mixtures, Combustion and Flame 167 (2016) 274–293. `doi:10.1016/j.combustflame.2016.02.001`.
URL `http://dx.doi.org/10.1016/j.combustflame.2016.02.001`

[25] C. Mandl, I. Obernberger, I. R. Scharler, Characterisation of fuel bound nitrogen in the gasification process and the staged combustion of producer gas from the updraft gasification of softwood pellets, Biomass and Bioenergy 35 (11) (2011) 4595–4604. `doi:10.1016/j.biombioe.2011.09.001`.
URL `http://dx.doi.org/10.1016/j.biombioe.2011.09.001`

[26] H. Sadig, S. A. Sulaiman, M. A. Said, Effect of producer gas staged combustion on the performance and emissions of a single shaft micro-gas turbine running in a dual fuel mode, Journal of the Energy Institute 90 (1) (2017) 132–144. `doi:10.1016/j.joei.2015.09.003`.
URL `http://dx.doi.org/10.1016/j.joei.2015.09.003`

[27] M. Frenklach, Reaction mechanism of soot formation in flames, Physical Chemistry Chemical Physics 4 (11) (2002) 2028–2037. `doi:10.1039/b110045a`.

[28] P. Glarborg, Hidden interactions—Trace species governing combustion and emissions, Proceedings of the Combustion Institute 31 (2007) 77–98. `doi:10.1016/j.proci.2006.08.119`.

[29] T. Kirch, P. R. Medwell, C. H. Birzer, P. J. Van Eyk, Influences of fuel bed depth and air supply on small-scale batch-fed reverse downdraft biomass conversion, Energy and Fuels 32 (2018) 8507–8518. `doi:10.1021/acs.energyfuels.8b01699`.

[30] T. Kirch, P. R. Medwell, C. H. Birzer, P. J. Van Eyk, Small-scale autothermal thermochemical conversion of various solid biomass feedstocks, Submitted to: Renewable Energy.

[31] T. Kirch, M. J. Evans, P. R. Medwell, V. H. Rapp, C. H. Birzer, A. J. Gadgil, Mixing uniformity of emissions for point-wise measurements in exhaust ducts, Proceedings of the 21st Australasian Fluid Mechanics Conference (December).

[32] M. Johnson, R. Edwards, V. Berrueta, O. Masera, New approaches to performance testing of improved cookstoves, Environmental Science and Technology 44 (1) (2010) 368–374. `doi:10.1021/es9013294`.

[33] M. Frenklach, D. W. Clary, W. C. Gardiner, S. E. Stein, Detailed kinetic modeling of soot formation in shock-tube pyrolysis of acetylene, Symposium (International) on Combustion 20 (1) (1985) 887–901. `doi:10.1016/S0082-0784(85)80578-6`.

[34] A. Indarto, A. Giordana, G. Ghigo, Formation of PAHs and soot platelets: multiconfiguration theoretical study of the key step in the ring closure – radical breeding polyyne-based mechanism, Journal of Physical Organic Chemistry 23 (2010) 400–410. `doi:10.1002/poc.1613`.

[35] A. Molino, S. Chianese, D. Musmarra, Biomass gasification technology: The state of the art overview, Journal of Energy Chemistry 25 (2016) 10–25. `doi:10.1016/j.jechem.2015.11.005`.
URL `http://linkinghub.elsevier.com/retrieve/pii/S2095495615001102`

[36] J. M. Jones, A. R. Lea-Langton, L. Ma, M. Pourkashanian, A. Williams, Pollutants Generated by the Combustion of Solid Biomass Fuels, Springer, London, 2014. `doi:10.1007/978-1-4471-6437-1`.
URL `http://link.springer.com/10.1007/978-1-4471-6437-1`

[37] K. L. Bignal, S. Langridge, J. L. Zhou, Release of polycyclic aromatic hydrocarbons, carbon monoxide and particulate matter from biomass combustion in a wood-fired boiler under varying boiler conditions, Atmospheric Environment 42 (39) (2008) 8863–8871. `doi:10.1016/j.atmosenv.2008.09.013`.
URL `http://dx.doi.org/10.1016/j.atmosenv.2008.09.013`

[38] Y. Huang, H. Liu, H. Yuan, X. Zhuang, S. Yuan, X. Yin, C. Wu, Release and Transformation Pathways of Various K Species during Thermal Conversion of Agricultural Straw. Part 1: Devolatilization Stage, Energy and Fuels 32 (2018) 9605–9613. `doi:10.1021/acs.energyfuels.8b02191`.
URL `http://dx.doi.org/10.1021/acs.energyfuels.8b02191`

[39] D. M. Quyn, H. Wu, C. Z. Li, Volatilisation and catalytic effects of alkali and alkaline earth metallic species during the pyrolysis and gasification of Victorian brown coal. Part I. Volatilisation of Na and Cl from a set of NaCl-loaded samples, Fuel 81 (2) (2002) 143–149. `doi:10.1016/S0016-2361(01)00127-2`.

[40] Y. Wang, H. Wu, Z. Sárossy, C. Dong, P. Glarborg, Release and transformation of chlorine and potassium during pyrolysis of KCl doped biomass, Fuel 197 (2017) 422–432. `doi:10.1016/j.fuel.2017.02.046`.
URL `http://dx.doi.org/10.1016/j.fuel.2017.02.046`

[41] X. Wei, U. Schnell, K. R. G. Hein, Behaviour of gaseous chlorine and alkali metals during biomass thermal utilisation, Fuel 84 (2005) 841–848. `doi:10.1016/j.fuel.2004.11.022`.

[42] B. S. Haynes, H. G. Wagner, Soot Formation, Progress in Energy and Combustion Science 7 (1981) 229–273. `doi:10.1016/0360-1285(81)90001-0`.
URL `http://www.csa.com/partners/viewrecord.php?requester=gs{&}collection=TRD{&}recid=A8214362AH`

[43] H. Wiinikka, R. Gebart, Critical parameters for particle emissions in small-scale fixed-bed combustion of wood pellets, Energy and Fuels 18 (4) (2004) 897–907. `doi:10.1021/ef030173k`.

[44] G. Habib, C. Venkataraman, T. C. Bond, J. J. Schauer, Chemical , Microphysical and Optical Properties of Primary Particles from the Combustion of Biomass Fuels, Environmental Science and Technology (2008) 8829–8834.

[45] T. C. Bond, D. G. Streets, K. F. Yarber, S. M. Nelson, J. H. Woo, Z. Klimont, A technology-based global inventory of black and organic carbon emissions from combustion, Journal of Geophysical Research D: Atmospheres 109 (14) (2004) 1–43. `doi:10.1029/2003JD003697`.

[46] G. Shen, S. Tao, S. Wei, Y. Zhang, R. Wang, B. Wang, W. Li, H. Shen, Y. Huang, Y. Chen, H. Chen, Y. Yang, W. Wang, W. Wei, X. Wang, W. Liu, X. Wang, S. L. Simonich, Reductions in emissions of carbonaceous particulate matter and polycyclic aromatic hydrocarbons from combustion of biomass pellets in comparison with raw fuel burning, Environmental Science and Technology 46 (11) (2012) 6409–6416. `doi:10.1021/es300369d`.

[47] J. Jetter, Y. Zhao, K. R. Smith, B. Khan, T. Yelverton, P. DeCarlo, M. D. Hays, Pollutant emissions and energy efficiency under controlled conditions for household biomass cookstoves and implications for metrics useful in setting international test standards, Environmental Science and Technology 46 (19) (2012) 10827–10834. `doi:10.1021/es301693f`.

[48] P. Arora, P. Das, S. Jain, V. V. N. Kishore, A laboratory based comparative study of Indian biomass cookstove testing protocol and Water Boiling Test, Energy for Sustainable Development 21 (1) (2014) 81–88. `doi:10.1016/j.esd.2014.06.001`.
URL `http://dx.doi.org/10.1016/j.esd.2014.06.001`

# Supporting Information:
# Feedstock Dependence of Emissions from Reverse Downdraft Gasifier Cookstove

Thomas Kirch[a,b,*], Paul R. Medwell[a,b], Cristian H. Birzer[a,b], Philip J. van Eyk[c]

[a]*School of Mechanical Engineering, The University of Adelaide, S.A. 5005, Australia*
[b]*Humanitarian and Development Solutions Initiative, The University of Adelaide, South Australia 5005, Australia*
[c]*School of Chemical Engineering, The University of Adelaide, S.A. 5005, Australia*

*Corresponding author
Email address:* `thomas.kirch@adelaide.edu.au` (Thomas Kirch )

### S1. S1 Materials and Methods

#### S1.1. S1.1 Particulate Measurements

As described in the paper the validity of the gaseous measurements at the measurement location has been numerically investigated and shown to be highly accurate in the current configuration [1]. The same cannot be assumed for the particulate measurements. Particulates may deposit on walls end bends of the exhaust hood. Further losses can be expected from impaction and diffusion on the baffles in the exhaust system. Sampling lines were kept as short as possible to minimise the associated losses.

#### S1.2. S1.2 Analysis

For the $PM_{2.5}$ emissions an estimation of the fraction of emissions released during shut-down is provided. This is calculated on the basis of the real-time PM measurements. The time step when the emissions increase substantially at the end of the process, was estimated, and the fraction of emissions released after this time time step was calculated.

### S2. S2 Results

Figure S1 presents the average nominal combustion efficiency (NCE) for all four fuels under investigation at various air supply rates, over the duration of the combustion process. In all configurations, transients at start-up and shut-down are apparent, while a continuous process is achieved in between those transients.

Lighting has previously been identified as a substantial source of emissions of incomplete combustion [2] and can be seen in the initial 500 s in all profiles, similar to Figure 2. Once a reaction front is formed in the solid fuel bed, it moves steadily downwards through the bed, releasing a continuous flow of combustible producer gas which is burned with high efficiency in all cases. Including transients, time weighted average NCE values $> 0.97$ are achieved for all fuels as presented in Table S1, demonstrating the high efficiency of the combustion process.

The highest performance can be noted when using WP as fuel. For fuel bed depths larger than one reactor diameter, time weighted average NCE values $> 0.99$ are achieved at all air supply rates. It can also be noticed in Figure S1(a) that the NCE increases over time. As it is more difficult to achieve complete combustion of tars than combustible gases, this reduction over time can be related to a decreasing tar content in the producer gas, similar to the $PM_{2.5}$ concentration in Figure 2.

For both manures, a high efficiency can be achieved at a low air supply, while it is lower at a high air supply rate. The influence of the high ash content of these fuels could lead to increasingly incomplete combustion. Although a lower NCE is achieved at high air supply rates for all fuels but WP, generally high average NCE values are recognised for all fuels, similar to those reported for pine pellets [3] and wood chips [4] burned in a comparable reactors. When comparing the presented results with those achieved with traditional stoves, using wood fuels and performing cooking tasks, higher values can be achieved here [5]. NCE values for all investigated fuels were within the range of a wide variety of stoves performing cooking tasks using only wood pellets as fuel, where transients, which generally lead to a reduction of the NCE, were not included [6]. Furthermore, all mean NCE values achieved here are higher than those reported not only for traditional stoves performing cooking tasks with wood, crop residues or dung as fuel, but also
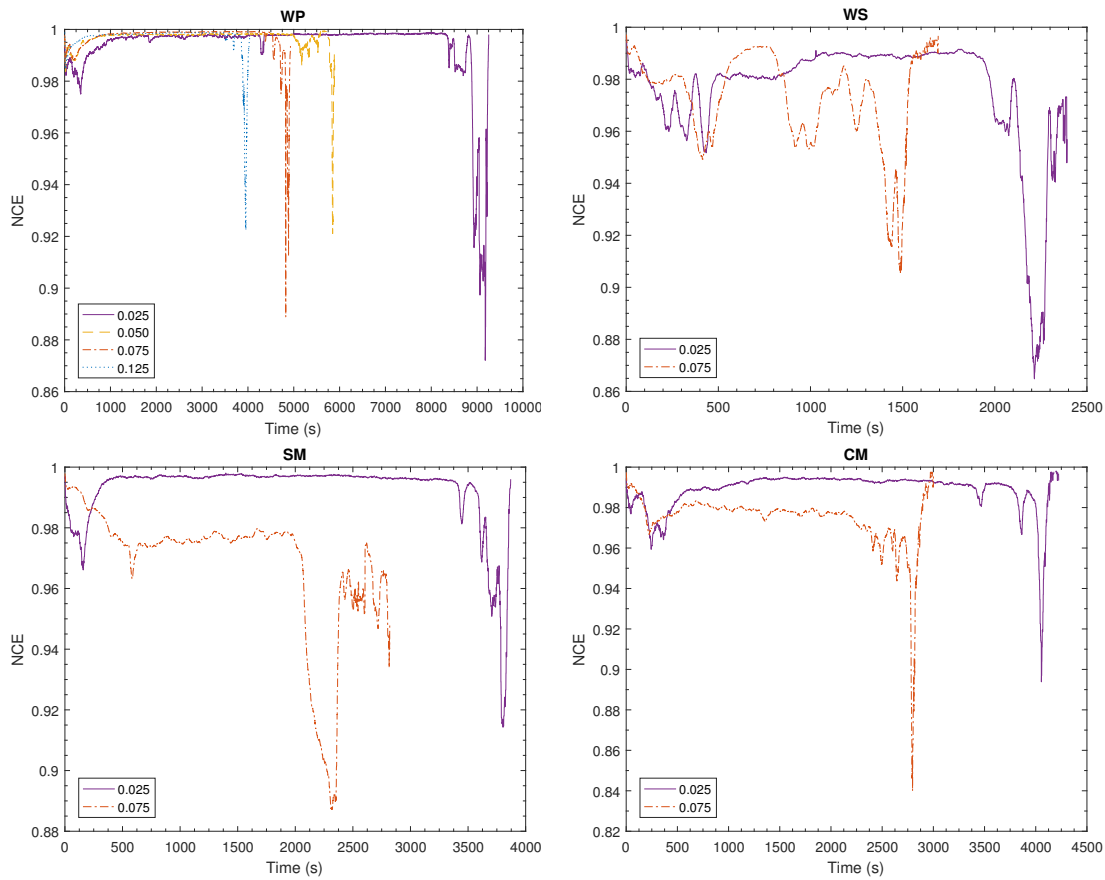
Figure S1: Temporal profiles of the nominal combustion efficiency (NCE = $CO_2$ / ($CO_2$ + CO)) are presented, for all fuels (a) wood pellets, (b) wheat straw, (c) sheep manure and (d) cow manure, with 4D fuel bed depth and the indicated air supply rates.

for an LPG burner [7]. These comparisons show that in the investigated reactor, high combustion efficiencies can be achieved even when non-woody biomass feedstock, WS, SM and CM, is utilised.

In Table S1 the approximate release of $PM_{2.5}$ during quenching is shown, based on the continuous measurements. It can be noticed that the impact of this transient is quite substantial but lower at higher air supply rates. It can also be seen that it is especially influential in the case of WS and SM, and for CM only at low air supply. In application, these emissions could be avoided by initially covering the combustion system with a lid before adding sufficient water for quenching. Therefore, it must be considered that in application lower emissions than presented here could ideally be achieved.

Table S1: Accumulated results for all tested configurations. Configuration parameters, fuel type, fuel bed depth and the primary air supply are provided. Furthermore, average results for the heat released, the NCE, as well as the emissions of CO and PM are presented.

| Fuel Type | Bed Depth (mm) | Primary Air (kg·m⁻²·s⁻¹) | Heat Release (W) | NCE (-) | CO mg·MJr | CO mg·kgc | PM$_{2.5}$ mg·MJr | PM$_{2.5}$ mg·kgc | PM$_{2.5}$ End (%) | PM$_{Total}$ mg·MJr | PM$_{Total}$ mg·kgc |
|---|---|---|---|---|---|---|---|---|---|---|---|
| Wood Pellets | 100 | 0.025 | 3760 ± 19 | 0.987 ± 0.017 | 555.4 ± 11.1 | 6245.5 ± 94.1 | 26.3 ± 8.8 | 364.1 ± 121.7 | 38.0 | 28.5 ± 15.9 | 395.0 ± 219.7 |
| | 100 | 0.050 | 4309 ± 10 | 0.993 ± 0.005 | 485.3 ± 41.0 | 6091.6 ± 506.3 | 12.4 ± 3.1 | 185.3 ± 46.5 | 12.9 | 25.0 ± 12.5 | 371.6 ± 186.1 |
| | 100 | 0.075 | 6142 ± 25 | 0.990 ± 0.009 | 407.4 ± 83.0 | 5374.2 ± 1100.2 | 20.0 ± 6.0 | 370.5 ± 67.9 | 33.6 | 39.6 ± 18.1 | 728.5 ± 268.0 |
| | 100 | 0.125 | 6544 ± 75 | 0.995 ± 0.004 | 275.5 ± 44.8 | 3765.5 ± 615.2 | 15.1 ± 5.7 | 234.3 ± 88.6 | 18.1 | 54.2 ± 27.2 | 842.6 ± 421.4 |
| | 200 | 0.075 | 6518 ± 46 | 0.994 ± 0.004 | 314.1 ± 25.2 | 4184.8 ± 353.7 | 8.1 ± 1.4 | 125.8 ± 22.1 | 5.4 | 12.8 ± 3.4 | 198.9 ± 51.9 |
| | 300 | 0.075 | 6542 ± 8 | 0.996 ± 0.004 | 180.2 ± 9.5 | 2353.1 ± 124.8 | 5.5 ± 1.4 | 83.5 ± 20.9 | 6.6 | 6.8 ± 2.7 | 104.0 ± 41.4 |
| | 400 | 0.025 | 3148 ± 8 | 0.994 ± 0.006 | 312.4 ± 24.9 | 3440.4 ± 273.9 | 5.8 ± 1.9 | 81.2 ± 26.5 | 26.0 | 9.4 ± 4.9 | 130.8 ± 68.1 |
| | 400 | 0.050 | 5201 ± 48 | 0.997 ± 0.002 | 216.3 ± 41.9 | 2642.6 ± 498.1 | 4.3 ± 1.2 | 63.7 ± 17.7 | 10.6 | 9.5 ± 2.4 | 140.2 ± 36.3 |
| | 400 | 0.075 | 6462 ± 33 | 0.997 ± 0.003 | 241.5 ± 57.7 | 3116.0 ± 735.5 | 7.4 ± 1.2 | 113.9 ± 18.5 | 7.2 | 7.8 ± 2.6 | 119.7 ± 40.6 |
| | 400 | 0.125 | 8417 ± 76 | 0.997 ± 0.003 | 243.5 ± 35.8 | 3464.4 ± 487.8 | 8.8 ± 2.9 | 141.4 ± 46.9 | 4.1 | 19.4 ± 4.8 | 312.1 ± 77.9 |
| Wheat Straw | 400 | 0.025 | 2403 ± 71 | 0.976 ± 0.012 | 1706.5 ± 207.6 | 15592.5 ± 1594.2 | 21.4 ± 0.6 | 288.0 ± 5.0 | 71.8 | 132.0 ± 57.1 | 1770.3 ± 751.1 |
| | 400 | 0.075 | 4511 ± 57 | 0.973 ± 0.009 | 2118.7 ± 617.8 | 25408.8 ± 7473.1 | 63.9 ± 7.3 | 1011.4 ± 114.8 | 28.4 | 237.1 ± 27.3 | 3751.9 ± 436.2 |
| Sheep Manure | 400 | 0.025 | 2297 ± 168 | 0.993 ± 0.006 | 473.8 ± 38.2 | 4109.8 ± 267.7 | 20.8 ± 4.3 | 332.1 ± 68.9 | 72.2 | 63.9 ± 20.6 | 1037.8 ± 380.6 |
| | 400 | 0.000 | 5214 ± 0 | 0.968 ± 0.008 | 2635.6 ± 500.5 | 35844.0 ± 6806.2 | 201.3 ± 46.0 | 4057.6 ± 887.6 | - | 405.7 ± 78.4 | 8081.8 ± 1638.3 |
| Cow Manure | 400 | 0.025 | 1985 ± 73 | 0.989 ± 0.006 | 864.4 ± 41.9 | 6497.5 ± 352.8 | 29.6 ± 10.1 | 442.3 ± 150.2 | 49.1 | 58.1 ± 4.1 | 871.9 ± 64.0 |
| | 400 | 0.075 | 3731 ± 83 | 0.975 ± 0.007 | 2047.3 ± 466.4 | 22443.4 ± 5137.0 | 349.1 ± 79.1 | 6130.4 ± 1432.5 | 8.9 | 497.1 ± 86.3 | 8716.3 ± 1574.5 |

[1] T. Kirch, M. J. Evans, P. R. Medwell, V. H. Rapp, C. H. Birzer, A. J. Gadgil, Mixing uniformity of emissions for point-wise measurements in exhaust ducts, Proceedings of the 21st Australasian Fluid Mechanics Conference (December).

[2] P. Arora, P. Das, S. Jain, V. V. N. Kishore, A laboratory based comparative study of Indian biomass cookstove testing protocol and Water Boiling Test, Energy for Sustainable Development 21 (1) (2014) 81–88. `doi:10.1016/j.esd.2014.06.001`.
URL `http://dx.doi.org/10.1016/j.esd.2014.06.001`

[3] G. Shen, S. Tao, S. Wei, Y. Zhang, R. Wang, B. Wang, W. Li, H. Shen, Y. Huang, Y. Chen, H. Chen, Y. Yang, W. Wang, W. Wei, X. Wang, W. Liu, X. Wang, S. L. Simonich, Reductions in emissions of carbonaceous particulate matter and polycyclic aromatic hydrocarbons from combustion of biomass pellets in comparison with raw fuel burning, Environmental Science and Technology 46 (11) (2012) 6409–6416. `doi:10.1021/es300369d`.

[4] T. Kirch, P. R. Medwell, C. H. Birzer, Natural draft and forced primary air combustion properties of a top-lit up-draft research furnace, Biomass and Bioenergy 91 (2016) 108–115. `doi:10.1016/j.biombioe.2016.05.003`.
URL `http://dx.doi.org/10.1016/j.biombioe.2016.05.003`

[5] M. Johnson, R. Edwards, V. Berrueta, O. Masera, New approaches to performance testing of improved cookstoves, Environmental Science and Technology 44 (1) (2010) 368–374. `doi:10.1021/es9013294`.

[6] C. L'Orange, J. Volckens, M. DeFoort, Influence of stove type and cooking pot temperature on particulate matter emissions from biomass cook stoves, Energy for Sustainable Development 16 (4) (2012) 448–455. `doi:10.1016/j.esd.2012.08.008`.
URL `http://dx.doi.org/10.1016/j.esd.2012.08.008`

[7] K. R. Smith, R. Uma, V. V. N. Kishore, K. Lata, V. Joshi, J. Zhang, R. Rasmussen, M. Khalil, Greenhouse gases from small-scale combustion devices in developing countries: Phase IIA; Household Stoves in India, Tech. rep., United States Environmental Protection Agency, Washington (2000). `doi:EPA-600/R-00-052`.

# Chapter 8

## Conclusions

## 8.1 Summary

This thesis investigated various aspects of the staged combustion process in gasifier cookstoves. Specifically designed research reactors were utilised to enable controlled air supplies of primary air to the fuel bed and secondary air downstream of the fuel bed, to the released products from the conversion process. Experimental facilities were developed for the measurement of products from the thermochemical conversion of the solid fuel, as well as from the secondary combustion process. The experimental work, presented in four independent research articles, contributes to our understanding of: the mode of air supply, in particular, via natural or forced draft; the relationship between the staged air supply, of primary to secondary air and the relative locations thereof; the fuel bed height; and the utilisation of a variety of fuels, with a wide range of ash contents. Specific attention has been paid to the overall combustion process and, in isolation, to the thermochemical conversion processes of the solid fuel and the oxidation of the released products in the secondary combustion region. The combined generation of heat and biochar is a central focus of this work and this should also be applicable to research more widely in the field.

## 8.2 Main Findings

An investigation of the mode of air supply found that providing a forced rather than natural draft air supply achieves a more steady and more efficient combustion process. Especially at start-up, it appears that a steady forced flow has beneficial implications for the release of emissions of incomplete combustion. When relying on a natural, buoyancy driven flow in the stove, initially temperature and thus density gradients are low, resulting in a low gas flow, which could be the cause of insufficient air supply to the igniting fuel. Different air supply requirements have been identified for the three subsequent phases of lighting, steady-state combustion

and char combustion, if the entire fuel is oxidised. In particular, high air requirements have been found for the conversion and efficient combustion of char in gasifier stoves. In the secondary combustion region, fuel lean conditions must be achieved for efficient combustion and a ratio of the primary to the secondary air supply of 1:4 has been found to provide these conditions. Furthermore, an increasing distance between the top of the fuel bed and the secondary combustion region reduces the efficiency of the combustion process, due to heat loss of the combustible gases. Therefore, an adjustable fuel grate, to adapt the depth of the fuel bed to the amount of fuel necessary for a specific cooking task, is suggested.

When focusing on the thermochemical conversion process within the fuel bed it was found that at low air supply rates to the fuel bed, substantial amounts of tars and char are produced, as expected. When increasing the air supply the fuel conversion is accelerated, leading to greater heat release and higher peak temperatures. However, the increase in fuel consumption is less severe when fuels with increasing ash contents are being utilised. Although generally higher reaction front temperatures are achieved when increasing the air supply, the peak reaction front temperature at a specific air supply rate may be related to the fuel bulk density. Higher reaction temperatures in the bed cause a reduction in tar and char yields, while greater amounts of gases, especially $H_2$, are released. This leads to an apparently feedstock-independent, nearly linear increase in the cold gas efficiencies, with higher peak reaction front temperatures. The conversion of tars to form gases can also be enhanced through the influence of the produced char. By increasing the fuel bed depth, for wood pellets in particular, tars released in the reaction front can decompose to form gases when passing through the layer of char at elevated temperatures. Greater fuel bed depths also reduce the impact of transients where the fuel conversion is less efficient. For manures, increasing the air supply leads to a more severe reduction in the conversion of fuel carbon to form char, when compared with wheat straw or wood pellets. With decreasing carbon and increasing ash content in

the char, the solid structure becomes less stable. Initially, ash appears liberated at the surface of the char particle. When there are further increases to the air supply, the ash becomes exposed to high temperatures, which leads to melting and fusing. Ash melting in the fuel bed is detrimental to the process. By limiting the air supply, the peak fuel bed temperature and the char consumption are restricted, and thus ash melting can be avoided. From all the investigated fuels, the produced biochars were found to be of highest classification. This was based on analyses of their elemental composition and evaluation, conforming to international guidelines.

The emissions from the producer gas combustion process downstream of the solid fuel bed were found to be relatively independent of variations in the combustible gas contents. Rather, they appear to be influenced by ash constituents. Although ash constituents were not specifically measured, clear trends in the emissions profiles from the tested fuels and observations of the produced chars enable deductions of their potential influence. For the low ash content wood pellets, a reduction in emissions of incomplete combustion can be related to the tar content in the producer gas. This impact is overshadowed by other mechanisms for higher ash content fuels, presumably that of the ash constituents. The influence of ash becomes apparent at high air supply rates, where little carbon remains in the solid char bed after conversion and the ash becomes liberated at the char particle surface, as described in the previous paragraph. Liberated ash can then be entrained by the surrounding gas flow. Increasing fuel bed temperatures will also lead to greater devolatilisation of certain ash constituents. Ash constituents present in the secondary combustion region may influence the combustion chemistry. At low air supply rates, where a larger fraction of ash constituents remains in the solid char, very high combustion efficiencies and low CO and PM emissions can be achieved for all the fuels investigated here. The substantial benefit of low air supply rates and moderate conversion temperatures needs to be highlighted.

## 8.3   Overall Conclusions

In each study of this thesis, the benefit of the combined production of char and producer gas in gasifier stoves is apparent. In Chapter 4 it is shown that even when utilising a forced air supply, where relatively clean combustion is achieved, the conversion and combustion of the char may lead to inefficiencies. These inefficiencies lead to the release of vast amounts of CO from gasifier stoves, due to incomplete combustion during the char combustion phase. Chapter 5 presents the influence of the char downstream of the reaction front on the conversion of tars and concludes that higher conversion to combustible gases, rather than tars, can be achieved. In Chapter 7, this conversion to combustible gases is found to reduce emissions of incomplete combustion. In Chapter 6 the production of char from high ash content fuels then avoids ash melting and fusing in the system. This is beneficial as ash melting has exhibited detrimental effects on the process performance and feasibility. Furthermore, the devolatilisation and entrainment of ash constituents is suggested in Chapter 7 to affect the combustion process substantially. An intact char body produced at low air supply rates and with moderate conversion temperatures may retain most of the ash. The retention of ash could be the reason for the very low emissions of CO and PM from the system, in comparison with similar devices. These findings combined show the great potential for emissions reductions, especially for the utilisation of high ash content fuels, due to char production. Furthermore, it is established that when producing char, even low value agricultural residues and manures can be combusted nearly as cleanly as high quality wood pellets under controlled conditions in gasifier stoves.

It has been confirmed that a substantial fraction of the emissions of incomplete combustion are released during transient events, at (1) start-up and (2) shut-down, or (3) during the combustion of the produced char. Here, it has been shown that a substantial mitigation of the release of pollutants can be achieved, by providing

sufficient air at start-up, via a forced air supply and by producing char as a solid product. Furthermore, it can be deduced that by quenching the process in an enclosed container further emissions reduction, particularly those of PM, could be achieved during shut-down.

## 8.4 Future work

In this thesis it has been shown that very low emissions from gasifier stoves can be achieved through the provision of certain controlled conditions. However, a further reduction is desired to achieve environmental as well as human health benefits. Significant work will be necessary to establish mechanisms that enable further reductions in pollutant emissions.

It has been shown that a forced air supply can reduce the emissions from the combustion process in gasifier stoves. Different air requirements have been identified for the three subsequent combustion phases, but here only constant air supply rates were investigated. The implementation and impact of a variable air control throughout the combustion processes, potentially automated, could be beneficial and worthy of investigative effort.

To enable a more in-depth understanding and potentially representative modelling of the secondary combustion process in gasifier stoves, a more detailed description of the products of the thermochemical conversion process would be beneficial. While the gaseous and solid products are analysed in this thesis, an investigation of the specific constituents of released tars could provide more detailed information again. Here, indications were found that cracking of tars in the char layer downstream of the fuel bed, which has been shown to occur for wood pellets as fuel, might be inhibited in higher ash content biomass fuels. The mechanisms that lead to tar conversion in gasifier stoves need further consideration.

Addressing the fate of fuel ash constituents is also a topic worthy of further work.

An investigation into the contribution of ash constituents to the PM emissions, potentially for specific particle sizes, would be beneficial. Simultaneously, a detailed analysis of the ash composition of the initial fuel and the produced char could enable an overall ash balance for the process. This could be followed by a more detailed discussion of measures that can achieve a reduction in the contribution of ash constituents to the PM emissions. As shown here, increasing the air supply, causes a reduction in the carbon content of the produced char and may lead to the liberation of ash constituents from the char particle surface. The potential limits of, for example, a minimum carbon content in the char, a maximum conversion temperature or a maximum superficial gas velocity in the fuel bed to reduce the influence of entrainment and devolatilisation of ash constituents, could be of significant interest in moving forward to optimised gasifier stove designs. Furthermore, a cold char bed in between the solid fuel bed and the secondary combustion region, to facilitate tar and ash deposition could be advantageous.

The benefit of the combined production of producer gas and char, in terms of pollutant emissions, has been demonstrated in the present thesis. From a user perspective, this is not necessarily a primary desire, as large amounts of the fuel's energy is being retained in the char, therefore users will need more fuel when producing char. Thus, clear incentives for users to produce char will certainly be necessary for this technology to be utilised and to achieve user acceptance.

This page intentionally left mostly blank.

# Appendix A

---

# Natural Draft and Forced Primary Air Combustion Properties of a Top-Lit Up-Draft Research Furnace

---

Research paper

# Natural draft and forced primary air combustion properties of a top-lit up-draft research furnace

Thomas Kirch[*], Paul R. Medwell, Cristian H. Birzer

*School of Mechanical Engineering, The University of Adelaide, S.A. 5005, Australia*

## ABSTRACT

Worldwide, over four million people die each year due to emissions from cookstoves. To address this problem, advanced cookstoves are being developed, with one system, called a top-lit up-draft (TLUD) gasifier stove, showing particular potential in reducing the production of harmful emissions. A novel research furnace analogy of a TLUD gasifier stove has been designed to study the TLUD combustion process. A commissioning procedure was established under natural draft and forced primary air conditions. A visual assessment was performed and the temperature and emissions profiles were recorded to identify the combustion phases. The efficiency was evaluated through the nominal combustion efficiency (NCE = $CO_2/(CO_2 + CO)$), which is very high in the migrating pyrolysis phase, averaging 0.9965 for the natural draft case. Forced primary air flows yield similar efficiencies. In the lighting phase and char gasification phase the NCE falls to 0.8404 and 0.6572 respectively in the natural draft case. When providing forced primary air flows, higher NCE values are achieved with higher air flows in the lighting phase, while with lower air flows in the char gasification phase. In the natural draft case high $H_2$ emissions are also found in the lighting and char gasification phases, the latter indicating incomplete pyrolysis. From the comparison of the natural draft with the forced draft configurations, it is evident that high efficiency and low emissions of incomplete combustion can only be achieved with high controllability of the air flow in the different phases of combustion.

© 2016 Elsevier Ltd. All rights reserved.

## 1. Introduction

Energy consumption in private households in developing countries is still primarily based on biomass fuels. This directly affects 2.7 billion people [1] who rely on traditional cooking methods, which typically have a very low efficiency and produce harmful emissions through incomplete combustion. This results in approximately 4.3 million premature deaths worldwide each year from cooking-related illnesses caused by household air pollution [2]. In order to achieve substantial health benefits, cleaner burning cookstoves than are currently in widespread use are needed [3,4]. One type of cookstove that has been recognised as potentially able to achieve this goal are "gasifier" stoves [5]. These stoves force volatile gases out of a solid fuel and burn them separately from the solid body [6]. This can reduce harmful emission production; however, there is a lack of scientific understanding to enable stove optimisation.

Gasifier cookstoves can be distinguished by the direction of the gasification air. Available designs of cookstoves use either updraft, downdraft or inverted downdraft, also called top-lit up-draft (TLUD), flow [7]. A TLUD stove is investigated in this study. To operate as a TLUD, the stove is filled with batches of fuel and lit from the top. Firstly, the top layer of biomass is ignited, typically by a kindling material, before a pyrolytic front forms, which moves downwards, opposite to the gas flow, through the fuel-stack, as illustrated in Fig. 1. In the enclosed space of the stove, the oxygen is quickly consumed in the oxidation process of the lighting phase. The heat released from the top layer causes lower layers to pyrolyse, which means that volatile matter is released from the fuel in an inert atmosphere [8]. This process is called a migrating pyrolytic front [9], which moves, in relation to the primary air, down the fuel-stack [10]. The pyrolysis products are liquids (water, heavier hydrocarbons, and tars), gases (such as CO, $CO_2$, or $CH_4$) and solid char [11]. The pyrolytic front is sustained by simultaneous gasification, in which the pyrolysis products can partially oxidise with the primary air into gases (CO, $CO_2$, $H_2$ and lesser quantities of
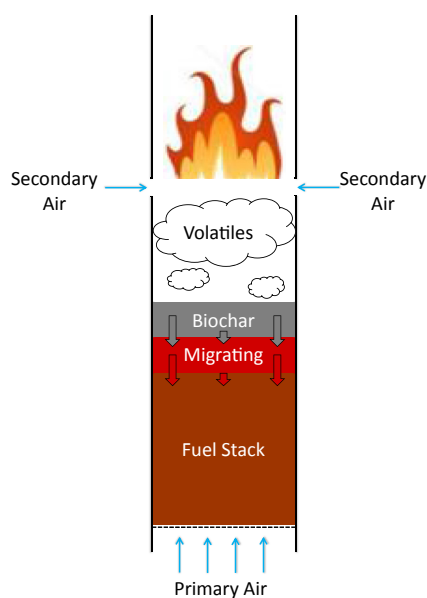
**Fig. 1.** Schematic diagram of TLUD operation.

hydrocarbon gases) [12]. In inverted downdraft gasifiers, heavier hydrocarbons and the liquid tar can crack into lighter components as they move through the high temperature zone of the char layer [10,13]. This process is highly complex, in part due to the thin char layer [14], and therefore the scientific understanding of these reactions in TLUD stoves is limited. Greater scientific understanding of the tar cracking processes for TLUD stoves is needed to ensure optimisation of systems in terms of emissions production.

The combustible pyrolysis products leave the fuel-stack at temperatures of $\approx 600\,^\circ$C [15], and are mainly composed of CO, $H_2$, $CH_4$ and some heavier hydrocarbons ($C_xH_y$) [16]. Once these gases reach the secondary air inlet, they are mixed with air and can be combusted if an ignition source is present, as shown in Fig. 1. As a result of gas-combustion and compared with other cookstoves, gasifier stoves have been shown to produce low CO and particulate matter (PM) emissions under laboratory conditions [17,18]. It has been shown that variations in the stove geometry and the utilized fuel have a significant impact on the stove's performance [19,20]. It has been observed that the heat transfer, to a vessel on the stove, is a strong function of the vessel diameter, while swirl of secondary air has a negligible impact [14]. It is clear that the design of the stove to optimise gas production for combustion, and for subsequent heat transfer are limited.

From the pyrolysis processes, char remains as a solid product. The char yield is mainly dependent on the superficial velocity, which is determined by the gas flow over the cross-sectional area [10] and the moisture content of the biomass [21,22]. This char can be further gasified and combusted in the stove or, if no further air is supplied and the oxidation process is quenched, it can be collected. If collected, the char can be used as either fuel or as a soil amendment (termed biochar). When using it as a soil amendment, the whole process could be seen as a mechanism for carbon sequestration [19,23]. If the quenching process is not conducted early enough, the char can continue to burn, producing high levels of harmful emissions, as well as produce ash, which cannot be used as a solid enhancer. It is therefore necessary to further develop the understanding of quenching of char for subsequent use, or for improved combustion in a process beneficial to the end user.

Uncertainty in the existing results is exacerbated by the influence of different standardised tests and kindling materials on the

performance of TLUD cookstoves. Arora et al. assessed different test protocols, and determined that, for given conditions, the emissions factors, (primarily of CO and PM), varied leading to differences in the cookstove performance. Wood, mustard stalks and kerosene were tested as kindling materials and it was observed that CO peaks would increase with lower calorific values of the kindling materials [24]. All of these studies have evaluated specific designs and analysed their performance while performing cooking tasks.

The previous paragraphs show that there are many gaps in scientific understanding of basic TLUD operation and design. These unknowns are extended when considering various fuel types and fuel quantities. Additionally, it is also known that these stoves can be used under natural draft conditions or with the assistance of a fan that creates a forced airflow. Altering the available flow rates can be beneficial, or detrimental, to the combustion processes. How these modifications influence the heat transfer, emissions production and burn rates are all crucial in development improved cookstoves and thus helping increase the quality of life for billions of people. However, much of the research has been conducted on stoves that do not allow for modification of these aspects. It is for this reason that a TLUD analogous furnace has been developed to allow for systematic studies of TLUD combustion. What is not completely known is how accurate the analogy is across all aspects of TLUD stove design.

The aim of the current paper is to present results from commissioning a TLUD analogy furnace and determine if forced draft flows can be used to simulate natural draft. Specifically, the study includes analysis of emissions and temperature profiles in natural draft as well as forced primary air TLUD operation, in order to characterise, understand and evaluate subsequent combustion processes.

## 2. Materials and methods

The research furnace, previously presented in Kirch et al. [25], was revised as a TLUD stove with the general characteristics of a primary air inlet at the bottom of the furnace, and a lateral secondary air inlet in the upper region. The furnace's dimensions were chosen to be larger than most extant commercial products and stoves in order to address scaling issues and achieve greater variability of the adjustable parameters. The furnace enables various combustion-relevant parameters to be controlled. The increased size of the research furnace allows the amount and location of the fuel to be widely altered which in turn permits the scaling from use in private households to use in communal kitchens to be studied, although this is outside the scope of the present study. The principal components of the research furnace are a stove body, a primary air inlet chamber and a secondary air inlet stove extension, which are shown in Fig. 2.

### 2.1. The TLUD research furnace

The central component of the research furnace is a 600-mm-tall steel cylinder with an inner diameter of 206 mm and 8 mm wall thickness, illustrated in Fig. 2. Inside the stove body, a grate is located, which holds the fuel-stack in place. The circular grate is perforated with 3-mm-diameter holes, with 26% open-area ratio. This allows air from beneath the grate to enter the fuel-stack. The fuel grate is located 420 mm below the top of the stove body and is easily removable for post-combustion analysis of the solid residual matter, as well as cleaning. The steel cylinder, in combination with the fuel grate, forms the stove body. It is placed on top of a steel frame that serves as the primary air inlet chamber.

The steel frame of the primary air inlet chamber has the following dimensions: 248 mm $\times$ 248 mm $\times$ 150 mm
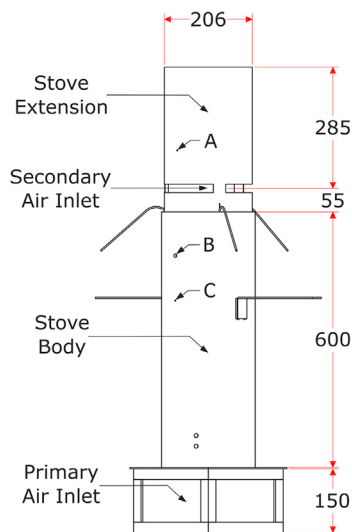
**Fig. 2.** Schematic TLUD research furnace configuration for natural draft conditions (all measurements in millimetres).



**Fig. 3.** Data collection set-up of the TLUD research furnace.

(length × width × height). The frame allows all sides to be closed off, so that air can be applied through only one inlet. The inlet can be connected to compressed air and the airflow is controlled by a needle valve and a rotameter. If the sides are not closed off, air enters freely.

The secondary air inlet is provided by a detachable stove extension to the top of the stove body. This extends the furnace height by 340 mm and is equipped with three 20 mm wide and 190 mm long lateral air inlets. The centre line of the air inlets is situated 55 mm above the top of the stove body as shown in Fig. 2. In all the tested configurations the secondary air inlets are unobstructed which allows secondary air to enter via natural draft induced by buoyancy.

### 2.2. Set-up of the data collection

Emissions data were collected at one central location while the temperature data were constantly measured at two locations. For emissions testing, the research furnace was placed under a hood, which was, in turn, attached to an extraction duct and a fan. The measuring probe of a Testo 350XL gas analyser was placed in the centre of the fume hood inlet at a distance of 830 mm above the exit plane of the research furnace extension, as presented in Fig. 3. The probe is located in the centre of the collection area of the fume hood and thus in the focus point of the emissions from the stove. The Testo 350XL was used to record the CO, $CO_2$ and $H_2$ concentrations at an interval of 1 Hz, on a dry basis. The resolution was 1 ppm for low emission levels (<2000 ppm) and 5 ppm for high emission levels (>2000 ppm) of CO measurements. The resolution for $CO_2$ measurements was 0.01%.

A normalisation process was performed for all the gathered emissions concentrations. This was necessary because the quantitative measurements were taken at a location of 830 mm above the stove, where flue gas from the combustion process is mixed with the surrounding air. The emissions data are related to the sum of all carbon emissions, here CO and $CO_2$. Other carbon-containing species were below the detection limits of the apparatus. Various emissions are each normalised with respect to the sum of the carbon emissions, because these can be attributed to the combustion process and provide the key relationship between the intensity of the combustion process and the release of certain products.
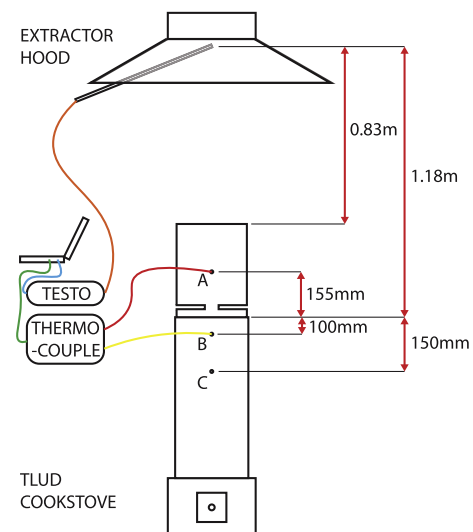
The temperature data were collected constantly via two K-type thermocouples, at locations A and B, and, when needed, via an infra-red thermometer at location C on the outer surface of the stove body. Both thermocouples were positioned in the centre of the stove body, as illustrated in Fig. 3. Location A, above the secondary air inlet, was chosen because it is expected to detect high temperatures when pyrolysis products burn with the secondary air inside the stove extension. The thermocouple at location B, in the stove body, is closer to the fuel-stack. Therefore it can capture when combustion occurs at the fuel-stack and can measure the temperature of the pyrolysis products during the migrating pyrolysis phase. The infra-red thermometer is used to measure the outside wall temperature of the stove, which is needed for the testing procedure, presented in Section 2.3.

### 2.3. The commissioning process

A testing procedure was established for the research furnace. To account for the influence of the thermal mass of the research furnace, with its wall thickness of 8 mm, on the combustion performance, it was ensured that the furnace is either pre-heated, or starts cold. For each test, a batch of 700 g of fuel was placed on the fuel grate and evenly distributed to achieve a level surface. The furnace was run once to pre-heat. Then for the pre-heated tests, which are presented here, the furnace was re-fuelled when the outer wall temperature at location C (see Fig. 3) reached 150 °C. As kindling material, approximately 5 mL of methylated spirits (96% ethanol) was poured evenly over the fuel. When the outer wall temperature at location C measured 135 °C a lit paper towel (approximately 190 mm × 100 mm) was dropped into the furnace to ignite the kindling material. The initial temperatures were chosen for the commissioning process to prevent volatilisation in the fuel, which starts at approximately 200 °C [26]. Data were recorded until only ash was left on the fuel grate. This meant that the biochar, as the solid pyrolytic product, was also gasified in order to obtain emissions data of all combustion phases.

Natural draft as well as various forced draft primary air flow configurations were tested in the present study. For the natural draft case, all sides of the primary air inlet chamber were open, as shown in Fig. 2 and air could enter the furnace freely. In the forced draft configuration, the sides of the primary air inlet chamber were closed off and controlled air flows of 0.048, 0.059, 0.071 and

0.083 kg m$^{-2}$ s$^{-1}$ respectively, were introduced into the furnace from the start of each test, as presented in Table 1. These air flow values were chosen as they should provide an oxygen-limited environment for the migrating pyrolysis, in accordance with previous studies on fixed bed reactors [27—31]. The same testing procedure was used for the natural draft and forced primary air configurations.

## 2.4. The tested fuel

The fuel for each test consisted of Radiata Pine (*Pinus radiata*) wood chips obtained, in 2014, from various locations across the Mt Lofty ranges of South Australia. They were sourced in-bulk, as pre-chipped material, and sieved through a 25 mm aperture, resulting in an average particle size of 24 mm × 8 mm × 3 mm (length × width × height). The bulk density of the fuel is approximately 210 kg m$^{-3}$. To avoid the influence of the wood chips' differing moisture content on the burning rate and the emissions [21], all the chips were dried to achieve a uniform moisture content throughout testing. This was done by keeping them for 16 h in a confined space at a constant temperature of 37 °C, created by an air conditioning unit. The drying process resulted in a fuel moisture content of approximately 7%, as determined by the American Society for Testing and Materials (ASTM) D4442-92(2003) standard procedure [32].

## 3. Results

Preliminary results were gathered through visual assessment. In further tests, emissions and temperature profiles were also recorded. By relating all the findings (visual, emissions and temperature measurements) to one another, a full picture of the process can be drawn.

### 3.1. Visual assessment

For the visual assessment, the stove extension was not connected to the stove body. This meant that the gasification products were burned as a non-premixed jet flame, issuing from the stove body into the surrounding air, which could, in turn, be observed without obstruction. Visual assessment is a powerful tool, especially for on-site use where other tools might not be available. Here it is applied to present and discuss visual indicators that can be observed in TLUD combustion. The key features are illustrated in Fig. 4.

After lighting, combustion takes place directly at the fuel-stack. This can be seen by flames spreading from the kindling material over the surface of the biomass. Once the upper layer of the fuel-stack is ignited, the temperature increases and small amounts of smoke start to be released, which can be seen in Fig. 4 (a). This suggests that the remaining water in the fuel evaporates and volatile compounds are released from the fuel.

A change can be observed once thick white smoke is released from the fuel-stack, as shown in Fig. 4 (b). The thick smoke is subsequently ignited and clean-burning, as displayed in Fig. 4 (c).

**Table 1**
Air flow and repetitions of the different test configurations.

|  | Repetitions | Primary air flow (kg m$^{-2}$ s$^{-1}$) |
|---|---|---|
| Natural draft | 8 | Natural draft |
| Varying primary air | 5 | 0.0472 |
|  | 4 | 0.0590 |
|  | 6 | 0.0708 |
|  | 6 | 0.0826 |

This indicates that a second phase, termed migrating pyrolysis, has begun. In the transition period from the lighting phase to the migrating pyrolysis, increasingly volatile compounds and the remaining moisture are released from the fuel, observable as thick white smoke. This thick white smoke was especially prominent in some cold start tests, where it was observed that the flames on top of the fuel-stack would not ignite a flame at the top of the stove body without an external influence (i.e. it was necessary to light manually), as is presented in the supplementary material. Supplementary video related to this article can be found at http://dx.doi.org/10.1016/j.biombioe.2016.05.003.

Once the volatile compounds are ignited, a bright yellow flame establishes that burns very cleanly, as shown in Fig. 4 (c). Above the flame, no smoke can be visually observed. The separation between the migrating pyrolysis taking place in the fuel-stack and the pyrolytic products being burned separately in time and location, at the secondary air inlet, is a distinctive characteristic of TLUD stoves [33]. The black char that can be seen on the fuel grate, while the bright yellow flame is present at the top of the stove body, reveals this separation.

The extinction of the flame at the secondary air inlet indicates the end of the migrating pyrolysis phase and the onset of char gasification. This phase begins because insufficient combustible gases are released from the fuel-stack to sustain the flame at the secondary air inlet. Although not presented, during testing, it could be seen that hot glowing char is left on the fuel grate, with small irregular flames above the char bed. If no more air were supplied or the process were quenched, the biochar, could be collected, as displayed in Fig. 4 (d). For the purposes of this research, however, the measurements and assessment of the emissions of the char gasification process are desired. Therefore the process is not ended, and it can be seen that the amount of hot glowing char decreases until only ash remains on the fuel grate.

### 3.2. Normalisation and mathematical phase separation

As described in Section 2.2, all emissions profiles were normalised to account for the influence of test-specific ambient conditions. This included the calculation of the so-called nominal combustion efficiency (NCE), which is defined as $CO_2/(CO + CO_2)$ [17]. The NCE is a key indicator of the stove's efficiency because it displays the proportion of products of complete combustion over the overall carbon emissions. Therefore the higher the NCE, the cleaner and more efficient the burning process.

Three phases can be identified in each of the four profiles presented in Fig. 5. The three phases are the lighting phase, the migrating pyrolysis phase and the char gasification phase. A mathematical separation of these three phases was performed. The combustion process in each phase is different and thus it is important to generate independent averaged data. A change in phase was identified when the temporal derivative of the normalised CO profile exceeded 0.002 s$^{-1}$. This value was determined following a rigorous verification based on inspection of the profiles and was found to be reliable at identifying each phase. To account for the differences in the combustion behaviour, with steady emissions profiles in the migrating pyrolysis phase as opposed to peak values in the lighting phase and multiple peaks in the char gasification phase, peak values as well as time-weighted-average (TWA) values are calculated. The average peak values were calculated for the lighting phase and the average TWA for the migrating pyrolysis phase. For the char gasification phase, average peak values, as well as average TWA values, were calculated. Table 2 presents the results of the above mentioned calculations with the standard deviation in parentheses underneath.
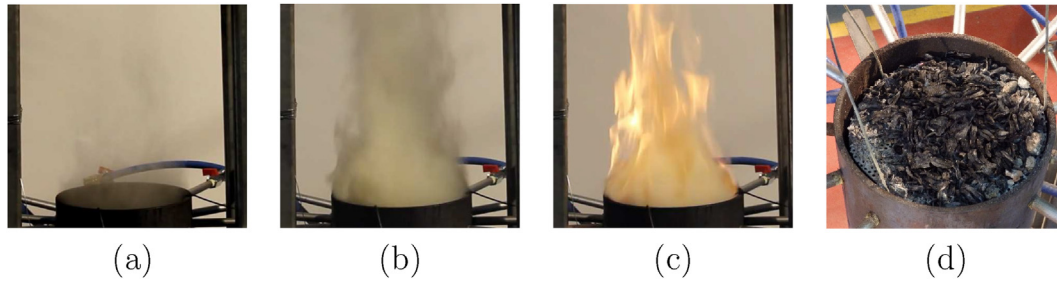
**Fig. 4.** Visual assessment: (a) smoke starts to be released, (b) thick smoke rising from fuel-stack prior to ignition of gaseous products, (c) combustion of volatiles after mixing with secondary air, (d) remaining biochar.
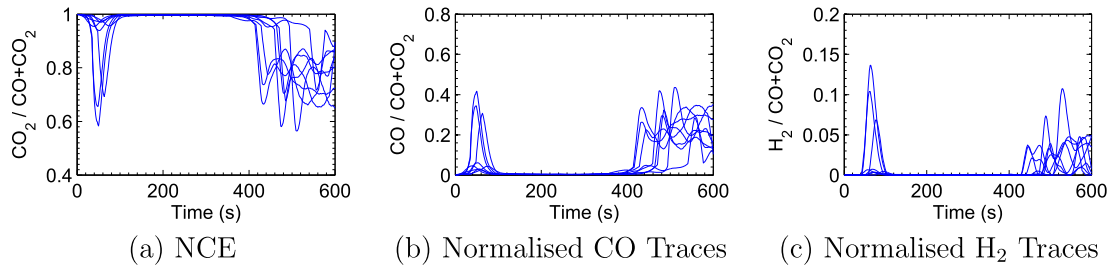


**Fig. 5.** Normalised emissions data of $CO_2$, $CO$ and $H_2$ measurements for eight individual tests.

### 3.3. Natural draft emissions profiles

It is apparent from Fig. 5 (a) that in the lighting phase, the NCE can be extremely low, with one peak reaching below 0.6 compared with an average of 0.9965, as presented in Table 2, in the migrating pyrolysis phase. This in turn means that there are high amounts of the products of incomplete combustion, seen in the CO and $H_2$ profiles in Fig. 5 (b, c).

At the onset of the migrating pyrolysis phase, a flame-front establishes at the secondary air inlet. The NCE simultaneously rises to an average of 0.9965, which is much higher than in the other phases, while the CO and $H_2$ emissions remain consistently low. In this phase, the migrating pyrolytic front moves steadily down the fuel-stack, which provides the necessary gaseous products for the flame at the secondary air inlet to be sustained. This phase is highly efficient and exhibits extremely low emissions of incomplete combustion.

In the char gasification phase, CO and $H_2$ emissions are relatively high, resulting in an NCE as low as 0.8518.

### 3.4. Natural draft temperature profiles

The temperature profiles, presented in Fig. 6, reflect the results from the emissions data. The three phases can be identified, based on the gradient of the temperature profiles. In the lighting phase, the gas temperature inside the stove body heats up much more quickly than in the stove extension because combustion takes place on top of the fuel-stack. Once the migrating pyrolysis phase starts and a flame-front establishes at the secondary air inlet, the gas temperature in the stove extension rises above the gas temperature in the stove body. Towards the end of the migrating pyrolysis phase, when the flame-front at the secondary air inlet extinguishes and combustion starts taking place on top of the fuel bed, the temperature inside the stove body starts increasing until it peaks in the char gasification phase.

### 3.5. Forced draft profiles

The time frames of the different air configurations are presented

**Table 2**
Averaged normalised peak values and time-weighted-average (TWA) values for the three phases, with the standard deviation of eight repeat tests in parentheses underneath.

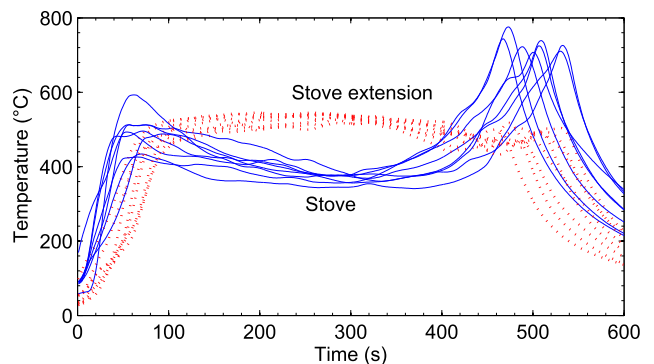|  | Lighting | Migrating pyrolysis | Char gasification |
|---|---|---|---|
| Time in Phase [s] | 95.1 (9.9) | 285.4 (27.7) | 221.5 (17.1) |
| Minimum NCE peak | 0.8404 (0.1658) | – | 0.6572 (0.0569) |
| Maximum $CO/(CO_2 + CO)$ peak | 0.1596 (0.1658) | – | 0.3428 (0.0569) |
| Maximum $H_2/(CO_2 + CO)$ peak | 0.0418 (0.0538) | – | 0.0556 (0.0240) |
| TWA - NCE | – | 0.9965 (0.0006) | 0.8518 (0.0427) |
| TWA − $CO/(CO_2 + CO)$ | – | 0.0035 (0.0006) | 0.1482 (0.0427) |
| TWA - $H_2/(CO_2 + CO)$ | – | 0.00013 (0.00015) | 0.01368 (0.00727) |



**Fig. 6.** Mean temperatures in the stove and in the stove extension.

in Fig. 7. The lowest air flow causes the lighting and char gasification phase to be longer than in the natural draft case, while the migrating pyrolysis phase is shorter. For all configurations, the char gasification phase is longer in the forced draft case, while the lighting and migrating pyrolysis phases are shorter. Thus it can be seen that it is not possible to simulate natural draft conditions by introducing a constant primary air flow. With higher airflows it can be observed that the standard deviation, of the time spent in a phase, subsides significantly leading to a higher repeatability of the test conditions.

The emissions from the system under forced draft conditions are illustrated in Fig. 8. In the lighting phase, the normalised peak NCE values are only considerably higher than in the natural draft configuration when the highest primary air flow is provided, and are significantly lower with the lowest air flow. The TWA NCE in the migrating pyrolysis phase is similar in both configurations, around the value of 0.9965 in the natural draft case. In contrast, in the char gasification phase, the influence of an increase in the primary air flow has a visible effect. The TWA NCE steadily falls, with the lower two values of the primary air flow achieving a higher efficiency, than the natural draft case, while the higher two values exhibit a lower efficiency.

A comparison of the emissions profiles in relation to the time frames spent in each phase provides further evidence that natural draft conditions cannot be simulated by introducing a forced primary air flow. The emission profiles of, for example, the migrating pyrolysis phase, in Fig. 8 (b), suggest that natural draft similar conditions are achieve with a forced air flow of 0.059 kg m$^{-2}$ s$^{-1}$, while the time frames in the phase, in Fig. 7 (b), suggest that a lower value than 0.048 kg m$^{-2}$ s$^{-1}$ would be necessary. Similarly contradicting results are noted for the lighting and char gasification phase.

## 4. Discussion

In the lighting phase, the profiles, seen in Fig. 5, can be related to the incomplete combustion of the kindling material and the top layer of the biomass. The combustion of the kindling material and the top layer of biomass takes place inside the stove body where the surrounding oxygen is rapidly consumed and insufficient primary air enters through the fuel-stack for complete combustion. As described, this CO peak in the lighting phase had previously been observed to increase with a lower calorific value of the kindling material [24]. Furthermore, it had been detected that the lighting phase contributed a large amount of the overall PM$_{2.5}$ emissions, which can also be the result of incomplete combustion [34]. It should be noted, though, that only three of the eight tests show very high CO peak values, which suggests that consistently lower emissions in this phase could be achieved. These deductions are supported by the results from the forced draft primary air tests, which are presented in Fig. 8 (a). It can be seen that the peak NCE rises with higher air flows achieving a maximum value of 0.9631 for

the highest air flow, which provides sufficient oxygen inside the stove body for more complete combustion.

The thick smoke, which was observed at the onset of the migrating pyrolysis phase, in Fig. 4 (b), indicates that there are high amounts of vaporised pyrolysis products, such as tars, heavier hydrocarbons and water, in the gas stream. This suggests that the process of cracking pyrolytic products into lighter hydrocarbons, which occurs at high temperatures and for which hot char particles act as a catalyst [11,13], is restricted. This observable amount of volatile compounds supports the hypothesis that cracking in gasifier-based stoves might be restrained due to the limited char bed thickness above the migrating pyrolysis front, resulting in a very short residence time of pyrolysis products in the char layer [14]. The released combustible products in the migrating pyrolysis phase, which exit the fuel-stack as thick smoke, are only partially oxidised inside the stove body because of the insufficient oxygen supply from the primary air inlet, and rise to the secondary air inlet. At the secondary air inlet, the thick smoke would typically be ignited, once it mixes with oxygen from the entering air, by the flames which were established in the lighting phase on the fuel-stack. This implies that the flames that establish in the lighting phase need to bridge the distance between the fuel-stack and the location where a combustible mixture of secondary air with gasification products from the fuel is present. Cases in which the flames on top of the fuel stack do not bridge this distance to ignite flames at the secondary air inlet were experienced when the stove extension was not connected to the stove body, as presented in the supplementary material, and also in some cold starts, when preheating the furnace. This has not previously been observed when testing smaller TLUD stoves and needs to be considered when designing larger TLUD stoves, where the distance between the fuel and the secondary air inlet increases.

Comparing the profiles of the migrating pyrolysis phase, in Figs. 5 and 8 (b) with the results of Johnson et al. [35] and Jetter et al. [17] it can be seen that very few stoves can achieve NCE values of this magnitude. It should be borne in mind, however, that this comparison is limited because Johnson et al. [35], presented averages of the NCE over water boiling tests (WBT) and minute-by-minute NCE ratios for normal stove use in homes, while Jetter et al. [17] measured the NCE over the high-power (cold start) phases of the WBT. Their results are only compared with the average of the migrating pyrolysis phase of this study. This comparison still verifies the high efficiency of the research furnace and the potential of this type of stove.

During the pyrolysis phase the endothermic reactions inside the stove body are mainly sustained by the heat released from the gasification of the pyrolysis products, which causes the temperature at location B to drop, as can be seen in Fig. 6. The gas temperature at location B, inside the stove body, reduces to below 400 °C, which means that the temperature of the pyrolysis products, once they reach the secondary air inlet, will be below this value. This drop of pyrolysis product temperature from ≈600 °C,



(a) Lighting phase      (b) Migrating pyrolysis      (c) Char gasification
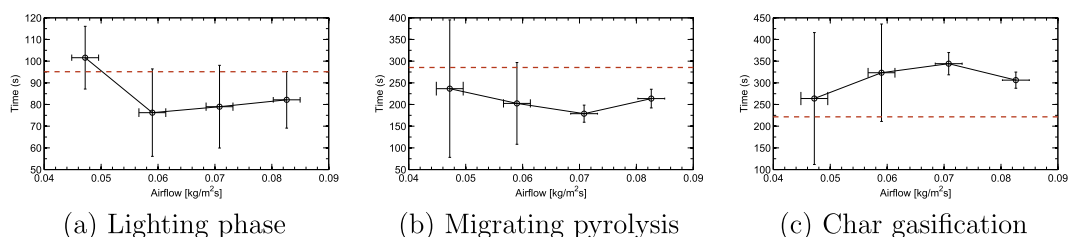
**Fig. 7.** Average time of the three phases of TLUD combustion with various forced primary air flows compared with natural draft conditions. The red dotted line demonstrates the respective result from the natural draft configuration. (For interpretation of the references to colour in this figure legend, the reader is referred to the web version of this article.)
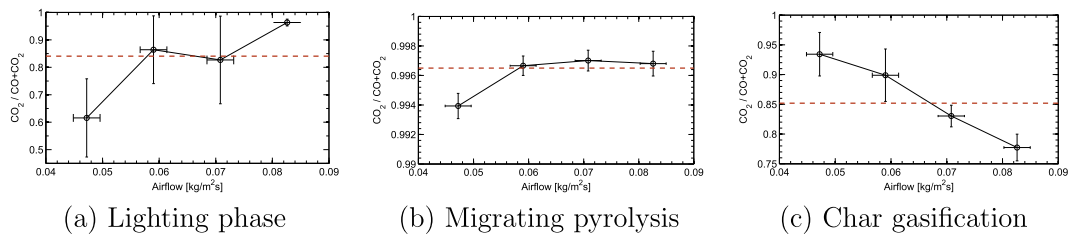
**Fig. 8.** Average peak nominal combustion efficiency (NCE) values for the lighting phase and time-weighed-average NCE values for the migrating pyrolysis and char gasification phase of various forced primary air flows compared with natural draft conditions of TLUD combustion. The red dotted line demonstrates the respective result from the natural draft configuration. (For interpretation of the references to colour in this figure legend, the reader is referred to the web version of this article.)

when leaving the fuel bed [15], to below 400 °C when reaching the secondary air inlet, suggests a cooling effect. This cooling effect can be assumed to be due to a combination of endothermic reactions of the gasification products and the heat loss through the furnace walls. Reducing this heat loss, either by insulating the stove body or by using released heat from the outer surface of the combustion chamber to pre-heat the secondary air, as is done in some TLUD designs, could further influence the combustion at the secondary air inlet positively.

The high CO emissions, which can be observed in the char gasification phase in Figs. 5 and 8 (c), were to be expected and had previously been detected [15]. An increase in the surface oxidation due to a higher relative surface area of the char particles can be assumed to cause these high CO emissions [36]. The lower NCE with a higher primary air flow, as seen in Fig. 8 (c), could be a result of more CO, the main gasification product, being transported out of the high temperature reaction zone of the char bed before being fully oxidised. This conclusion is supported by the results from the natural draft case. The highest CO emissions, as presented in Fig. 5 (b), were measured when the gas temperatures inside the stove, as illustrated in Fig. 6, were at their peak, thus when it can be assumed that the buoyancy force, and in turn the primary air flow, was at its greatest.

The high $H_2$ emissions in the char gasification phase, in Fig. 5 (c), should also be noted carefully because they cannot necessarily be explained by char gasification. These emissions might indicate that the release of hydrocarbons in the migrating pyrolysis phase is incomplete. Therefore it might be possible, through further study, to optimise the migrating pyrolysis phase to achieve a higher overall efficiency of TLUD stoves.

## 5. Conclusions

In order to better understand the combustion process in TLUD stoves, and to enable future optimisation of TLUD designs for various conditions, a research furnace has been commissioned. In the lighting phase, high primary air flows lead to an increase in peak NCE values and are therefore desirable to reduce emissions of incomplete combustion during this phase. In the migrating pyrolysis phase, an increase in forced primary air flows has little advantage over natural draft conditions in terms of NCE values, but lower primary air flows lead to higher CO emissions.

In the char gasification phase, the NCE values are significantly higher with low forced draft primary air flows, as compared with natural draft or with high forced draft primary air flows, due to the reduced residence time within the high temperature reaction zone of the char be facilitating less complete oxidation to $CO_2$. These findings demonstrate that high controllability of the air flow in each of the distinct combustion phases of a TLUD enables an improvement in the efficiency of the combustion system and a reduction in the emissions of incomplete combustion.

## References

[1] S. Bonjour, H. Adair-Rohani, J. Wolf, N.G. Bruce, S. Mehta, A. Prüss-Ustün, et al., Solid fuel use for household cooking: country and regional estimates for 1980-2010, Environ. Health Perspect. 121 (7) (2013) 784—790.
[2] WHO, Household Air Pollution and Health — Fact Sheet N 292, 2014. URL, http://www.who.int/mediacentre/factsheets/fs292/en/.
[3] K.R. Smith, J.P. McCracken, M.W. Weber, A. Hubbard, A. Jenny, L.M. Thompson, et al., Effect of reduction in household air pollution on childhood pneumonia in Guatemala (RESPIRE): a randomised controlled trial, Lancet 378 (2011) 1717—1726.
[4] J. Baumgartner, K.R. Smith, A. Chockalingam, Reducing CVD through improvements in household energy: implications for policy-relevant research, Glob. Heart 7 (3) (2012) 243—247.
[5] G.L. Simon, R. Bailis, J. Baumgartner, J. Hyman, A. Laurent, Current debates and future research needs in the clean cookstove sector, Energy Sustain. Dev. 20 (2014) 49—57.
[6] P.S. Anderson, T.B. Reed, Biomass gasification: clean residential stoves, commercial power generation, and global impacts, in: LAMNET Project International Workshop. Viña del Mar, Chile, 2004.
[7] K.B. Sutar, S. Kohli, M.R. Ravi, A. Ray, Biomass cookstoves : a review of technical aspects, Renew. Sustain. Energy Rev. 41 (2015) 1128—1166.
[8] V. Kirubakaran, V. Sivaramakrishnan, R. Nalini, T. Sekar, M. Premalatha, P. Subramanian, A review on gasification of biomass, Renew. Sustain. Energy Rev. 13 (1) (2009) 179—186.
[9] C. Roth, Micro-Gasification : Cooking with Gas from Dry Biomass, 2014. URL, http://www.giz.de/fachexpertise/downloads/giz2014-en-micro-gasification-manual-hera.pdf.
[10] T. Reed, R. Walt, S. Ellis, A. Das, S. Deutch, Superficial velocity — the key to downdraft gasification, in: 4th Biomass Conference of the Americas. Oakland, California, 1999, pp. 1—8.
[11] P. Basu, Pyrolysis, in: Biomass Gasification, Pyrolysis and Torrefaction, second ed., Elsevier Inc., 2013, pp. 147—176 chap. 5.
[12] A. Bridgwater, Renewable fuels and chemicals by thermal processing of biomass, Chem. Eng. J. 91 (2—3) (2003) 87—102.
[13] P. Basu, Tar production and destruction, in: Biomass Gasification and Pyrolysis, second ed., Elsevier Inc., 2013, pp. 177—198 chap. 6.
[14] S. Varunkumar, N.K.S. Rajan, H.S. Mukunda, Experimental and computational studies on a gasifier based stove, Energy Convers. Manag. 53 (1) (2012) 135—141.
[15] H.S. Mukunda, S. Dasappa, P.J. Paul, N.K.S. Rajan, M. Yagnaraman, D. Ravi Kumar, et al., Gasifier stoves — science, technology and field outreach, Curr. Sci. 98 (5) (2010) 627—638.
[16] P. Raman, J. Murali, D. Sakthivadivel, V.S. Vigneswaran, Performance evaluation of three types of forced draft cook stoves using fuel wood and coconut shell, Biomass Bioenergy 49 (2013) 333—340.
[17] J. Jetter, Y. Zhao, K.R. Smith, B. Khan, T. Yelverton, P. DeCarlo, et al., Pollutant emissions and energy efficiency under controlled conditions for household biomass cookstoves and implications for metrics useful in setting international test standards, Environ. Sci. Technol. 46 (19) (2012) 10827—10834.
[18] J.J. Jetter, P. Kariher, Solid-fuel household cook stoves: characterization of performance and emissions, Biomass Bioenergy 33 (2) (2009) 294—305.
[19] C. Birzer, P. Medwell, G. MacFarlane, M. Read, J. Wilkey, M. Higgins, et al., A biochar-producing, dung-burning cookstove for humanitarian purposes, Procedia Eng. 78 (2014) 243—249.
[20] J. Tryner, B.D. Willson, A.J. Marchese, The effects of fuel type and stove design

on emissions and efficiency of natural-draft semi-gasifier biomass cookstoves, Energy Sustain. Dev. 23 (2014) 99—109.

[21] Y. Huangfu, H. Li, X. Chen, C. Xue, C. Chen, G. Liu, Effects of moisture content in fuel on thermal performance and emission of biomass semi-gasified cookstove, Energy Sustain. Dev. 21 (1) (2014) 60—65.

[22] T.B. Reed, E. Anselmo, K. Kircher, Testing & modeling the wood-gas turbo stove, Prog. Thermochem. Biomass Convers. Conf. (2000) 693—704.

[23] E. Pârpăriță, M. Brebu, M. Azhar Uddin, J. Yanik, C. Vasile, Pyrolysis behaviors of various biomasses, Polym. Degrad. Stab. 100 (1) (2014) 1—9.

[24] P. Arora, P. Das, S. Jain, V.V.N. Kishore, A laboratory based comparative study of Indian biomass cookstove testing protocol and water boiling test, Energy Sustain. Dev. 21 (1) (2014) 81—88.

[25] T. Kirch, P.R. Medwell, C. Birzer, L. Holden, The role fo primary and secondary air on wood combustion in cookstoves, Int. J. Sustain. Energy (2016), http://dx.doi.org/10.1080/14786451.2016.1166110.

[26] M. Kumar, S. Kumar, S. Tyagi, Design, development and technological advancement in the biomass cookstoves: a review, Renew. Sustain. Energy Rev. 26 (2013) 265—285.

[27] M. Fatehi, M. Kaviany, Adiabatic reverse combustion in a packed bed, Combust. Flame 99 (1) (1994) 1—17.

[28] M. Rönnbäck, M. Axell, L. Gustavsson, H. Thunman, B. Lecher, Combustion processes in a biomass fuel bed — experimental results, in: A.V. Bridgwater (Ed.), Progress in Thermochemical Biomass Conversion, Blackwell Science Ltd, Oxford, UK, 2001, pp. 743—757 chap. 59.

[29] M. Horttanainen, J. Saastamoinen, P. Sarkomaa, Operational limits of ignition front propagation against airflow in packed beds of different wood fuels, Energy Fuels 16 (3) (2002) 676—686.

[30] J. Porteiro, D. Patiño, J. Collazo, E. Granada, J. Moran, J.L. Miguez, Experimental analysis of the ignition front propagation of several biomass fuels in a fixed-bed combustor, Fuel 89 (1) (2010) 26—35.

[31] J. Porteiro, D. Patiño, J. Moran, E. Granada, Study of a fixed-bed biomass combustor: influential parameters on ignition front propagation using parametric analysis, Energy Fuels 24 (7) (2010) 3890—3897.

[32] American Society for Testing and Materials. ASTM D4442—92(2003), Standard Test Methods for Direct Moisture Content Measurement of Wood and Wood-based Materials, 2003.

[33] P.S. Anderson, T.B. Reed, P.W. Wever, Micro-gasification: what it is and why it works, Boil. Point 53 (53) (2007) 35—37.

[34] E.M. Carter, M. Shan, X. Yang, J. Li, J. Baumgartner, Pollutant emissions and energy efficiency of chinese gasifier cooking stoves and implications for future intervention studies, Environ. Sci. Technol. 48 (11) (2014) 6461—6467.

[35] M. Johnson, R. Edwards, V. Berrueta, O. Masera, New approaches to performance testing of improved cookstoves, Environ. Sci. Technol. 44 (1) (2010) 368—374.

[36] P.S. Arora, S. Jain, Estimation of organic and elemental carbon emitted from wood burning in traditional and improved cookstoves using controlled cooking test, Environ. Sci. Technol. 49 (2015) 3958—3965.

This page intentionally left mostly blank.

# Appendix B

## The Role of Primary and Secondary Air on Wood Combustion in Cookstoves

Taylor & Francis
Taylor & Francis Group

# The role of primary and secondary air on wood combustion in cookstoves

Thomas Kirch [ID], Cristian H. Birzer [ID], Paul R. Medwell [ID] and Liam Holden

School of Mechanical Engineering, The University of Adelaide, Adelaide, SA, Australia

## ABSTRACT

A two-stage solid fuel research furnace was used to examine the claim that through forced draught greater mixing and more complete combustion could be achieved. By varying the primary air (PA) and secondary air (SA) flow the influence on the combustion process was investigated. In the first part of the combustion, when the release of volatile compounds predominates, the variation of neither PA nor SA had a significant influence. In the second part when mainly char is oxidised an increase in both PA and SA lead to a rising nominal combustion efficiency $(NCE = CO_2/(CO_2 + CO))$, with a greater impact observed with SA. Furthermore higher air flows caused the heat transfer, to a pot above the furnace, to decline. Therefore forced draught does lead to greater mixing and mitigation of emissions, but in the presented configuration a trade-off between a higher NCE and a lower heat transfer needs consideration.

## 1. Introduction

Currently, and consistently over the last three decades, 2.9 billion people rely on solid fuels as a primary source for cooking (Bonjour et al. 2013). Traditional open fires or basic cookstoves, that are primarily used for burning solid fuels, result in the emission of significant amounts of toxic products of incomplete combustion leading to health, social, and environmental problems. Worldwide, household air pollution from solid fuels is a major contributor to the burden of disease, especially for women, for whom it is second only to high blood pressure in disability-adjusted-life-years (Lim 2012), and children, for whom it is responsible for 50% of premature deaths under five years of age (WHO 2014). Addressing the issue of pollution from open fires and basic cookstoves is therefore important to help improve the quality of life for billions of people.

To reduce the problems related to traditional cooking methods there are a multitude of improved cooking systems on the market (Urmee and Gyamfi 2014), with some showing promising results (Jetter et al. 2012; Johnson et al. 2013). However, as noted by MacCarty, Still, and Ogle (2010), not all new stove designs necessarily improve the emission of products of incomplete combustion, such as carbon monoxide (CO) and particulate matter (PM). To ensure the optimisation of cookstoves for the future, the development of improved combustion science for these systems is essential (Simon et al. 2014).

It is widely known that a key attribute for complete combustion is to create sufficient mixing of oxygen with the fuel. Without adequate mixing, and the necessary feedback from the hot combustion products, emissions of incomplete combustion will remain high. Recognising the importance of mixing in the improvement of efficiency and reduction of pollutants, an increasing number of improved cookstoves seek to incorporate forced draught. Stoves that apply the assistance of blowers or fans

increase the stove price dramatically, however with low-cost computer-based blowers being available now this problem can be ameliorated (Kshirsagar and Kalamkar 2014). It has been observed that when using forced air the heat transfer to a vessel would increase, and products of incomplete combustion, foremost CO and PM, would decrease, compared to other cookstoves (MacCarty, Still, and Ogle 2010; Aprovecho Research Center 2011; Kumar, Kumar, and Tyagi 2013; Raman, Ram, and Gupta 2014). The increase in the heat transfer is related to higher velocity of hot flue gases around the cooking vessel while the emissions reduction is believed to be caused by greater mixing of air with combustible gases. On the contrary it has been found that forced air stoves, though more energy efficient, are not necessarily more emission efficient (Kshirsagar and Kalamkar 2014) and although emitting relatively less $PM_{2.5}$ mass the number of ultra-fine particles can increase (Jetter et al. 2012).

There is an increasing trend for improved cookstoves to feature forced air (Kshirsagar and Kalamkar 2014) with the widespread belief that forced air necessarily leads to greater mixing and thus increased performance. The analysis of the validity of this claim over a range of conditions is the purpose of this study. A two-stage solid fuel research furnace, analogous to a cookstove, which allows the air flow rate through a primary and a secondary inlet to be controlled was used to investigate advantages and disadvantages of forced draught in cookstoves. The measurement of emissions from the combustion and the temperatures inside the furnace enable the evaluation of the process. Especially the incorporation of secondary air (SA), also called over-fire air, which is a key feature of gasifier type stoves could be beneficial for the presented combustion furnace.

## 2. Equipment and techniques

### 2.1. Research furnace

Experiments were conducted in a research furnace, shown in Figure 1, which was designed to provide control over multiple air flow rates, geometry, and fuel/air locations. The furnace has an inner
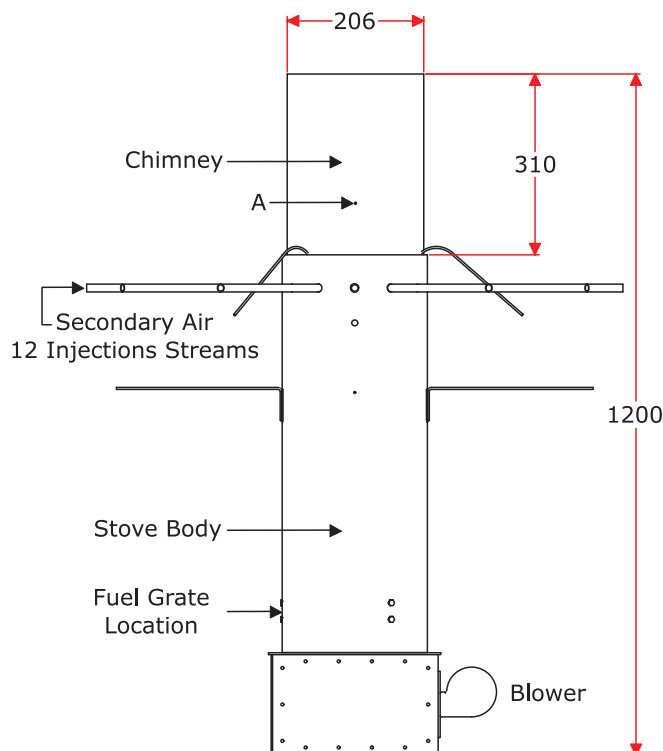


**Figure 1.** Schematic research furnace (all measurements in ( mm )).

diameter of 206 mm and a height of 1200 mm. This size is larger than most stoves which are designed for household use, to be able to address scaling issues and to enable a greater variability of adjustable parameters. These parameters include the location and the depth or amount of the fuel, which can have an influence on the combustion process, but an investigation of these parameters is outside the scope of the present study which is focused on the effect of the air supply. The research furnace consists of the primary air (PA) inlet chamber, the stove body, in which the fuel grate is located, and the furnace extension, as presented in Figure 1. On top of the research furnace a pot and pot-stand were added to the set-up. The pot was filled with 2 L of water, and the water temperature was monitored with a K-type thermocouple. The tip of the water thermocouple was inserted through a small hole in the top of the lid of the pot to ensure that it was submersed in the water.

The PA flow rate can be controlled by using a small blower situated on the outside of the furnace, as shown in Figure 1. This blower is designed for the purpose of cooling personal computers. It was chosen for this application because for in-field construction of forced draught cookstoves the use of this kind of blower could achieve a far reaching impact. Personal computer blowers are readily available in many parts of the world and have previously been used for the purpose of providing forced draught in cookstoves (Anderson and Reed 2004). The blower can be adjusted using a pulse width modulator with five settings to adjust the PA flow rate in relation to the maximum airflow of 14.6 L/s.

To control the global equivalence ratio of the furnace, without changing the air flow rate through the fuel bed, compressed air was injected into the furnace as SA. The SA flow enters the furnace downstream of the fuel bed via 12 equi-spaced radial injection streams. The injection streams consist of 290 mm long pipes, with an inner diameter of 12 mm, and a 1.2 m long flexible hose. All hoses are connected to a manifold to ensure uniform flow rate through the SA injection streams. The flow rates are controlled using a rotameter situated upstream of the manifold.

## 2.2. Fuel

Wood chips were the fuel used for the experiments reported in this paper. These wood chips were produced from Radiata Pine (*Pinus Radiata*) trees sourced from a timber processing plant in Jamestown, South Australia. Pine bark also accounts for a small portion of the chips (less than 10%). A sample tested was found to include chips varying from $75 \times 25 \times 3$ mm to $8 \times 5 \times 2$ mm with the average size approximately $30 \times 20 \times 3$ mm. A controlled moisture content of approximately 10% was established for all experiments. Wood chips were chosen as fuel because wood is the most commonly combusted biomass (Yevich 2003). The mass of fuel used for all tests was 1.0 kg.

## 2.3. Measurements

Emissions were measured using a Testo 350 Flue Gas Analyser. Measurements included oxygen ($O_2$), CO, and carbon dioxide ($CO_2$). The flue gas measurements were taken at 830 mm above the exit plane of the furnace extension, along the central axis of the furnace. All concentrations recorded are on a dry basis. Mean gas-phase temperature measurements were obtained using a K-type thermocouple mounted in location A, as shown in Figure 1 and the water temperature inside a pot was measured, as described in Section 2.1.

## 2.4. Test procedure for varying PA

Investigations into the effect of PA flow rate were conducted with a furnace extension height set at 310 mm, a distance from the furnace extension to the pot of 50 mm and the SA flow rate set at 6.4 L/s. Tests were conducted at the PA flow rates of 14.6 , 8.8 , and 5.9 L/s, each repeated three times. To minimise thermal variations between tests, the furnace was pre-heated to approximately 65°C. For each experiment 1 kg of fuel was loaded onto the fuel grate. During testing the research furnace was placed under a fume extraction duct and the pot containing 2 L of water was placed

above the exit plane of the furnace extension. The pot was placed onto the pot-stand and visually aligned with the flue to ensure the exhaust gases flowed evenly around the outside of the pot. The temperature of the water in the pot, and the time taken to achieve water boiling, give an indication of the heat transfer from the hot gases issuing from the furnace to the pot.

To ignite the biomass, approximately 50 mL of methylated spirits (96% ethanol) was poured into the furnace over the biomass fuel. The PA and the SA were turned on after 1 min to the predetermined value for each experiment. The experiments were conducted for 13 min, with both airflows turned off after 11 min. The experiments were run in a continuous cycle to ensure that the furnace always started at the same temperature, being pre-heated by the previous experiment. For each set of parameters the test was repeated three times and the arithmetic mean of the results is presented. Due to the variability of stove testing more tests would be advantageous (Wang et al. 2014) but the observations were found to be repeatable, such that the trends are not affected by a bias due to the limited sample size.

### 2.5. Test procedure for varying SA

Consistent with the test procedure for varying PA presented in Section 2.4, the same procedure was used for a second set of experiments, but instead the SA was varied. The PA was kept constant at 14.6 L/s and the SA was adjusted. Experiments were performed at SA flow rates of 1.3 , 3.8 , 6.4 , and 9.0 L/s.

## 3. Results and discussion

### 3.1. Varying PA flow rate

#### 3.1.1. Oxygen profile.

Figure 2 shows the mean oxygen concentration from three independent test measurements, at each of the three various PA flow rates. At the beginning of the burn-cycle the initial concentration of oxygen ($O_2$) is approximately 21%, as expected. During the combustion process the $O_2$ concentration decreases as a function of time for all levels of PA until it reaches a minimum at approximately 350 s. It can be assumed that at this point, after 350 s, the combustion intensity is greatest, consuming the oxygen and leading to these low values. In all cases it is noted that the lowest $O_2$ concentration is greater than 5% (on a volumetric basis). This measurement is influenced due to the fact that the emissions were measured at 830 mm above the top of furnace extension, where they have been mixed with surrounding air. The high $O_2$ concentrations suggest though that with all the PA flow rates the system operates fuel-lean.

Of particular note from Figure 2 is that the oxygen concentration returns to 21% at approximately the same time for all PA flow rates. This indicates that the burn-time for all cases is approximately 650 s. The average air to fuel ratios ($A/F = \mathrm{kg_{air}/kg_{fuel}}$ ), for the complete combustion of all fuel over the time period of 650 s are presented in Table 1. These values are calculated assuming a molar ratio of the biomass fuel of approximately $CH_{1.4}O_{0.6}$, as has been suggested to be an average for woods, with a resulting $A/F$ of 6.3 for complete combustion (Saravanakumar et al. 2007). The presented calculations in Table 1 are highly simplified, since they are based on many assumptions, such as a uniform fuel consumption during the combustion process. Bearing these assumptions in mind the values in Table 1 give an indication which supports the suggestion of constantly fuel-lean conditions. In all cases, except for a PA flow of 5.9 L/s, overall fuel-lean conditions appear to be achieved by the PA flow.

The SA is introduced downstream of the flame front, such that the PA flow rate should control the combustion of the solid fuel. The addition of SA serves predominately to create mixing of air and the primary combustion products, and is aimed to lead to the complete combustion.
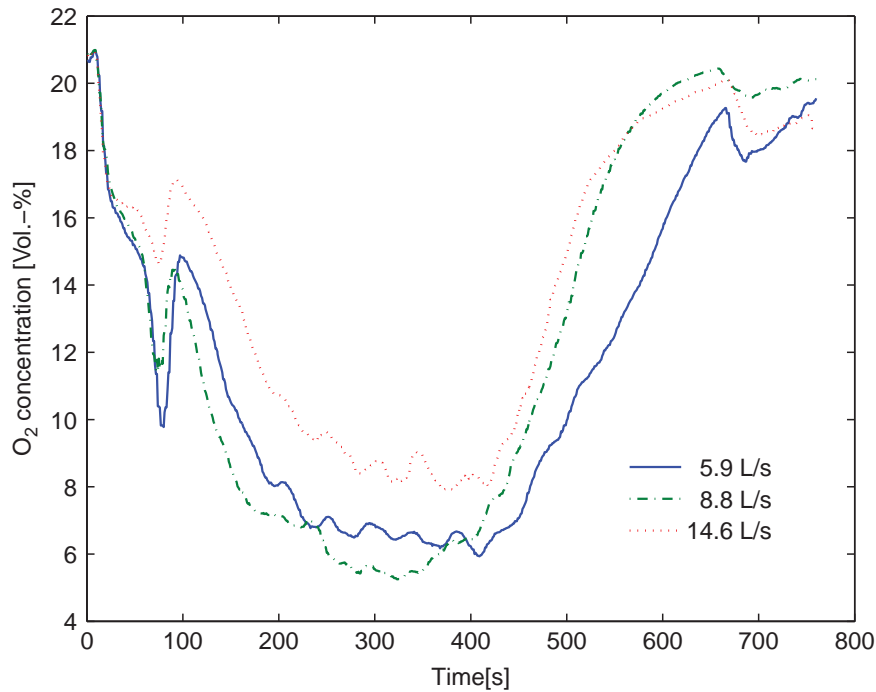
**Figure 2.** Mean $O_2$ concentrations with varying PA.

### 3.1.2. The nominal combustion efficiency.

Figure 3 presents the nominal combustion efficiency (NCE), the relation of $CO_2$ emissions normalised by the sum of CO and $CO_2$ emissions (Jetter et al. 2012), for varying PA flows. This normalisation procedure was performed because the emissions were measured at a position of 830 mm above the furnace where they have been mixed with surrounding air. Due to this mixing effect the measured concentrations have been diluted and could be misleading. The NCE provides a relation of the carbonaceous emissions of complete combustion, $CO_2$, to the intensity of the combustion process, represented by the sum of all measured carbonaceous emissions, CO and $CO_2$. This normalisation is independent of location of the measurement and therefore allows an evaluation of the combustion process. High NCE values, which can be seen in the first part of the process up to approximately 450 s, represent a high combustion performance and low emissions of incomplete combustion. The rapid fall of all curves after the initially steadily high values is assumed to be due to the transition from primarily volatile combustion to primarily char combustion (Jones et al. 2014). In the second part of the process mainly charcoal remains as fuel, which usually accounts for about 20–30% of the initial mass (Huangfu et al. 2014). The produced charcoal has a highly porous

**Table 1.** The PA and SA flow, the average air/fuel (A/F) ratio for the PA flow as well as the overall A/F ratio for the consumption of all fuel over the whole burn-cycle of 650 s and the average NCE for all configurations.

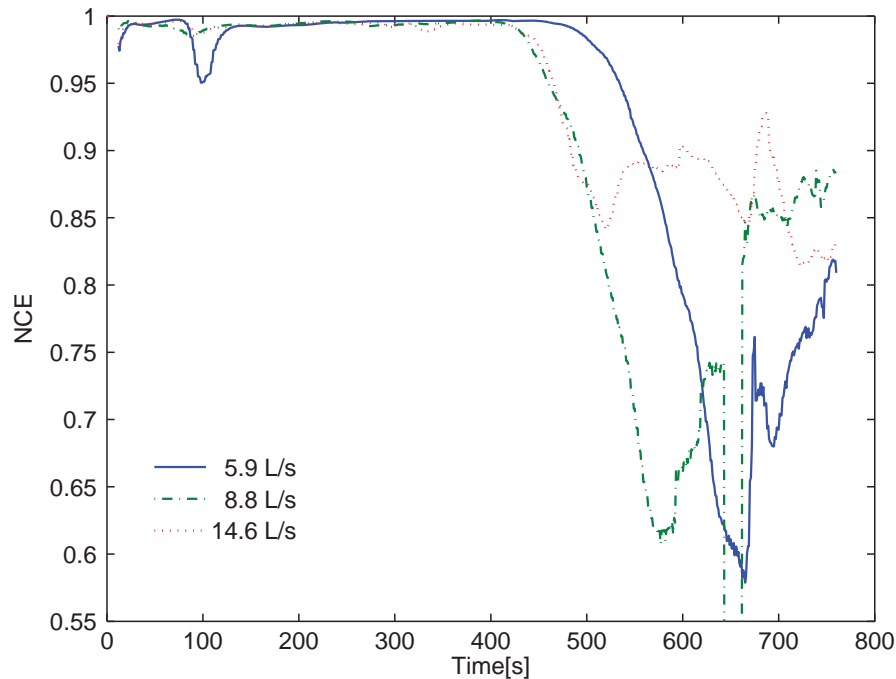| Air flow | | A/F ratio | | NCE |
|---|---|---|---|---|
| Primary ( L/s ) | Secondary ( L/s ) | Primary ( $kg_{air}/kg_{fuel}$ ) | Overall ( $kg_{air}/kg_{fuel}$ ) | |
| *Varying PA flow* | | | | |
| 5.9 | 6.4 | 5.1 | 10.6 | 0.919 |
| 8.8 | 6.4 | 7.6 | 13.2 | 0.916 |
| 14.6 | 6.4 | 12.7 | 18.2 | 0.944 |
| *Varying SA flow* | | | | |
| 14.6 | 1.3 | 12.7 | 13.8 | 0.923 |
| 14.6 | 3.8 | 12.7 | 16.0 | 0.932 |
| 14.6 | 6.4 | 12.7 | 18.2 | 0.944 |
| 14.6 | 9.0 | 12.7 | 20.4 | 0.951 |

**Figure 3.** NCE values for varying PA.

structure and it consists primarily of carbon. The carbon reacts with oxygen on its surface, largely inside the porous structure (Emmons and Atreya 1982). This surface oxidation causes high emissions of CO which can subsequently oxidise further to form $CO_2$ if sufficiently high temperatures and oxygen are available (Glassman, Yetter, and Glumac 2015). Although with all three PA flows sufficient oxygen is supplied for complete combustion, as shown in Section 3.1.1, the CO emissions are high in the char combustion phase. Table 1 presents the average NCE over the burn-time for the respective tests, which shows that the NCE value increases only by 2.5% with a 2.5 times greater PA /fuel ratio. This shows that by only increasing the PA flow no drastic reduction of emissions of incomplete combustion can be achieved. In the first two cases, of 5.9 and 8.8 L/s PA, the average NCE is similar to the average of an open fire during a day of in-home use (Johnson et al. 2010). This lead to the choice of 14.6 L/s of PA for the tests of varying SA, as the goal is to achieve a NCE as high as possible.

## 3.2. Varying SA flow rate

### 3.2.1. Carbonaceous emissions.
Figure 4 presents the NCE profiles from varying SA flow rates. It shows that the NCE, similar to the profiles of varying PA, is relatively high in the first part and low in the second part of the burn-cycle. In the beginning, predominantly combustion of volatile compounds, that are released from the fuel stack, is taking place. The consistently high NCE shows that a variation in SA air flow does not have an influence on this part of the combustion process. Towards the end, when most of the volatiles from the fuel are combusted, char remains. The NCE falls during the char combustion, which occurs after the peak intensity of combustion ($\sim 350$ s, as mentioned in Section 3.1.1). The CO levels are highest for the lowest SA flow rate of 1.3 L/s SA.

When char combustion occurs in the fuel bed, the oxidation process could be assumed to be controlled by the PA flow rate rather than the SA. This is reflected in the 3.8, 6.4, and 9.0 L/s SA cases, which all show similar profiles. Table 1 shows that the average NCE increases with a higher SA airflow. This indicates that there is a relationship between the SA and the fuel bed. It is hypothesised
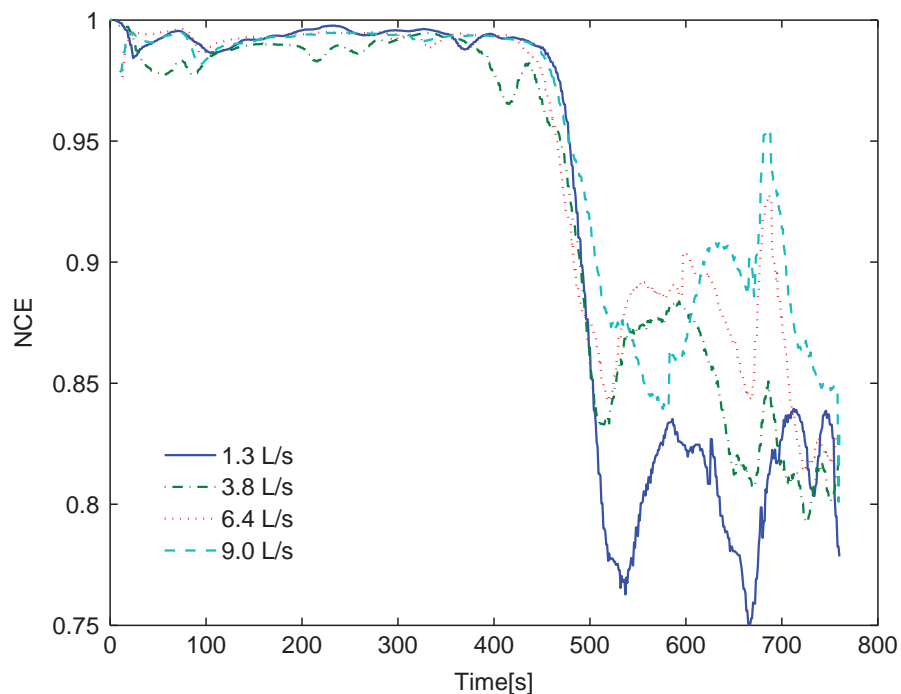
**Figure 4.** NCE values for varying SA.

that at the higher SA flow rates some of the air is directed downward onto the fuel bed, assisting in the char combustion and thus reducing the CO emissions.

### 3.2.2. Flue gas temperature and heat transfer profile.

Figure 5 shows in part (a) the gas-phase temperature in the furnace extension and in part (b) the water temperature inside the pot for the four SA flow rates considered. It can be seen in Figure 5 (a) that when the SA flow rate of 1.3 L/s was used, the flue temperature was considerably higher, up to 200°C greater than at 9.0 L/s SA. The lower temperature with the higher SA flow rates does not indicate lower heat output, but that the heat is diluted by the additional air (thus lowering the temperature). Depending on the application, the additional air (thus increased gas velocity) may be advantageous, while other applications may require the higher temperature. The average of the water temperature, as presented in Figure 5(b), reaches boiling point at 1.3 L/s SA (100°C) approximately 200 s before the measurements at 9 L/s SA. This shows that at 1.3 L/s SA flow, with the highest flue gas temperatures, the heat transfer is greatest in this combustion system.

### 3.3. Discussion

In Figures 3 and 4 it can be seen that in all cases the emissions of incomplete combustion are low in the first part of the combustion process and high in the second part. The first part of the process appears to be influenced by the variation of neither PA nor by SA. The volatile compounds which are released from the fuel are burned cleanly. The combustion in the second part of the process is, opposite to the first part, influenced by both PA and SA flow. With an increase of PA flow the NCE also increases, as can be seen in Figure 3, and the lowest SA flow displays the lowest NCE in Table 1. These emissions profiles need to be related to the information that the heat transfer to the pot, presented in Section 3.2.2, is significantly greater with lower SA. This finding is in agreement with previously reported lower heat transfer with higher air flows in a biomass combustion furnace (Selim et al. 2011). Therefore a trade-off needs to be considered between a higher NCE and lower
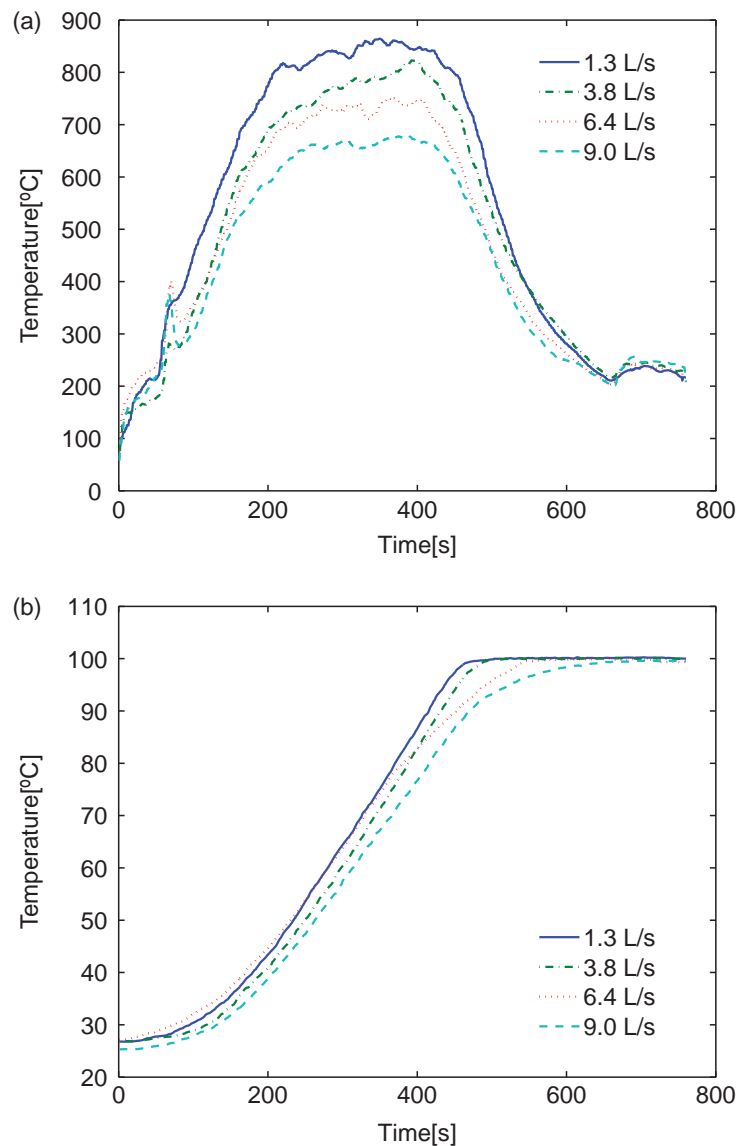
**Figure 5.** (a) The gas temperatures in the furnace extensions and (b) the water temperatures during varying SA tests.

heat transfer with a greater air flow against a higher heat transfer and lower NCE with a lower air flow.

## 4. Conclusions

The present study was performed on a two-stage research furnace to investigate the influence of the application of PA as well as SA on the combustion process of cookstoves. Two sets of experiments were performed. In one set the SA was held constant while the PA was varied. In another set the PA was held constant while the SA was varied. This allowed the influence of air flows over a range of conditions to be studied.

The results show that the first part of the combustion process, where the combustion of volatile compounds prevails, exhibits similar emissions profiles for all air flow applications, with low emissions of incomplete combustion. In the second part of the process, where mostly char combustion is taking place, higher PA flows cause a higher NCE, but even an excessive supply of air does not lead to a significant reduction of products of incomplete combustion. Furthermore although an increase in

SA supply steadily raises the NCE it has to be considered that it also lowers the heat transfer to a pot on the stove.

Thus it has been shown that both forced PA and forced SA do have an influence on the stove performance. The increase of PA and laterally introduced SA aid in the mixing of fuel and air and lower the emissions of products of incomplete combustion, but also they cause a lower heat transfer. Therefore the application of forced draught for PA as well as SA should be further investigated to achieve greater mixing and higher NCE values without increasing the amount of air, introduced into the system. Also it should be considered that different air flow rates in the first and second part of the combustion process could be advantageous.

## Acknowledgments

## Disclosure

## ORCID

*Thomas Kirch* http://orcid.org/0000-0002-6288-7466
*Cristian H. Birzer* http://orcid.org/0000-0002-7051-9137
*Paul R. Medwell* http://orcid.org/0000-0002-2216-3033

## References

Anderson, P. S., and T. B. Reed. 2004. *Biomass Gasification: Clean Residential Stoves, Commercial Power Generation, and Global Impacts.* LAMNET Project International Workshop, Viña del Mar.

Aprovecho Research Center. 2011. *Test Results of Cook Stove Performance.* Technical Report.

Bonjour, S., H. Adair-Rohani, J. Wolf, N. G. Bruce, S. Mehta, A. Prüss-Ustün, M. Lahiff, E. A. Rehfuess, V. Mishra, and K. R. Smith. 2013. "Solid Fuel Use for Household Cooking: Country and Regional Estimates for 1980–2010." *Environmental Health Perspectives* 121 (7): 784–790.

Emmons, H. W., and A. Atreya. 1982. "The Science of Wood Combustion." *Proceedings of the Indian Academy of Sciences Section C: Engineering Sciences* 5 (4): 259–268.

Glassman, I., R. A. Yetter, and N. G. Glumac. 2015. *Combustion of Nonvolatile Fuels.* 5th ed. Waltham, MA: Elsevier.

Huangfu, Y., H. Li, X. Chen, C. Xue, C. Chen, and G. Liu. 2014. "Effects of Moisture Content in Fuel on Thermal Performance and Emission of Biomass Semi-gasified Cookstove." *Energy for Sustainable Development* 21 (1): 60–65.

Jetter, J., Y. Zhao, K. R. Smith, B. Khan, T. Yelverton, P. Decarlo, and M. D. Hays. 2012. "Pollutant Emissions and Energy Efficiency Under Controlled Conditions for Household Biomass Cookstoves and Implications for Metrics Useful in Setting International Test Standards." *Environmental Science and Technology* 46 (19): 10827–10834.

Johnson, M., R. Edwards, V. Berrueta, and O. Masera. 2010. "New Approaches to Performance Testing of Improved Cookstoves." *Environmental Science and Technology* 44 (1): 368–374.

Johnson, M. A., V. Pilco, R. Torres, S. Joshi, R. M. Shrestha, M. Yagnaraman, N. L. Lam, et al. 2013. "Impacts on Household Fuel Consumption from Biomass Stove Programs in India, Nepal, and Peru." *Energy for Sustainable Development* 17 (5): 403–411.

Jones, J. M., A. R. Lea-Langton, L. Ma, M. Pourkashanian, and A. Williams. 2014. *Pollutants Generated by the Combustion of Solid Biomass Fuels.* London: Springer.

Kshirsagar, M. P., and V. R. Kalamkar. 2014. "A Comprehensive Review on Biomass Cookstoves and a Systematic Approach for Modern Cookstove Design." *Renewable and Sustainable Energy Reviews* 30: 580–603.

Kumar, M., S. Kumar, and S. Tyagi. 2013. "Design, Development and Technological Advancement in the Biomass Cookstoves: A Review." *Renewable and Sustainable Energy Reviews* 26: 265–285.

Lim, S. S. 2012. "A Comparative Risk Assessment of Burden of Disease and Injury Attributable to 67 Risk Factors and Risk Factor Clusters in 21 Regions, 1990–2010: A Systematic Analysis for the Global Burden of Disease Study 2010." *The Lancet* 380 (9859): 2224–2260.

MacCarty, N., D. Still, and D. Ogle. 2010. "Fuel Use and Emissions Performance of Fifty Cooking Stoves in the Laboratory and Related Benchmarks of Performance." *Energy for Sustainable Development* 14 (3): 161–171.

Raman, P., N. K. Ram, and R. Gupta. 2014. "Development, Design and Performance Analysis of a Forced Draft Clean Combustion Cookstove Powered by a Thermo Electric Generator with Multi-utility Options." *Energy* 69: 813–825.

Saravanakumar, A., T. M. Haridasan, T. B. Reed, and R. K. Bai. 2007. "Experimental Investigation and Modelling Study of Long Stick Wood Gasification in a Top Lit Updraft Fixed Bed Gasifier." *Fuel* 86 (17–18): 2846–2856.

Selim, M. Y. E., S. A. B. Al-Omari, S. M. S. Elfeky, and M. S. Radwan. 2011. "Utilization of Extracted Jojoba Fruit as a Fuel." *International Journal of Sustainable Energy* 30 (Suppl. 1): S106–S117.

Simon, G. L., R. Bailis, J. Baumgartner, J. Hyman, and A. Laurent. 2014. "Current Debates and Future Research Needs in the Clean Cookstove Sector." *Energy for Sustainable Development* 20: 49–57.

Urmee, T., and S. Gyamfi. 2014. "A Review of Improved Cookstove Technologies and Programs." *Renewable and Sustainable Energy Reviews* 33: 625–635.

Wang, Y., M. D. Sohn, Y. Wang, K. M. Lask, T. W. Kirchstetter, and A. J. Gadgil. 2014. "How Many Replicate Tests Are Needed to Test Cookstove Performance and Emissions? – Three Is Not Always Adequate." *Energy for Sustainable Development* 20: 21–29.

WHO. 2014. *Household Air Pollution and Health – Fact Sheet N 292.*

Yevich, R. 2003. "An Assessment of Biofuel Use and Burning of Agricultural Waste in the Developing World." *Global Biogeochemical Cycles* 17 (4): 6-1–6-40.

This page intentionally left mostly blank.

# Appendix C

## Assessment of Natural Draft Combustion Properties of a Top-Lit Up-Draft Research Furnace

# Assessment of natural draft combustion properties of a top-lit up-draft research furnace

T. Kirch[*], P.R. Medwell, C.H. Birzer

School of Mechanical Engineering
The University of Adelaide, SA 5005, Australia

## Abstract

Worldwide, over four million people die each year due to emissions from cookstoves. To address this problem advanced cookstoves are being developed with one system, called a top-lit up-draft (TLUD) gasifier stove, showing particular potential in reducing the production of harmful emissions. A novel research furnace analogy of a TLUD gasifier stove has been designed to study the TLUD combustion process. A commissioning procedure was performed under natural draft conditions. This included an assessment to establish the design operates as a TLUD gasifier and described the visual attributes of the TLUD's performance for in-field evaluation. Emissions profiles were recorded to identify combustion phases. The efficiency was evaluated through the nominal combustion efficiency ($NCE = CO_2/(CO_2 + CO)$) which is very high in the migrating pyrolysis phase, averaging 0.997. A value of this magnitude has previously not been reported for a cookstove. In the lighting phase and char gasification phase the NCE falls to 0.841 and 0.657 respectively. High $H_2$ emissions are also found in the lighting and char gasification phases, the latter indicating incomplete pyrolysis. The low NCE in the lighting and char gasification phase, compared to the NCE of an open fire, clearly demonstrate the need for combustion optimisation and emissions mitigation of these phases. The precise description of all the combustion phases, in combination with the emissions profiles and efficiency evaluation provide the means for in-field stove evaluation, aid in determining stove deficiencies and set baseline measurements against which TLUD stove designs can be compared.

*Keywords: Top-lit up-draft, Natural draft, Gasification, Pyrolysis, Cookstove.*

## 1. Introduction

Energy consumption in private households in developing countries is still primarily based on biomass fuels. Over the last three decades, and into the foreseeable future, 2.7 billion people [1] consistently rely on traditional, open fires and simple cookstoves to satisfy their cooking needs. These methods have very low efficiency and produce harmful emissions through incomplete combustion. In addition to the potential environmental consequences of deforestation and the contribution to climate change, there are major health problems related to traditional household cooking methods.

Worldwide, approximately 4.3 million premature deaths occur each year from cooking-related illnesses: more than 50% of premature deaths of children under the age of five years are the result of household air pollution [2]. The implementation of more efficient cookstoves that could decrease the consumption of biomass fuels would reduce the environmental consequences as well as people's exposure to pollutants, offering both health and environmental benefits [3].

In order to achieve substantial health benefits, cleaner burning cookstoves than are currently in use are needed [4,5]. One type of cookstove that has been recognised as potentially able to achieve this goal are gasifier stoves [6]. These use the thermochemical process of gasification to transform the fuel into combustible gases and burn them separately in time and location [7].

Gasifier stoves can be used under natural draft conditions, as in the present study, or with the assistance of a fan that creates a forced airflow. Compared with other cookstoves, gasifier stoves have been shown to produce low carbon monoxide (CO) and particulate matter (PM) emissions under laboratory conditions [8,9]. Specific studies on the TLUD combustion behaviour are limited but it has been shown that variation in stove geometry and the utilized fuel have an important impact on the stove performance [10,11]. It has been observed that the burn rate of wood increases with the initial wood density [12] and that the heat transfer to a vessel on the stove is a strong function of the vessel diameter while swirl of secondary air has a negligible impact [13]. Arora *et al.* [14] compared the influence of different standardised tests, kindling material and fuel feeding intervals on the cookstove performance. With different test protocols as well as fuel feeding intervals the emissions factors, primarily of CO and PM, showed variation and increased with lower calorific value of the kindling material. All of these studies have evaluated specific designs and analysed the performance while performing cooking tasks. An analysis of the unobstructed combustion process could lead to a deeper understanding and present further optimization possibilities to reduce harmful emissions consistently.

In the current study, a research furnace was specifically designed to study the operational properties of TLUD stoves in order to optimise for combustion and fuel efficiency. The designed furnace allows for various combustion-relevant parameters to be individually altered and is larger than normal household stoves, to be able to address scaling issues for stoves for communal use versus stoves for private households. Furthermore the increase in size enables a greater variability of adjustable parameters, such as amounts and locations of

_____
\* Corresponding author:
Phone: (+61) 8313 5460
Email: thomas.kirch@adelaide.edu.au

the fuel within the combustion chamber, to be studied. Through the commissioning test procedure, under natural draft conditions, the combustion phases will be determined, both visually and through emissions testing over the whole burning cycle. Furthermore, the phases will be clearly separated and analysed individually. This will allow future studies on TLUD cookstoves to be compared with these basic natural draft conditions to determine how design alternations affect the combustion process. An investigation of what is visually perceptible, in addition to the emissions profiles of all combustion phases, is especially relevant for in-field stove assessment. This article, therefore, provides the means to relate visual findings to emissions profiles and sets a baseline against which to compare TLUD stove designs.

## 2. Experimental details

The research furnace was designed as a TLUD stove with the general characteristics of a primary air inlet at the bottom of the furnace, and a lateral secondary air inlet in the upper region, as shown in Fig. 1.

The central component of the research furnace is the stove body, consisting of a cylindrical steel cylinder (600 mm tall, 206 mm inner diameter, 8 mm wall thickness) and a fuel grate. The perforated fuel grate (26% open-area ratio) is located inside the cylinder to hold the fuel stack in place. The depth of the fuel grate is adjustable. The stove body is placed on top of a steel frame, which serves as the primary air inlet chamber. The steel frame of the primary air inlet allows all sides to be closed off, so air can be applied through only one inlet. If the sides are not closed off, air enters freely. In the present study air can enter freely via natural draft over the whole stove diameter. The secondary air inlet is provided by a detachable stove extension to the top of the stove body. There are two possible stove extensions. The first extension is equipped with a diffuser ring around the air inlet that it can be attached to compressed air to control the in-flow. The second extension, which was used for testing in this study, allows air to enter by natural draft.

Emissions data was collected in one central location while the temperature data was constantly measured in
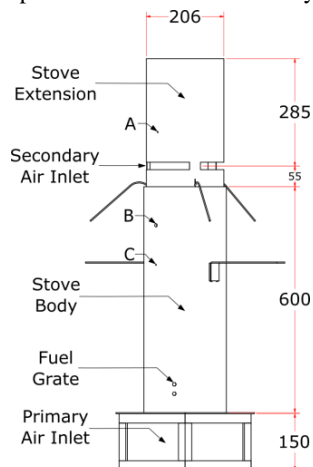


**Figure 1: Schematic TLUD research furnace configuration for natural draft conditions**

two locations. For emissions testing a measuring probe of a Testo 350XL was placed in the centre of a fume hood inlet at a distance of 0.83 m above the exit plane of the extension. The Testo 350XL was used to record the CO, $CO_2$, $H_2$ concentrations, on a dry basis. Temperature data were collected via two K-type thermocouples (locations A and B in Fig. 1) and via an infra-red thermometer (location C).

A normalisation process was performed for all gathered emissions concentrations. The emissions data are related to the sum of all carbon emissions, here CO and $CO_2$. The emissions are each normalised with respect to the sum of the carbon emissions because these can be attributed to the combustion process and provide the relationship between the intensity of the combustion process and the release of certain products.

The fuel for each test consisted of 700 g of dried locally sourced pine bark chips. Bark chips were chosen as fuel because wood is the most commonly combusted biomass [15]. In every test the furnace was pre-heated, supplied with one batch of fuel and lit at the top, using 5 mL of methylated spirits to aid ignition.

## 3. Results

Preliminary results were gathered through visual assessment. In further tests, emissions and temperature profiles were also recorded. Through the emissions measurements, the performance of the stove in terms of the nominal combustion efficiency (NCE) (defined as $CO_2/(CO + CO_2)$ [9]) was evaluated and a mathematical separation of the combustion phases was conducted. By relating all the findings (visual, emissions and temperature measurements) to one another, a full picture of the process could be drawn.

After lighting, combustion takes place directly at the fuel stack. This can be seen by flames spreading from the kindling material over the surface of the biomass. Once the upper layer of the fuel stack is ignited, the temperature increases and small amounts of smoke start to be released. This suggests that the remaining water evaporates and volatile compounds are released from the fuel. A change can be observed once thick white smoke is released from the fuel stack which is subsequently ignited and clean burning. This indicates that a second phase, termed *migrating pyrolysis*, has begun.

In the transition period from the lighting phase to the migrating pyrolysis volatile compounds are released from the fuel, observable as thick white smoke. The thick smoke indicates that there are high amounts of vaporised pyrolysis products, such as tars, heavier hydrocarbons and water, in the gas stream. This suggests that the process of cracking pyrolytic products into lighter hydrocarbons, which occurs at high temperatures and for which hot char particles act as a catalyst [16], is restricted. Varunkumar *et al.* [13] hypothesised that cracking in gasifier based stoves might be restrained due to the limited char bed thickness.

The thick smoke released from the fuel rises to the secondary air inlet where it should be ignited, after mixing with oxygen from the entering air. In the pre-

heated tests the flames that established on the fuel stack in the lighting phase ignite the thick smoke at the secondary air inlet. In some cold start tests, it was observed that the flames on top of the fuel stack would not ignite a flame at the secondary air inlet. This implies that the flames that establish in the lighting phase need to bridge the distance between the fuel stack and the location where a combustible mixture of secondary air with gasification products from the fuel is present. This has previously not been observed when testing smaller TLUD stoves and needs to be considered when designing bigger TLUD stoves, where the distance between fuel and secondary air inlet increases. Once the thick smoke is ignited a bright yellow flame establishes that burns very cleanly. This separation between the migrating pyrolysis taking place in the fuel stack and the pyrolytic products being burned separately in time and location, at the secondary air inlet, is a distinctive characteristic of TLUD stoves [17].

The end of the migrating pyrolysis phase is indicated by the extinction of the flame at the secondary air inlet. The char gasification phase begins because insufficient combustible volatiles are released from the fuel stack to sustain the flame at the secondary air inlet. It can be seen that hot glowing char remains, with small irregular flames above the char bed until only ash is left on the fuel grate.

Tests were carried out with the natural draft stove and emissions concentrations were recorded, as presented in Fig. 2. Three phases can be identified in each of the profiles presented in Fig. 2. The three phases are the lighting phase, the migrating pyrolysis phase and the char gasification phase. Numerically, a change in phase is identified here when the temporal derivative of the normalised CO profile exceeds $\pm 0.002$ s$^{-1}$. This value was determined following a rigorous verification based on inspection of the profiles and found to be reliable at identifying each phase. Table 1 presents the results of the combustion phase specific calculations of time weighted average (TWA) values for all emissions and peak values for the nominal combustion efficiency (NCE) and $H_2$ emissions.

It is apparent from Fig. 2 that in the lighting phase, the NCE can be extremely low, with one peak reaching below 0.6 compared to an average of 0.9965 in the migrating pyrolysis phase (see Table 1). These profiles can be related to incomplete combustion of the kindling material and the top layer of the biomass. In the lighting phase the combustion of kindling material and the top layer of biomass takes place inside the stove body where the surrounding oxygen is quickly consumed and insufficient primary air enters through the fuel stack for complete combustion. It should be noted, though, that only three of the eight tests show very low $CO_2$ peak values, which suggests that a consistently higher NCE in this phase could be achieved. To find ways to ensure lower emissions in this phase requires further investigation.

Once a flame front establishes at the secondary air inlet, the NCE rises to an average of 0.9965, which is much higher than in the other phases, while the $H_2$

**Table 1: Averaged normalised data for the three phases, with the standard deviation of eight tests in parentheses underneath**

|  | Lighting | Migrating pyrolysis | Char gasification |
|---|---|---|---|
| Time in Phase [s] | 95.1 (9.9) | 285.4 (27.7) | 221.5 (17.1) |
| Min NCE | 0.8404 (0.1658) | – | 0.6572 (0.0569) |
| Time to Peak [s] | 54.4 (10.5) | – | 523.4 (40.9) |
| Peak $H_2/(CO_2 + CO)$ | 0.0418 (0.0538) | – | 0.0556 (0.0240) |
| Time to Peak [s] | 71.9 (11.4) | – | 539.1 (41.9) |
| TWA - NCE | – | 0.9965 (0.0006) | 0.8518 (0.0427) |
| TWA - $CO/(CO_2 + CO)$ | – | 0.0035 (0.0006) | 0.1482 (0.0427) |
| TWA - $NO_x/(CO_2 + CO)$ | – | 0.00059 (0.00005) | 0.00036 (0.00007) |
| TWA - $H_2/(CO_2 + CO)$ | – | 0.00013 (0.00015) | 0.01368 (0.00727) |
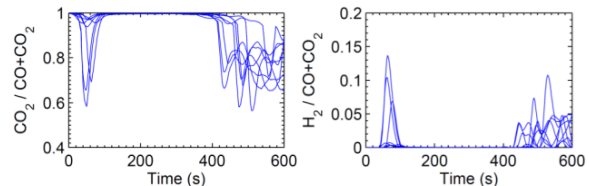


**Figure 2: Normalised emissions data of $CO_2$ and $H_2$ measurements for eight tests**

emissions remain consistently low (Fig. 2). In this phase the migrating pyrolytic front steadily moves down the fuel stack, which provides the necessary gaseous products for the flame at the secondary air inlet to be sustained. This phase is highly efficient and exhibits extremely low emissions. Comparing these with the results of Jetter *et al.* [9] and Johnson *et al.* [18] it can be seen that only very few stoves can achieve a NCE of this magnitude. It should be borne in mind, though, that this comparison is limited because the test conditions in the compared studies are different. The comparison still clearly verifies the high efficiency of the research furnace and the potential of this type of stove.

In the char gasification phase, average CO and $H_2$ emissions are higher than in the other phases, resulting in a low NCE. The high CO emissions were to be expected and were also detected by Mukunda *et al*. [19]. These emissions can be explained by an increase in the surface oxidation due to a higher relative surface area [20]. The high $H_2$ emissions should be noted carefully in this phase because they cannot necessarily be explained by char gasification. These emissions might indicate that the release of hydrocarbon compounds in the migrating pyrolysis phase is incomplete. Therefore it might be possible, through further study, to optimise the migrating pyrolysis phase to achieve a higher overall efficiency.

The temperature profiles presented in Fig. 3 reflect the results from both the visual assessment and the emissions data. The three phases can be identified, based on the slope of the temperature profile. In the lighting phase, the gas temperature inside the stove body heats up much more quickly than in the stove extension because combustion takes place on the fuel stack.

Once the migrating pyrolysis phase starts and a flame front establishes at the secondary air inlet, the gas temperature inside the stove extension rises above the
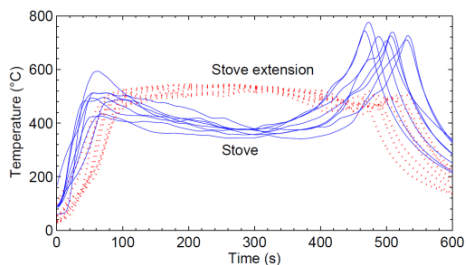
**Figure 3: Mean temperatures in the stove (location B in Fig. 1) and in the stove extension (location A)**

temperature in the stove body. In the stove body, the endothermic (energy absorbing) pyrolysis is mainly sustained by the released energy from the partial oxidation of the pyrolysis products, which causes the temperature to drop. The gas temperature inside the stove body reduces to below 400 °C, which means that the temperature of the pyrolysis products, once they reach the secondary air inlet, can be below this value. This drop of pyrolysis product temperature from ≈ 600 °C, when leaving the fuel bed [19], to below 400 °C when reaching the secondary air inlet suggests a cooling effect. This cooling effect can be assumed to be due to the heat loss through the furnace walls and would increase with the size of the stove. Especially when increasing the size, beyond the size of the presented research furnace, the condensation of liquid pyrolysis products could occur. This cooling effect needs to be considered when designing large stoves. Towards the end of the migrating pyrolysis phase, the gas temperature inside the stove body starts increasing until it peaks in the char gasification phase. This can be explained by the decline of endothermic, pyrolytic reactions with a simultaneous increase of exothermic, char gasification reactions inside the fuel bed. Highest temperatures can be achieved in the char gasification phase within the stove body, as has previously been observed [11, 12].

## 4. Conclusions

In order to better understand the combustion process in TLUD stoves, and to enable future optimisation of TLUD designs for various conditions, a research furnace has been designed, built and commissioned. A visual assessment presented the attributes of TLUD stoves that can be observed; primarily the separation of the solid fuel and the combustion of the gasification products. Furthermore, the emissions profiles were normalised and presented to show the combustion behaviour of TLUD stoves under natural draft conditions. Three distinct phases: the lighting phase, the migrating pyrolysis phase and the char gasification phase, were identified. The lighting and char gasification phases are characterised by low nominal combustion efficiency (NCE) and high emissions of incomplete combustion. It has been seen that a consistently shorter and more efficient lighting phase should be possible to achieve. Also scaling issues are shown to occur when increasing the distance between the fuel bed and the secondary air inlet. These issues include ignition problems at the secondary air inlet and heat loss between the fuel bed and the secondary air inlet. The migrating pyrolysis phase, conversely to the

other two phases, displayed an extremely high NCE. High traces of $H_2$ emissions in the char gasification phase suggest that the pyrolysis process is incomplete in the migrating pyrolysis phase. The high emissions in the lighting phase and char gasification phase are in contrast to the low emissions in the migrating pyrolysis phase. This leads to the conclusion that further research to prolong the migrating pyrolysis phase, while mitigating the release of emissions of incomplete combustion in the lighting and char gasification phases, could be of benefit to future stove designs.

These results identify research topics that need to be addressed to optimise stove performance and shed light on relevant parameters that need to be considered when designing larger TLUD stoves for communal use. Additionally they enable the in-field visual assessment of TLUD stoves and set a baseline against which such stoves can be compared.

## 5. Acknowledgements

## 6. References

[1] S. Bonjour, H. Adair-Rohani, J. Wolf, N. G. Bruce, S. Mehta, A. Prüss-Ustün, M. Lahiff, E. a. Rehfuess, V. Mishra, and K. R. Smith, Environ. Health Perspect., **121** (7) ( 2013), pp. 784–790.
[2] WHO, (2014). [Online]. Available: http://www.who.int/iris /handle/10665/141496. [Accessed: 04-Aug-2015].
[3] C. A. Ochieng, C. Tonne, and S. Vardoulakis, Biomass and Bioenergy, **58** (2013), pp. 258–266.
[4] K. R. Smith, J. P. McCracken, M. W. Weber, A. Hubbard, A. Jenny, L. M. Thompson, J. Balmes, A. Diaz, B. Arana, and N. Bruce, Lancet, **378** (2011), pp. 1717–1726.
[5] J. Baumgartner, K. R. Smith, and A. Chockalingam, Glob. Heart, **7** (3) (2012), pp. 243–247.
[6] G. L. Simon, R. Bailis, J. Baumgartner, J. Hyman, and A. Laurent, Energy Sustain. Dev., **20** (2014), pp. 49–57.
[7] P. S. Anderson and T. B. Reed, LAMNET Project International Workshop (2004).
[8] J. J. Jetter and P. Kariher, Biomass and Bioenergy, **33** (2) (2009), pp. 294–305.
[9] J. Jetter, Y. Zhao, K. R. Smith, B. Khan, T. Yelverton, P. Decarlo, and M. D. Hays, Environ. Sci. Technol., **46** (19) (2012), pp. 10827–10834.
[10] C. Birzer, P. Medwell, J. Wilkey, T. West, M. Higgins, G. Macfarlane, and M. Read, J. Humanitarian Eng., **2** (1) (2013), pp. 1–8.
[11] J. Tryner, B. D. Willson, and A. J. Marchese, Energy Sustain. Dev., **23** (2014), pp. 99–109.
[12] S. Varunkumar, N. K. S. Rajan, and H. S. Mukunda, Combust. Sci. Technol., **183** (11) (2011), pp. 1147–1163.
[13] S. Varunkumar, N. K. S. Rajan, and H. S. Mukunda, Energy Convers. Manag., **53** (1) (2012), pp. 135–141.
[14] P. Arora, P. Das, S. Jain, and V. V. N. Kishore, Energy Sustain. Dev., **21**, (1) (2014), pp. 81–88.
[15] R. Yevich, Global Biogeochem. Cycles, **17** (4) (2003).
[16] P. Basu, Elsevier Inc., 2013, p. 118.
[17] P. S. Anderson, T. B. Reed, and P. W. Wever, Boil. Point, **53** (53) (2007), pp. 35–37.
[18] M. Johnson, R. Edwards, V. Berrueta, and O. Masera, Environ. Sci. Technol., **44** (1) (2010), pp. 368–374.
[19] H. S. Mukunda, S. Dasappa, P. J. Paul, N. K. S. Rajan, M. Yagnaraman, D. Ravi Kumar, and M. Deogaonkar, Curr. Sci., **98** (5) (2010), pp. 627–638.
[20] P. S. Arora and S. Jain, Environ. Sci. Technol., **49** (2015), pp. 3958 – 3965.

This page intentionally left mostly blank.

# Appendix D

---

# Mixing Uniformity of Emissions for Point-Wise Measurements in Exhaust Ducts

---

# Mixing uniformity of emissions for point-wise measurements in exhaust ducts

**T. Kirch**[1,2]**, M. J. Evans**[1]**, P. R. Medwell**[1,2]**, V. H. Rapp**[3]**, C. H. Birzer**[1,2] **and A. J. Gadgil**[3,4]

[1]School of Mechanical Engineering, The University of Adelaide, South Australia 5005, Australia

[2]Humanitarian and Development Solutions Initiative, The University of Adelaide, South Australia 5005, Australia

[3]Environmental Technologies Area, Lawrence Berkeley National Laboratory, Berkeley, CA 94720, USA

[4]Department of Civil and Environmental Engineering, University of California, Berkeley, CA 94720, USA

## Abstract

Exhaust hoods are commonly used to capture all emissions from stationary combustion systems that are open to the environment, such as residential heaters or stoves. For experimental purposes, emissions are sampled at one, or more, discrete locations downstream in the exhaust duct. Point-wise measurements in the duct are often taken with the assumption that the emissions are homogeneously distributed across the duct cross-section, because the flow is turbulent and therefore believed to be thoroughly mixed. However, the length of such systems is rarely sufficient to ensure fully-developed flow, and the actual homogeneity is seldom assessed. In the present work the mixing within the duct is investigated by simulating the emissions distribution within various hood and duct configurations. The simulations include a straight duct with and without baffles and two different exhaust hood configurations, namely at the Stove Testing Lab at Lawrence Berkeley National Laboratory (LBNL) and at the University of Adelaide that meet standard requirements. The air flow in the ducts was simulated using Reynolds-averaged (RANS) turbulence modelling, with carbon monoxide (CO) as a representative combustion product, injected at three locations in the straight duct and two locations (centre and side) in the exhaust hoods. Simulations predict that, in isolation, neither a straight duct without baffles, nor a hood with a 90° elbow followed by a straight duct without baffles, provide sufficient mixing to achieve a near uniform distribution of CO at the sampling locations. However, simulations show that adequate mixing of dilution air and CO is achieved with baffles-induced flow detachment and recirculation, not from turbulent mixing in the straight section of the duct itself. The simulations also suggest that elbows, baffles, expansions or other geometrical features are needed to induce thorough mixing. For example, in the Stove Testing Lab at LBNL, flow disturbance is induced by an expansion into a larger diameter straight duct immediately downstream of the hood and the 90° elbow. Although these two systems demonstrate sufficient mixing of CO within the exhaust, the RANS simulations in this study suggest that other systems relying solely on mixing within a specified duct length (viz. 8–12 diameters) may not be sufficient.

## Introduction

The evaluation of the combustion properties and efficiency of stationary appliances, such as cookstoves, is often based on measurements of emissions. In order to provide representative measurements of these emissions, the released products typically need to be captured. In laboratory studies, exhaust hoods are often used to capture all emissions of combustion systems that do not have a flue or other exhaust system, which are then transported outside via ducting. The hood generally spans over a larger area to ensure it captures all the emissions from the appliance, which is often quite a localised source. In the region under the hood, the draft velocity is low to avoid disturbing the combustion itself. The flow velocity increases in the contrac-

tion of the hood, is turbulent within the duct and is therefore believed to be thoroughly mixed. Nevertheless, large spatial inhomogeneities of the emissions under the hood could persist throughout the duct if sufficient mixing is not ensured. Within the duct, point-wise measurements rely on homogeneous emissions distribution to determine the performance of the combustor in a representative, repeatable and affordable manner. The present study numerically investigates the mixing behaviour of a representative gaseous combustion product within different exhaust systems to evaluate the validity of measurements taken at specific locations in exhaust ducts.

An exhaust hood typically includes a contraction hood, followed by ducts, of various geometries, and a blower or fan, to create a forced air flow. The necessary requirement—as well as the challenge—is to measure representative combustion emissions within the duct. Existing designs of exhaust hoods for emissions measurements are represented in standard methods, such as AS/NSZ 4013:2014 or US EPA Title 40 §60. While both suggest two 90° elbows and a straight section before the measuring location, US EPA guidelines suggest two baffles (semi-circular obstruction) in between the 90° elbows; but also allows for alternative measurements after eight or, if not feasible, after two diameters of straight ducting. A specific test protocol for cookstoves (ISO 19867-1, 2018), stipulates one 90° elbow followed by baffles and 12 diameters (12D) of straight duct upstream of the sampling location. With these different options, and many more found in the literature for the design of exhaust hoods, it is unclear which specifications achieve comparable and representative measurements. The evaluation of the mixing behaviour of gaseous emissions through computational fluid mechanics could therefore provide insights into the necessary flow characteristics to achieve sufficient mixing.

To assess the mixing behaviour in an exhaust system, initially an understanding of mixing in a straight pipe is required. Previously, it has been suggested that in turbulent straight pipes, fully developed flow can be achieved at 100–130 diameters downstream of any disturbance [1]. While the turbulence properties of fully-developed flow are not a necessity for a well-mixed gas flow, turbulence is the dominant mixing mechanism in a straight pipe. A shorter length could be insufficient to achieve homogeneous distribution of constituents in ducts. Furthermore, it has been shown that tracer gas measurements in a straight duct at 9D downstream of a 90° elbow deviate approximately 20% from the mean and obstructions or mixing elements need to be introduced to reduce this value [2]. The lack of certainty in the mixing of various systems may render any data erroneous or misleading. Simulations enable a deeper understanding of the influence of the length of the straight pipe section, as well as geometrical specifications on gaseous mixing in the duct to ensure reliable point-wise measurements.

A numerical study of mixing of emissions from stationary combustion systems with dilution air in exhaust hoods is provided

to investigate the validity of point-wise measurements within ducts. Point-release of a tracer gas is used to investigate the impact of non-homogenous release of pollutants across the duct inlet, to assess the mixing homogeneity and to identify a reliable sampling measure at a single point downstream in the duct. Specifically, the influence of flow obstructing baffles, in a straight pipe and a representative exhaust hood, as well as geometrical specifications, elbows and expansions, in two representative exhaust hoods are addressed. While the focus of the present study is the mixing behaviour in exhaust hoods, the results might also be relevant for direct emissions measurements within flues or exhaust pipes.

## Methods

### Modelling

Three exhaust systems were modelled, specifically; the gas flow in a straight pipe with and without baffles; the facilities at the Stove Testing Lab at Lawrence Berkeley National Laboratories (LBNL); and those used at the University of Adelaide (UofA) with and without baffles. Model specifications and boundary conditions for all five variations are presented in Table 1.

The steady Reynolds-averaged Navier-Stokes (RANS) simulations were conducted with ANSYS CFX 17.2, using the shear-stress transport (SST) turbulence model [3]. All simulations employ a second-order coupled solver for turbulent flows and convergence was better than $10^{-4}$. The inlet turbulence intensity was 5%. Smooth, no slip walls were employed. For the more complex hood structures, transitional turbulence using the Gamma Theta model [5] with reattachment modification was used. In the region of the elbow and baffles the boundary layer was resolved, while in the straight duct of all models, a low 0.0002–0.0007 mm first inflation layer thickness and a subsequent growth of 1.2 was employed. A structured, quadrilateral, computational mesh, was created in the straight duct while the enclosures and duct intersection in the UofA cases were unstructured, based on mesh independence studies. In the duct $y^+ < 5$ was widely achieved. The wall-treatment switched between resolving the boundary layer for sufficiently low $y^+$, and standard k–ω wall functions. Transport of CO is modelled using binary Fickian diffusion and a turbulent Schmidt number of 0.9, which has previously been validated [6].

**Table 1: Model specifications of the geometries the straight pipe with (SP-B) and without (SP-N) baffles, the LBNL, and the UofA with (-B) and without (-N) baffles.**

|        | Outlet | Tracer flow | Elements | Re |
|--------|--------|-------------|----------|----|
|        | kg·s$^{-1}$ | L/min | ·$10^6$ | ·$10^3$ |
| SP-N   | 0.112  | Isokinetic  | 7.45     | 30 |
| SP-B   | 0.112  | Isokinetic  | 1.37     | 30 |
| LBNL   | 0.112  | 100 L/min   | 2.83     | 30 |
| UofA-N | 0.078  | Isokinetic  | 4.30     | 35 |
| UofA-B | 0.078  | Isokinetic  | 4.81     | 35 |

### Straight pipe

The straight pipe model has an inner diameter of 250 mm and 30 m length. CO is introduced separately in three locations (L1–L3) in a 10° wedge, spanning from 100 mm$<r<$250 mm, as presented in Figure 1(c). The entrance plane is defined as an opening to ensure isokinetic flow, while the mass flow through the pipe is specified at the outlet. Simulations were also performed with baffles, 300 mm and 600 mm downstream of the inlet, oriented such that the first baffle obstructs half the flow path (B1), while the second obstructs the opposite half (B2). The three cell thick baffles were removed from the geometry.

### Exhaust system at Lawrence Berkeley National Laboratories

The exhaust system used at LBNL consists of a hood with vertical walls, of different height, and a door at the front [7, 8]. The front is of 460 mm height, partially covered by 300 mm high doors, while the back wall extends to 760 mm below the hood. As the back wall extends further than the front from the hood, the sides are of trapezoidal shape, with the diagonal side extending from front wall corner to the back wall corner. Air can enter into the hood from all sides from below the walls. The 1,370 mm by 860 mm hood contracts into a 152.4 mm (6 in) diameter duct. The hood is followed by a 90° elbow and a stepwise expansion to 254 mm (10 in) duct. To assess the uniformity of the mixing, the tracer gas, CO, is introduced in two different locations, (1) coaxial (along the centre line of the duct connected to the hood), and (2) circumferential (off the centre line, on the side of the hood). The tracer gas inlet is modelled as a square opening with an equivalent area to the 6 mm hose used in validation experiments previously published by LBNL [4].

### Exhaust system at The University of Adelaide

The UofA hood covers a square enclosure of 600 mm by 600 mm with a height of 1800 mm. Three sides of the enclosure are sealed, while the front consists of a door spanning from 600 mm above the floor to the top. Thus a 600 mm by 600 mm opening below the door allows air to enter. The hood has a 45° inclination leading into a 150 mm diameter duct at its centre. At the top of the square contraction, a 90° elbow into a straight vertical duct with an inlet for dilution flow (which is considered closed in all simulations). The straight duct extends 40 diameters (6 m). When baffles are introduced, the first baffle is located downstream of the elbow, obstructing the top half of the duct, and the second baffle is located 300 mm downstream of the first, obstructing the bottom half of the duct. CO is introduced along the centre of the enclosure at a height of 700 mm from the floor.

## Results

### Straight pipe

In Figure 1 the normalised CO mass concentration (the local mass fraction divided by the mean mass fraction across the duct cross-section) profile is presented across cross sectional slices of the pipe at certain locations. Pipe cross sectional planes at 12 and 100 diameter (D) length downstream of the inlet are presented in Figures 1(a) and 1(b), respectively. Three configurations of the straight pipe with baffles at 12 D downstream of the second baffle are also shown. In the configuration with baffles, three separate injection locations (L1–L3) were simulated, with respect to the baffle locations, as shown in the profile in Figure 1(c). The three locations at the circumference of the inlet are L1 at the centre of the first baffle (B1), L2 at the centre of the second baffle (B2), and L3 at the edge of the baffles, with the results presented in Figures 1(d), 1(e) and 1(f), respectively.
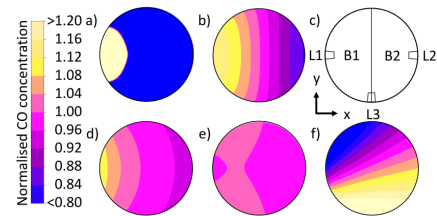


**Figure 1: Normalised CO profiles at in the straight pipe: (a) no baffles, 12D; (b) no baffles, 100D; (c) profile indicating baffle and tracer locations; (d) baffles, tracer L1, 12D; (e) baffles, tracer L2, 12D; (f) baffles, tracer L3, 12D.**
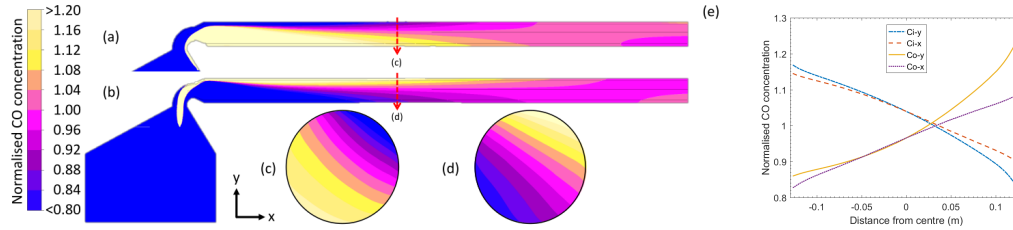
**Figure 2:** The normalised CO profiles along the centre plane, (a) and (b), and at the measuring location 8 diameters downstream of the expansion, (c) and (d), for circumferential (Ci) and coaxial (Co) tracer injection respectively LBNL facilities. The graph (e) shows the simulated normalised CO value along the x- and y-axes at the measuring location.

In case of the unobstructed spatially developing flow, it can be seen in Figure 1(a) that the CO distribution is biased towards the tracer injection location at 12D, with notable CO concentrations extending approximately 0.4D from the circumference. Previously, approximately 100 D have been suggested to ensure fully developed pipe flow [1], which is often believed to be sufficient to ensure homogeneous mixing of gas phase constituents. In Figure 1(b) it can be seen that even at 100D downstream of the inlet the CO mass fraction displays a bias toward the side of the tracer injection: with a variation of over $\pm 35\%$ across the duct in x-direction. Therefore, although fully developed pipe flow can be assumed after 100D of a straight pipe, this does not mean that all gaseous constituents are homogeneously mixed.

Adding baffles to the pipe enhances mixing, but the effects are dependent on the tracer injection location. The most homogeneous CO profile can be noted when injecting in location L2, while the greatest bias results from location L3 where the impact of the baffles is lower, because of less path obstruction.

It is evident that to achieve sufficient mixing, extremely large pipe length or specific flow disturbing elements are necessary to promote mixing. In the straight pipe at 100D downstream of the inlet, there is still a substantial bias in the tracer gas concentration, which demonstrates that under turbulent flow conditions, homogeneous constituent distribution cannot be assumed, even if the flow is fully developed.

### Exhaust system at Lawrence Berkeley National Laboratories

Figure 2 presents the system at LBNL that has been extensively used for cookstove emissions testing [4, 7, 8]. The cross-sectional plane along the length of the system, for the two different injection strategies: circumferential injection and coaxial injection, are shown in Figures 2(a) and 2(b), respectively. Additionally, the normalised CO profiles in the duct cross sectional area at the measuring locations (viz. 8D downstream of the elbow) are shown in Figures 2(c) and 2(d). Figure 2(e) presents the simulated normalised CO mass fraction at the measuring location 8D downstream of the expansion, across the x- and y-axes (refer to 2(c) and 2(d)).

In Figure 2(a) and 2(b) it can be seen that flow detachment and a large recirculation zone is induced by the expansion downstream of the elbow. Flow detachment, especially at the bottom of the duct, leads to the formation of a substantial recirculation zone. While in 2(a) the coaxial release of CO leads to recirculation of low CO concentration gas, the opposite is the case for the circumferential CO release. Downstream of the flow disturbance, low and high concentration gases mix more rapidly.

At the measuring location shown in Figures 2(c) and 2(d), a low bias of the normalised CO mass fraction can be noted for both cases. A more uniform profile is achieved for coaxial tracer injection compared with circumferential injection. This shows

the dependence of the mixing outcome on the source location, as also noted in the straight pipe simulations. It is evident that in both cases, the CO mass fraction is especially close to the mean value around the centre of the duct, where samples are generally extracted. A comparison with previously performed experiments [4] and the numerical results show qualitatively similarity, supporting the validity of the presented results and underlining that sufficient mixing is achieved.

### Exhaust system at the University of Adelaide

Figure 3 shows the normalised CO mass fraction along the central cross-sectional plane of the UofA exhaust system (Figures 3(a) and 3(b)) and across the measuring plane within the duct at 12D downstream of the elbow or second baffle in Figures 3(c) and 3(d), respectively. Additionally, the values of the normalised CO mass fraction along the x- and y-axes at the measuring location are presented in 3(e).

When considering the configuration without baffles in Figures 3(a), 3(c) and 3(e) a largely inhomogeneous profile can be seen. Values of the normalised CO concentration along the x-axis range from 0.67 to 1.52 and a value of 0.76 can be noted at the centre of the duct, the typical location of sample extraction. It can be seen that the combination of the vertical front opening with the 90° elbow of the duct leads to a substantial bias of the CO concentration towards the front and top side of the duct. In this geometry, no zone of intensive mixing is created. Extending the measuring location further downstream, better mixing can be seen at 20D and 30D but with diminishing returns. A bias is still notable at 40D, which marks the boundary of the simulated domain. This shows that a 90° elbow followed by a straight duct, without flow disturbing elements, does not achieve sufficient mixing of gaseous constituents in this exhaust duct.

When baffles are incorporated into the duct, the first baffle, constricting the top section of the duct, leads to build up of high CO concentration flow and mixing as this flow is directed towards the low CO concentration flow at the bottom of the duct (see Figure 3(b)). The second baffle then leads to build up of the remaining low CO concentration flow. Flow detachment and recirculation in the wake of both baffles causes further mixing of CO within the flow. With baffles, a discrepancy between opposite sides of duct of less than 5% is achieved, as shown in Figure 3(d) and 3(e). Especially at the centre of the duct, values are particularly close to the expected mean concentration. Therefore, sufficient mixing at the measuring location is achieved when baffles are introduced into the system.

### Discussion

In all simulations, the tracer gas is introduced in small concentrations and specific locations into the system and must therefore be considered "worst case" scenarios. In application, a combustion appliance is a much more dispersed source and
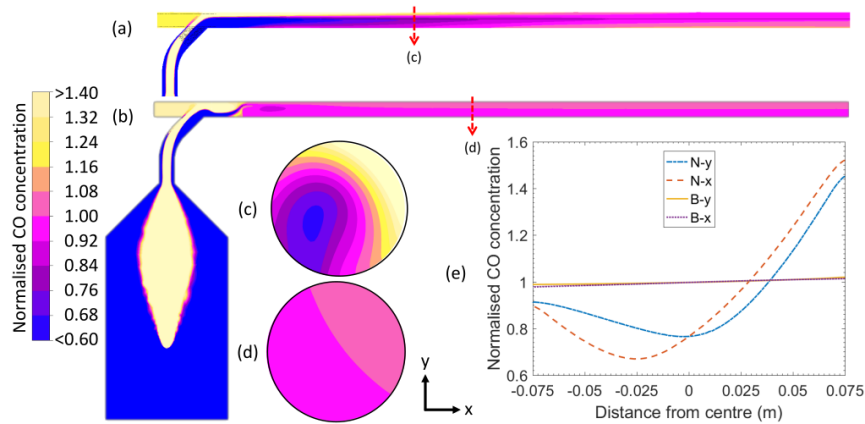
**Figure 3: The normalised CO profiles of the UofA system along the centre plane, (a) and (b), and at the measuring location 12D downstream, (c) and (d) for the cases without and with baffles, respectively. In (e) the values along the x- and y-axes of the measuring location are presented.**

more homogeneous mixing can be expected.

The influence of flow disturbing elements on multi-phase flows (combustion appliance exhaust gases generally contain substantial amounts of particulate matter) have not been considered in the simulations. For example, the Stokes number of $< 10~\mu m$ diameter particles (density $\approx 2250$ kg·m$^{-3}$), in the UofA system, is $< 0.1$. Particles with a Stokes numbers of $< 1$ are considered to respond and follow flow. Therefore, valid particle measurements are expected, as most particles from cookstoves are of sub-micron size [9]. However, this considers neither the influence of the dilution air on particle morphology and size distribution [10] nor the Stokes number dependence of particle size distribution within the duct [11]. Furthermore, when baffles are introduced, the large surface area of impaction might have a more substantial influence on the particle size distribution and reduce measured concentrations. Further research regarding the influence of dilution air and flow disturbing elements on particulate measurements is required.

## Conclusions

Simulations of multiple exhaust geometries and the exhaust systems used at the Stove Testing Lab at the Lawerence Berkeley National Laboratories (LBNL) and the University of Adelaide (UofA) were performed to evaluate the mixing behaviour within ducts. Large spatial inhomogeneities between localised emissions sources and the surrounding area underneath exhaust hoods could propagate throughout the duct if sufficient mixing is not ensured. Sufficient mixing is required to enable valid point-wise measurements within the ducting. Results show that a straight duct or a 90° elbow followed by a straight duct achieve insufficient mixing of combustion products and dilution air within reasonable duct length. To enhance mixing, specific flow disturbances need to be introduced into the exhaust system. Sufficient mixing is achieved through a duct expansion after an elbow and the introduction of baffles into the straight duct section, in the LBNL and UofA systems respectively. These results highlight the necessity to verify the mixing patterns within a specific hood geometry when being used for exhaust sampling.

## Acknowledgements

## References

[1] Pitts, W.M. and Kashiwagi, T., The application of laser-induced Rayleigh light scattering to the study of turbulent mixing, *J Fluid Mech*; **141**, 1984, 391–428.

[2] Gupta, R., Turbulent mixing and deposition studies for single point aerosol sampling, *Thesis*, Texas A&M, 1999.

[3] Menter, F., 2-Equation eddy-visocity turbulence models for engineering applications, *AIAA Journal*; **32**, 1994, 1598–1605.

[4] Wilson, D.L., Rapp, V.H., Caubel, J.J., Chen, S.S. and Gadgil, A.J., Verifying mixing in dilution tunnels How to ensure cookstove emissions samples are unbiased, *LBNL*, 2017, LBNL–2001088.

[5] Menter, F. *et al.*, A Correlation-based transition model using local variables – Part I: Model Formulation, *J Turbomach*; **128**, 2006, 413–422.

[6] Ekambara, K., Joshi, J.B., Axial mixing in pipe flows: Turbulent and transition regions, *Chem Eng Sci*; **58**, 2003, 2715–2724.

[7] Caubel, J.J., Rapp, V.H., Chen, S.S. and Gadgil, A.J., Optimization of Secondary Air Injection in a Wood-Burning Cookstove: An Experimental Study, *Environ Sci Technol*; **52**, 2018, 4449–4456.

[8] Rapp, V.H., Caubel, J.J., Wilson, D.W. and Gadgil, A.J., Reducing ultrafine particle emissions using air injection in wood-burning cookstoves, *Environ Sci Technol*; **50**, 2016, 8368–8374.

[9] Li, X. *et al.*, Emission characteristics of particulate matter from rural household biofuel combustion in China, *Energy Fuels*; **21**, 2007, 845–851.

[10] Arora, S. *et al.*, A review of chronological development in cookstove assessment methods: Challenges and way forward, *Renewable and Sustainable Energy Reviews*; **55**, 2016, 203–220.

[11] Lau, T. and Nathan, G., Influence of Stokes number on the velocity and concentration distributions in particle-laden jets, *J Fluid Mech*; **757**, 2014, 432–457.